VOLUME 49, NUMBER 8

**August, 1961**

*published monthly by The Institute of Radio Engineers, Inc.*

# Proceedings of the IRE®

*contents*

Poles and Zeros ..... 1261

Anthony B. Giordano, Director, 1961–1962 ..... 1262

Scanning the Issue ..... 1263

PAPERS

Antiferroelectric Ceramics with Field-Enforced Transistions: A New Nonlinear Circuit Element, *Bernard Jaffe* ..... 1264
Large-Signal Circuit Theory for Negative-Resistance Diodes, in Particular Tunnel Diodes, *M. Schuller and W. W. Gärtner* ..... 1268
IRE Standards on Solid-State Devices: Definitions of Terms for Nonlinear Capacitors, 1961 ..... 1279
Self-Oscillation in a Transmission Line with a Tunnel Diode, *J. Nagumo and M. Shimura* ..... 1281
IRE Standards on Solid-State Devices: Measurement of Minority-Carrier Lifetime in Germanium and Silicon by the Method of Photoconductive Decay ..... 1292
Detection Range Predictions for Pulse Doppler Radar, *S. A. Meltzer and S. Thaler* ..... 1299
Low-Level Garnet Limiters, *F. R. Arams, M. Grace, and S. Okwit* ..... 1308

CORRESPONDENCE

The Silicon Cryosar, *H. Izumi* ..... 1313
Noise Figure and Stability of Negative Conductance Amplifiers, *Alan C. Macpherson* ..... 1314
Tunnel-Diode One-Shot and Triggered Oscillator, *T. W. Flowerday and D. D. McKibbin* ..... 1315
A Tunnel-Diode Slot Transmission Amplifier, *Melvin E. Pedinoff* ..... 1315
Neural Analogs, *L. D. Harmon and A. E. Brain* ..... 1316
On Self-Organizing Systems, *P. D. Coleman* ..... 1317
Stable Low-Noise Tunnel-Diode Frequency Converter, *F. Sterzer and A. Presser* ..... 1318
Thin-Film Cryotrons, *V. L. Newhouse and H. H. Edwards* ..... 1318
Are Electronics Engineers Educated?, *R. W. Johnson* ..... 1319
A Note on Sugai's Class of Solutions to Riccati's Equation, *David C. Stickler* ..... 1320
A New RMS Describing Function for Single-Valued Nonlinearities, *J. E. Gibson and K. S. Prasanna-Kumar* ..... 1321
A Proposed Test of the Constancy of the Velocity of Light, *Pascal M. Rapier* ..... 1322
Notes on the Structure of Logic Nets, *Robert M. Stewart* ..... 1322
Suppression of Emission from Portions of Barium-Activated Tungsten Dispenser Cathodes and Adjoining Electrodes, *R. Levi and E. S. Rittner* ..... 1323
Transmission Line Model, *J. D. Wallace* ..... 1324
Antenna Siting Tests at 3480 and 9640 Mc on a 173-Mile Tropospheric Scatter Path, *N. D. La Frenais and W. J. Lucas* ..... 1325
On the Linear Circuit Aspects of Cryotrons, *P. M. Chirlian and V. A. Marsocci* ..... 1326
A Method for Determining the Base Voltage and Contact Resistance of a Conductivity-Modulated Diode, *J. M. Swartz and H. C. Gorton* ..... 1326
Receivers with Zero Intermediate Frequency, *M. D. Rubin* ..... 1327
A Magnetic Shield for Beam Frequency Standards, *F. S. Barnes* ..... 1328
A Monopulse Instrumentation System, *Frederic P. Storke, Jr.* ..... 1328
A Traveling-Wave Maser Using Chromium-Doped Rutile, *E. S. Sabisky and H. J. Gerritsen* ..... 1329
Shaping of Distributed RC Networks, *B. L. H. Wilson and R. B. Wilson* ..... 1330
Proposed Technique for Modulation of Coherent Light, *A. K. Kamal and S. D. Sims* ..... 1331
A Generalization of "Mutual Information," *N. M. Blachman* ..... 1331
A Broad-Band Termination for IF Coaxial Lines, *A. Susini and F. A. Ferger* ..... 1332
Tracking and Display of Earth Satellites, *A. Van Gelder, Jr.* ..... 1332
High-Level Microwave Detector Using Avalanche Injection, *H. M. Day and A. C. MacPherson* ..... 1333
Coherent Generation of Microwave Power by Annihilation Radiation of a Prebunched Beam, *B. W. Hakki and H. J. Krumme* ..... 1334
WWV and WWVH Standard Frequency and Time Transmissions, *National Bureau of Standards* ..... 1335
Self-Educating Machines for Recognition and Classification of Patterns, *P. A. Clavier* ..... 1335
On Parametric Amplification in Transistors, *J. Lindmayer, C. Wrigley, V. W. Vodicka, and R. Zuleeg* ..... 1335
Multiple Burst Detection, *Francis Corr* ..... 1337
An Analytical Expression for Describing the Write Process in Magnetic Recording, *T. C. Ku* ..... 1337
A Potential Microwave Computer Element, *R. W. Couch, A. F. Rashid, and R. Spence* ..... 1338
A Solution to the Shannon Switching Game, *A. Lehman* ..... 1339

COVER

The array of curves shown on the cover portray the characteristics of a new dielectric ceramic circuit element capable of antiferroelectric-to-ferroelectric transitions, as described on page 1264.

AUGUST

World Radio History

*published monthly by The Institute of Radio Engineers, Inc.*

# Proceedings of the IRE

*continued*

The Wide Tuning Range of Backward Traveling-Wave Parametric Amplifiers, *H. Hsu and S. Wanuga* ..... 1339
Correction to "Negative Resistance in Transistors Based on Transit-Time and Avalanche Effects," *R. A. Pucel and H. Statz* ..... 1340
Correction to "Communications Satellites Using Arrays," *R. C. Hansen* ..... 1340

REVIEWS

Books:
"Transistor Circuit Analysis," by M. V. Joyce and K. K. Clarke, *Reviewed by J. T. Lynch and J. J. Karew* ..... 1343
"IRE Dictionary of Electronic Terms and Symbols (Compiled from IRE Standards)," *Reviewed by R. F. Shea* ..... 1343
"Printed Circuits—Their Design and Application," by J. M. C. Dukes, *Reviewed by Thomas A. Prugh* ..... 1343
"Line Waves and Antennas," by R. G. Brown, R. A. Sharpe, and W. L. Hughes, *Reviewed by Carl E. Smith* ..... 1344
"Time-Harmonic Electromagnetic Fields," by Roger F. Harrington, *Reviewed by Charles H. Papas* ..... 1344
"Theory of Microwave Valves," by S. D. Gvozdover, *Reviewed by C. W. Barnes* ..... 1344
"Lectures on Communication System Theory," Elie J. Baghdady, Ed., *Reviewed by M. R. Aaron* 1345
"Electronic Drafting Handbook," by Nicholas M. Raskhodoff, *Reviewed by R. T. Haviland* .... 1345
"Electronics," by P. M. Chirlian and A. H. Zemanian, *Reviewed by W. R. Hill* ..... 1346
"Progress in Semiconductors, Vol. 5," A. F. Gibson, F. A. Kröger, and R. F. Burgess, Eds., *Reviewed by W. M. Bullis* ..... 1346
"Essentials of Dielectromagnetic Engineering," by H. M. Schlicke, *Reviewed by Charles F. Pulvari* ..... 1347
"Radio Waves in the Ionosphere," by K. G. Budden, *Reviewed by M. G. Morgan* ..... 1347
"Scientific Russian," by James W. Perry, *Reviewed by S. D. Browne* ..... 1347
"Electrical Noise," by W. R. Bennett, *Reviewed by H. A. Haus* ..... 1348
Recent Books ..... 1348
Scanning the TRANSACTIONS ..... 1348

ABSTRACTS

Abstracts of IRE TRANSACTIONS ..... 1349
Abstracts and References ..... 1358

IRE NEWS AND NOTES

Current IRE Statistics ..... 14A
Calendar of Coming Events and Authors' Deadlines ..... 14A
Professional Group News ..... 18A
Programs:
Western Electronics Show and Conference (WESCON) ..... 20A
Joint Nuclear Instrumentation Symposium ..... 28A
National Symposium on Space Electronics and Telemetry ..... 28A
Ninth Annual Engineering Management Conference ..... 30A
Industrial Electronics Symposium ..... 32A

DEPARTMENTS

Contributors ..... 1341
IRE People ..... 54A
Industrial Engineering Notes ..... 34A
Meetings with Exhibits ..... 8A
Membership ..... 140A
News—New Products ..... 128A
Positions Open ..... 102A
Positions Wanted by Armed Forces Veterans ..... 108A
Professional Group Meetings ..... 39A
Section Meetings ..... 133A
Advertising Index ..... 153A

AUGUST

BOARD OF DIRECTORS, 1961
*L. V. Berkner, *President*
*J. F. Byrne, *Vice President*
Franz Ollendorff, *Vice President*
*S. L. Bailey, *Treasurer*
*Haraden Pratt, *Secretary*
*F. Hamburger, Jr., *Editor*
*Ernst Weber
*Senior Past President*
*R. L. McFarlan
*Junior Past President*

1961
C. W. Carnahan (R7)
B. J. Dasher (R3
A. N. Goldsmith
*P. E. Haggerty
C. F. Horne
R. E. Moe (R5)
D. E. Noble
B. M. Oliver
J. B. Russell, Jr. (R1)

1961 1962
A. B. Bereskin (R4)
M. W. Bullock (R6)
A. B. Giordano (R2)
W. G. Shepherd
G. Sinclair
B. R. Tupper (R8)

1961–1963
E. F. Carter
L. C. Van Atta

*Executive Committee Members

EXECUTIVE SECRETARY
George W. Bailey

John B. Buckley, *Chief Accountant*

Laurence G. Cumming, *Professional Groups Secretary*

Joan Kearney, *Assistant to the Executive Secretary*

Emily Sirjane, *Office Manager*

ADVERTISING DEPARTMENT
William C. Copp, *Advertising Manager*

Lillian Petranek, *Assistant Advertising Manager*

EDITORIAL DEPARTMENT
Alfred N. Goldsmith, *Editor Emeritus*
F. Hamburger, Jr., *Editor*
E. K. Gannett, *Managing Editor*
Helene Frischauer, *Associate Editor*

EDITORIAL BOARD
F. Hamburger, Jr., *Chairman*
T. A. Hunter, *Vice Chairman*
E. K. Gannett
T. F. Jones, Jr.
J. D. Ryder
G. K. Teal
Kiyo Tomiyasu
A. H. Waynick

AUDITED PAID CIRCULATION ABC

PROCEEDINGS OF THE IRE, published monthly by The Institute of Radio Engineers, Inc., at 1 East 79 Street, New York 21, N. Y. Manuscripts should be submitted in triplicate to the Editorial Department. Correspondence column items should not exceed four double-spaced pages (illustrations count as one-half page each). Responsibility for contents of papers published rests upon the authors, and not the IRE or its members. All republication rights, including translations, are reserved by the IRE and granted only on request. Abstracting is permitted with mention of source.

Thirty days advance notice is required for change of address. Price per copy: members of the Institute of Radio Engineers, one additional copy $1.25; non-members $2.25. Yearly subscription price: to members $9.00, one additional subscription $13.50; to non-members in United States, Canada, and U. S. Possessions $18.00; to non-members in foreign countries $19.00. Second-class postage paid at Menasha, Wisconsin, under the act of March 3, 1879. Acceptance for mailing at a special rate of postage is provided for in the act of February 28, 1925, embodied in Paragraph 4, Section 412, P. L. and R., authorized October 26, 1927. Printed in U.S.A. *Copyright © 1961 by The Institute of Radio Engineers, Inc.*

World Radio History

*August, 1961*
*Vol. 49 No. 8*

**Proceedings of the IRE**

# Poles and Zeros

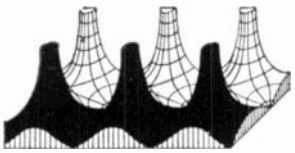

**WESCON 1961.** This month (August 22–25) the West Coast puts on its "Big Show" for the electronics profession, second only in importance to the IRE International Convention. It is anticipated that 35,000 persons will be present. Each of the forty technical sessions will be comprised of three papers with a panel of authorities who will provide a critique of each. There will be 1180 exhibits in the WESCON show.

The emphasis of this year's program is on the field of radio/radar astronomy. It fits well the coincidence of the convention of the International Astronomical Union, in Berkeley, the dates of which overlap those of WESCON, in San Francisco. The over-all program places emphasis on masers, lasers, and parametric amplifiers related to astronomical programs and to quantum electronics. A joint session featuring speakers from IAU is scheduled.

The IRE WESCON CONVENTION RECORD, which was initiated in 1957, will not be published this year. WESCON management, after very careful consideration, decided that the abandonment of the RECORD would release more papers for later publication in the PROCEEDINGS and the TRANSACTIONS OF IRE. They feel that this new policy has attracted more high-quality papers since the authors have greater freedom to seek publication in the journal of their choice. The Managing Editor, in cooperation with WESCON, has issued information to all WESCON authors concerning the submission of their WESCON papers to IRE journals. This change in the publication policy of WESCON holds no implication for the IRE INTERNATIONAL CONVENTION RECORD; its publication will continue.

For the fifth year WESCON will feature the Future Engineers Show. This outstanding student affair should be a must on the schedule of every attendee at WESCON. Youngsters from high schools throughout the West (including Alaska and Hawaii) gather for a "junior WESCON." They exhibit their own works, have their own technical sessions, and compete for scholarship awards. The forty participants are chosen from regional and area science fairs by local IRE committees. The student exhibits are judged by leaders in the electronics field based on the demonstration, presentation, and content of their displays. The Future Engineers Show, conceived as a service to students, will again this year open the eyes and attract the ears of the "older engineers" attending WESCON.

Poles and Zeros salutes the WESCON Board, Albert J. Morris, O. H. Brown, John V. N. Granger, Calvin K. Townsend, Bruce S. Angwin, Donald C. Duncan, Edward C. Bertolet, and S. H. Bellue. The detailed program, for which they, and nearly 300 Bay Area electronics men and women deserve congratulations, will be found in the IRE News and Notes section of this issue.

**Information Retrieval.** Poles and Zeros, in October, 1960, discussed the growth of engineering and scientific publication to point up the increasing "problem of too little time for too much to read." Comment was made in that note concerning the helpfulness of various indexing, abstracting, and reviewing services. Although no solution to this complex problem has yet been brought forth it is satisfying to be able to report an increase in IRE services in the form of abstracting and reviewing.

A growing number of the IRE TRANSACTIONS are publishing abstracts or literature review sections. For example, PGANE published abstracts of the *Journal of the Institute of Navigation* (London); PGCT reviews current literature; PGEC provides abstracts of current computer literature and reviews of books and papers in the computer field; PGEWS publishes book reviews; PGIT gives both abstracts and book reviews; and PGBME publishes abstracts. These TRANSACTIONS are to be congratulated on this extra service to IRE and Professional Group members.

This service, supplementing as it does the Abstracts and References section and the Book Review section of the PROCEEDINGS, is only one phase of the contribution to the solution of the literature problem being made by the TRANSACTIONS. One cannot ignore the significance of the publication of bibliographies as a literature aid. An outstanding example is the "Bibliography on Medical Electronics," compiled by the Medical Electronics Center of the Rockefeller Institute and published by the Professional Group on Bio-Medical Electronics. This particular bibliography and its two annual supplements cover some 7,600 references in that field.

Not to belabor, but to emphasize, the importance of contributions of this type one may note that both sales figures for the electronics industry and IRE membership have tripled in size in the last decade. Publication volume has correspondingly increased. IRE, for example, published approximately 200 letters and papers in one journal in 1950. In 1960 it published approximately 2,000 items in 32 publications.

It is to be hoped that, pending a unique and radical solution to the problem, additional TRANSACTIONS will emulate the example of those listed above.

**Career Brochure.** Poles and Zeros reported, in September, 1960, the issuance of the brochure "Electronics—Career for the Future" as a result of the work and energy of the Cedar Rapids Section. The brochure was so well received that the original printing has been exhausted. It is a pleasure to report that a new printing of a revised brochure will be available this fall through the cooperation of the Electronic Industries Association. Distribution is planned to 28,000 high schools throughout the country.—F. H., Jr.

World Radio History

# A. B. Giordano

*Director, 1961–1962*

Anthony B. Giordano (SM'46–F'58) was born on February 1, 1915, in New York, N. Y. He attended the Polytechnic Institute of Brooklyn, Brooklyn, N. Y., and received the following degrees from that institution: the B.E.E. in 1937, the M.E.E. in 1939, and the D.E.E. in 1946. Also, he was honored with a Certificate of Distinction in 1957 for contributions to education and research.

He joined the academic staff of the Polytechnic Institute of Brooklyn in 1939 as Instructor of Electrical Engineering, became Assistant Professor in 1945, and, in 1952, as Associate Professor, he administered the graduate program in electrical engineering, and launched and coordinated the Polytechnic Graduate Study Program in Mineola, L. I. He was made Professor in 1953, Associate Dean in 1957, and Dean of the Graduate School in 1960, as well as Director of Special Studies.

During World War II he devoted part of his effort to microwave research. As a member of Dr. Ernst Weber's original research team, he assisted in the development of the first microwave precision attenuator. The group was reorganized as the Microwave Research Institute, and he directed several research contracts which led to the development of a series of precision waveguide attenuators. He also guided the program on microwave measurements and has authored over twenty-five research reports and articles in microwaves and related fields.

As a member of the New York Section of the IRE, Dr. Giordano was Secretary during 1952–1953, Vice Chairman during 1953–1954, and Chairmen during 1954–1955. He has also participated in the activities of the Long Island Section, the Professional Group on Microwave Theory and Techniques, the Antennas and Waveguide Committee, and the Professional Group on Circuit Theory.

Dr. Giordano holds membership in Eta Kappa Nu, Sigma Xi, Tau Beta Pi, AAAS, ASEE, and AIEE. In the New York Section of the AIEE, he is now a member-at-large of the Executive Committee. He is also a member of the AIEE Committee on Electronic and High Frequency Measurements and Commission 1 of URSI. Through an impetus provided by Dr. McFarlan, he organized during 1958 an Engineering Advisory Committee for the Board of Education of the City of New York to study the high school curriculum in physics.

World Radio History

# Scanning the Issue

**Antiferroelectric Ceramics with Field-Enforced Transitions: A New Nonlinear Circuit Element** (Jaffe, p. 1264)—Any material that exhibits nonlinear characteristics is potentially useful as a circuit element. Indeed, many of the most important devices of the past decade depend on nonlinearity for their operation. The nonlinearity of certain antiferroelectric ceramics has been known for a number of years. An antiferoelectric is characterized by rows of dipoles, with each row polarized in the opposite direction to that of its neighbor. Under special conditions, an applied field will switch alternate rows so that all rows are polarized in the same direction. This antiferroelectric-to-ferroelectric transition produces a double hysteresis loop characteristic which has a linear central region, rather like a tilted integral sign with a loop on each end. As mentioned above, this transition has been observed in certain materials before, but only within a very narrow temperature range in the 200° C region. This effect has therefore remained little more than a marginal scientific curiosity. This paper demonstrates that the transition can now be made to occur over much wider temperature ranges and in a temperature region of much greater practical interest, namely, from −60° C to over 100° C. What was once a scientific curiosity has thus been transformed into a phenomenon which has a promising future in a number of important applications, including nonlinear capacitors, energy storage devices and electromechanical transducers.

**Large-Signal Circuit Theory for Negative-Resistance Diodes, in Particular Tunnel Diodes** (Schuler and Gärtner, p. 1268)—The complications of analyzing a device that is nonlinear can usually be circumvented satisfactorily by making approximations which are easier to handle mathematically. The simplification frequently takes the form of substituting an equivalent linear parameter for a nonlinear one. This approach is especially effective in studying small-signal situations. In the case of tunnel diodes, an entire small-signal theory has been satisfactorily developed on this basis by assuming a linear negative resistance. For large-signal applications, however, the entire range of positive and negative resistances of the device are important, and the linear model becomes inaccurate. This paper develops a system of nonlinear differential equations which accurately describes the true large-signal behavior of a tunnel diode, without any of the customary simplifications. The equations are then solved by a computer. The solutions are worked out in detail for large-signal operation of tunnel diodes as oscillators and switches. Since tunnel diode switching applications appear to be a large and important field, these "exact" solutions will be of substantial interest and importance. Equally significant is the fact that the approach presented here can be used to solve a wide class of nonlinear problems.

**IRE Standards on Solid-State Devices: Definitions of Terms for Nonlinear Capacitors** (p. 1279)—The nonlinearity of semiconductor diode capacitors gives them special characteristics which make them a valued member of the electronic component family. Their nonlinearity also raises a need for special concepts and terminology for describing these special characteristics. This need has now been met by the list of nineteen terms and definitions provided in this standard.

**Self-Oscillation in a Transmission Line with a Tunnel Diode** (Nagumo and Shimura, p. 1281)—This paper presents an analysis, complete with experimental verification, of the self-oscillations that occur when a transmission line is connected to a negative resistance element, such as a tunnel diode. Both the method of analysis and the particular application discussed make this a paper of more than ordinary interest and importance. The authors have gone back some 25 years in the literature to draw upon a study of the self-oscillations that occur in a violin string. The method of analysis has important application to the broad study of transmission lines with nonlinear terminations, but until now it apparently never received much attention because the original analysis dealt with an acoustic problem and was published in a somewhat inaccessible journal. The specific application discussed here, namely, tunnel diode oscillators that make use of transmission line circuits, is of substantial interests in itself. Now that tunnel diodes capable of operating up to 10 Gc appear feasible, oscillators incorporating simple microwave structures are an attractive prospect. The authors' analysis takes into account the nonlinearities of such a system.

**IRE Standards on Solid-State Devices: Measurement of Minority-Carrier Lifetime in Germanium and Silicon by the Method of Photoconductive Decay** (p. 1292)—The importance of carrier lifetime to the operation of semiconductor devices is fundamental. Because of the extremely high degree of purity that can be obtained in semiconductor crystals, it has become possible to observe and measure recombination processes in much finer detail than was once possible. Although a number of methods for measuring carrier lifetime have been developed, the one which has gained most widespread use consists of deliberately creating excess carriers in a sample by exposing it to a short burst of optical radiation and then monitoring the voltage drop across the material as the excess carriers recombine. This standard specifies the methods for carrying out this important and basic measurement.

**Detection Range Predictions for Pulse Doppler Radar** (Meltzer and Thaler, p. 1299)—The subject of this paper, pulse Doppler radar, is a field fast becoming of interest to weapons systems engineers. The study presented here is probably the first serious attempt to set up a mathematical model exclusively tailored to predicting the range of this type of radar. The model allows the variation of most of the important radar parameters and is sufficiently flexible to predict the range of most pulse Doppler radar search systems. Not only is a study of this type much needed today, but it is not unlikely that this paper may become a basic reference.

**Low-Level Garnet Limiters** (Arams, *et al.*, p. 1308)—There has long been a need for limiters which would protect microwave receivers against overload or burnout, and for power levelers which would eliminate power output variations in microwave power sources. At present, suitable limiters are not available on the market and very little information on these devices is contained in the literature. This paper is representative of what can be done in the area of low-level limiting. The authors describe, and give experimental results for, garnet limiters developed for L and S bands, including such novel types as electronically tunable preselectors, and cavity-type and comb-type limiters. The fact that this is a new and rapidly moving field makes this information especially timely.

**Scanning the Transactions** appears on page 1348.

World Radio History

# Antiferroelectric Ceramics with Field-Enforced Transitions: A New Nonlinear Circuit Element*

BERNARD JAFFE†

*Summary*—**Ceramic dielectrics capable of field-enforced antiferroelectric-to-ferroelectric transitions from below −60°C to over 100°C have been made. The transition manifests itself by a $D/E$ hysteresis figure with a linear central region and loops showing saturation on either end. Previously studied materials have exhibited this phenomenon only in a very limited temperature range. Conditions for obtaining the effect over a wide temperature range are: 1) a polymorphic inversion from ferroelectric to antiferroelectric with ascending temperature, and 2) a relatively high-peak dielectric constant at the antiferroelectric-paraelectric transition temperatures. Nonlinear capacitance, usefulness for capacitive energy storage, and novel transducer properties are described.**

## Introduction

THIS PAPER describes ceramic dielectrics that have a field-enforced antiferroelectric-to-ferroelectric transition. Examples of this phenomenon have been known for some time, but have been restricted to very limited temperature ranges just under a dielectric-constant maximum that varies from one composition to another. Now, however, this range has been extended widely, from below −60°C to over 100° or 125°C. In this form, these ceramics seem to constitute a new class of nonlinear circuit element.

An antiferroelectric is characterized by rows of dipoles, with the dipole moment of adjacent rows equal but antiparallel.[1] This arrangement can be regarded as two interpenetrating sublattices of equal and opposite polarization, with no net spontaneous polarization. We shall use the term "soft" to describe those antiferroelectrics in which an attainable applied field can switch the direction of polarization of the sublattice it opposes. Most antiferroelectric crystalline materials would break down before switching in this way. They would behave as linear, low-loss capacitors.

It is well known that crystal or ceramic $PbZrO_3$ is capable of undergoing such a change for a few centigrade degrees below 230°C, its temperature of maximum dielectric constant. In this field-enforced phase change, the structure changes from a staggered orthorhombic arrangement[2,3] to a polar arrangement, probably rhombohedral,[4] whenever the applied field exceeds a certain threshold value. This manifests itself by a double hysteresis loop with a linear central region and open areas on either end (Fig. 1). It was first described by Shirane, Sawaguchi, and Takagi[5] and has been studied further.[6,7] Similar instances of soft antiferroelectricity with slightly greater temperature range, perhaps 30 centigrade degrees in a region near 200°C, have been described[6,8] for $PbZrO_3$ modified with small amounts of $Ti^{+4}$ or $Ba^{+2}$. A related phenomenon has been observed by Merz[9] in $BaTiO_3$ just over its Curie temperature. In this case, the linear central region of the hysteresis loop denotes a paraelectric ground state rather than an antiferroelectric one, and the temperature range of this effect is very small.

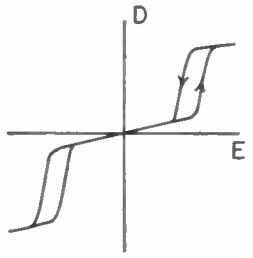


Fig. 1—Hysteresis loop for an antiferroelectric with a field-enforced ferroelectric transition.

## Method of Achieving Soft Antiferroelectricity over a Wide Temperature Range

Shirane, Sawaguchi, and Takagi[5] ascribed the anomalous hysteresis loop and the existence of the dielectric-constant maximum in $PbZrO_3$ to a ferroelectric phase, itself unstable, having free energy slightly greater than that of the stable antiferroelectric phase. The energy

* Received by the IRE, November 1, 1960; revised manuscript received, April 17, 1961.

† Electronic Res. Div., Clevite Corp., Cleveland, Ohio.

[1] C. Kittel, "Theory of antiferroelectric crystals," *Phys. Rev.*, vol. 82, pp. 729–732; June, 1951.

[2] E. Sawaguchi, H. Maniwa and S. Hoshino, "Antiferroelectric structure of lead zirconate," *Phys. Rev.*, vol. 83, p. 1078; September, 1954.

[3] F. Jona, G. Shirane, F. Mazzi and R. Pepinsky, "Neutron diffraction study of antiferroelectric lead zirconate, $PbZrO_3$," *Phys. Rev.*, vol. 105, pp. 849–856; February, 1957.

[4] G. Shirane and S. Hoshino, "X-Ray study of phase transitions in $PbZrO_3$ containing Ba or Sr," *Acta Cryst.*, vol. 7, pp. 203–210; February, 1954.

[5] G. Shirane, E. Sawaguchi and Y. Takagi, "Dielectric properties of lead zirconate," *Phys. Rev.*, vol. 84, pp. 476–481; November, 1951.

[6] E. Sawaguchi, "Ferroelectricity versus antiferroelectricity in the solid solutions of $PbZrO_3$ and $PbTiO_3$," *J. Phys. Soc. (Japan)*, vol. 8, pp. 615–629; September–October, 1953.

[7] A. P. DeBretteville, Jr., "Threshold field and free energy for the antiferroelectric-ferroelectric phase transition in lead zirconate," *Phys. Rev.*, vol. 94, pp. 1125–1128; June, 1954.

[8] G. Shirane, "Ferroelectricity and antiferroelectricity in ceramic $PbZrO_3$ containing Ba or Sr," *Phys. Rev.*, vol. 86, pp. 219–227; April, 1952.

[9] W. J. Merz, "Double hysteresis loop of $BaTiO_3$ at the Curie point," *Phys. Rev.*, vol. 91, pp. 513–517; August, 1953.

World Radio History

gap between the two possible phases governs the threshold field necessary to excite the anomalous hysteresis loop.

To achieve a soft antiferroelectric stable over an extended temperature range, it was desired to have a low and stable threshold field. The ideal way to do this would be to make an antiferroelectric ceramic extremely close in composition to a morphotropic-(composition dependent-temperature independent) phase boundary between antiferroelectric and ferroelectric phases. However, no such boundary is perfectly morphotropic. Accordingly two criteria were adopted. They were: 1) the sequence of change with heating was to be ferroelectric-to-antiferroelectric-to-paraelectric, and 2) the dielectric-constant maximum at the antiferroelectric-to-paraelectric transition was to be as high as possible. This would ensure equal energy between the ferroelectric and antiferroelectric states at the ferroelectric to antiferroelectric inversion temperature and almost equal energy at the antiferroelectric-to-paraelectric inversion temperature. It would also favor reasonably uniform properties within the antiferroelectric range.

The desired sequence of the phase changes is exemplified in Fig. 2, which shows the low-field dielectric constant and loss for a composition that changes from ferroelectric to antiferroelectric at about 90°C. The low losses at temperatures above this are typical of antiferroelectrics, and the loss peak associated with the dielectric-constant maximum in a ferroelectric is clearly absent.

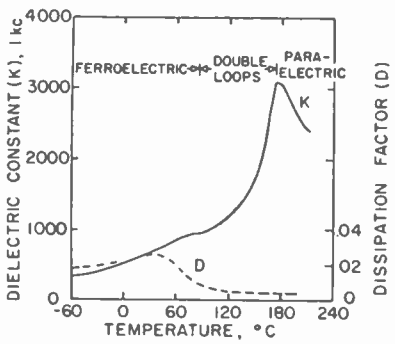


Fig. 2—Low-field dielectric constant and loss for a composition that shows the field-enforced antiferroelectric-ferroelectric transition above 90°C.

## Results

### *Hysteresis Loops at Varying Temperatures*

These conditions have been realized in a series of related ceramic compositions that show the anomalous hysteresis loops from temperatures as low as −60°C or lower, to over 100°C. The dielectrics studied are pseudocubic perovskite solid solutions. They are based on antiferroelectric $Pb(Zr, Sn)O_3$ compositions, which are orthorhombic perovskites, isostructural with $PbZrO_3$ and showing similar superstructure lines in their X-ray pattern.[10] These antiferroelectrics have been modified by compositional additives, so that they show ferroelectricity at low temperatures, as outlined in the preceding section. The type and amount of the additives govern the temperature of the ferroelectric-to-antiferroelectric transition. For most compositions studied, the dielectric-constant maximum, which represents an antiferroelectric-to-paraelectric transition, occurs between 150° and 200°C.

The series of 60-cps hysteresis loops, shown in Fig. 3, for one of these compositions illustrates the results achieved. Somewhere below −50°C the material shown is ferroelectric. Above 125°C as the temperature of the dielectric-constant maximum is approached, the character of the *D-E* loop gradually approaches a closed saturating-type figure (Fig. 3, 128°C). There is no sharply defined upper temperature limit for obtaining the double loop. Its character is entirely subdued when the temperature of the dielectric-constant maximum is reached. The ferroelectric parts of the loop gradually become slimmer (less lossy) with increasing temperature.

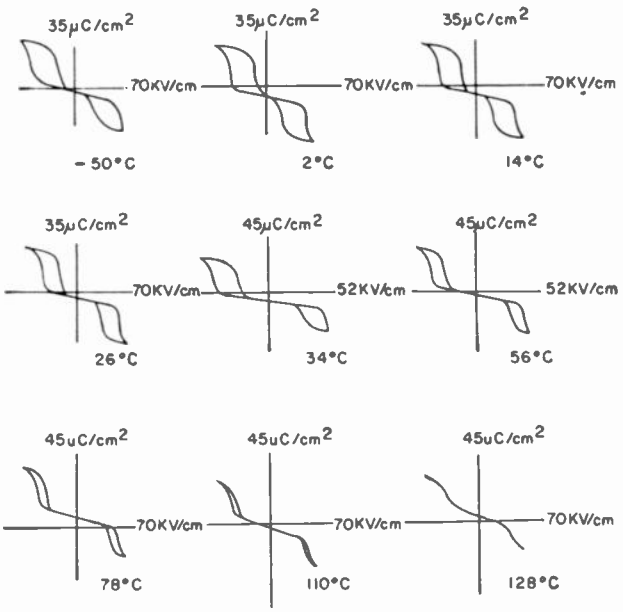


Fig. 3—Hysteresis loops for a composition showing field-enforced transition from below −50°C to above 125°C. Because of the high threshold fields, some were poorly saturated.

### *Capacitance Nonlinearity*

Inasmuch as the slope of the hysteresis loop indicates the differential (dc) capacitance of the sample, it is apparent that this parameter increases sharply as the field passes the threshold for inducing the ferroelectric state.

[10] B. Jaffe, R. S. Roth and S. Marzullo, "Properties of piezoelectric ceramics in the solid-solution series lead titanate-lead zirconate-lead oxide: tin oxide and lead titanate hafnate," *J. Res. N.B.S.*, vol. 55, pp. 239–254; November, 1955.

World Radio History

It then drops as the loop saturates, and increases again as the field falls through the range where the polarization drops sharply and the antiferroelectric state appears. Thus in each half cycle, we have two intervals of high differential dielectric constant, corresponding to the two steep parts of the loop. Inasmuch as typical values at room temperature are 700 at low field and 5000 for the average (tip-to-tip) value at high fields, it can be seen that the differential value during dipole swtiching is quite high.

In contrast to the behavior of the differential (dc) dielectric constant, the small-field incremental (ac) dielectric constant, measured with a small 1000-cps alternating field superimposed on slowly varying bias, increases slowly with increasing bias through the antiferroelectric range, then drops as the threshold field is exceeded and approaches a saturation value. Because of the hysteresis, it remains low until the bias field falls enough to allow reversion to the antiferroelectric state, then rises to the original value. Typical values of the dielectric constant are 700 to 1000 at low bias and half that at saturation. This behavior is shown diagramatically for soft antiferroelectric and conventional ferroelectric samples in Fig. 4.

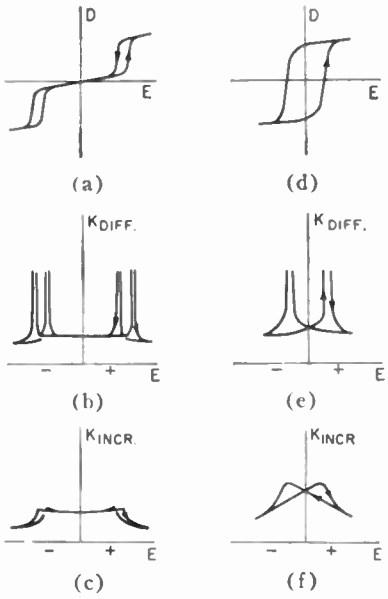


Fig. 4—Hysteresis loop, differential dielectric constant (slope of loop) and incremental dielectric constant (1000-cycle measuring field with slowly-varying bias) for: (a)–(c) a soft antiferroelectric, and (d)–(f) a normal ferroelectric.

*Energy Storage*

It has been suggested by H. Jaffe of this laboratory that such a dielectric would have advantages as a high-energy-storage capacitor. In Fig. 5, typical *D-E* Lissajous figures for a soft antiferroelectric, a normal ferroelectric, and a linear dielectric are shown. The energy recoverable from each is denoted by the shaded areas. In the ferroelectric, much of the charging energy

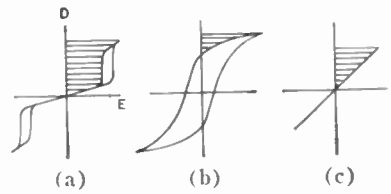


Fig. 5—Hysteresis figures for (a) a soft antiferroelectric, (b) a normal ferroelectric, and (c) a linear capacitor. The shaded area denotes the discharge energy.

is absorbed by domain switching, and remains as remanence. It is available only as pyroelectricity or as irreversible piezoelectricity at pressures greater than those used to produce a linear piezoelectric effect. Remanence can be avoided in part by the use of compositional additives that minimize it. Dielectrics of this nature frequently saturate at relatively low fields. Once saturated, an increment of field causes little additional energy storage. Another way of avoiding remanence is to use a ferroelectric in its paraelectric condition, just above the Curie temperature. Here, too, easy saturation is likely to limit the energy storage.

In the linear capacitor, no remanence occurs, but the dielectric constants are generally low. Storage of appreciable charge requires very high field and, consequently, extreme dielectric strength. The soft antiferroelectrics, too, are free of remanence. A particular advantage of the soft antiferroelectrics is the approach of the "energy area" to a square instead of a triangle. This allows, in principle, energy storage exceeding $D \cdot E/2$, and approaching $D \cdot E$. Typical charges stored are about 25 $\mu C/cm^2$ at peak fields of 40 to 50 kv/cm. In the presently explored materials, these fields approach breakdown for thick sections. The working voltages are thus limited because it is necessary to use thin pieces (1 to $1\frac{1}{2}$ mm at present). It is expected that continued work will improve the dielectric strength.

*Transducer Properties*

It has been suggested by Dr. R. Gerson and demonstrated by C. P. Germano of this laboratory that the onset of field-enforced ferroelectricity is accompanied by large strain effects parallel to the field. These strains are of the order of $4 \times 10^{-4}$.

The types of electromechanical effects are shown in Fig. 6. Hard antiferroelectrics show quadratic electrostriction, like all other solids. Ferroelectrics, due to domain switching, give the well-known butterfly loops shown. They can be poled and used at remanence to produce a linear piezoelectric response, like piezoelectric crystals. The soft antiferroelectrics produce the abrupt incremental strain shown in the figure. This constitutes a sort of quasi-electrostriction of large magnitude. Samples biased by a dc- or low-frequency field to a point beyond the threshold field respond as a piezoelectric to small signal fields, especially at mechanical resonance. Thus the bias field can act as a controlling or modulating means. It also seems probable that samples can be

World Radio History

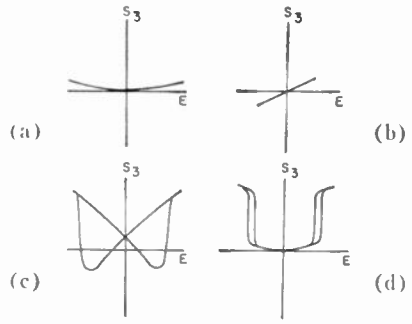


Fig. 6—Strain vs field in (a) electrostriction, (b) piezoelectricity, (c) ferroelectricity, and (d) soft antiferroelectricity.

driven at mechanical resonances by strong signals of half the resonant frequency, but this has not yet been demonstrated.

## Improvements Needed

Like other ceramic dielectrics, these soft antiferroelectrics are subject to breakdown at high fields. This factor most strongly limits their utility. Although it is possible to obtain much lower threshold fields by raising the ferroelectric-to-antiferroelectric transition temperature, the lowest threshold field yet found in a composition antiferroelectric down to $-60°C$ is about 40 kv/cm. Although operation at fields of this strength is tolerable in thin specimens, it is undesirable where high voltage applications are desired, such as in energy storage. It is also desirable to have low threshold fields for the nonlinear capacitor and transducer applications. Here, low-voltage operation is usually desired, and although thin specimens can be used, there is a practical minimum to thickness. This indicates two development objectives: increasing the dielectric strength and finding compositions with lower threshold fields. There is hope that both of these can be improved.

## Conclusion

Soft antiferroelectrics are those capable of field-enforced transitions to a ferroelectric state at fields below breakdown. They show a characteristic double hysteresis loop with a linear central region and a saturated loop on either end. Previous examples of this phenomenon have had limited temperature range. The effect can be produced over a wider temperature range by 1) a polymorphic inversion from ferroelectric-to-antiferroelectric-to-paraelectric states with increasing temperature, and 2) a relatively high dielectric-constant maximum at the antiferroelectric-to-paraelectric inversion temperature. An example of such a dielectric is shown, with the desired type of behavior occurring through the temperature range of below $-50°$ to above 125°C. With fields passing the threshold for the field-enforced transition, the differential (dc) capacitance increases greatly, while the incremental (ac) capacitance drops. Simultaneously, strain of the order of $10^{-4}$ occurs. The shape of the hysteresis loop is favorable for energy storage. Present utility is limited by dielectric strength.

## Acknowledgment

In addition to the contributions of my colleagues mentioned in the text, the help and interest of D. Berlincourt and H. H. A. Krueger, and the careful work of R. Wolfe, Miss M. E. Christopher, F. Brunarski and B. Kost are gratefully acknowledged.

World Radio History

# Large-Signal Circuit Theory for Negative-Resistance Diodes, in Particular Tunnel Diodes*

M. SCHULLER†, MEMBER, IRE, AND W. W. GÄRTNER†, SENIOR MEMBER, IRE

*Summary*—**The large-signal, high-frequency circuit applications of a tunnel diode as an oscillator and as a monostable and bistable switch have been analyzed quantitatively, without any of the customary simplifications, by solving on a computer the system of nonlinear differential equations which describe the diode and the external circuitry. Frequency, amplitude, distortion and switching times are calculated with high accuracy as functions of operating point and circuit inductance. The results are in very good agreement with actual measurements.**

## Introduction

MOST circuit theory is based on a linearization of the characteristic of the component used. Nonlinear theories usually depend either on relatively simple analytical approximations of the component characteristics such as the exponential or square-law characteristics of diodes used in mixing and frequency conversion, etc., or on a piece-wise linearization of the complicated component characteristic, which is commonly used in negative-resistance circuit theory. In practically no case do these approaches yield quantitative answers to such typical large-signal nonlinear problems as the determination of output waveform, harmonic content, large-signal switching time, etc., although they usually give satisfactory results in an analysis of stability.[1,2]

In this paper we propose to develop a large-signal circuit theory for negative-resistance diodes in which the device and its external circuit are characterized by a system of accurate nonlinear differential equations and the solutions are obtained by an electronic computer. This approach is very general and can be applied to any nonlinear electronic device. It is worked out below in detail to describe the large-signal operation of tunnel diodes as oscillators and switches.

## Characterization of the Tunnel Diode

For small-signal applications the tunnel diode is satisfactorily characterized by its differential negative resistance ($-R$), its junction capacitance $C_j$ and series bulk resistance $r_s$, as shown in Fig. 1(a).[3] This equivalent circuit has been employed successfully to derive expressions for the gain, bandwidth, etc., of small-signal tunnel-diode amplifiers, and the cutoff frequency of tunnel-diode oscillators. Linear fourpole equations for the tunnel diode based on this circuit[4] can be used to formulate the entire small-signal circuit theory for tunnel diodes. It is obvious, however, that this small-signal equivalent circuit cannot be used to accurately describe large-signal applications in which the entire range of positive and negative resistances is important, such as large-signal oscillators and monostable and bistable switches. Therefore, the equivalent circuit of Fig. 1(a) was extended. The proposed large-signal equivalent circuit used in this paper consists of a nonlinear current source in parallel to the capacitance of the *p-n* junction and a series resistance presenting the bulk and contact resistances. This circuit is shown in Fig. 1(b). The tunnel phenomenon is very fast and no delay effects are included in the current generator. The junction capacitance represents all the storage mechanisms in this device. The junction capacitance has been chosen to be constant over the whole voltage range. This is a slight simplification because the capacitance of a forward-biased junction depends on the voltage across it. The simplification seems to be justified because the capacitance is much less dependent on the voltage than the junction current in the voltage range of interest, so that the voltage dependence of the capacitance introduces negligible corrections in the cases discussed in this paper.

The generalization of the approach used here for a voltage-dependent junction capacitance is obvious. The series bulk resistance is also considered constant in our analysis because the current densities during operation are not high enough to cause high-injection resistance modulation. Again, this assumption could be easily removed if the need became apparent.

The equations describing the large-signal operation of the tunnel diode are therefore:

$$v_D = v_J + i_D r_s \tag{1}$$

$$i_D = C_j \frac{dv_J}{dt} + i(v_J). \tag{2}$$

Fig. 2 shows the measured dc characteristics $i(v_D)$ of the tunnel diode used in the analysis and the experiments. Because of the small series resistance of $r_s = 0.3$ ohm, in

* Received by the IRE, March 7, 1961; revised manuscript received, April 18, 1961.

† CBS Labs., Stamford, Conn.

[1] W. J. Cunningham, "Introduction to Nonlinear Analysis," McGraw-Hill Book Co., Inc., New York, N. Y., ch. 5; 1958.

[2] B. G. Farley, "Dynamics of transistor negative-resistance circuits," PROC. IRE, vol. 40, pp. 1497–1507; November, 1952.

[3] H. S. Sommers, Jr., "Tunnel diodes as high-frequency devices," PROC. IRE, vol. 47, pp. 1201–1206; July, 1959.

[4] W. W. Gärtner, "Tunneldioden," Elektronische Rundschau, Berlin, Germany, vol. 14, pp. 265–271; July, 1960.

World Radio History

this case, the device voltage $v_D$ and the junction voltage $v_J$ are practically the same for dc. The junction capacitance of 390 pf was measured at the valley point.

## Oscillator

Analyzing the oscillations of negative-resistance elements has long been an electrical engineering problem[1,2] and while it is rather simple to show that a negative resistance with the approximate load will oscillate, it is quite an involved problem to find the exact output waveform of the oscillator. To solve the problem analytically, the characteristic of the negative element must be oversimplified and the results are only in qualitative agreement with the exact solutions. Graphical methods are tedious when accurate solutions must be obtained. Both methods are useful only when a small number of nonlinearities appear in the circuit. The approach used here to obtain an exact answer to the tunnel-diode oscillator problem was to find on a digital computer the exact stable solution to the set of exact nonlinear differential equations which describe the device and circuit.

### *External Circuits*

Since the device itself has an internal capacitance, it is enough to add an external inductance to excite oscillations when the diode is biased in the negative-resistance region. This simplest oscillator circuit, shown in Fig. 3, will be used to illustrate the proposed approach, generalizations to more complicated external circuitry being obvious. The external inductance has been assumed lossless, and any losses can be included simply in the series bulk resistance of the device $r_s$. We are now in a position to write down the entire set of differential equations which describe the oscillator operation:

$$\left.\begin{aligned} v_D &= v_J + i_D \cdot r_s \\ i_D &= C_j \frac{dv_J}{dt} + i(v_J) \end{aligned}\right\} \text{device} \qquad (1), (2)$$

$$v_L = L \frac{di_L}{dt} \text{ external circuit} \qquad (3)$$

$$\left.\begin{aligned} v_D &= v_0 + v_L \\ i_L &= -i_D \end{aligned}\right\} \text{relations connecting device and external circuit.} \qquad (4), (5)$$

The only nonlinearity entering this set of equations is the relation between junction current and voltage in (2). This function has been obtained by measurement and has been plotted in Fig. 2.

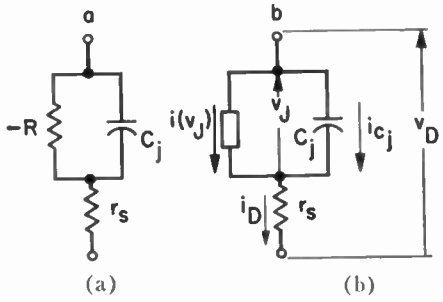


Fig. 1—(a) Small-signal and (b) large-signal equivalent circuits for tunnel diodes.

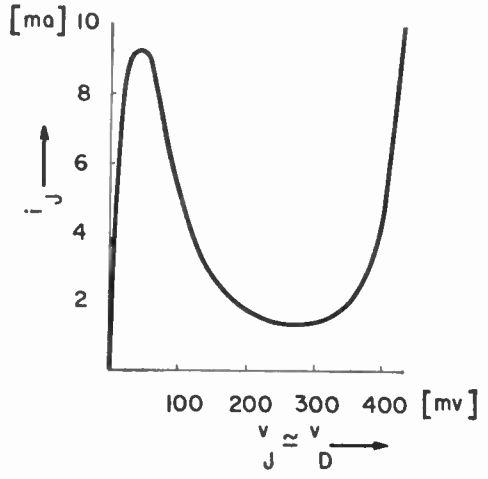


Fig. 2—Measured junction-current vs junction-voltage characteristic of tunnel diode (germanium) used for theory and experiments.

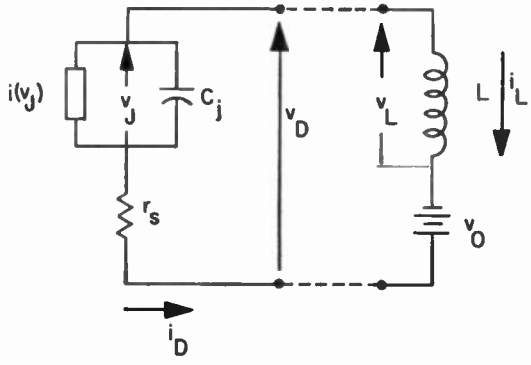


Fig. 3—Tunnel-diode oscillator circuit.

World Radio History

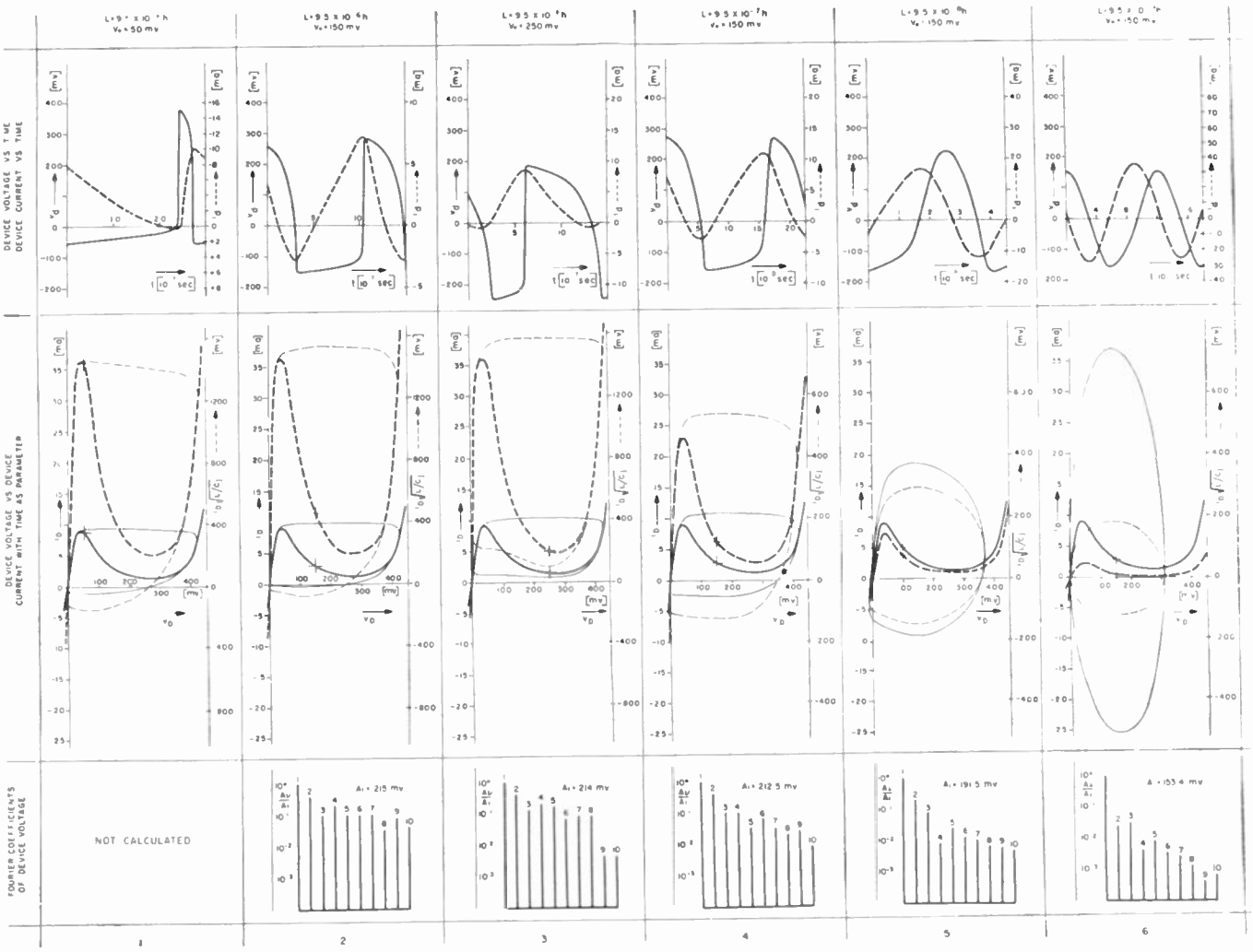


Fig. 4—Upper row: ac device voltage $v_d$ (solid lines) and device current $i_d$ (dashed lines) as functions of time $t$ for six combinations of operating point and external circuit inductance.

Middle row: dc device characteristic (heavy lines) and limit cycle, *i.e.*, instantaneous device current vs device voltage (light lines) for six cases depicted in the upper row. The solid curves compare the limit cycles in the various cases plotted to identical scales. The dashed lines give the same information with each graph normalized so that the limit cycle for a strictly sinusoidal oscillation would appear as a circle.

Lower row: The first ten Fourier coefficients of the device voltage plotted on a logarithmic scale.

*Solution*

This system of differential equations has been solved on a digital computer with starting values chosen in such a way as to get the stable solution within a small number of periods. Fig. 4 shows some of the oscillation patterns achieved for different operating points and external inductances. The first row of graphs represents the ac components of the device current $i_d$, and of the device voltage $v_d$, with the bias point as the origin. The second row shows the device characteristic (heavy) and the limit cycle (light) of the oscillation plotted in the $i_D$-$v_D$ plane (solid) and in the transformed ($i_D\sqrt{L/C_j}$)-$v_D$ plane (dashed). The latter transformation has been chosen because in this plane the limit cycle for a sinusoidal oscillation will appear as a circle and any deviation from the circular pattern indicates harmonic content. The third row shows the Fourier analysis of the device-voltage $v_d$.

The photographs of oscilloscope traces given in Fig. 5 were obtained from an actual circuit using a diode with the characteristic of Fig. 2 and employing the operating points and external inductance given in the first three columns of Fig. 4. One observes excellent agreement with the theoretical predictions.

Various qualitative features of the output waveform and the limit cycle may be illustrated by Fig. 4. When the external inductance $L$ is rather large as in the first three columns of Fig. 4, the limit cycle (second row in Fig. 4) consists of the positive branches of the dc-device characteristic and almost straight lines through the peak and valley points, parallel to the current axis. These parallel lines correspond to very rapid changes in device voltage. Whereas this limit cycle pattern is relatively independent of the operating point, one observes that the latter has a pronounced influence on the output waveform (period, amplitude, and harmonic con-

World Radio History

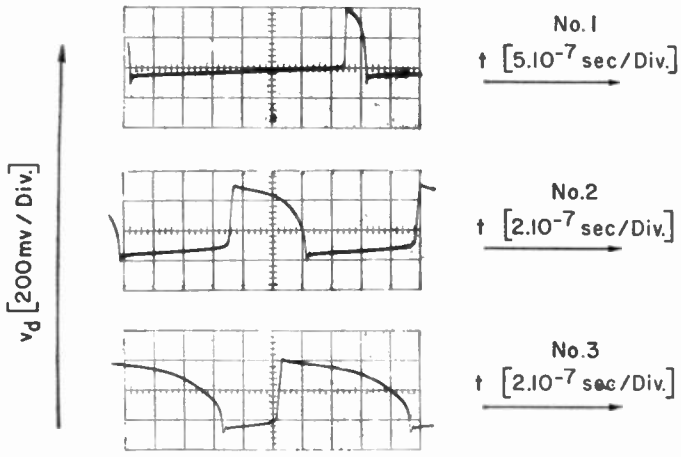


Fig. 5—Photographs of oscilloscope traces showing device voltage vs time obtained in the circuit of Fig. 3 using a diode with the characteristic of Fig. 2. Operating points and external circuit inductance are as follows:

| Curve No. | $V_0[m_v]$ | $L[h]$ |
|---|---|---|
| 1 | 50 | $9.5\times10^{-6}$ |
| 2 | 150 | $9.5\times10^{-6}$ |
| 3 | 250 | $9.5\times10^{-6}$ |

tent). This applies in particular, also, to the dc component of the output current which modifies the assumed operating point. For small bias voltages the dc component of the device current is negative; for large bias voltages it is positive.

The following table gives this dc component for the six cases shown in Fig. 4:

| Column in Fig. 4 | 1 | 2 | 3 | 4 | 5 | 6 |
|---|---|---|---|---|---|---|
| DC Component of Output Current in ma | −3.70 | 2.34 | 3.24 | 3.96 | 2.66 | 1.80 |

Incidentally, the output voltage across the device has no dc component because of (3) and (4). This shifting of the operating point for oscillating tunnel diodes is a well-known fact and can be observed frequently on oscilloscope traces displaying the characteristic of the tunnel diode.[5] This shift in bias current depends also on the external inductance, as can be seen in the last three columns of Fig. 4, where for the same bias voltage the external inductance has been decreased. The oscillation becomes more and more sinusoidal, the smaller the inductance. This is in keeping with the observation that for $L$ approaching a limiting value $L_{min}$ (see next section) the limit cycle in the $(i_D\sqrt{L/C_j})$-$v_D$ plane becomes a circle with decreasing radius. The Fourier coefficients of the higher harmonics also decrease with decreasing inductance.

[5] R. Trambarulo and C. A. Burrus, "Esaki diode oscillators from 3 to 40 kMc, PROC. IRE, vol. 48, pp. 1776–1777; October, 1960.

*Analytical Approximation*

While it is impossible to give an exact analytical solution for the general tunnel diode oscillator, one may obtain a certain amount of qualitative information when the device characteristic is replaced by a simple three-order polynomial. Under this assumption one may calculate how the amplitude of oscillation changes with external inductance (or frequency) and how much the frequency of oscillation differs from the pure sine-wave frequency, calculated for the $LC$-resonant tank circuit.

Combining (1) through (5) one obtains the following ordinary differential equation for the junction voltage $v_J$.

$$LC_j\frac{d^2v_J}{dt^2}+\left(r_sC_j+L\frac{di}{dv_J}\right)\frac{dv_J}{dt}+r_si_J(v_J)+v_J-v_0=0. \quad (6)$$

Separating dc and ac voltages,

$$v_J=v_j(t)+v_0 \quad (7)$$

leads to an equation for the ac junction voltage only:

$$LC_j\frac{d^2v_j}{dt^2}+\left(r_sC_j+L\frac{di}{dv_j}\right)\frac{dv_j}{dt}+r_si_j(v_j)+v_j=0 \quad (8)$$

where

$$i_j(v_j)=i_J(v_j+v_0). \quad (9)$$

For the functional dependence of $i_j$ on $v_j$ we now assume a simple third-order polynomial of the form

$$i_j=(g/v_0^2)v_j(v_j^2-v_0^2). \quad (10)$$

Eq. (10) has been plotted in Fig. 6 explaining the meaning of the parameters $g$ and $v_0$. With (10), (8) can be transformed into

$$\frac{d^2v}{d\tau^2}+\nu(v^2-1)\frac{dv}{d\tau}+v\left\{1-gr_s+\frac{r_sv^2}{3}\left(g-r_s\frac{C_j}{L}\right)\right\}=0 \quad (11)$$

where

$$v=\frac{v_j}{v_0}\sqrt{\frac{3Lg}{Lg-r_sC_j}} \quad (12)$$

$$\tau=\frac{t}{\sqrt{LC_j}} \quad (13)$$

and

$$\nu=\sqrt{\frac{L}{C_j}}\left(g-r_s\frac{C_j}{L}\right). \quad (14)$$

World Radio History

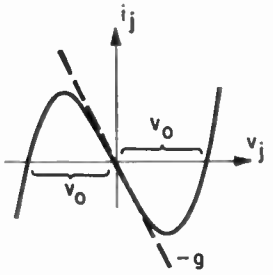


Fig. 6—Symmetrical dc characteristic used for the analysis of tunnel-diode oscillator.

With the device characteristics fixed, the only free parameter in (11) is the external inductance $L$. One may now ask how the external inductance affects the amplitude and frequency of oscillation. From (12) one concludes that there exists a minimum value for $L$,

$$L_{\min} = \frac{r_s C_j}{g} \tag{15}$$

where $v_j = 0$.

For values of $L$ close to this minimum value $L_{\min}$, (11) reduces to the equation of a sine wave oscillation:

$$\frac{d^2v}{d\tau^2} + v(1 - gr_s) = 0. \tag{16}$$

If $\tau$ in (16) is replaced by $t$ according to (13), the frequency of this sine wave oscillation can be calculated to be

$$f = \frac{\sqrt{1 - gr_s}}{2\pi\sqrt{LC_j}}. \tag{17}$$

Taking into consideration that $L$ can be replaced by $L_{\min}$ according to (15), we obtain the well-known maximum cutoff frequency ($f_{\max}$) of a tunnel-diode oscillator:

$$f_{\max} = \frac{1}{2\pi C_j}\sqrt{\frac{g(1 - r_s g)}{r_s}}. \tag{18}$$

For inductance values $L > L_{\min}$, one must go back to the exact equation (11). Assuming that $r_s$ is zero, one finds

$$\frac{d^2v}{d\tau^2} + \nu(v^2 - 1)\frac{dv}{d\tau} + v = 0. \tag{19}$$

This is the well-known van der Pol equation.[1]

The steady-state solution of this equation shows[6] that the period depends strongly on the parameter $\nu$ (Fig. 7, solid) but that the steady-state amplitude is practically constant and equal to unity (Fig. 7, dashed). One may use this solution of the van der Pol equation as an approximate solution of (11) provided that $gr_s \ll 1$ because then the correction term

$$gr_s - \frac{r_s v^2}{3}\left(g - r\frac{C_j}{L}\right) \leqq gr_s$$

in (11), will be negligible for all values of $L$. The condition that $gr_s \ll 1$ is usually well fulfilled in tunnel diodes. For the diode used in our exact solution, $gr_s$ had a value equal to 0.03.

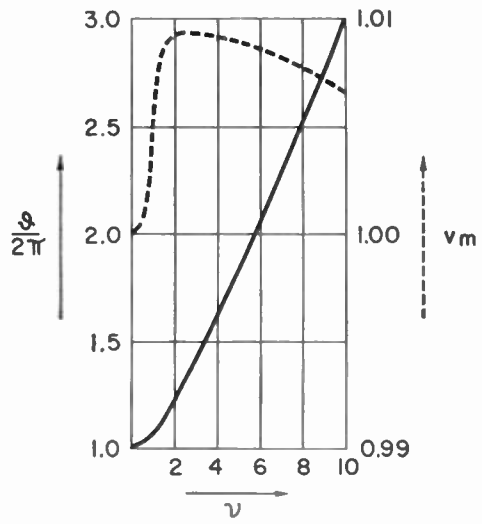


Fig. 7—Period $\theta$ (solid) and amplitude $v_m$ (dashed) of the solution of van der Pol equation as function of the parameter $\nu$.

Using (12) and (14), one may therefore transform the solutions of the van der Pol equation in Fig. 7 into solutions of (11) for the steady-state amplitude and frequency of the ac tunnel-diode junction voltage $v_j$. Since the amplitude of $v$ is approximately unity one finds from (12) the following dependence of the amplitude of $v_j$ on the inductance $L$:

$$v_{jm} = v_0\sqrt{\frac{Lg - r_s C_j}{3Lg}}. \tag{20}$$

For small values of $gr_s \ll 1$ the amplitude of $v_d$ follows the same dependence, which has been plotted in Fig. 8(a) for various values of $g$.

The period of oscillation $\theta$ depends on $\nu$ as shown in Fig. 7 (solid). Analytical expressions have been derived[6] for small $\nu$ ($\nu < 2.5$) and large $\nu$ ($\nu \geqq 6$):

$$\theta = 2\pi\left(1 + \frac{\nu^2}{16} - \frac{5\nu^4}{3072} + \cdots\right) \quad \text{for } \nu < 2.5 \tag{21}$$

$$\theta = 1.6137\nu + 7.0143\nu^{-1/3} - \frac{22}{9}\frac{\ln \nu}{\nu} + \cdots \text{ for } \nu > 6. \tag{22}$$

Between these ranges, the period can be interpolated. Remembering that the relation of normalized time ($\tau$) to actual time ($t$) is given by (13), we find the actual period of oscillation ($T$) from the normalized ($\theta$) by

$$T = \theta\sqrt{LC_j}. \tag{23}$$

[6] E. Fisher, "The period and amplitude of the van der Pol limit cycle," *J. Appl. Phys.*, vol. 25, pp. 273–274; March, 1954.

World Radio History

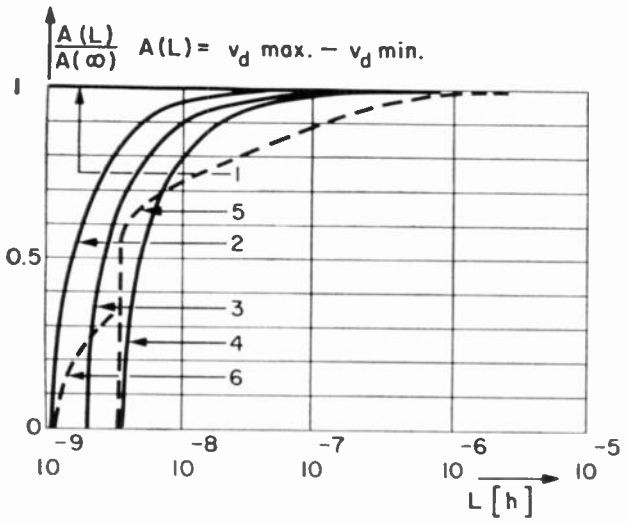


(a)

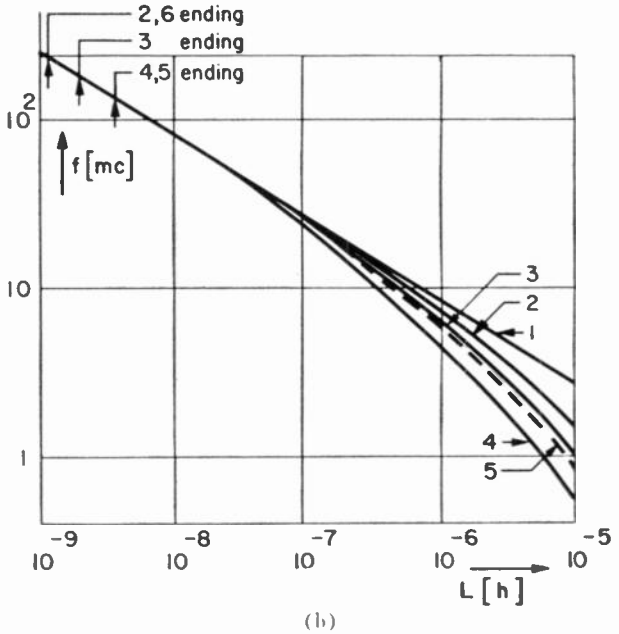


(b)

$C_j = 3.9 \times 10^{-10} f$

| Nº | | 1 | 2 | 3 | 4 | | | 5 | 6 |
|---|---|---|---|---|---|---|---|---|---|
| $r_s$ | ohm | 0 | 0.3 | 0.3 | 0.3 | $r_s$ | ohm | 0.3 | 0.3 |
| g | mho | 0 | 0.1 | 0.0326 | 0.06 | $V_0$ | mv | 150 | 75 |
| | | Analysis | | | | | | Computer | |

Fig. 8—(a) Normalized amplitude and (b) frequency of tunnel-diode oscillator as a function of circuit inductance $L$, for analytical approximation (solid line) and for exact computer solution (dashed lines). Parameter: $g$, $r_s$, and $V_0$.

Since $\theta$ is a function of $\nu$ and $\nu$ according to (14) is a function of inductance $L$, $T$ is a function of $L$. The frequency $f$ (by definition $1/T$), therefore, is also a function of inductance. This dependence of frequency on inductance $L$ has been plotted in Fig. 8(b) for different values of $g$. The results of the computer calculations have been plotted in the same figure. For the extreme cases of small and large inductances the following analytical expressions for the frequency can be derived:

$L \approx L_{min}$:

$$f \approx \left\{2\pi\sqrt{LC_j}\left[1 + \frac{1}{16}\frac{L}{C_j}\left(g - r_s\frac{C_j}{L}\right)\right]\right\}^{-1} \tag{24}$$

$L$ large:

$$f \approx (1.6137gL)^{-1}. \tag{25}$$

The results obtained from the analytical approximation as compared to those from the exact computer solution show that the frequency of oscillation can be predicted reasonably well except for large values of $L$. There is, however, a considerable difference between the amplitudes predicted by the approximate treatment and their exact values. An interesting feature which is absent from the analytical approximation occurs in the actual oscillator when it is not biased into the point of steepest negative slope. While for the analytical solution the amplitude of oscillation is decreasing steadily to zero for increasing inductances, the amplitude of the actual oscillator may collapse from a finite value when a certain inductance value is reached. This phenomenon has not been completely explained but the reason seems to be that when the device is not biased at the voltage with the highest negative slope, there exist two limit cycles, a smaller and a bigger one. The small limit cycle is determined mainly by the negative slope at the bias point while the bigger limit cycle is determined by the average negative slope which is higher than the slope in the bias point. The cutoff frequencies of these two limit cycles do not seem to be the same. Thus, for the same inductance, two oscillations with different amplitudes may exist. Whether the large or the small amplitude is excited depends on whether the oscillation is started close to the bias point or reasonably far away. Suitable pulses could switch the circuit from one mode of oscillation to the other.

Fig. 9 shows this situation for the bias point $V_0 = 150$ mv and an inductance value of $3.5 \times 10^{-9}$ h. While the inner curve 1 is decreasing to zero, there exists a finite

World Radio History

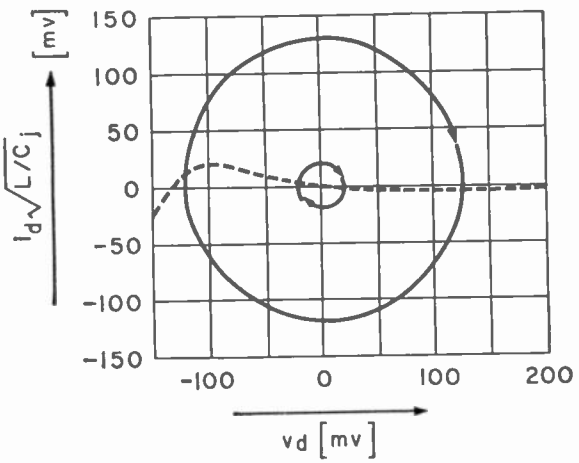


Fig. 9—Two different limit cycles for one inductance value. $V_0=150$ mv, $L=3.5\times10^{-9}$ h.

limit cycle 2 which is stable. When the device is biased at the voltage with the highest negative slope, the amplitude is decreasing steadily to zero with decreasing inductance, as in the analytical case [curve no. 6 in Fig. 8(a)].

## Monostable Switch

### *External Circuit*

To use the tunnel diode as a monostable switch, the same circuit as for the oscillator can be used. The only difference between the two cases is that for the monostable switch the device must be biased in the positive-resistance region.

### *Trigger Pulse*

When biased in the positive region the device is stable. To achieve switching action it must be triggered. To avoid an interaction between trigger and switching pulses in our calculations, the trigger pulse has been assumed to be much faster than the resulting switching pulse. Mathematically this is achieved by giving only a starting value in the differential equation.

### *Solution*

Fig. 10 (p. 1276) shows some of the switching plots achieved for different operating points, trigger pulses and external inductances. Column 1 in Fig. 10 shows the trigger output when the device is biased close to the peak point. The inductance has a medium value. For very large inductance values the trace would jump to the opposite positive branch of the device immediately after triggering, in the same way as in the oscillator. For smaller external inductance values (column 2 in Fig. 10) the switching trace changes similar to the oscillator pattern, *i.e.*, the peak current increases and the voltage swing decreases. Column 3 shows the switching plots when the device is biased close to the valley point. Comparing columns 1 and 3, one notices that when the device is biased near the peak point, much smaller trigger pulses suffice to produce large output signals. Therefore, when the monostable switch is used as pulse amplifier, an operating point close to the peak gives highest gains. Column 3 also shows that the output amplitude can be very sensitive to the amplitude of the trigger pulse. A small change in trigger pulse (curves A and B) results in a large change of output waveform.

## Bistable Switch

### *External Circuit*

Fig. 11(a) shows the circuit used to analyze the bistable switch. The only addition to the oscillator and monostable switching circuit is the load resistance $r_L$.

It follows from this figure that a set of differential equations for the bistable switching circuit can be derived from (1)–(5) if one replaces $r_s$ by $r_s+r_L$:

$$\frac{dv_J}{dt}=\frac{1}{C_j}\left[i_D-i(v_J)\right] \tag{26a}$$

$$\frac{di_D}{dt}=\frac{1}{L}\left[v_0-v_J-i_D(r_s+r_L)\right]. \tag{26b}$$

The load resistance and the bias voltage are adjusted to produce three intersections with the device characteristic, as shown in Fig. 11(b). In general, two of the points of intersection (1, 2) are stable and one is unstable (3).

### *Solution*

Fig. 12 shows the forward and backward switching of the bistable circuit for different trigger pulses and inductances. Column 1 illustrates the case where the circuit is triggered from the high-current, low-voltage state (stable point 1) to the low-current, high-voltage state (stable point 2). The circuit will switch to point 2 only when the trigger pulse is larger than a certain critical amplitude (curves A and B). For trigger amplitudes below this level the device will go back to stable point 1 (curve C). The same is true for back-triggering from 2 to 1 (column 2 in Fig. 12). For the special load resistance and bias point considered here, the back-trigger pulse must be much larger than the forward-trigger pulse. This feature of the bistable circuit results from the fact that there exists a characteristic curve in the device current and device voltage plane (called separatrix) which separates all switching paths into two categories, one ending at stable point 1 [Fig. 11(b)] and the other at stable point 2. To trigger the circuit from one stable state to the other, it is necessary that the trigger pulse bring the device voltage and current beyond the separatrix. Otherwise, the circuit will return to the respective starting point. Column 3 in Fig. 12 gives the forward-triggering case for small inductances. It is interesting to note that after an initial drop in current the trace follows the load lines closely. Comparing columns 1 and 3, one also observes that the critical trigger amplitude depends on the external inductance.

World Radio History

*Analysis*

Some of the characteristic features of the bistable operation of the tunnel diode shall be explained by the following approximate calculations. We propose to show: 1) how the separatrix, which gives the minimum trigger amplitude for positive switching, can be calculated, when the device characteristic is approximated by straight lines; 2) how the device characteristic and the load line limit the switching speed of the tunnel diode in fast bistable operation.

1) When the device characteristic is approximated by a straight line through the unstable point 3 in Fig. 11(b) with a slope equal to that of the actual characteristic at this point, then the separatrix will also be a straight line through point 3. Its slope may be determined by the following argument.

Transforming (25a) and (26b) such that the unstable point is at the origin and replacing the device characteristic $i(v_J)$ by a straight line with slope $(i/r_d)$, and then dividing (25a) by (26b) one gets

$$\frac{di_D}{dv_J} = \frac{di_d}{dv_j} = \frac{C_j}{L} \frac{[-v_j - i_d(r_s + r_L)]}{\left[i_d - \frac{1}{r_d} v_j\right]}. \tag{27}$$

Substituting in (27),

$$\frac{di_d}{dv_j} = \frac{i_d}{v_j} = m, \tag{28}$$

we find the slopes of the solution curves for this differential equation through the unstable point

$$m_{1,2} = \frac{1}{2}\left[\frac{1}{r_d} - \frac{r_s + r_L}{L} C_j \pm \sqrt{\left(-\frac{r_s + r_L}{L} C_j + \frac{1}{r_d}\right)^2 - \frac{4C_j}{L}}\right]. \tag{29}$$

For large values of $L$, $m$ simplifies to

$$m_{1\infty} = \frac{1}{r_d} \tag{30}$$

$$m_{2\infty} = 0 \tag{31}$$

and for small $L$ values one finds

$$m_{10} = -\frac{r_s + r_L}{L} \cdot C_j \tag{32}$$

$$m_{20} = -\frac{1}{r_s + r_L}. \tag{33}$$

These extreme cases are plotted in Fig. 13 (p. 1278).

The separatrices for all other values of $L$ lie in the shaded area between $m_{10}$ and $m_{1\infty}$. Comparing this result with the actual calculated trigger pulses in Fig. 12 one observes that for the forward-trigger pulse (columns 1 and 3) there is good agreement with the approximate calculations. The backward-trigger pulse, however, is not predicted well enough because in this case the straight line approximation for the separatrix is too inaccurate.

2) For small values of $L$ the switching path and time can be predicted very well. When triggered beyond the separatrix the current will decrease very fast with the voltage constant until it hits the load line. Then it follows the load line until it settles at the stable point 2. Because this first drop in current at constant voltage is very fast, the switching time $T$ is given by (25a) with $i_D = i_{DL}$ and $v_J \approx v_D$.

$$T = C_j \int_{v_{D0}}^{v_{D1}} \frac{dv_D}{i_{DL} - i(v_D)}. \tag{34}$$

Fig. 14 explains the symbols used in (34). From (34) the switching times for different trigger pulses have been determined by graphical integration using the device and load resistance employed in the computations (Fig. 12, Column 1). The upper limit in the integration has been chosen 10 mv below the stable point. Fig. 15 shows the results of these approximate calculations in comparison with the results obtained by the computer, solving the exact differential equations for different starting values. The agreement is reasonable.

From (34) and Fig. 14, one may conclude what tunnel-diode characteristics are desirable for very fast bistable operation:

1) $C_j$ small,
2) peak current large,
3) peak current to valley current ratio high.

## Conclusion

The preceding discussion tried to show how a computer can be used successfully to solve nonlinear circuit problems quantitatively. We only gave a very small selection of the problems which could be attacked in this way. This approach could be extended readily to such nonlinear problems as diode mixers, parametric amplifiers, distortion of low-frequency transistor oscillators and so on. All these problems have in common that the device and circuit can be described by nonlinear dc quantities and capacitances leading to a set of nonlinear but ordinary differential equations. A drastic extension of this approach must be made, when storage effects and time delays due to diffusion become important. A feasible approach to these more complicated problems would be to start with the nonlinear time-dependent transport equations in the different regions of the active semiconductor device and combine them into a set of nonlinear partial differential equations, in which arbitrary constants and functions are determined by measurements on the finished device.

World Radio History

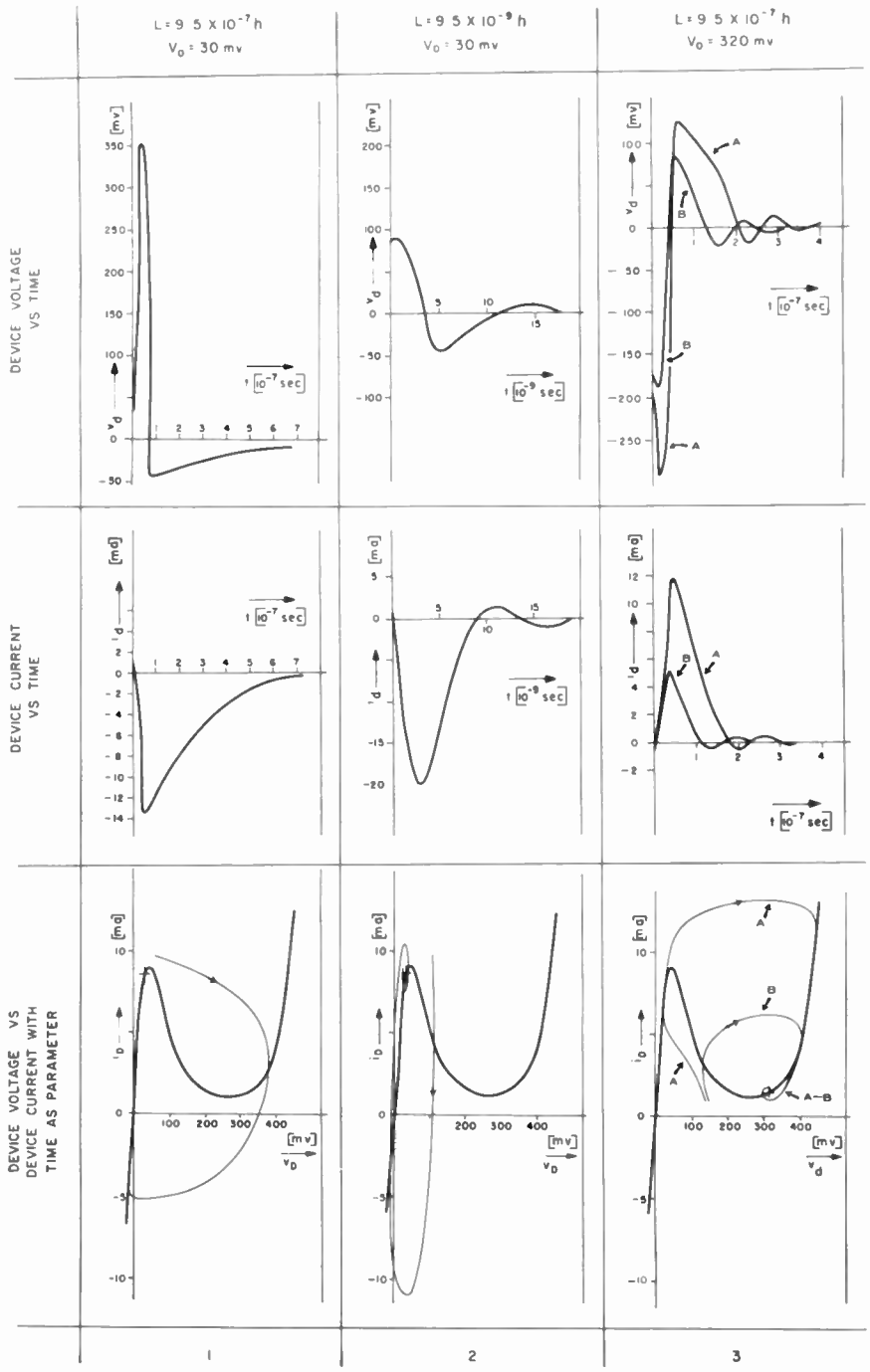


Fig. 10—Monostable switch.
Upper row: ac device voltage $v_d$ as a function of time for three combinations of operating point and external inductance.
The third column shows the output patterns for two different trigger pulse amplitudes ($A$, $B$).

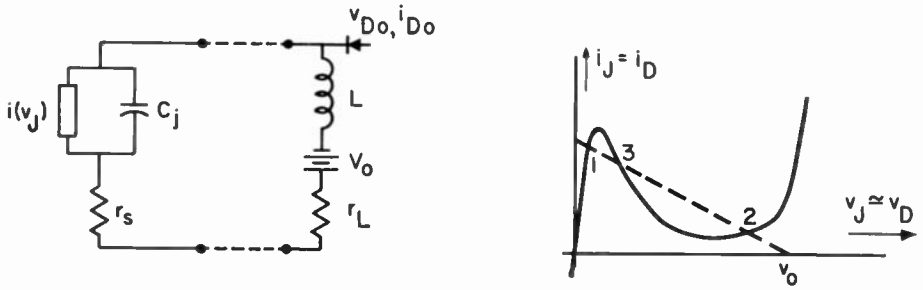


Fig. 11—(a) Circuit and (b) position of load line for operation of the tunnel diode as a bistable switch.

World Radio History

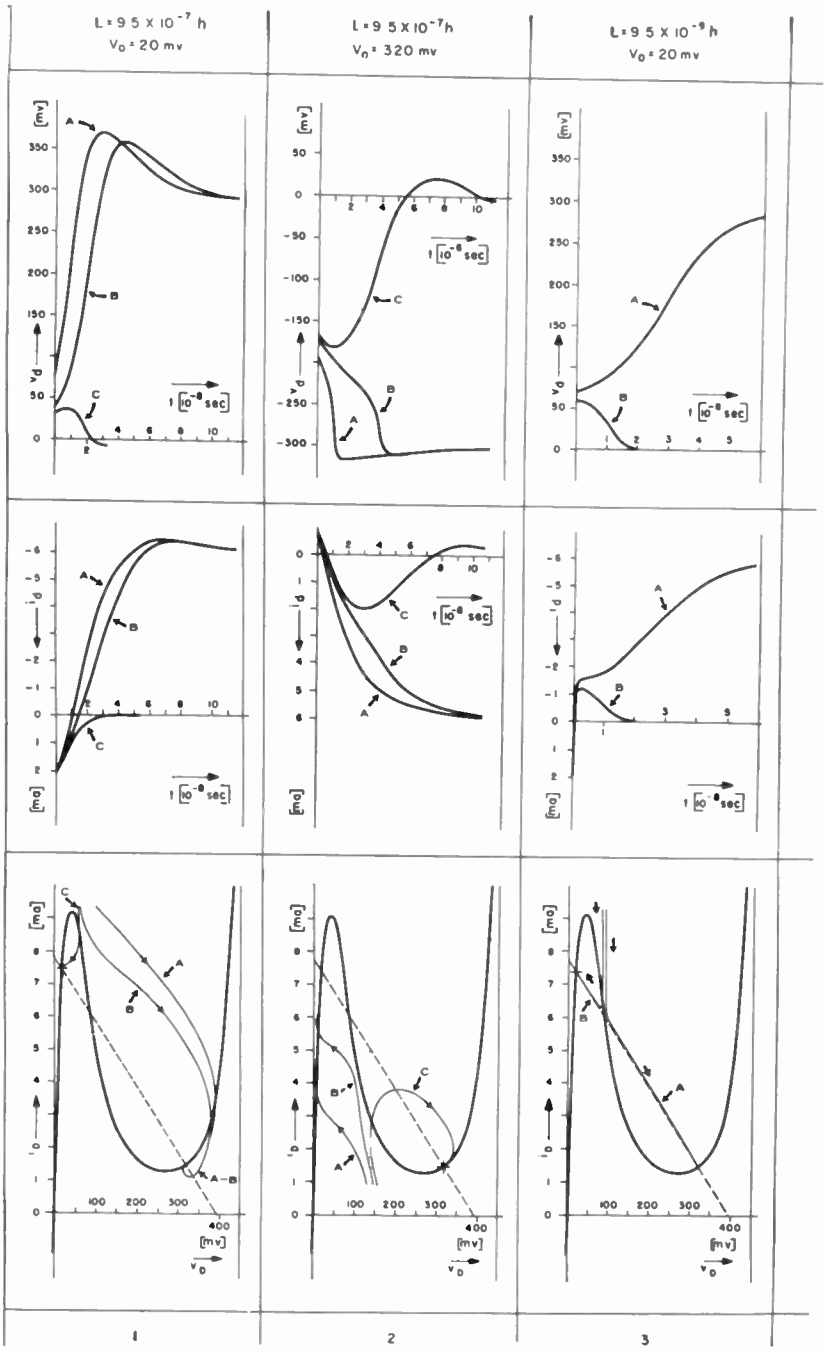


Fig. 12—Bistable switch

Upper row: ac device voltage $v_d$ as a function of time for three combinations of operating point and external inductance under different trigger conditions.

Middle row: ac device current $i_d$ as a function of time for different cases depicted in the upper row.

Lower row: dc device characteristic (heavy lines) and switching path, *i.e.*, instantaneous device current vs device voltage (light lines) for the cases depicted in the upper two rows.

World Radio History

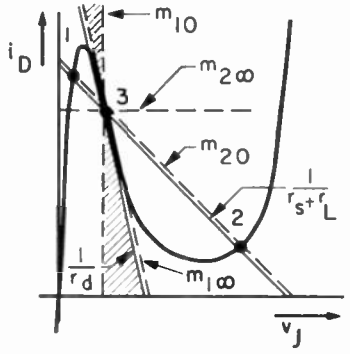


Fig. 13—Solutions of differential equations for bistable circuit in vicinity of the unstable point 3, when the nonlinear device characteristic in 3 is replaced by the tangent through this point. Cases shown are for large and small inductances.

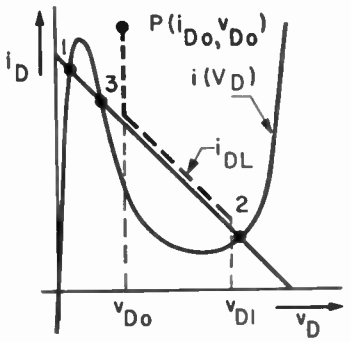


Fig. 14—Bistable swtiching path for small inductance (heavy dashed line), which can be used to calculate the switching time $T$ for fast switching.

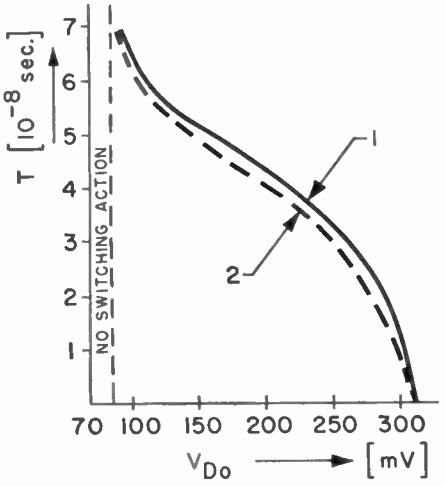


Fig. 15—Switching time of fast bistable switch vs trigger voltage. Curve no. 1 (solid) shows the results obtained by computer, solving the exact differential equations for different starting values, and curve no. 2 (dashed) the approximate results of graphically integrating (34). The bias point and the load line are the same as for Fig. 12, Column 1.

## Acknowledgment

The authors would like to thank J. B. Herder from the U. S. Army Research and Development Laboratory of Fort Monmouth, N. J., for carrying out all the computer calculations.

World Radio History

# IRE Standards on Solid-State Devices: Definitions of Terms for Nonlinear Capacitors, 1961*

61 IRE 28. S1

## COMMITTEE PERSONNEL

### Task Group on Nonlinear Capacitor Definitions

1956–1960

E. A. Sack, *Chairman* 1956–1958
P. N. Wolfe, *Chairman* 1958–1960

T. W. Butler
H. Diamond
R. A. Fotland
N. R. Kornfield
E. E. Loebner
E. F. Mayer
C. F. Pulvari
C. F. Spitzer
S. W. Tehon

### Subcommittee on Dielectric Devices

1955–1960

C. A. Rosen, *Chairman* (IRE) 1955–1957
H. Epstein, *Chairman* (AIEE) 1955–1958
E. E. Loebner, *Chairman* (IRE) 1957–1960
F. A. Schwertz, *Chairman* (AIEE) 1958–1960
P. N. Wolfe, *Chairman* (IRE) 1960

J. H. Armstrong
R. E. Benn
W. Bixby
W. D. Bolton
J. Bramley
R. B. DeLano, Jr.
H. Diamond
D. P. Faulk
L. A. Finzi
W. Gardner
R. Gerson
R. B. Gray
F. P. Hall
R. E. Halsted
S. R. Hoh
H. F. Ivey
B. Jaffee
N. R. Kornfield
E. F. Mayer
G. R. Mott
A. Myerhoff
H. I. Oshry
C. F. Pulvari
J. R. Roeder
N. Rudnick
E. A. Sack
R. M. Schaffert
E. Schwenzfeger
F. A. Schwertz
G. Shaw
A. C. Sheckler
B. R. Shepard
C. F. Spitzer
L. A. Walkup

### Solid-State Devices Committee

1959–1961

R. L. Pritchard, *Chairman* 1959–1961
R. H. Rediker, *Vice Chairman* 1960–1961
E. O. Johnson, *Vice Chairman* 1959–1960
V. P. Mathis, *Secretary* 1959–1961

J. B. Angell
S. J. Angello
J. S. Blakemore
A. Coblenz
L. Davis, Jr.
W. C. Dunlap, Jr.
J. M. Early
H. J. Evans
P. A. Fleming
J. R. Hyneman
B. K. Kazan
N. R. Kornfield
A. W. Lampe
E. E. Loebner
J. R. Roeder
B. J. Rothlein
S. Sherr
A. E. Slade
B. N. Slade
M. E. Talaat
R. W. Ure, Jr.
W. M. Webster
P. N. Wolfe

* Approved by the IRE Standards Committee, December 8, 1960. Reprints of this Standard 60 IRE 13. S1, may be purchased while available from the Institute of Radio Engineers, 1 East 79 Street, New York, N. Y., at $0.25 per copy. A 20 per cent discount will be allowed for 100 or more copies mailed to one address.

World Radio History

**Standards Committee**

**1960 1961**

C. H. Page, *Chairman*
J. G. Kreer, Jr., *Vice Chairman*
H. R. Mimno, *Vice Chairman*
L. G. Cumming, *Vice Chairman*

J. H. Armstrong
J. Avins
G. S. Axelby
M. W. Baldwin, Jr.
W. R. Bennett
J. G. Brainerd
A. G. Clavier
S. Doba, Jr.
R. D. Elbourn
G. A. Espersen
R. J. Farber
D. G. Fink
G. L. Fredendall
E. A. Gerber
A. B. Glenn
V. M. Graham
R. A. Hackbusch
R. T. Haviland
A. G. Jensen
R. W. Johnston
I. Kerkey
E. R. Kretzmer
W. Mason
D. E. Maxwell
R. L. McFarlan
P. Mertz
H. I. Metz
E. Mittelmann
L. H. Montgomery, Jr.
S. M. Morrison
G. A. Morton
R. C. Moyer
J. H. Mulligan, Jr.
A. A. Oliner
M. L. Phillips
R. L. Pritchard
P. A. Redhead
C. M. Ryerson
G. A. Schupp, Jr.
R. Serrell
W. A. Shipman
H. R. Terhune
E. Weber
J. W. Wentworth
W. T. Wintringham

**Definitions Coordinator**

H. R. Mimno

**Alternating Charge Characteristic.** The function relating the instantaneous values of the alternating component of *transferred charge*, in a steady state, to the corresponding instantaneous values of a specified applied periodic *capacitor voltage*.

*Note:* The nature of this characteristic may depend upon the nature of the applied voltage.

**Capacitance Ratio.** The ratio of maximum to minimum capacitance over a specified voltage range, as determined from a capacitance characteristic, such as a *differential capacitance characteristic*, or a *reversible capacitance characteristic*.

**Capacitor Voltage.** The voltage across two terminals of a capacitor.

**Differential Capacitance.** The derivative with respect to voltage of a charge characteristic, such as an *alternating charge characteristic* or a *mean charge characteristic*, at a given point on the characteristic.

**Differential Capacitance Characteristic.** The function relating *differential capacitance* to voltage.

**Ideal Capacitor.** A capacitor whose *transferred charge characteristic* is single-valued.

**Initial Differential Capacitance.** *Differential capacitance* at zero *capacitor voltage*.

**Initial Reversible Capacitance.** *Reversible capacitance* at a constant bias voltage of zero.

**Mean Charge.** The arithmetic mean of the *transferred charges* corresponding to a particular *capacitor voltage*, as determined from a specified *alternating charge characteristic*.

**Mean Charge Characteristic.** The function relating *mean charge* to *capacitor voltage*.

*Note: Mean charge characteristic* is always single-valued.

**Nonlinear Capacitor.** A capacitor having a *mean charge characteristic* or a *peak charge characteristic* that is not linear, or a *reversible capacitance* that varies with bias voltage.

**Nonlinear Ideal Capacitor.** An *ideal capacitor* whose *transferred charge characteristic* is not linear.

**Peak Charge Characteristic.** The function relating one half the peak-to-peak value of *transferred charge* in the steady state, to one half the peak-to-peak value of a specified applied symmetrical alternating *capacitor voltage*.

*Note: Peak charge characteristic* is always single-valued.

**Reversible Capacitance.** The limit, as the amplitude of an applied sinusoidal *capacitor voltage* approaches zero, of the ratio of the amplitude of the resulting in-phase fundamental-frequency component of *transferred charge* to the amplitude of the applied voltage, for a given constant bias voltage superimposed on the sinusoidal voltage.

**Reversible Capacitance Characteristic.** The function relating the *reversible capacitance* to the bias voltage.

**Transferred Charge (Capacitor).** The net electric charge transferred from one terminal of a capacitor to another via an external circuit.

**Transferred Charge Characteristic.** The function relating *transferred charge* to *capacitor voltage*.

**Voltage Coefficient of Capacitance.** The derivative with respect to voltage of a capacitance characteristic, such as a *differential capacitance characteristic* or a *reversible capacitance characteristic*, at a point, divided by the capacitance at that point.

**Voltage Sensitivity (Nonlinear Capacitor).** See *Voltage Coefficient of Capacitance*.

World Radio History

# Self-Oscillation in a Transmission Line with a Tunnel Diode*

J. NAGUMO†, MEMBER, IRE, AND M. SHIMURA†

*Summary*—Self-oscillation is observed in a transmission line with a tunnel diode on one end. The voltage waveform across and the current waveform through the tunnel diode are, in general, pulse form or stair-case form. This paper discusses the theoretical analysis of the circuit, and also presents the experimental results, which are in good agreement with the analysis.

This circuit can be used as a pulse or staircase wave generator, pulse-frequency modulator with discontinuous levels, analog-digital converter, etc. It is simple in construction, requires little source power, and has a wide frequency range (*e.g.*, $\mu$sec ~ m$\mu$sec).

## I. Introduction

SELF-OSCILLATION is usually a problem associated with lumped constant systems. In this paper, self-oscillation in a distributed constant system is discussed.

In general, self-oscillation in a distributed constant system is described by a nonlinear partial differential equation, but it may also occur in a distributed constant system described by a linear partial differential equation (wave equation) and a nonlinear boundary condition.

Witt has considered the self-oscillation occurring in a string of a violin (the self-oscillation of the latter type), and has developed an elegant method of analysis.[1] Following this method, we have discussed the self-oscillation in a transmission line with a negative resistance element, *e.g.*, tunnel diode, *p-n-p-n* diode and others.

## II. Circuit and Fundamental Equation

A transmission line with the tunnel diode is shown in Fig. 1. In the following analysis, it is assumed that there are no losses in the line. The relation of the voltage $v$ and the current $i$ in the line becomes

$$\frac{\partial v}{\partial x} = -L\frac{\partial i}{\partial t}, \qquad \frac{\partial i}{\partial x} = -C\frac{\partial v}{\partial t}. \tag{1}$$

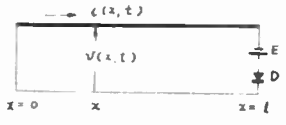


Fig. 1—Fundamental circuit of the tunnel diode connected to a transmission line.

where $L$ is the series inductance, and $C$ is the parallel capacitance per unit length of the line. Accordingly, eliminating $i$ (or $v$),

$$\frac{\partial^2 v}{\partial x^2} = LC\frac{\partial^2 v}{\partial t^2} \qquad \left(\frac{\partial^2 i}{\partial x^2} = LC\frac{\partial^2 i}{\partial t^2}\right). \tag{2}$$

As the line is shorted at $x=0$ and connected with the tunnel diode at $x=l$, boundary conditions are

$$v(0, t) = 0 \tag{3}$$

$$i(l, t) = f(v(l, t) + E), \tag{4}$$

where $E$ is the dc bias voltage, and $I=f(V)$ is the expression representing the characteristic curve of the tunnel diode.

It is assumed that the voltage along the line at $t=0$ is $\alpha(x)$ and the current is $\beta(x)$. Therefore, the initial conditions may be written as follows:

$$v(x, 0) = \alpha(x) \qquad (0 < x < l), \tag{5}$$

$$i(x, 0) = \beta(x) \qquad (0 < x < l), \tag{6}$$

where $\alpha(0)=0$.

The d'Alembert's solution of (2) is of the form

$$v(x, t) = \phi_1\left(t - \frac{x}{w}\right) + \phi_2\left(t + \frac{x}{w}\right), \tag{7}$$

where $w=(LC)^{-1/2}$ is the propagation velocity. From (1) and (7) it follows immediately that

$$i(x, t) = \frac{1}{Z}\left\{\phi_1\left(t - \frac{x}{w}\right) - \phi_2\left(t + \frac{x}{w}\right)\right\}, \tag{8}$$

where $Z=(L/C)^{1/2}$ is the characteristic impedance of the line.

The combination (3) and (7) gives

$$\phi_1(t) + \phi_2(t) = 0. \tag{9}$$

With the substitution of (9) into (7) and (8), the results are

$$v(x, t) = \phi_1\left(t - \frac{x}{w}\right) - \phi_1\left(t + \frac{x}{w}\right), \tag{10}$$

$$i(x, t) = \frac{1}{Z}\left\{\phi_1\left(t - \frac{x}{w}\right) + \phi_1\left(t + \frac{x}{w}\right)\right\}. \tag{11}$$

From (4), (10) and (11) we have

$$\phi_1\left(t - \frac{T}{2}\right) + \phi_1\left(t + \frac{T}{2}\right) = Zf\left(\phi_1\left(t - \frac{T}{2}\right) - \phi_1\left(t + \frac{T}{2}\right) + E\right), \tag{12}$$

where $T/2=l/w$: the propagation time of waves in the line.

* Received by the IRE, March 8, 1961.

† Dept. of Applied Physics, Faculty of Engineering, University of Tokyo, Tokyo, Japan.

[1] A. Witt, "Sur la théorie de la corde de violon," *Tech. Phys. USSR*, vol. 4, pp. 261–288; April, 1937.

World Radio History

Eq. (12) may be written as follows:

$$\phi_1\left(t+\frac{T}{2}\right)=g\left[\phi_1\left(t-\frac{T}{2}\right)\right]. \tag{13}$$

This equation is a difference equation with the difference $T$. If $\phi_1(t)$ is given for $-T/2<t<T/2$, $\phi_1(t)$ may be successively determined for $T/2<t<3T/2$, $3T/2<t<5T/2$, $\cdots$.

As can be seen later, $g[\phi_1(t)]$ is a single-valued function or a triple-valued function. Especially when it is single valued, $\phi_1(t)$ is determined uniquely for $t>T/2$.

Now, from (5) and (10)

$$\phi_1\left(-\frac{x}{w}\right)-\phi_1\left(\frac{x}{w}\right)=\alpha(x) \qquad (0<x<l), \tag{14}$$

and from (6) and (11)

$$\phi_1\left(-\frac{x}{w}\right)+\phi_1\left(\frac{x}{w}\right)=Z\beta(x) \qquad (0<x<l). \tag{15}$$

Accordingly,

$$\phi_1\left(-\frac{x}{w}\right)=\frac{1}{2}\{\alpha(x)+Z\beta(x)\} \qquad (0<x<l), \tag{16}$$

$$\phi_1\left(\frac{x}{w}\right)=-\frac{1}{2}\{\alpha(x)-Z\beta(x)\} \qquad (0<x<l). \tag{17}$$

Eq. (16) gives $\phi_1(t)$ for $-T/2<t\leq 0$, and (17) for $0\leq t<T/2$. The value of $\phi_1(t)$ for $-T/2<t<T/2$, therefore, is determined by combining (16) with (17).

Thus, we intend to discuss the difference equation (12) or (13) in order to carry the analysis further.

## III. Asymptotic Behavior

Introducing a new function $\varphi(t)$ by

$$\varphi(t)\equiv\phi_1\left(t-\frac{T}{2}\right),$$

(13) becomes as follows:

$$\varphi(t+T)=g[\varphi(t)]. \tag{18}$$

It is assumed that the initial function is of the form

$$\varphi(t)=\varphi_0(t), \tag{19}$$

where $\varphi_0(t)$ is a known function of $t$ for $0<t<T$.

Let $t_0$ be a fixed time, and define a sequence $\{\varphi_n\}$ by

$$\begin{aligned}
\varphi_0&=\varphi_0(t_0),\\
\varphi_1&=\varphi_0(t_0+T)=g[\varphi_0(t_0)],\\
\varphi_2&=\varphi_0(t_0+2T)=gg[\varphi_0(t_0)],\\
&\cdots\cdots\cdots\cdots\\
\varphi_n&=\varphi_0(t_0+nT)=gg\cdots(n)\cdots g[\varphi_0(t_0)].
\end{aligned}$$

Then the sequence $\{\varphi_n\}$ has two possible steady states as follows when $n\to\infty$.

1) There exists a certain value $\varphi_\infty$ such that

$$\varphi_n=\varphi_\infty, \qquad \text{for } n=0, 1, 2, \cdots.$$

In this case, $\varphi_\infty$ is given by

(Fig. 2). $$\varphi_\infty=g[\varphi_\infty]. \tag{20}$$

2) The steady state takes $m$ alternative different values

$$\underbrace{\varphi_\infty^{(1)}\varphi_\infty^{(2)}\cdots\varphi_\infty^{(m)}}\ \underbrace{\varphi_\infty^{(1)}\varphi_\infty^{(2)}\cdots\varphi_\infty^{(m)}}\ \underbrace{\varphi_\infty^{(1)}\cdots}$$

cyclically (Fig. 3). In this case, $\varphi_\infty^{(s)}(1\leq s\leq m)$ satisfies the following relations:

a) $$\varphi_\infty^{(s+1)}=g[\varphi_\infty^{(s)}] \qquad (1\leq s\leq m), \tag{21}$$

where $\varphi_\infty^{(m+1)}\equiv\varphi_\infty^{(s)}$.

b) $$\varphi_\infty^{(s)}=gg\cdots(m)\cdots g[\varphi_\infty^{(s)}]. \tag{22}$$

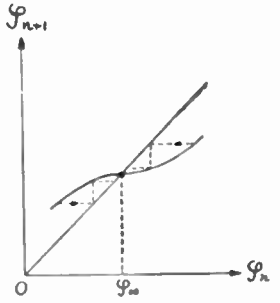


Fig. 2—When $|dg/d\varphi|<1$, the sequence $\{\varphi_n\}$ converges to $\varphi_\infty$, and no oscillation can occur.

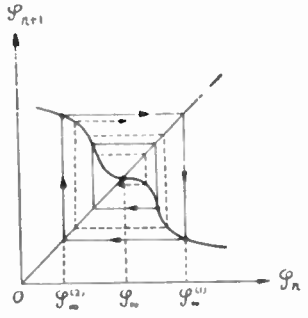


Fig. 3—The steady state takes two steady operating points ($\varphi_\infty^{(1)}$ and $\varphi_\infty^{(2)}$), alternatively.

Now let us consider the stability of these steady states. The steady state of case 1) is called stable when every sequence converges to $\varphi_\infty$, of which sequence the initial value is in the $\epsilon$ neighborhood of $\varphi_\infty$ at time $t=t_0$, where $\epsilon$ is some positive constant. The steady state which is not stable is called unstable. The stability of the periodic steady state [case 2)] may be defined as the same as case 1) for each $\varphi_\infty^{(s)}$ $(1\leq s\leq m)$.

World Radio History

For these definitions, the following stability criterion holds.

1) If

$$\left|\frac{dg[\varphi]}{d\varphi}\right|_{\varphi=\varphi_\infty} < 1, \tag{23}$$

then the steady state $\varphi_\infty$ is stable (Fig. 2).

2) If

$$\left|\frac{dgg\cdots(m)\cdots g[\varphi]}{d\varphi}\right|_{\varphi=\varphi_\infty{}^{(m)}} < 1 \quad \text{for } 1 \le s \le m, \tag{24}$$

then the periodic steady state is stable (Fig. 3).

Eq. (24) can be rewritten as follows:

$$\left|\prod_{s=1}^{m}\left[\frac{dg[\varphi]}{d\varphi}\right]_{\varphi=\varphi_\infty{}^{(s)}}\right| < 1. \tag{25}$$

In general, $\{\varphi_n\}$ tends to a stable steady state as $n\to\infty$. It is worth mentioning that the above discussion does not give the complete explanation of the steady state, since the steady state discussed here depends upon the individual initial value $\varphi_0(t_0)$. (See Section V.)

## IV. Steady State

Eq. (12) may be written in the form

$$\varphi(t) + \varphi(t+T) = Zf(\varphi(t) - \varphi(t+T) + E), \tag{26}$$

where

$$\varphi(t) \equiv \phi_1(t - T/2).$$

With new variables $\xi$ and $\eta$, (26) becomes

$$\eta = \frac{Z}{\sqrt{2}} f(\sqrt{2}\xi + E), \tag{27}$$

where

$$\xi = \frac{1}{\sqrt{2}}\{\varphi(t) - \varphi(t+T)\},$$

$$\eta = \frac{1}{\sqrt{2}}\{\varphi(t) + \varphi(t+T)\}. \tag{28}$$

Obviously, $\xi$ and $\eta$ are related with $v(l, t)$ and $i(l, t)$ by

$$\xi = \frac{1}{\sqrt{2}} v(l, t),$$

$$\eta = \frac{Z}{\sqrt{2}} i(l, t).$$

The voltage-current characteristic of the tunnel diode is illustrated in Fig. 4. The relation between $\xi$ and $\eta$, therefore, becomes as shown in Fig. 5. Hence, the relation between $\varphi(t)$ and $\varphi(t+T)$ is obtained by rotating the curve of Fig. 5 45° to the right. This is shown in Fig. 6. In this relation, it is apparent that $|dg/d\varphi| < 1$ in the region where the resistance is positive ($f'(V) > 0$), and $|dg/d\varphi| > 1$ where negative ($f'(V) < 0$).

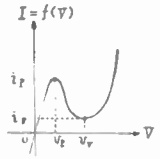


Fig. 4—The V-I characteristic of the tunnel diode.

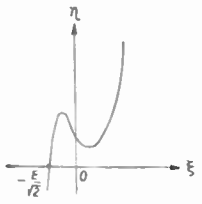


Fig. 5—The characteristic of the tunnel diode mapped on $(\xi, \eta)$-plane.

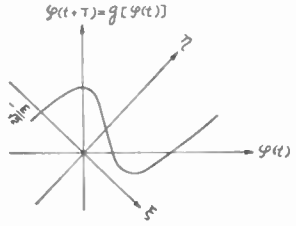


Fig. 6—The curve of the function $g$ is obtained by rotating the $\xi$ and $\eta$ axes 45° to the right.

Let us write the negative resistance as

$$\rho(V) = -\left(\frac{dI}{dV}\right)^{-1} \quad (\rho(V) > 0),$$

and define $\rho_0$ as

$$\rho_0 = \operatorname*{Min}_{\rho(V)\ge 0} \rho(V).$$

If

$$Z < \rho_0, \tag{29}$$

the function $g$ of Fig. 6 is single valued, but if $Z > \rho_0$, it becomes triple valued in some region.

The steady state shows much difference owing to the dc bias voltage $E$ and the characteristic impedance $Z$ of the line. We must, therefore, discuss various cases.

A. $E < v_P$ or $E > v_V$

In this case, the curve $g$ has a single intersection with $\eta$ axis (45° line), and at the point, $|dg/d\varphi|$ is smaller than unity. Fig. 7 shows the case $E < v_P$, and Fig. 8 shows the case $E > v_V$.

World Radio History

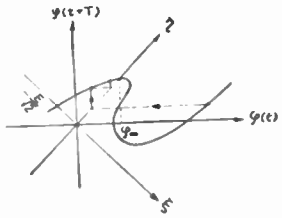

Fig. 7—The bias voltage $E$ is smaller than $v_P$.

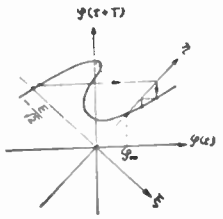

Fig. 8—The bias voltage $E$ is larger than $V_V$.

Evidently, every sequence $\{\varphi_n\}$ with arbitrary initial value converges to $\varphi_\infty$ as $n \to \infty$, where $\varphi_\infty$ corresponds to this intersection. Therefore, $v(l, t)$ tends to zero as $t \to \infty$ for arbitrary initial condition. From this fact it is easily seen that no oscillation can occur in this case.

B. $v_P < E < v_V$

$|dg/d\varphi|$ is larger than unity at the intersection of the curve $g$ with $\eta$ axis (unstable). Thus, it is possible for various types of self-oscillations to occur. Some typical examples are discussed below.

1) Fig. 9 illustrates the case where the steady state takes two alternative values $\varphi_\infty^{(1)}$ and $\varphi_\infty^{(2)}$. In Fig. 10 let

$$\eta_P = \frac{Z}{\sqrt{2}} i_P,$$

$$\eta_V = \frac{Z}{\sqrt{2}} i_V,$$

and write three values of $\xi$ corresponding to $\eta(\eta_V < \eta < \eta_P)$ as $\xi_1 > \xi_0 > \xi_2$, respectively ($\xi_0$ is not shown in the figure). Put

$$\xi_M = \tfrac{1}{2}(\xi_1 + \xi_2).$$

Then, the locus of the point $(\xi_M, \eta)$ in the $(\xi, \eta)$-plane makes a curve by varying $\eta$ in the interval $\eta_V \leq \eta \leq \eta_P$. The edge points of this curve are $(\xi_V^*, \eta_V)$ and $(\xi_P^*, \eta_P)$. Let $\eta^*$ be the ordinate of the above mentioned curve corresponding to an arbitrary value of $\xi^*$, which lies in the intervals $(\xi_P, \xi_V)$ and $(\xi_V^*, \xi_P^*)$ in common. Also, let $\xi_1^*$ and $\xi_2^*$ represent the values of $\xi_1$ and $\xi_2$ corresponding to $\eta = \eta^*$. Thus, it is evident that

$$\xi_1^* - \xi^* = \xi^* - \xi_2^*.$$

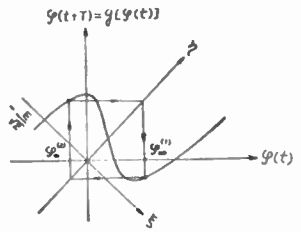

Fig. 9—When $v_P < E < V_V$, the steady state takes two steady operating points alternatively, and self-oscillation can occur.

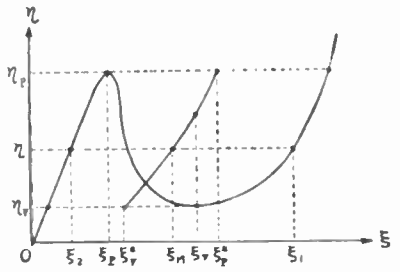

Fig. 10—The locus of the point $(\xi_M, \eta)$.

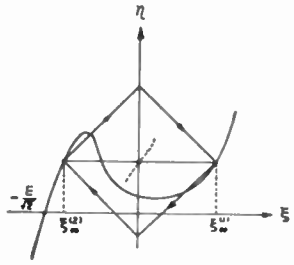

Fig. 11—One steady operating point is on the left positive resistance region, and one is also on the right. This is the case called $m=1$, $n=1$.

Fig. 11 shows the result in the case where the bias voltage is set at $E = \sqrt{2}\xi^*$, where $\xi_\infty^{(1)}$ and $\xi_\infty^{(2)}$ are given by

$$\xi_\infty^{(1)} = \xi_1^* - \xi^* = \frac{1}{\sqrt{2}}\left\{\zeta_\infty^{(1)} - \varphi_\infty^{(2)}\right\},$$

$$\xi_\infty^{(2)} = \xi_2^* - \xi^* = \frac{1}{\sqrt{2}}\left\{\varphi_\infty^{(2)} - \varphi_\infty^{(1)}\right\}.$$

Apparently, this steady state is stable.

If the characteristic impedance of the line is too high, it becomes not as in Fig. 11 but as in Fig. 15.

The voltage $V$ across the tunnel diode, corresponding to $\xi_\infty^{(1)}$ and $\xi_\infty^{(2)}$, are

$$v_\infty^{(1)} = \sqrt{2}\xi_1^* = \sqrt{2}\left(\xi_\infty^{(1)} + \frac{E}{\sqrt{2}}\right),$$

$$v_\infty^{(2)} = \sqrt{2}\xi_2^* = \sqrt{2}\left(\xi_\infty^{(2)} + \frac{E}{\sqrt{2}}\right).$$

The voltage waveform is a square wave with period $2T$.

World Radio History

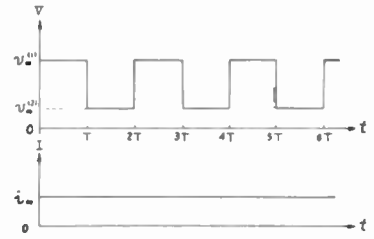

Fig. 12—The voltage and the current waveforms in the case $m=1$, $n=1$. The voltage waveform is a square one.

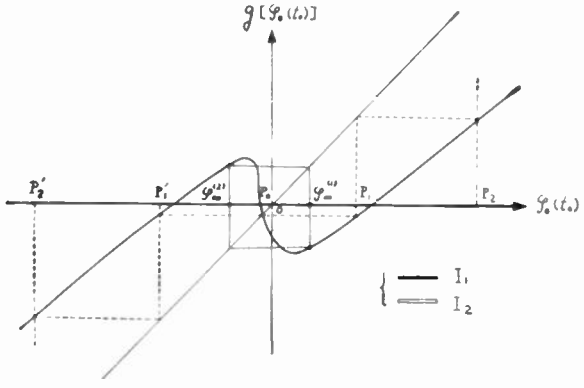

Fig. 13—An illustration of the effect of the initial condition.

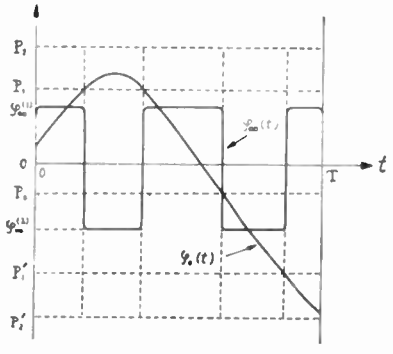

Fig. 14—The relation between the initial function $\varphi_0(t)$ and $\varphi(t)$ at the steady state. For the initial condition $\varphi_0(t_0)\in I_1$, the value of the steady operating point is $\varphi_\infty^{(1)}$, whereas for $\varphi_0(t_0)\in I_2$, the value is $\varphi_\infty^{(2)}$.

Let the current $I$ through the tunnel diode be $i_\infty^{(1)}$ and $i_\infty^{(2)}$ corresponding to the voltage $v_\infty^{(1)}$ and $v_\infty^{(2)}$. Then the relation

$$i_\infty^{(1)} = i_\infty^{(2)} = i_\infty = \frac{\sqrt{2}}{Z}\eta^*$$

holds, showing that the current is constant (Fig. 12).

2) We will now discuss briefly the relation between the value of $\varphi(t)$ at the steady state ($\varphi_\infty^{(1)}$ or $\varphi_\infty^{(2)}$) and the initial value ($\varphi_0(t)$ at $t=t_0$). In Fig. 13 two kinds of intervals ($I_1$ and $I_2$) on the horizontal axis show the relation between the initial value $\varphi_0(t_0)$ and the value $\varphi(t)$ at the steady state ($\varphi_\infty^{(1)}$ or $\varphi_\infty^{(2)}$). If $\varphi_n\to\varphi_\infty^{(1)}$ for $\varphi_0(t_0)\in I_1$, then $\varphi_n\to\varphi_\infty^{(2)}$ for $\varphi_0(t_0)\in I_2$. Fig. 14 shows these circumstances situating for a half period $T$. The figure for the next half period is obtained by interchanging $\varphi_\infty^{(1)}$ and $\varphi_\infty^{(2)}$ in Fig. 14.

It is possible, therefore, to generate square waves with the period $2T/\nu$ ($\nu$ is an integer larger than 1) by choosing a suitable initial function $\varphi_0(t)$. When the initial voltage and the current distributions $\alpha(x)$ and $\beta(x)$ $(0<x<l)$ are nearly equal to zero, then

$$\zeta_0(t) = \phi_1\left(t-\frac{T}{2}\right) \fallingdotseq 0 \qquad (0<t<T).$$

Hence, the voltage waveform becomes as in Fig. 12 but not as in Fig. 14.

3) It is seen from (27) that the curve is stretched along the $\eta$ axis with increasing $Z$. Fig. 15 shows this case when the bias voltage is set on near $v_P$.[2] Fig. 16 shows the voltage and the current waveforms of this case with the period $3T$.

There are two steady operating points on the left side of the characteristic curve in Fig. 15, and one point on the right side. This follows from the fact that the bias voltage is nearer to $v_P$ than $v_V$. If the bias voltage, therefore, is nearer to $v_V$ than $v_P$, the number of the steady operating points is two on the right and one on the left. The case when $Z$ is higher than that of Fig. 15 is shown in Fig. 17 and Fig. 18.

4) As the characteristic impedance $Z$ becomes higher, the number of the steady operating points becomes greater. In Fig. 19 the bias voltage is set on near the middle point between $v_P$ and $v_V$, and the number of the steady operating points are two on the left and three on the right. Fig. 20 shows the voltage and the current waveforms.

5) With a suitable bias voltage, the number of the steady operating points remain the same as in Fig. 19; however, the path from point to point is different, as shown in Fig. 21. The voltage and the current waveforms are illustrated in Fig. 22.

6) Let us consider the limit case as $Z\to\infty$. With very high $Z$, the figure compressed along the $\eta$ axis becomes as in Fig. 23. Fig. 24 shows its voltage and current waveforms.

The self-oscillation in this case is quite near to the relaxation oscillation. In fact, it can be shown that the limit becomes the relaxation oscillation, as discussed below.

In Fig. 25 we have

$$\overline{DE} = \overline{BD} - \overline{BE} = \overline{BD} - \overline{EC} = \overline{BD} - \overline{DE}\tan\theta,$$

and hence

$$\overline{DE} = \frac{\overline{BD}}{1+\tan\theta} \fallingdotseq \frac{\overline{BD}}{\tan\theta}.$$

[2] Refer to the Appendix for the method of construction.

World Radio History

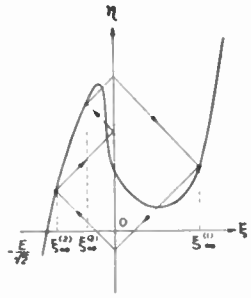

Fig. 15—The case $m=2$, $n=1$.

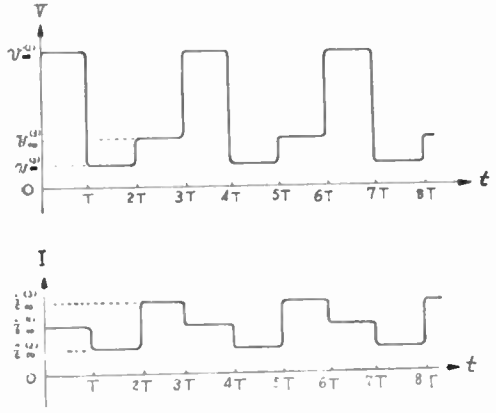

Fig. 16—The voltage and the current waveforms with period $3T$ in the case of Fig. 15.

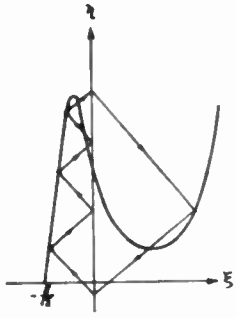

Fig. 17—The case $m=3$, $n=1$.

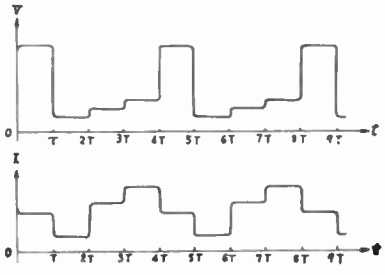

Fig. 18—The voltage and the current waveforms with period $4T$.

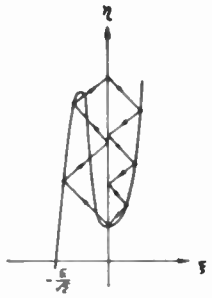

Fig. 19—The case $m=2$, $n=3$.

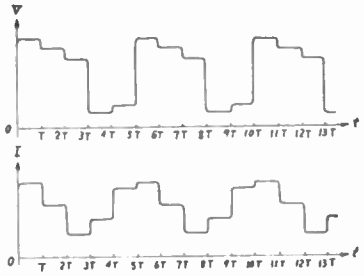

Fig. 20—The voltage and the current waveforms with period $5T$.

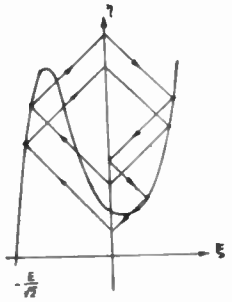

Fig. 21—The number of $m$ and $n$ is quite equivalent with that of Fig. 19. However, the path from point to point is different.

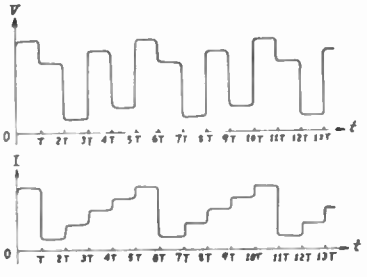

Fig. 22—The voltage and the current waveforms show many differences from those of Fig. 20.

World Radio History

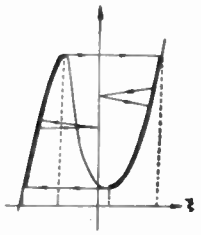

Fig. 23—The curve of the function $g$ compressed along the $\eta$ axis when $Z$ is very large. In addition this figure shows the jump condition.

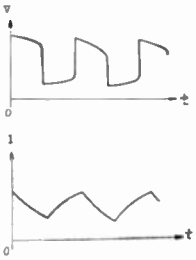

Fig. 24—The voltage and the current waveforms of Fig. 23 approach those of the relaxation oscillation as $Z \to \infty$.

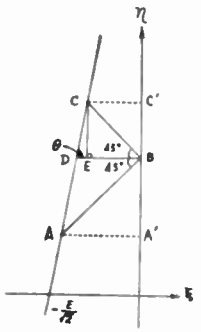


Fig. 25—A portion of the characteristic curve of the tunnel diode on $(\xi, \eta)$-plane.

As it is evident that

$$\tan\theta = \frac{d\eta}{d\xi} = Zf'(\sqrt{2}\xi + E) = Zf'(v + E),$$

the result is

$$\Delta\xi \fallingdotseq \frac{-2\xi}{Zf'(v+E)} = \frac{-2\xi}{\sqrt{L/C}\,f'(v+E)},$$

where

$$\overline{BD} = -\xi, \qquad \Delta\xi = \overline{AA'} - \overline{CC'} \fallingdotseq 2\overline{DE}.$$

If we write the time needed for the steady operating point running from $A$ to $C$ as

$$\Delta t = T = 1/2l\sqrt{L/C},$$

then

$$\frac{\Delta\xi}{\Delta t} \fallingdotseq \frac{-\xi}{lLf'(v+E)},$$

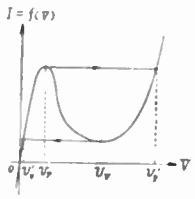


Fig. 26—Arrows show the jumping path of the relaxation oscillation.

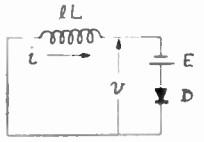


Fig. 27—The relaxation oscillation occurs in this circuit.

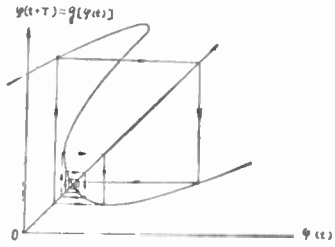

Fig. 28—When the bias voltage $E$ is set on near the valley point of the tunnel diode characteristic, the steady operating points are observed on the negative-resistance region.

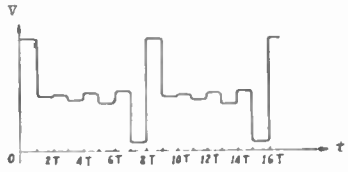


Fig. 29—The voltage waveform of Fig. 28.

or

$$\frac{\Delta v}{\Delta t} \fallingdotseq \frac{-v}{lLf'(v+E)}. \tag{30}$$

This difference equation may be approximated by the following differential equation:

$$\frac{dv}{dt} = \frac{-v}{lLf'(v+E)}. \tag{31}$$

In addition, from Fig. 26 the jump condition is obtained:

$$v_V \to V'_V, \qquad v_P \to V'_P \qquad (V = v + E). \tag{32}$$

On the other hand, if $C=0$, in Fig. 1, this circuit becomes that of Fig. 27. From Kirchhoff's law,

$$v = -lL\frac{di}{dt}, \qquad i = f(v+E). \tag{33}$$

Therefore, the differential equation of this circuit coincides with (31), and the jump condition with (32).

World Radio History

7) When the bias voltage $E$ is set on near the valley point of the negative-resistance characteristic, the steady operating points are observed in the negative-resistance region. In this case, several rotations of the operating point are observed around the valley point, as shown in Fig. 28.

The number of rotations is restricted by the stability criterion:

$$\left| \prod_{s} \left[ \frac{dg[\varphi]}{d\varphi} \right]_{\varphi=\varphi_{\infty}^{(s)}} \right| < 1.$$

If the number of rotations is too large, the left side of the above inequality becomes larger than unity, and the steady state will turn out unstable. Fig. 29 illustrates the voltage and the current waveforms. This case does not seem to be so stable.

## V. General Conclusions

Summing up these results, we arrive at the following general conclusions. When the bias voltage $E$ is set in the negative resistance region ($v_P < E < v_V$), self-oscillation is observed to occur in the transmission line. If this oscillation is observed by the voltage across the tunnel diode or the current through it, the oscillation generally has a staircase waveform. This waveform displays many differences, according to the characteristic impedance $Z$ and the bias voltage $E$.

If the bias voltage $E$ is set near the middle point between $v_P$ and $v_V$, the number of the steady operating points on the left positive-resistance region ($m$) is nearly equal to that on the right ($n$). In the case where $Z$ is low, $m=1$, $n=1$. The voltage waveform is a square one, and the current is constant. When $Z$ increases, $m(=n)$ becomes greater, and the oscillation approaches a relaxation oscillation.

In general, $m$ is larger than $n$ when $E$ is near to $v_P$, and is smaller when $E$ is near to $v_V$. There is more than one steady state which corresponds to the same $m$ and $n$ (except for the case $m=1$, $n=1$).

In any case, the period is $(m+n)T$. Thus, the period $2T$, corresponding to $m=1$, $n=1$, may be considered as the basic period, although it is not the shortest period as already seen in Section IV-B, 2).

## VI. Effect of the Parallel Capacitance of the Tunnel Diode

In the previous sections we have neglected the parallel capacitance of the tunnel diode. If the parallel capacitance $C_0$ is considered in the circuit of Fig. 1, (4) becomes as follows:

$$i(l,t) = f(v(l,t) + E) + C_0 \frac{\partial v(l,t)}{\partial t}. \tag{34}$$

Therefore, (12) takes the form

$$\phi_1\left(t - \frac{T}{2}\right) + \phi_1\left(t + \frac{T}{2}\right) = Zf\left(\phi_1\left(t - \frac{T}{2}\right) - \phi_1\left(t + \frac{T}{2}\right) + E\right) + ZC_0 \left\{ \frac{d\phi_1\left(t - \frac{T}{2}\right)}{dt} - \frac{d\phi_1\left(t + \frac{T}{2}\right)}{dt} \right\}. \tag{35}$$

This is a differential-difference equation with the difference $T$.

By the initial conditions (5) and (6), the value of $\phi_1(t)$ for $-T/2 < t < T/2$ is given as (16) and (17). Besides, the value of $d\phi_1(t)/dt$ can be determined for $-T/2 < t < T/2$ by the equations

$$\frac{d\phi_1\left(-\frac{x}{w}\right)}{dx} = -\frac{w}{2}\left\{\frac{d\alpha(x)}{dx} + Z\frac{d\beta(x)}{dx}\right\} \qquad (0 < x < l), \tag{36}$$

$$\frac{d\phi_1\left(\frac{x}{w}\right)}{dx} = -\frac{w}{2}\left\{\frac{d\alpha(x)}{dx} - Z\frac{d\beta(x)}{dx}\right\} \qquad (0 < x < l). \tag{37}$$

If the values of $\phi_1(t)$ and $d\phi_1(t)/dt$ are given for $-T/2 < t < T/2$, (35) becomes a first-order differential equation of $\phi_1(t)$ for $T/2 < t < 3T/2$. Therefore, assuming that $\phi_1(t)$ is continuous at $t = T/2$, $\phi_1(t)$ may be determined for $T/2 < t < 3T/2$. In a like manner, $\phi_1(t)$ may be successively determined for $3T/2 < t < 5T/2$, $5T/2 < t < 7T/2$, $\cdots$.

Now, setting $\varphi(t) \equiv \phi_1(t - T/2)$, (35) may be written

$$C_0 \frac{d\varphi(t+T)}{dt} = G\left(\varphi(t+T), \varphi(t), C_0 \frac{d\varphi(t)}{dt}\right), \tag{38}$$

where

$$G\left(\varphi(t+T), \varphi(t), C_0 \frac{d\varphi(t)}{dt}\right) = f(\varphi(t) - \varphi(t+T) + E) - \frac{1}{Z}\{\varphi(t+T) + \varphi(t)\} + C_0 \frac{d\varphi(t)}{dt}.$$

Let us consider this differential-difference equation under the initial function:

$$\varphi(t) = \varphi_0(t) \qquad (0 \le t \le T), \tag{39}$$

where $\varphi_0(t)$ is a given function of $t$ for $0 \le t \le T$. Henceforth, we assume that the initial function and its first derivative are continuous for $0 \le t \le T$. Clearly, this assumption is satisfied if $d\alpha(x)/dx$ and $d\beta(x)/dx$ are continuous for $0 \le x \le l$, and $d\beta(x)/dx = 0$ at $x = 0$.

In order that the solution of this equation has physical significance, it must be "stable" in some sense. It seems reasonable for us to define the stability of the solution of (38) as follows. Let $\varphi(t|\varphi_0(t))$ be the solution of (38) corresponding to the initial function $\varphi_0(t)(0 \le t \le T)$. The solution $\varphi(t|\varphi_0(t))$ is said to be

World Radio History

stable if we can find a $\delta=\delta(\epsilon)>0$ for every $\epsilon>0$, such that, for any initial function $\varphi_0^*(t)(0\leq t\leq T)$ which satisfies

$$\text{Max}\ |\varphi_0(t)-\varphi_0^*(t)|<\delta,$$
$$\text{Max}\ |d\varphi_0(t)/dt-d\varphi_0^*(t)/dt|<\delta \qquad \text{for } 0\leq t\leq T,$$

we have

$$|\varphi(t|\varphi_0(t))-\varphi(t|\varphi_0^*(t))|<\epsilon \qquad \text{for } t\geq T.$$

If $C_0=0$, (38) takes the form

$$G(\varphi(t+T),\varphi(t),0)=0. \tag{40}$$

This equation is called a "degenerate equation," corresponding to (38), and is nothing but the difference equation (18). It is already known that (40) has the discontinuous periodic solution (staircase waveform) under suitable conditions.

We are now in a position to investigate the following problems.

1) Does the differential-difference equation (38) have a periodic solution, and especially, a stable one? If it does, how do its waveform and period depend upon the value of $C_0$? This problem has practical importance in relation to the rise time of pulses when this circuit is used as a pulse generator.

2) In the case where (38) has a stable periodic solution, which one of the discontinuous periodic solutions of the degenerate equation (40) does the stable periodic solution of (38) approach as $C_0\to 0$?

As discussed, three $\varphi(t+T)$ correspond to one $\varphi(t)$, when the function $g$ is triple-values. Which one of these three is actually selected is a problem which is closely connected with the latter problem mentioned above.

To establish a complete explanation of all the circuit behaviors, it is necessary to investigate these problems fully. We shall refrain from doing so, however, but we shall indicate the direction of the further approach.

## VII. Synchronization of the Self-Oscillation

It is well known that self-oscillation may be generally synchronized by the external periodic oscillation. The same phenomenon was seen concerning the self-oscillation discussed in this paper. The fractional synchronization was also observed, but the basic synchronization had wider synchronous region. This problem can be analyzed by treating the periodic solution of the period $2\pi/\omega$ of the nonautonomous differential-difference equation which is obtained by replacing $E+e\sin\omega t$ for $E$ in (38).

## VIII. Use of the Current-Controlled Negative-Resistance Element

When the current-controlled negative-resistance element (*e.g.*, *p-n-p-n* diode, double-base diode, electric discharge tube and arc, etc.) is used instead of the tunnel diode (voltage-controlled element), the transmission line must be open at the end $x=0$ (Fig. 30). In the case, the analysis can be made in the same manner as above by interchanging voltage and current, impedance and admittance.

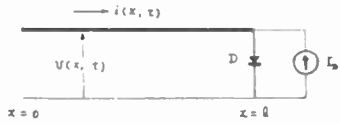


Fig. 30—A circuit using a current-controlled negative-resistance element.

## IX. Experimental Results

As a transmission line, we used an LC lumped-constant delay line, conventional delay line, coaxial line, parallel wires (feeder line for television) and Lecher wires.

Using the LC lumped-constant delay line with $Z=220$ Ω, we observed various types of self-oscillations, $m=1, 2, 3, 4$, $n=1, 2, 3$. Some of these waveforms are shown in Figs. 31–36. We could also observe three modes for the case $m=1$, $n=1$, corresponding to different initial conditions.

The effect of the parallel capacitance of the tunnel diode increases the rise and fall times of a pulse.

Figs. 31(a) and 32(a) show steady operating points as determined graphically. Bright spots on the V-I characteristic curve of Figs. 31(b), 32(b) and 33(a) indicate those points as they appeared on a cathode-ray tube. These waveforms were observed by a 30-Mc synchroscope.

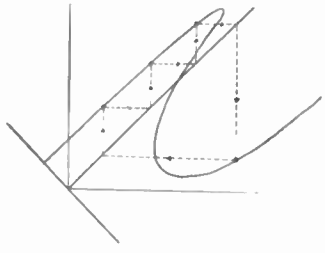

(a)

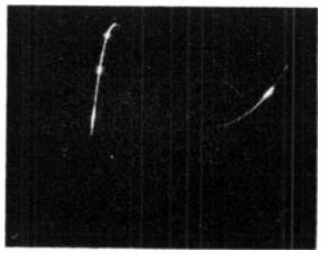

(b) The V-I characteristic.

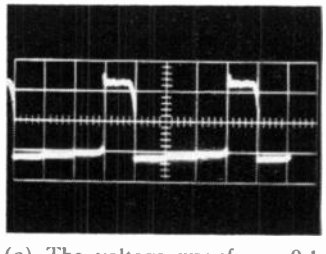

(c) The voltage waveform. 0.1 volt/division (vertical). 900 μsec/division (horizontal).

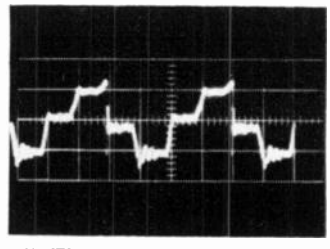

(d) The current waveform. 2 ma/division (vertical). 900 μsec/division (horizontal).

Fig. 31—The case $m=3$, $n=1$. (3:1) $Z=220$ Ω. $T/2=450$ μsec. $E=0.140$ volt.

World Radio History

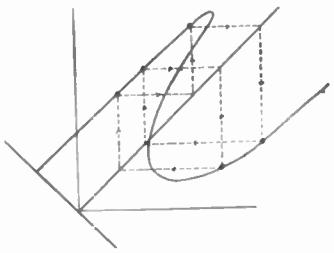

(a)

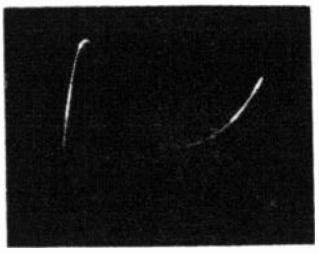

(b) The V-I characteristic.

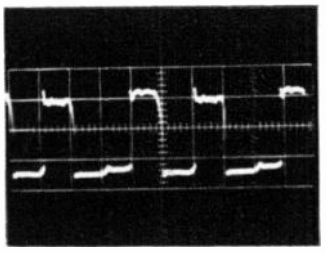

(c) The voltage waveform. 0.1 volt/division (vertical). 900 μsec/division (horizontal).

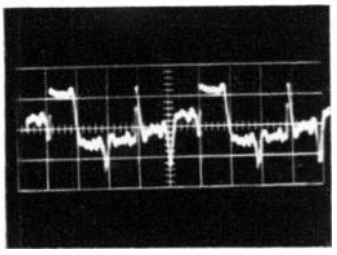

(d) The current waveform. 2 ma /division (vertical). 900 μsec /division (horizontal).

Fig. 32—The case $m=3$, $n=2$. $[(2:1)\rightleftarrows(1:1)]$ $Z=220\ \Omega$. $T/2=450$ μsec. $E=0.223$ volt.

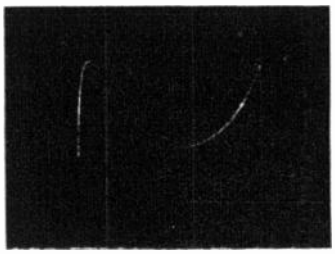

(a) The V-I characteristic.

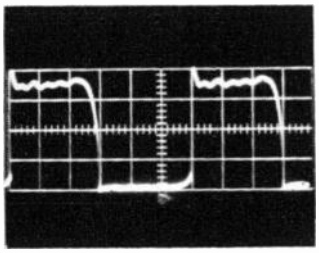

(b) The voltage waveform of the fundamental mode (Mode 1).

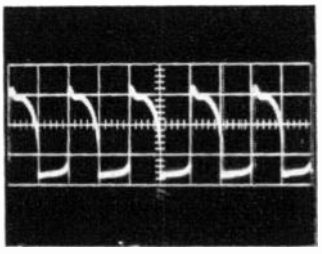

(c) Mode 2.

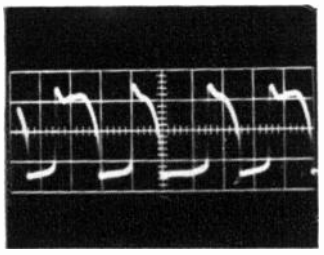

(d) Mode 3.

Fig. 33—The three modes of the case $m=1$, $n=1$, corresponding to the different conditions. $Z=220\ \Omega$. $T/2=450$ μsec. $E=0.240$ volt. Each division indicates 0.1 volt (vertical) and 300 μsec (horizontal).

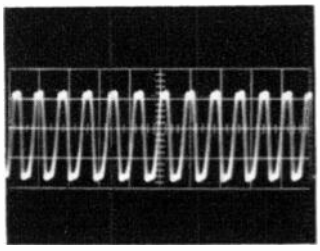

(a) The case $m=1$, $n=1$. $E=0.120$ volt.

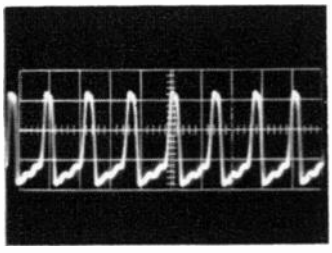

(b) The case $m=3$, $n=1$. $E=0.082$ volt.

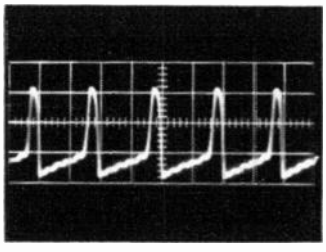

(c) The case $m=5$, $n=1$. $E=0.067$ volt.

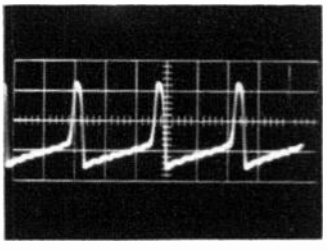

(d) The case $m=7$, $n=1$. $E=0.060$ volt.

Fig. 34—The voltage waveforms when the coaxial lines with $Z=75\ \Omega$ and $T/2=13$ mμsec is used. Each division indicates 0.1 volt (vertical) and 100 mμsec (horizontal).

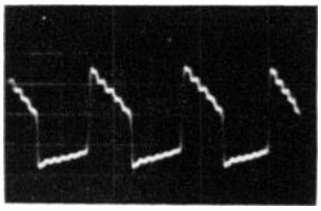

(a) $E=0.133$ volt.

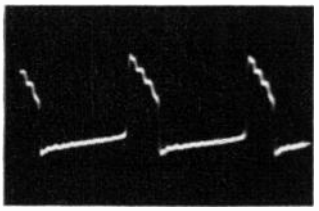

(b) $E=0.093$ volt.

Fig. 35—The voltage waveforms with use of the parallel line (feeder line for television) with $Z=300\ \Omega$ and $T/2=20$ mμsec. 0.1 volt /division (vertical) and 150 mμsec/division (horizontal).

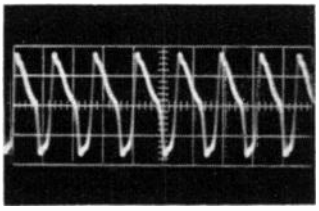

(a) $E=0.068$ volt.

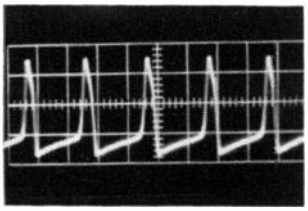

(b) $E=0.172$ volt.

Fig. 36—The voltage waveforms with use of the Lecher wires with $Z=260\ \Omega$ and $T/2=8.5$ mμsec. 0.1 volt/division (vertical) and 100 mμsec/division (horizontal).

World Radio History

## X. Remarks

The self-oscillation discussed in this paper can be explained as the periodic solution of the linear wave equation with a nonlinear (negative-slope) boundary condition. If the nonlinear boundary condition is resistive, the problem reduces to a nonlinear difference equation, while, if reactive, it becomes a nonlinear differential-difference equation.

Many examples represented by this scheme are seen in mechanical systems. Table I shows the correspondence between such examples and the circuit considered in this paper. From this table, we conclude that this circuit is a simulator of almost all stringed and wind instruments.

## Appendix

### Method of Construction

In Fig. 37 the curve $A'B'$ is the mapping of the right portion $AB$ of the characteristic curve. If we write the coordinate of the point $A$ as $(\varphi(t), g[\varphi(t)])$, that of the point $A'$ is $(g^{-1}[\varphi(t)], g[\varphi(t)])$. The mirror image of the curve $CD$ is drawn for the 45° line, and its intersection with the curve $A'B'$ is obtained. When this point is shifted horizontally into the right portion of the characteristic, the new point gives one of the steady operating points of the case $m=1$, $n=2$, provided that the shifted point falls in the interval $(p, q)$. If the curve $A''B''$, mapped once again, is used instead of $A'B'$, one of the steady operating points of the case $m=1$, $n=3$ is obtained. In the same way, the intersection of the curve $A''B''$ with the mirror image of the curve $C'D'$, the mapping of the left portion $CD$, gives one of the steady operating points of the case $m=2$, $n=3$.

TABLE I

| Mathematical Expression | | Linear Wave Equation | Nonlinear (Negative-Slope) Boundary Condition | | |
|---|---|---|---|---|---|
| System | Example | Distributed Constant System | Element | Position | Characteristic |
| Electric system | Our circuit | Transmission line | Tunnel diode | One edge of the line | Voltage-current |
| Mechanical system | Violin | String | Coulomb friction | Contact point of string with bow | Frictional force-relative velocity |
| Fluid system | Water hummer | Water duct | Valve | One edge of the duct | Pressure-flow |
| Sound system | Wind instruments | Air duct | Lips | One edge of the duct | Pressure-flow |

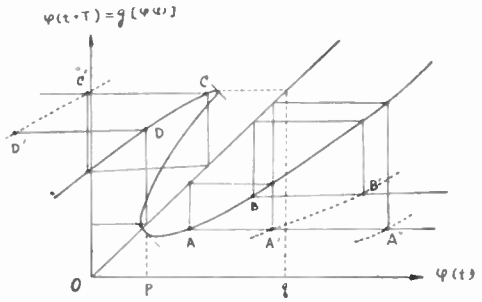


Fig. 37—Steady operating points can be obtained graphically. The curve $A'B'$ is obtained by mapping the curve $AB$ as shown in the figure.

World Radio History

# IRE Standards on Solid-State Devices: Measurement of Minority-Carrier Lifetime in Germanium and Silicon by the Method of Photoconductive Decay*

61 IRE 28. S2

## COMMITTEE PERSONNEL

### Task Group on Methods of Test for Bulk Semiconductors
1959–1960

E. N. Clarke, *Chairman*

G. Bemski
J. S. Blakemore
D. C. Cronemeyer
I. Drukaroff
A. L. Kestenbaum
M. F. Lamorte
J. Mandelkorn
D. T. Stevenson

### Solid State Devices Committee
1959–1961

R. L. Pritchard, *Chairman* 1959–1961
R. H. Rediker, *Vice Chairman* 1960–1961
E. O. Johnson, *Vice Chairman* 1959–1960
V. P. Mathis, *Secretary* 1959–1961

J. B. Angell
S. J. Angello
J. S. Blakemore
A. Coblenz
L. Davis, Jr.
W. C. Dunlap, Jr.
J. M. Early
H. J. Evans
P. A. Fleming
J. R. Hyneman
B. K. Kazan
N. R. Kornfield
A. W. Lampe
E. E. Loebner
J. R. Roeder
B. J. Rothlein
S. Sherr
A. E. Slade
B. N. Slade
M. E. Talaat
R. W. Ure, Jr.
W. M. Webster
P. N. Wolfe

### Subcommittee on Semiconductor Devices
1959–1960

J. M. Early, *Chairman* (IRE)
A. C. Sheckler, *Chairman* (AIEE)
S. K. Ghandhi, *Chairman* (AIEE)

G. Abraham
J. B. Angell
E. N. Clarke
A. Coblenz
C. G. Currin
J. M. Goldey
B. Jacobs
J. D. Johnson
C. H. Knowles
R. P. Lyon
R. Morrison
C. W. Mueller
M. B. Prince
R. L. Pritchard
B. J. Rothlein
H. N. Sachar
D. E. Sawyer
A. P. Stern
R. L. Trent
R. W. Ure, Jr.

* Approved by the IRE Standards Committee, November 10, 1960. Reprints of this Standard 61 IRE 28. S2, may be purchased while available from the Institute of Radio Engineers, 1 East 79 Street, New York, N. Y., at $0.60 per copy. A 20 per cent discount will be allowed for 100 or more copies mailed to one address.

World Radio History

**Standards Committee**
**1960–1961**

C. H. PAGE, *Chairman*
J. G. KREER, JR., *Vice Chairman*
H. R. MIMNO, *Vice Chairman*
L. G. CUMMING, *Vice Chairman*

J. H. Armstrong
J. Avins
G. S. Axelby
M. W. Baldwin, Jr.
W. R. Bennett
J. G. Brainerd
A. G. Clavier
S. Doba, Jr.
R. D. Elbourn
G. A. Espersen
R. J. Farber
D. G. Fink
G. L. Fredendall
E. A. Gerber
A. B. Glenn
V. M. Graham
R. A. Hackbusch
R. T. Haviland
A. G. Jensen
R. W. Johnston
I. Kerney
E. R. Kretzmer
W. Mason
D. E. Maxwell
R. L. McFarlan
P. Mertz
H. I. Metz
E. Mittelmann
L. H. Montgomery, Jr.
S. M. Morrison
G. A. Morton
R. C. Moyer
J. H. Mulligan, Jr.
A. A. Oliner
M. L. Phillips
R. L. Pritchard
P. A. Redhead
C. M. Ryerson
G. A. Schupp, Jr.
R. Serrell
W. A. Shipman
H. R. Terhune
E. Weber
J. W. Wentworth
W. T. Wintringham

**Measurements Coordinator**

J. G. KREER, JR.

## 1. GENERAL

### *1.1 Scope*

This standard describes a particular method for measuring carrier lifetime, namely, that of photoconductive decay. Lifetime (volume) is defined[1] as: "the average time interval between the generation and recombination of minority carriers in a homogeneous semiconductor." Numerous methods for measuring carrier lifetime have been described, but this present standard concerns itself with the technique which has gained most widespread use. Discussion of basic theory and reference to other techniques will be found in the review paper by Bemski.[2]

This standard concerns measurements on both germanium and silicon, and in particular, describes the analysis of nonexponential decays often found in the case of silicon measurements.

The smallest lifetime measurable by this method is determined by the turnoff time of the light sources as described in Section 2.2.1. The maximum measurable lifetime is determined by the diffusion constant $D$ and the sample dimensions. Detailed limits for both $n$- and $p$-type germanium and silicon are presented in Table I (see Appendix).

[1] "IRE Standard on Solid-State Devices, Definitions of Semiconductor Terms, 1960: 60 IRE 28. S1," PROC. IRE, vol. 48, pp. 1772–1775; October, 1960.
[2] G. Bemski, "Recombination in semiconductors," PROC. IRE, vol. 46, pp. 990–1004; June, 1958.

### *1.2 General Procedure*

In the photoconductive-decay method, a constant current is passed through a semiconducting filament equipped with ohmic contacts, and the voltage drop down the filament is monitored continuously. For a short period, excess carriers are deliberately created in the body of the filament—usually by exposure to visible or near infrared illumination, though high-energy electromagnetic rays or beams of high-energy particles may be used.

It is not usually desirable to employ exciting rays which are too strongly absorbed by the semiconductor, for then most of the excess carriers are created near the front surface of the specimen and tend to recombine on this surface. A filter made of the same semiconductor as the specimen itself is often interposed between the light source and the specimen. This eliminates the short-wavelength nonpenetrating photons, but passes a fair proportion of those wavelengths near the absorption edge which can be absorbed reasonably uniformly throughout the thickness of the specimen.

In thermal equilibrium, the voltage drop along the section of the specimen to be illuminated is $V_0$ for a given constant current. When illumination starts, the voltage decreases, since additional carriers are being provided to support the current. The excess-carrier lifetime can be determined from observations of the change in voltage, $\Delta V = (V_0 - V)$ during the period of conductance buildup; however, it is more useful to study the

World Radio History

decay of $\Delta V$ when the light is suddenly turned off. During the latter period excess holes and electrons are progressively made unavailable for conduction through recombining and trapping processes.

The two excess populations are equal in density only when recombination is the dominant factor. During the decay the excess conductivity $\Delta\sigma$ varies as

$$\Delta\sigma \propto \Delta p = \Delta n \propto \exp\left[-t/\tau\right], \tag{1}$$

where $\Delta p$ and $\Delta n$ are, respectively, the concentrations of excess holes and excess electrons, and $\tau$ is a characteristic time constant.

For a specimen operated under constant-current conditions, voltage is inversely proportional to conductance. Hence, for small deviations from thermal-equilibrium conditions, $\Delta V$ is directly proportional to excess conductance but is of the opposite sign. (Corrections for large modulation appear in Section 2.4.2.) Accordingly, the effective measured lifetime, ordinarily called the filament lifetime, $\tau f$ at any instant is given by

$$\tau f = -\Delta V\left[d(\Delta V)/dt\right]^{-1} \quad \text{when} \quad \Delta V \ll V_0 \tag{2}$$

and by an appropriately modified form for strongly modulated conditions. The recombination mechanisms which jointly determine $\tau f$ will include both volume and surface effects. It is necessary to take precautions to calculate the surface contribution if volume lifetime is to be measured adequately.

The time scale of decay does not correctly portray the lifetime behavior if trapping is serious, either in the recombination levels or in separate traps of poor recombinative efficiency. Excess holes and electrons then will contribute to the photoconductance in a manner which changes as the trapping proceeds. While excess carriers of one type are trapped, a corresponding concentration of the opposite type is forced to remain in circulation; these contribute a long-period tail to the photoconductance, which declines slowly as the traps finally empty.

Trapping is most serious at low temperatures, but in silicon it can be significant at room temperature for small light intensities. In these cases it is still often possible to measure the lifetime corresponding to large excess concentrations, since traps may tend to become saturated. The necessary conditions can be arranged either by observing the early stages of decay following an intense flash of light or by using a weaker light flash in conjunction with strong continuous illumination.

## 2. Detailed Procedure

### 2.1 Preparation of Samples

*2.1.1 Surface Preparation:* The surface should be sandblasted or ground. This provides a reference surface for which the surface recombination rate of the fundamental mode is

$$\nu_s = \pi^2 D\left[\frac{1}{a^2} + \frac{1}{b^2} + \frac{1}{c^2}\right], \tag{3}$$

where $a$, $b$ and $c$ are the dimensions of the sample, and should be expressed in centimeters if the diffusion constant $D$ is given in cm²/sec. In general, the ambipolar diffusion constant, defined by (4),

$$D = \left[\frac{n+p}{\left(\frac{n}{D_p}\right) + \left(\frac{p}{D_n}\right)}\right] \tag{4}$$

should be used in the calculation of the surface-recombination rate; however, this reduces to $D_p$ for strongly $n$-type material and to $D_n$ for strongly $p$-type material. Only with germanium of higher resistivity than 20 ohm-cm is it imperative to use $D$ in the form of (4).

Once the surface-recombination rate $\nu_s$ has been calculated, it is possible to compute the volume lifetime $\tau B$ from the filament lifetime $\tau f$, using

$$\tau B = \left[\frac{1}{\tau f} - \nu_s\right]^{-1} \tag{5}$$

and subject to the restriction that penetrating light is employed (see Section 2.2 below).

*2.1.2 Sample Shape and Size:* Three standard sizes of samples are given in the Appendix. Table I of the Appendix gives the maximum values of volume lifetime measurable with the different sizes; Table II of the Appendix gives the surface-recombination rate $\nu_s$ calculated from (3) and used in (5). If no knowledge of lifetime range is available before the measurement, the largest size sample possible should be used. In addition to providing a calculable surface effect, sandblasting or grinding of the surfaces greatly reduces the importance of surface cleanliness and ambient gas.

*2.1.3 Contact Preparation:* End contacts should cover the entire ends and should not make contact with the sides of the sample. The contacts should be nonrectifying. This condition should be tested by observing the voltage across the sample corresponding to each polarity of the constant-current source. If these two voltages are within 2 per cent of each other, the contacts can be regarded as satisfactory for a lifetime measurement. It is recommended that the necessary ohmic contacts on germanium be applied by soldering or by plating. In the case of silicon it is recommended that the necessary ohmic contacts be applied by an ultrasonic soldering method. For $p$-type silicon pure indium, and for $n$-type silicon, an alloy of 95 per cent tin, 5 per cent antimony, gives satisfactory behavior.

*2.1.4 Resistivity Uniformity:* The resistivity profile of the sample is measured according to presently accepted

World Radio History

techniques.[3] The lowest resistivity should not differ from the highest resistivity by more than 10 per cent.

*2.1.5 Photo Voltage:* With the sample current set at zero any photovoltaic signal should have a peak amplitude less than 1 per cent of the desired photoconductive signal.

### 2.2 Optical Requirements

The illuminating system is required to deliver a pulse of light with a very short turn-off time. An arrangement of mirrors and/or lenses is usually included to collect as much of the available light as possible and direct this to the front face of the specimen. The inclusion of a filter (made from the same semiconductor as the specimen) in the optical path insures that nonpenetrating light does not reach the specimen. Since radiation of wavelengths longer than the absorption edge does not produce free hole-electron pairs, it is only the intensity in a wavelength interval immediately around 1.1 $\mu$ (for silicon) or 1.7 $\mu$ (for germanium) which determines the carrier generation rate in the specimen. The amount of this light depends on the type of light source as discussed below.

*2.2.1 Desired Behavior of Light Source:* Several types of pulsed light sources have been used successfully. These included mechanical choppers, rotating mirror systems, short-duration arc sources and electro-optical shutters. The light intensity normally should be maintained at a level such that the filament conductance changes by less than 5 per cent. When measurements are made with larger modulation, it is necessary to follow the procedure of Section 2.4.2 for correcting $\Delta n$ and $\tau$. The turn-off time of the light sources must be short compared with the filament lifetime (light intensity down to 10 per cent in 0.2 $\tau f$ or less). An $n$-type germanium sample with $a=1.0$ cm, $b=0.4$ cm, $c=0.025$ cm, with all surfaces ground or sandblasted may be used to test the turn-off time of the pulsed light source. This sample will have a filament lifetime of less than about 1 $\mu$sec regardless of the bulk lifetime of the germanium used. In the case of silicon, a sample 0.010 cm thick would be required to insure a filament lifetime less than 1 $\mu$sec.

In one preferred type of source a capacitor is charged to several thousand volts and discharged through a spark gap or Xenon flash tube. With a capacitor of some 0.01 $\mu$f a bright discharge can be obtained which reaches maximum intensity within 0.3 $\mu$sec and is down to less than 5 per cent of this intensity in an additional 0.5 $\mu$sec. The fast decay of light intensity is necessary, for otherwise falsely long lifetimes will be ascribed to material in which the rate of carrier recombination is comparable with the rate of light decay. When measuring a sample with a lifetime of less than 5 $\mu$sec, it is preferable to use a smaller capacitor for a shorter pulse duration, even though the total available light flux is then smaller. A triggered repetition rate of the order of 20 to 60 cps for the light source will result in a steady oscillographic display which is convenient to adjust and not fatiguing to the eyes.

In a different kind of light source, the output of a continuously operated lamp (usually a tungsten ribbon at 3000°K) is modulated by a rotating mirror or Kerr cell. This form of source is less efficient than a spark gap or flash tube in that the heated ribbon is capable of providing only 10 per cent as many photons per square centimeter of source per second at 1.1 $\mu$. When a mirror is rotated fast enough to produce a pulse which decays in less than 1 $\mu$sec, the light intensity at the sample may be small. The Kerr cell has the advantage that the length and shape of the light pulse can very easily be made variable.

*2.2.2 Optical Filtering:* The light is passed through a polished filter of the same semiconductor as the lifetime sample with thickness and temperature comparable with that of the sample. The filter is perpendicular to the beam and parallel to the sample. Considerable displacement of the light occurs if the two are misoriented because of the high refractive indices of silicon and germanium. A good position for the filter is immediately in front of the specimen.

*2.2.3 Sample Area to be Illuminated:* The region surrounding the end contacts is shielded from light. It is further recommended that masking strips should be placed along the specimen so that only approximately the center half of the total width is exposed to light. When measurements are made under these conditions, the electric field within the sample should satisfy the inequality

$$E \leq \frac{300}{\sqrt{\tau\mu}} \frac{\text{volt}}{\text{cm}}. \tag{6}$$

where $\tau$ is here expressed in microseconds and

$$\mu = \frac{\mu_n\mu_p \left| n_0 - p_0 \right|}{n_0\mu_n + p_0\mu_p} \frac{\text{cm}^2}{\text{volt} - \text{sec}}. \tag{7}$$

For material which is strongly $n$-type or $p$-type the latter expression becomes $\mu_p$ or $\mu_n$, respectively.

With the specimen masked as described, the exposed area should be illuminated as uniformly as possible.

*2.2.4 Background Illumination:* Occasionally background light has been used to saturate traps in silicon. However, in the general case it is recommended that a background light should not be used. The presence of traps in a particular sample should be noted and the lifetime qualified. (See Section 2.4.1.)

[3] See for example, L. B. Valdes, "Resistivity measurement on germanium for transistors," PROC. IRE, vol. 42, pp. 420–427; February, 1954.

World Radio History

*2.3 Electric Circuit and Operating Procedure*

The components of the measuring system to be used are shown in Fig. 1. The current source may either be a battery or a hum-free power supply. In series with this is a nonreactive low-noise resistor $R_L$, whose resistance must be at least 20 times greater than the sample resistance (so that a constant current is preserved during illumination). A multirange micro- and milliammeter is desirable for observing the actual current I. $V_B$ and $R_L$ will normally be adjustable either continuously or in steps. The photoconductive-decay pattern should be observed for both polarities of the constant-current source. It is convenient to take the output signal to the preamplifier and oscilloscope from the side of the reversing switch remote from the specimen, so that the oscilloscope display is not inverted when the specimen current is reversed. When a flash of light occurs, the oscilloscope may be triggered either directly from the light source or from the rise of the photoconductive signal $\Delta V$. It is preferable to trigger the scope by the light source, since this guarantees that the entire decay can be viewed.

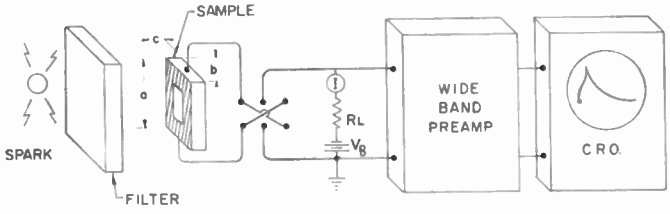


Fig. 1—Schematic circuit arrangement.

*2.3.1 Precaution:* The specimen is to be mounted in a metal box which provides adequate electrical shielding. All connections between parts of the system are to be made with shielded cables which must be kept as short as possible. "Sweep-out" of charge carriers must be obviated by use of a sufficiently small electric field in the sample. For specimens of $\tau < 100$ μsec, a field of up to 0.5 v/cm may be permissible, but a smaller field must be used for material of longer lifetime in accordance with (6). The criterion of satisfactory field for any specimen must finally rest on the observation that the lifetime does not depend on the magnitude or polarity of the impressed current.

*2.3.2 Pre-amplifier and Oscilloscope Requirements:* The requirements for the performance of pre-amplifier and oscilloscope should be considered together. The more responsive one unit is, the less sensitivity is required of the other. Taken together, they should have the following characteristics:

a) Calibrated vertical deflection sensitivity of 2 cm/mv or better.
b) Vertical gain and deflection linear to within 3 per cent.
c) Rise time not more than 0.2 μsec.

In addition, the oscilloscope should:

d) Have a calibrated time base correct to 3 per cent and linear to within 3 per cent.
e) Be capable of being triggered by the signal being studied or by an external signal.
f) Be fitted with a reticule marked in centimeter squares on the back face (*i.e.*, the face nearest the CRT) on which is marked a curve, the height of which above the reticule base line decays exponentially with distance from the left, *i.e.*, $y = y_0 \exp(-x/L)$. Fig. 2 illustrates this, the curve (a) in the figure satisfying the equation $y = 6 \exp(-x/2.5)$ with $x$ and $y$ in scale divisions.

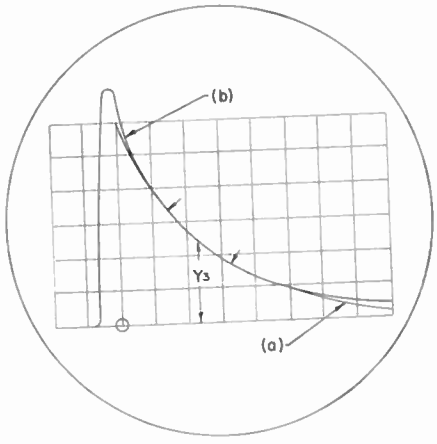


Fig. 2.

*2.3.3 Suggested Measurement Procedure:*

1) For reasonably small modulation (see Sections 2.2.1 and 2.4.2), the photoconductive signal voltage $\Delta V$ is proportional to the total number $n$ of excess carriers in a filament. The mean volume concentration of excess carriers $\Delta\bar{n}$ through the affected region of the specimen is of course related to $n$ by a simple geometric multiplying factor. Under these conditions the time constant of voltage decay $\tau v$ equals $\tau f$, the time constant of excess carrier decay.
2) When illumination has ceased, $\tau f$ is defined by the rate of decay of $\Delta\bar{n}$. Thus

$$(1/\tau f) = -(1/\Delta\bar{n})(d\Delta\bar{n}/dt) = -d(\ln \Delta\bar{n})/dt, \quad (8)$$

or

$$\Delta\bar{n} = A \exp(-t/\tau f). \quad (9)$$

3) The quantity $\tau f$ need not be constant during a decay, and certainly will not be if there are recombination processes present for which the recombination rate does not vary linearly with the local excess carrier density. But in the *simple* case, $\tau f$ does *not* depend on $\Delta\bar{n}$, and the decay exempli-

World Radio History

fied by (9) follows a pure exponential when higher-order modes of surface decay have become sufficiently attenuated.

4) The single time constant of a purely exponential photoconductive decay signal is to be measured by matching the decay of $\Delta V$ against the drawn exponential [curve (a)] of Fig. 2 on the oscilloscope face. The sequence of operations is as follows:

   a) Using a slow time sweep so that the screen width encompasses many lifetimes, the vertical shift control is adjusted to coincidence between the base line of the marker curve and base line of the decay itself.
   b) The time base is expanded to produce a decay trace similar to that of the marker (using either the signal itself or a separate synchronizing pulse to trigger the oscilloscope), and the horizontal shift, vertical amplification, and time-base-sweep speed controls are adjusted until the decay exactly matches the marker curve.
   c) If the decay *is* pure exponential, the match of decay and marker will be equally good when the vertical amplification is increased or decreased and the horizontal shift moved an appropriate amount to left or right. In making such a check, take care that no stage of the amplification system is driven into nonlinear conditions.
   d) If the marker curve is drawn to attenuate by a factor of $e=2.718$ in $L$ cm, and the trace follows the same decay when the time base sweep is set at $S_1$ $\mu$sec/cm, then the filament lifetime is

$$\tau f = LS_1 \ \mu\text{sec}. \tag{10}$$

5) It should be noted that the above procedure requires an oscilloscope for which the time base is continuously calibrated. However, many oscilloscopes have only a number of fixed calibrated sweep rates, the interpolated rates being uncalibrated. With such an instrument, proceed as follows:

   a) Carry out the steps described in 4)-a), -b), and -c) in order to verify that the decay *is* pure exponential.
   b) Turn the sweep speed to the nearest calibrated position, say $S_2$ $\mu$sec/cm. Measure the horizontal distance, say $M$ cm between any two points on the decay whose amplitudes are in a ratio of 2:1. Then the filament lifetime is

$$\tau f = \frac{MS_2}{\ln 2} = 1.44MS_2 \ \mu\text{sec}. \tag{11}$$

6) From (8) it is evident that in measuring lifetime we are measuring the logarithmic decay slope of $\Delta\bar{n}$. This is simple when $\tau f$ is constant, for then the curve is a pure exponential which has the same logarithmic slope throughout. In many experimental cases, however, the logarithmic slope changes through the course of the decay, *i.e.*, $\tau f$ is a function of $\Delta\bar{n}$. It is still possible to measure lifetime, but now the filament must be described by a series of pairs of values for $\tau f$ and $\Delta\bar{n}$.

7) In the general case, then, a lifetime is determined from the slope and amplitude of decay at a single instant. This may be done by matching the decay rate at a given point to the decay rate of an exponential marker curve, as in Fig. 2. The two curves have identical slopes at a certain amplitude (say $y=y_3$) when the sweep speed is $S_3$ $\mu$sec/cm; thus

$$\tau f = LS_3 \ \mu\text{sec}$$

for

$$y = y_3, \qquad \Delta\bar{n} = \Delta\bar{n}_3 \tag{12}$$

but there will be a finite region of the decay, indicated by a pair of arrows, for which the difference between the two curves is imperceptible. The more strongly $\tau$ depends on $\Delta\bar{n}$, the shorter will this region of apparent coincidence be, and the more important will it be to measure $\tau f$ for a number of values of $\Delta\bar{n}$.

8) The procedure of Section 7) can be carried out only with an oscilloscope of continuously calibrated sweep. Using an instrument with only fixed calibrated points, it is necessary to adopt the procedure of Section 5) for any decay, whether pure exponential or not. This has the effect of measuring the *average logarithmic slope* of decay between points corresponding with an amplitude ratio of 2:1. When $\tau$ is a gradual function of $\Delta n$, the error involved in such a procedure is not large. But $\tau$ can be a rapid function of $\Delta n$ in $p$-type silicon, and the error involved in taking such a wide range average may then be severe.

9) Even when the lowest mode of bulk and surface recombination is purely exponential in decay, higher modes will interfere in the early stages. Then $\Delta V$ will be a rapid function of $t$ at first, approaching the behavior of the lowest mode as the decay proceeds. No measurement of the decay slope should be made until the signal has decayed to less than 60 per cent of the peak value if half or less of the width of the filament is exposed to illumination. On the other hand, if more than half the entire width of the specimen is illuminated, no measurement should be made until the signal is less than 25 per cent of the peak value.

World Radio History

### 2.4 Interpretation

*2.4.1 Analysis of Nonexponential Decay:* Often, in the case of silicon measurements, the decay curve will not consist of a single exponential. Three general cases can arise as follows:

A) Trapping (see Fig. 3). It may be determined whether the longer time constant for the final decay at room temperature is due to trapping, by heating the sample to 50–70°C and observing whether the long time constant disappears. If the tail does disappear with heating, one has trapping, and a reliable lifetime determination will not be possible by the present method. When trapping is present to no greater extent than 5 per cent of the total amplitude, a determination of lifetime can still be made by matching the exponential. A steady background light might also be used to test for traps, and this is perhaps simpler than the heating of the sample.

B) The initial part of the decay, representing usually less than 40 per cent of the amplitude, should be ignored, since it does not represent the true lifetime (see Fig. 4). The initial decay is a function mainly of higher modes associated with surface recombination.

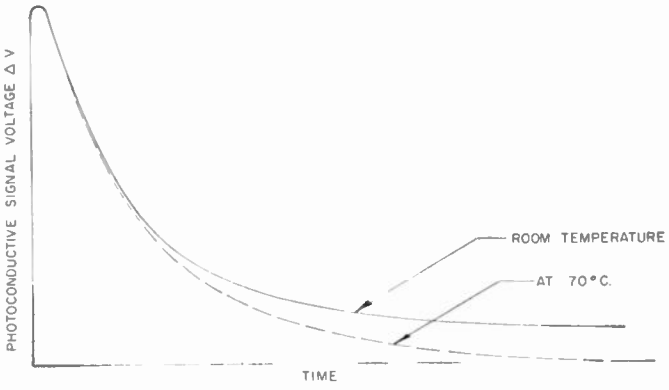


Fig. 3—Evidence of trapping.

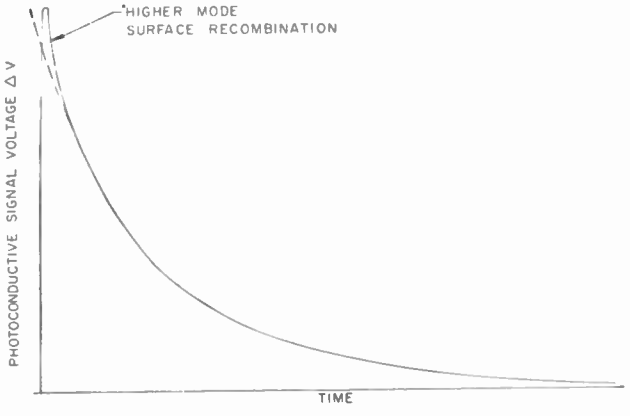


Fig. 4—Evidence of surface recombination.

C) In some cases, even after taking under consideration parts A) and B), it still will not be possible to match the decay curve to the simple exponential. (For example, $\tau B$ is a function of $\Delta n$ in $p$-type silicon.) One can, however, match a portion of the curve representing a particular concentration of excess carriers, which may be calculated from the amplitude as described below.

*2.4.2 Evaluation when Modulation is Finite:*

A) *Relation of carrier and conductivity modulation to signal voltage:* As remarked previously, the sample conductance and potential drop change by the same fractional amount in a constant-current circuit *if the modulation is very small.* For a finite (but not too large) modulation of carrier concentration, the change $\Delta V$ in voltage still can be related to the change in bulk conductivity. Thus, consider a sample of conductivity $\sigma_0$, in which by illuminating a fraction $\beta$ of the width, the conductivity in that fraction is caused to increase to a mean value $(\sigma_0+\Delta\bar{\sigma})$. Then, if $V_0$ was the normal potential drop along the *illuminated* part of the sample length,

$$\Delta\bar{\sigma} = \frac{(\sigma_0)}{\beta}\cdot\frac{(\Delta V/V_0)}{1-(\Delta V/V_0)}, \qquad (\Delta V/V_0) \leq 0.1. \quad (13)$$

Since $\sigma_0$ will customarily be measured on any sample prior to a lifetime determination, a given $\Delta V$ can be converted into the corresponding $\Delta\bar{\sigma}$. When trapping is absent, the relation

$$\Delta\bar{n} = \frac{\Delta\bar{\sigma}}{e(\mu_n+\mu_p)}, \qquad \Delta\bar{n} \leq \frac{n_0}{20} \text{ or } \frac{p_0}{20} \quad (14)$$

may be used to go a stage further, and permit the mean volume concentration of excess carriers to be deduced from the conditions of the measurement.

Only when results of high precision are required is it necessary to use (13) rather than the simple limiting form for small modulation,

$$\Delta\bar{\sigma} = (\sigma_0/\beta)\cdot(\Delta V/V_0), \qquad (\Delta V/V_0) \ll 1. \quad (15)$$

The assumption that an excess carrier will provide the same current impulse wherever it is created in a sample is only valid if the concentration of such carriers is everywhere small compared with the permanent majority-carrier concentration. Thus the preceding discussion requires that the majority-carrier concentration be modulated by not more than 5 per cent.

Indeed, measurement should not normally be made with a modulation anywhere near this large, unless there is a specific need to know $\tau B$ for a certain excess pair density. In the characterization of bulk material, measurements involving very small departures from thermal equilibrium are usually most reproducible and, therefore, most useful.

*B) Voltage- and carrier-decay coefficients for finite modulation:* When measurements must be made for

World Radio History

more than one per cent carrier-concentration modulation, not only should (13) be used rather than (15), but a distinction should also be made between the time constant of *voltage* decay $\tau v = -\Delta V(dt/d\Delta V)$ and the *filament* lifetime $\tau f = -\Delta\bar{n}(dt/d\Delta\bar{n})$. These two time constants are equal for very small modulation, but for finite modulation

$$\tau f = \tau v[1 - (\Delta V/V_0)]. \tag{16}$$

The quantity experimentally determined is $\tau v$, but by using (16) it is a simple matter to obtain $\tau f$. The surface correction may then be applied to yield the volume lifetime

$$\tau B = [(1/\tau f) - \nu_s]^{-1}. \tag{17}$$

## Appendix

Data are given below for the three standard sample sizes:

| *Type* | *Length* | *Cross Section* |
|---|---|---|
| A | 1.5 cm | 0.25×0.25 cm² |
| B | 2.5 | 0.5 ×0.5 |
| C | 2.5 | 1.0 ×1.0 |

The value of the maximum volume lifetime measurable for each of these sample sizes is given in Table I, and the corresponding surface recombination rate $\nu_s$ used to determine the maximum lifetime is given in Table II. The maximum value of lifetime here is set by the condition that $\tau B$ should not be larger than $1/\nu_s$. When this condition is reached, $\tau f = \tau B/2 = 1/2\nu_s$. Thus, $\tau f$ should not exceed half the value listed here for each specimen size. In the starred cases, it may be desirable to stretch the upper limit to 1000 μsec ($\tau f = 320$ μsec for $p$-type germanium, $\tau f = 490$ μsec for $n$-type germanium), recognizing that uncertainty in the surface term will have a greater effect on the final result. Values of $D_n = 101$, $D_p = 49$ cm²/sec for germanium, and $D_n = 35$, $D_p = 13.1$ cm²/sec for silicon were used in calculating the values given in Tables I and II.

TABLE I
Maximum Measurable Values of Volume Lifetime $\tau B$

| Sample | Type A | Type B | Type C | |
|---|---|---|---|---|
| $p$-type Ge | 32 μsec | 125 μsec | 460 μsec | * |
| $n$-type Ge | 64 | 250 | 950 | * |
| $p$-type Si | 90 | 350 | 1340 | |
| $n$-type Si | 240 | 950 | 3600 | |

TABLE II
Surface-Recombination Rate $\nu_s$

| Sample | Type A | Type B | Type C |
|---|---|---|---|
| $p$-type Ge | 32,300 sec⁻¹ | 8130 sec⁻¹ | 2150 sec⁻¹ |
| $n$-type Ge | 15,750 | 3960 | 1050 |
| $p$-type Si | 11,200 | 2820 | 745 |
| $n$-type Si | 4,200 | 1050 | 279 |

# Detection Range Predictions for Pulse Doppler Radar*

S. A. MELTZER†, SENIOR MEMBER, IRE, AND S. THALER‡, MEMBER, IRE

*Summary*—**A mathematical model of sufficient flexibility to describe most pulse Doppler radar search systems is constructed and used to predict detection ranges. It is applicable to situations where thermal noise and/or sidelobe clutter limits detection range. The sidelobe clutter is assumed to be statistically similar to thermal noise. The model allows the variation of most of the important radar parameters. The receiver is assumed to have a number of rectangular, nonoverlapping range gates followed by narrow-band, Gaussian shaped Doppler filters, and then a square-law envelope detector followed by a postdetection filter consisting of one or two stages having exponential weighting functions. Single scan and cumulative probabilities of detection are calculated for both steady and scintillating targets.**

* Received by the IRE, March 18, 1960; revised manuscripts received, October 17, 1960 and February 3, 1961.

† Res. and Dev. Labs., Hughes Aircraft Co., Culver City, Calif.
‡ West Coast Missile and Surface Radar Div., RCA, Van Nuys, Calif. Formerly with Hughes Aircraft Co., Culver City, Calif.

## I. Introduction

ALTHOUGH the literature dealing with the performance of radar systems is extensive, there are only a few[1,2] treatments of pulse Doppler radar systems. The case of a "matched filter" radar has been analyzed by Siebert.[3] The object of this paper is to predict the detection capability of a pulse Doppler radar where the Doppler filter bandwidth is much wider than the bandwidth of each spectral line in the received signal.

[1] J. J. Bussgang, P. Nesbeda, and H. Safran, "A unified analysis of range performance of CW, pulse, and pulse Doppler radar," Proc. IRE, vol. 47, pp. 1753–1762; October, 1959.
[2] E. J. Barlow, "Doppler radar," Proc. IRE, vol. 37, pp. 340–355; April, 1949.
[3] W. McC. Siebert, "A radar detection philosophy," IRE Trans. on Information Theory, vol. IT-2, pp. 204–221; September, 1956.

World Radio History

Unlike those papers which use false alarm probabilities, this paper considers the false alarm rate as one of the fundamental design parameters. (The false alarm rate is proportional to the amplitude density of the noise,[4] whereas the false alarm probability is proportional to the cumulative probability density of the noise.) Moreover, this treatment introduces a mathematical model of sufficient flexibility to predict detection ranges for many pulse Doppler radar search systems. It is applicable to situations where thermal noise and/or sidelobe clutter limits detection range. The sidelobe clutter is assumed to be statistically similar to thermal noise. The model allows the variation of most of the important radar parameters. The antenna beam shape is assumed to be Gaussian; however, the scan speed and beamwidth remain general. The receiver is assumed to have a number of rectangular, nonoverlapping range gates, each followed by a multiplicity of Gaussian shaped Doppler filters. The number and width of gates and filters are left open. The output of the Doppler filter is passed through a square-law envelope detector followed by a postdetection filter consisting of one or two stages having exponential weighting functions. A block diagram of the radar receiver is found in Fig. 1.

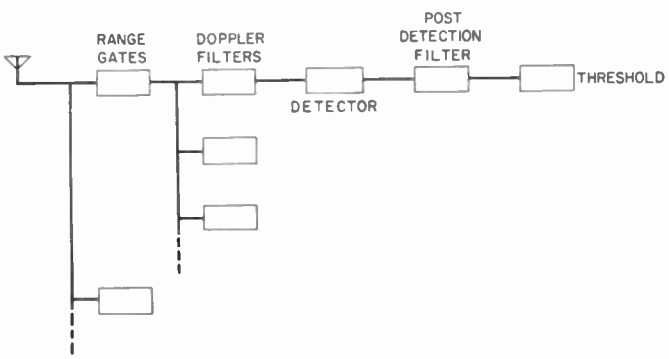


Fig. 1—Block diagram of a pulse Doppler receiver.

It is assumed that the received signal falls in the center of the Doppler filter. However, the power lost by not having the signal in the center of the filter becomes important only when the filter gain at the crossover becomes less than about 2 db. With this degree of overlap, the detection range does not change much with the frequency of the received signal.

The square-law envelope detector was selected for analysis mainly for mathematical convenience. Nevertheless, on the basis of a "Monte Carlo" simulation of the detection process on a digital computer,[5] the detection range with a linear envelope detector is not appreciably different from that of the square-law device. Marcum[6] has also found in his studies very little difference in results between linear and square-law detectors.

Single-scan detection probabilities are computed by calculating the probability that signal plus noise (or noise plus clutter) exceeds a threshold at the time for which the ensemble average of signal plus noise is maximum. The aforementioned "Monte Carlo" simulation indicates that the calculation of the probability of detection at the peak signal-to-noise ratio is an excellent approximation.

The model allows the target either to be steady or to scintillate slowly with a Rayleigh amplitude distribution; that is, the target cross section remains constant during the time on target but may vary randomly from scan to scan.

## II. Detailed Calculations

### A. *Notation*

$A$ = amplitude of the received signal
$f_c$ = carrier frequency of the received signal
$t$ = time
$\Psi$ = phase factor
$W$ = pulse width
$T$ = pulse repetition period
$g(t)$ = two-way voltage gain of the normalized antenna pattern
$\dot{\theta}$ = antenna scan rate
$\theta_{HP}$ = half-power beamwidth of the one-way antenna pattern
$s(t)$ = signal output of the Doppler filter
$n(t)$ = noise output of the Doppler filter
$x(t)$ = component of the noise
$y(t)$ = component of the noise
$E(t)$ = signal-plus-noise output of the Doppler filter
$f$ = frequency
$W(f)$ = power spectrum of the noise
$\gamma$ = noise power per cycle at the Doppler filter input

[4] S. Thaler and S. A. Meltzer, "The amplitude distribution and false alarm rate of noise after post-detection filtering," Proc. IRE, vol. 49, pp. 479–485; February, 1961.
[5] Hughes Aircraft Co., Culver City, Calif., internal rept.
[6] J. I. Marcum, "A statistical theory of target detection by pulsed radar," IRE Trans. on Information Theory, vol. IT-6, pp. 59–144; April, 1960.

World Radio History

$B$ = noise bandwidth of the Doppler filter
$U(t)$ = low-frequency output of the square-law detector
$V(t)$ = output of the postdetection filter
$h(t)$ = weighting function of the postdetection filter
$\tau_0$ = time constant of the single low-pass postdetection filter
$J(t)$ = Signal-to-noise ratio (SNR) after the low-pass filter
$V_n(t)$ = noise output of the low-pass filter when there is no signal present
$N$ = noise power after postdetection filtering
$F$ = SNR in the Doppler filter
$\alpha$ = time on target
$P_D$ = single-scan detection probability
$\alpha$ = threshold setting
$K$ = number of range gates
$D$ = range-gate width
$P_C$ = cumulative probability of detection
F.A.R. = false-alarm rate per Doppler channel
$M$ = expected number of positive crossings of the mean of the noise after postdetection filtering
$Q(\alpha)$ = probability density of the noise amplitude after postdetection filtering

$$\Phi(x) = \frac{1}{\sqrt{2\pi}} \int_0^x e^{-t^2_1/2} dt.$$

### B. Output of the Doppler Filter

The signal at the receiver consists of a periodically pulsed, coherent sinusoid whose amplitude is modulated by the antenna pattern as the beam linearly sweeps the target and whose frequency differs from that of the transmitter by a Doppler shift. It is assumed at this point that the received pulse falls completely within the range gate and that the target is not scintillating. These restrictions will be removed in later sections of this paper. This signal can be represented as the product of a Doppler-shifted sinusoid

$$A \cos (2\pi f_c t + \Psi), \tag{1}$$

a pulsing function

$$\frac{W}{T} + \sum_{n=1}^{\infty} \frac{2}{n\pi} \sin \frac{n\pi W}{T} \cos 2\pi \frac{n}{T} t, \tag{2}$$

and an amplitude modulation proportional to the two-way voltage gain of the normalized antenna pattern, assumed to be Gaussian and denoted by $g(t)$,

$$g(t) = \exp\left[-\left(\frac{\dot{\theta} t}{\theta_{HP}}\right)^2 4 \ln 2\right] \tag{3}$$

where $f_c$ is the carrier frequency of the received signal, $W$ is the pulse width, $T$ is the pulse repetition period, $\dot{\theta}$ is the antenna scan rate, $\theta_{HP}$ is the half-power beamwidth of the antenna one-way power pattern, and the target is on the peak of the beam at time $t = 0$.

If it is assumed that the width of the Doppler filter is such that only the center line of the received spectrum (along with the modulation sidebands due to the antenna pattern) is passed, the output of the Doppler filter, denoted by $s(t)$, is

$$s(t) = \frac{AW}{T} \exp\left\{-\left(\frac{\dot{\theta} t}{\theta_{HP}}\right)^2 4 \ln 2\right\} \cos (2\pi f_c t + \Psi). \tag{4}$$

This result also assumes that the Doppler filter is wide compared to the bandwidth of each spectral line in the received signal. If this assumption is not true (4) must be modified accordingly.

The output of the Doppler filter also includes noise, $n(t)$, and/or clutter. Since the clutter is assumed to be statistically similar to random noise, it will merely be necessary to study the case where noise alone is present, and then to modify the results to account for the clutter. The total Doppler-filter output is the sum of signal and noise, which is denoted by $E(t)$.

$$E(t) = s(t) + n(t). \tag{5}$$

The process $n(t)$, which consists of white Gaussian noise, passed through the Doppler filter, is assumed to be stationary and ergodic. Narrow-band noise can be represented by[7]

$$n(t) = x(t) \cos 2\pi f_c t - y(t) \sin 2\pi f_c t, \tag{6}$$

where $x(t)$ and $y(t)$ are independent Gaussian processes with zero means and equal variances. It is assumed that the center of the Doppler filter is at $f_c$ and that the filter is Gaussian in shape. Thus, the power spectrum of the noise is

$$W(f) = \frac{\gamma}{2} \left[e^{-(\pi(f-f_c)^2)/B^2} + e^{-(\pi(f+f_c)^2)/B^2}\right], \tag{7}$$

where $B$ is the noise bandwidth of the Doppler filter and $\gamma$ is the noise power per cycle at its input. The average noise power out of the Doppler filter is equal to $\gamma B$.

$$E(t) = \frac{AW}{T} g(t) \cos (2\pi f_c t + \Psi) + x(t) \cos 2\pi f_c t - y(t) \sin 2\pi f_c t. \tag{8}$$

### C. Low-Frequency Output of the Square-Law Detector

The square-law detector is followed by a low-pass filter, so the high-frequency output of the square-law device will be filtered out. The low-frequency output, denoted by $U(t)$, is

$$U(t) = \frac{1}{2}\left\{\frac{A^2W^2}{T^2} g^2(t) + x^2(t) + y^2(t) + \frac{2AW}{T} g(t)[x(t) \cos \Psi + y(t) \sin \Psi]\right\} \tag{9}$$

[7] S. O. Rice, "Mathematical analysis of radar noise," *Bell Sys. Tech. J.*, vol. 24, p. 75; January, 1945.

World Radio History

*D. Output of the Postdetection Filter*

The output of the postdetection filter, denoted by $V(t)$, is

$$V(t) = \int_{-\infty}^{t} h(t-\tau)U(\tau)d\tau, \tag{10}$$

where $h(t)$ is the filter weighting function, or impulsive response.

Two weighting functions for the postdetection filter will be considered. The first is assumed to be exponential.

$$h_1(t) = \begin{cases} \dfrac{1}{\tau_0} e^{-t/\tau_0} & 0 \le t \\ 0 & 0 > t. \end{cases} \tag{11}$$

$\tau_0$ is the time constant of the filter. The output of this filter, $V_1(t)$, is

$$V_1(t) = \int_{-\infty}^{t} \frac{1}{\tau_0} e^{-(t-\tau)/\tau_0} U(\tau)d\tau. \tag{12}$$

The second weighting function is obtained by cascading two filters, each having an exponential weighting function. The resulting weighting function is

$$h_2(t) = \begin{cases} \dfrac{t}{\tau_0^2} e^{-t/\tau_0} & 0 \le t \\ 0 & 0 > t. \end{cases} \tag{13}$$

The filter output, $V_2(t)$, is

$$V_2(t) = \int_{-\infty}^{t} \frac{(t-\tau)}{\tau_0^2} e^{-(t-\tau)/\tau_0} U(\tau)d\tau. \tag{14}$$

*E. The Time Constant of the Postdetection Filter*

The signal-to-noise ratio after the postdetection filter, designated by the symbol $J(t)$ will be defined as the ratio of the increase in the expected value of the filter output when signal is present to the standard deviation of the noise fluctuations out of the filter with no signal present.

$$J(t) = \frac{\langle V \rangle - \langle V_n \rangle}{[\langle V_n^2 \rangle - \{\langle V_n \rangle\}^2]^{1/2}}, \tag{15}$$

where $V_n(t)$ is the output of the low-pass filter when there is no signal present.

The notation $\langle\ \rangle$ indicates the ensemble average of the quantity enclosed. The ensemble averages of $V_n$ and $V_n^2$ are assumed to be independent of time. However, the ensemble average of signal plus noise, $\langle V \rangle$, is a function of time. To simplify future equations, let $\langle V_n^2 \rangle$, the noise power out of the postdetection filter, be denoted by $N$. The value of the filter time constant will be selected to maximize this SNR.

1. *Single Low-Pass Filter:* From (12) and (39) it is seen that

$$\langle V_1(t) \rangle = \gamma B + \frac{A^2 W^2}{2\tau_0 T^2} \int_{-\infty}^{t} e^{-(t-\tau)/\tau_0} g^2(\tau)d\tau, \tag{16}$$

and

$$\langle V_n(t) \rangle = \gamma B. \tag{17}$$

The value of $N_1$ is given by equation (50). The SNR, $J_1(t)$, is

$$J_1(t) = \frac{2^{3/4} B^{1/2} F}{\tau_0^{1/2}} \int_{-\infty}^{t} e^{-(t-\tau)/\tau_0} g^2(\tau)d\tau \tag{18}$$

where $F$, the SNR in the Doppler filter, is defined by

$$F = \frac{A^2 W^2}{2T^2 \gamma B}. \tag{19}$$

The SNR at the output of the single low-pass filter, $J_1(t)$, considered as a function of $\tau_0$ and $t$, takes on its maximum value at $\tau_0 = 0.62a$ and $t = 0.31a$. The symbol $a$ stands for the time on target defined by

$$a = \frac{\theta_{HP}}{\dot{\theta}}. \tag{20}$$

This maximum value is

$$J_1 = 0.77 B^{1/2} a^{1/2} F. \tag{21}$$

2. *Cascaded Low-Pass Filter:* From (14) and (39) it is seen that

$$\langle V_2(t) \rangle = \gamma B + \frac{A^2 W^2}{2\tau_0^2 T^2} \int_{-\infty}^{t} (t-\tau) e^{-(t-\tau)/\tau_0} g^2(\tau)d\tau. \tag{22}$$

The value of $N_2$ is found from (53). The SNR $J_2(t)$ is

$$J_2(t) = \frac{2^{5/4} B^{1/2} F}{\tau_0^{3/2}} \int_{-\infty}^{t} (t-\tau) e^{-(t-\tau)/\tau_0} g^2(\tau)d\tau. \tag{23}$$

$J_2(t)$ takes on its maximum value for $\tau_0 = 0.29a$ at $t = 3/2\tau_0$. The maximum value of the SNR is

$$J_2 = 0.84 B^{1/2} a^{1/2} F. \tag{24}$$

*F. Probability of Detection*

The single-scan probability of detection calculated at the instant of time at which the SNR out of the postdetection filter is maximum will be denoted by $P_D$. The event of detection will be said to have occurred if the output of the postdetection filter exceeds the threshold setting in the threshold device. The detection probability during the time interval when the output SNR is near its peak value can be obtained by making the very reasonable assumption that the amplitude statistics of the output of the low-pass filter are approximately Gaussian. Let the threshold setting be given by a constant $\alpha$ times the standard deviation of the noise fluctuations out of the low-pass filter when no signal is present. Then from (21) and (61), the probability of detection for the system having the single low-pass filter is

$$P_D(F) = \frac{1}{2} - \Phi\left\{\frac{\alpha - 0.77 B^{1/2} a^{1/2} F}{(1 + 2.12F)^{1/2}}\right\}. \tag{25}$$

World Radio History

1961

.d setting $\alpha$ is measured
f the postdetection filter
It is to be noted that the thresh
from the mean noise level. (24) and (64) are utilized
when no signal is present
to determine the p
having the case $\Phi\left\{\frac{\alpha - 0.84B^{1/2}a^{1/2}F}{(1 + 2.22F)^{1/2}}\right\}$. (26)

of detection for the system
pass filter.

) yield the single-scan probability of
e case where the pulse train received
suffers no degradation due to obscuring
nitter or by straddling of the range gates.
e, (25) and (26) hold only for a nonscintil-
get. It is not difficult to modify these equations
ve these restrictions.

1. *Range Gating:* For the purpose of this calculation, the following assumptions are made:

1) The receiver has $K$ nonoverlapping range gates, each of time duration $D$.
2) The relative time of reception of pulses within a range gate does not alter during the on-target period.
3) From scan to scan, the reception of the pulse train will commence with equal probability anywhere within the interval between pulses (pulse repetition period).

It is further assumed that

$$D \geq W, \tag{27}$$

where $W$ is the pulse width and $D$ the gate width. Eq. (19) shows that the SNR, $F$, is proportional to $W^2$. Thus, the probability of detection averaged over all possible reception times of the received pulse train within a pulse repetition period, denoted by $\overline{P_D(F)}$, is

$$\overline{P_D(F)} = K\left(\frac{D}{T} - \frac{W}{T}\right)P_D(F) + 2\frac{W}{T}\int_0^1 P_D(x^2F)dx + (K-1)\frac{W}{T}\int_0^1 P_D(x^2F)\left[2 - P_D\left\{(1-x)^2F\right\}\right]dx. \tag{28}$$

The first term in (28) accounts for the return pulse being completely within the range gate; the second term accounts for the effect of its straddling the leading edge of the first gate or the trailing edge of the $K$th gate; and the third term accounts for its straddling the boundary between two gates. Thus, for a nonscintillating target, the single-scan probability of detection for the system having the single low-pass filter is found by combining (25) and (28), and the probability of detection for the system having the cascaded low-pass filter is found by combining (26) and (28).

2. *Target Scintillation:* The case of slow scintillation —that is, when the cross section remains constant during the time on target but may vary randomly from scan to scan—will be considered here. We will assume that the radar cross section, which is directly proportional to $F$, is exponentially distributed. (This implies that the envelope statistics of the target return is Rayleigh distributed.) Then the single-scan probability of detection, averaged over the target's scintillation and denoted by $\langle\overline{P_D(F)}\rangle$, is

$$\langle\overline{P_D(F)}\rangle = \int_0^\infty e^{-y}\,\overline{P_D(yF)}\,dy. \tag{29}$$

3. *Cumulative Probability of Detection:* Let the cumulative probability of detection at the $n$th scan be defined as the probability that the target has been detected at least once by the $n$th scan. Then the cumulative probability of detection is given by

$$P_C^{(n)} = P_C^{(n-1)} + \left[1 - P_C^{(n-1)}\right]P_D^{(n)}, \tag{30}$$

where

$P_C^{(n)}$ is the cumulative probability of detection and
$P_D^{(n)}$ is the single-scan probability of detection for the $n$th scan.

## G. False Alarm Rate

An extensive study[4] has been carried out on an IBM 709 to determine the false-alarm rate for the detector and postdetection filtering assumed in this paper. It was concluded that the false-alarm rate (F.A.R) could be represented by

$$\text{F.A.R.} = \frac{MQ(\alpha)}{Q(0)}. \tag{31}$$

where $M$ is the expected number per second of positive crossing of the mean of the noise out of the postdetection filter, $Q$ is the probability density of this noise amplitude, and $\alpha$ is the threshold level, measured from the mean output in standard deviations of the noise out of the postdetection filter. The above formula holds in the region where false alarms are relatively rare, *i.e.*, much less than one false alarm during the time on target. Rice's[8] formula for Gaussian noise for the expected number of positive crossings of a threshold is the same form as (31).

Explicit expressions for $M$ have been derived in Appendix IV. If these expressions are evaluated for the optimum time constants for the respective postdetection filters, it is found that

$$M_1 = 0.34(B/a)^{1/2} \tag{32}$$

for the single low-pass filter, and

$$M_2 = \frac{0.55}{a} \tag{33}$$

for the cascaded low-pass filter. $Q(\alpha)$ is graphed for each postdetection filter in Figs. 2 and 3, respectively.

[8] S. O. Rice, "Mathematical analysis of random noise," *Bell Sys. Tech. J.*, vol. 24, p. 55; Eqs. 3.3-14; January, 1945.

World Radio History

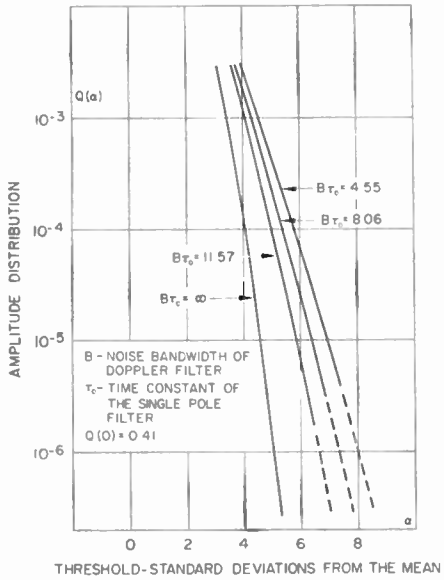


Fig. 2—Amplitude distribution after postdetection filtering (square-law detector, single-pole filter).

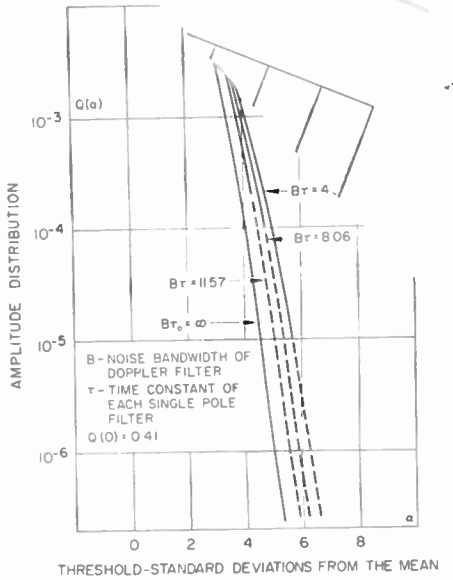


Fig. 3—Amplitude distribution after postdetection filtering (square-law detector, double-pole filter).

## III. Detection Range Predictions

The system parameters in conjunction with the radar range equation can be used to calculate the SNR in the Doppler filter. Denoting this SNR by $F$ [refer to (19)], we have

$$F = \frac{P_{av}(W/T)G_0^2\lambda^2\bar{\sigma}L}{(4\pi)^3(D/T)kT_EBR^4}, \tag{34}$$

where

$P_{av}$ = average transmitter power
$W$ = transmitted pulse width
$T$ = pulse repetition period
$G_0$ = antenna axial gain (one-way)
$\lambda$ = carrier wavelength
$\bar{\sigma}$ = mean target cross section
$L$ = real system losses (plumbing, radome, atmospheric attenuation)
$D$ = time duration of the range gate
$k$ = Boltzmann's constant ($1.38\times10^{-23}$ joules per degree Kelvin)
$T_E$ = effective noise temperature of the receiver in degrees Kelvin
$B$ = noise bandwidth of Doppler filter
$R$ = range.

The range at which the value of $F$ is unity is denoted by $R_0$.

$$R_0 = \left[\frac{P_{av}(W/T)G_0^2\lambda^2\bar{\sigma}L}{(4\pi)^3(D/T)kT_EB}\right]^{1/4} \tag{35}$$

Thus it follows that

$$F = \left[\frac{R_0}{R}\right]^4 \tag{36}$$

In the sidelobe clutter region, the only modification to the detection theory is that $R_0$ must be modified to

$$R_0 = \left\{\frac{P_{av}(W/T)G_0^2\lambda^2\bar{\sigma}L}{(4\pi)^3[C + (D/T)kT_EB]}\right\}^{1/4} \tag{37}$$

where $C$ is the clutter power after Doppler filtering.

The single-scan probability of detection as a function of range is computed from (28) and (29), or from (28) alone, depending on whether the target is slowly scintillating or nonscintillating. These equations require as an input either (25) or (26), depending on the type of postdetection filter. A new input equation would be required for types of postdetection filters not covered in this paper. The relationship between the radar parameters and the range is given by (35) and (37). The cumulative probability of detection as a function of range is found from (30). These computations require the specification of the following parameters:

1) Time on target ($a$), determined from (20).
2) Doppler filter noise bandwidth ($B$).
3) Number of range gates ($K$).
4) Transmitter duty factor ($W/T$).
5) Range-gate duty factor ($D/T$).
6) Initial range separation between target and interceptor ($R_I$).
7) Threshold setting ($\alpha$), determined from (31) and Figs. 2 and 3.
8) The range at which the signal-to-noise (or noise-plus-clutter) ratio in the Doppler filter equals unity ($R_0$), determined from (35) and (37).
9) Change in range between scans ($\Delta R$). For a collision course, the change in range between scans, $\Delta R$, equals the product of range closing rate and scan time.

Because of the complicated form of (28) required to account for range-gate straddling and eclipsing by the

World Radio History

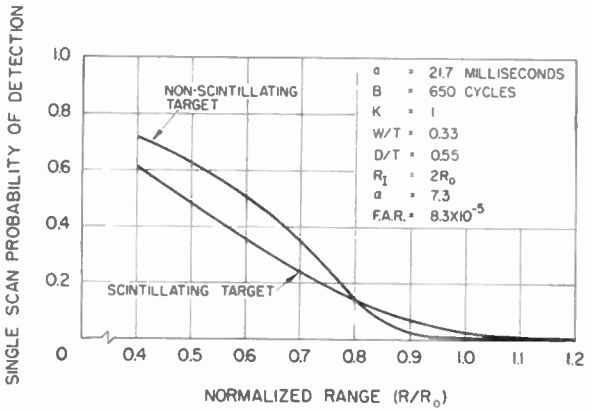


Fig. 4—Single-scan probability of detection (square-law detector, single-pole filter).

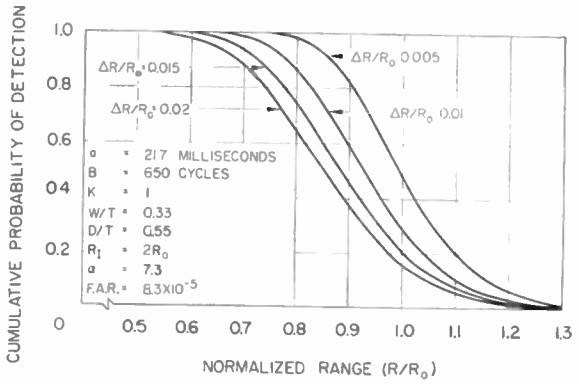


Fig. 5—Cumulative probability of detection of a scintillating target (square-law detector, single-pole filter).

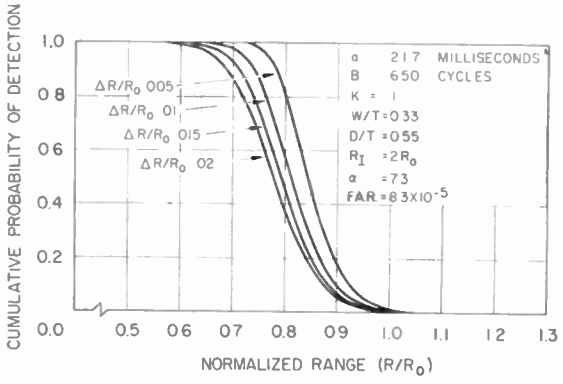


Fig. 6—Cumulative probability of detection of a nonscintillating target (square-law detector, single-pole filter).

transmitter of the received signal, it was found necessary to program these equations for a computer.

Once the false-alarm rate per Doppler channel has been specified, (31) and (32) or (33) enable one to calculate the numerical value of $Q(\alpha)$, the probability density of the noise after postdetection filtering, required to give that false-alarm rate. Fig. 2 or 3 is then used to yield the appropriate value of $\alpha$, the threshold setting. These figures contain plots of the amplitude distribution of the noise after postdetection filtering vs $\alpha$, the threshold setting, for four different ratios of predetection-to-postdetection bandwidth. In most cases, it is necessary to interpolate between these curves to determine the appropriate value of $\alpha$. Typical results obtained by using this detection model are graphed in Figs. 4–6. Graphs of results for the cascaded postdetection filter have been omitted since this filter provides less than 1 db improvement in performance.

## Appendix I

### Low-Frequency Noise Power Spectrum Out of the Square-Law Detector

It is seen from (9) that if no signal is present, the low-frequency noise out of the detector, denoted by $n_0(t)$, is

$$n_0(t) = \tfrac{1}{2}[x^2(t) + y^2(t)]. \tag{38}$$

The correlation function of $n_0(t)$ is designated $R(\tau)$. By definition,

$$\langle x(t)x(t+\tau)\rangle = \langle y(t)y(t+\tau)\rangle = \gamma B\rho(\tau) \tag{39}$$

where $\rho(\tau)$ is the normalized correlation function. Further, since $x$ and $y$ are independent Gaussian processes,

$$\begin{aligned}\langle x^2(t)x^2(t+\tau)\rangle &= \langle y^2(t)y^2(t+\tau)\rangle \\ &= (\gamma B)^2[1 + 2\rho^2(\tau)]\end{aligned} \tag{40}$$

from which it follows that

$$R(\tau) = \langle n_0(t)n_0(t+\tau)\rangle = (\gamma B)^2[1 + \rho^2(\tau)]. \tag{41}$$

Using (6) and (7), we can easily show that

$$\rho(\tau) = e^{-\pi B^2\tau^2}. \tag{42}$$

Representing the low-frequency power spectrum of the noise out of the detector by $N(f)$, we have

$$N(f) = (\gamma B)^2 \int_{-\infty}^{\infty} [1 + e^{-2\pi B^2\tau^2}] \cos 2\pi f\tau d\tau. \tag{43}$$

This equals

$$N(f) = (\gamma B)^2 \left[\delta(f) + \frac{1}{\sqrt{2}\,B} e^{-\pi f^2/2B^2}\right] \tag{44}$$

World Radio History

## Appendix II

### Noise Power Out of the Postdetection Filter

It can be shown that the noise power out of the postdetection filter, denoted by $N$, is equal to

$$N = \int_{-\infty}^{\infty} |Y(f)|^2 N(f) df \tag{45}$$

where $Y(f)$, the filter frequency response function, is the Fourier transform of the filter weighting function.

$$Y(f) = \int_{-\infty}^{\infty} h(\tau) e^{i2\pi f\tau} d\tau. \tag{46}$$

*A. Single Low-Pass Filter*

The exponential weighting function is given by (11).

$$Y_1(f) = \int_0^{\infty} \frac{1}{\tau_0} e^{-\tau/\tau_0} e^{i2\pi f\tau} d\tau. \tag{47}$$

Thus,

$$|Y_1(f)|^2 = \frac{1}{1 + 4\pi^2 f^2 \tau_0^2}. \tag{48}$$

Using (44) and (48), the noise power, $N_1$, out of the single low-pass filter is given by

$$N_1 = (\gamma B)^2 \int_{-\infty}^{\infty} \frac{1}{1 + 4\pi^2 f^2 \tau_0^2} \cdot \left\{\delta(f) + \frac{1}{\sqrt{2}\,B} e^{-\pi f^2/2B^2}\right\} df. \tag{49}$$

Integrating equation (49) and assuming that $4\pi B^2\tau_0^2 \gg 1$, we get

$$N_1 = (\gamma B)^2 \left\{1 + \frac{1}{2\sqrt{2}B\tau_0}\right\} \tag{50}$$

*B. Cascaded Low-Pass Filter*

The weighting function of this filter is given by (13). The frequency response function of this filter is the square of that for the single low-pass filter. Thus,

$$|Y(f)|^2 = \frac{1}{[1 + 4\pi^2 f^2 \tau_0^2]^2}. \tag{51}$$

By use of (44), the noise power, $N_2$, out of the cascaded low-pass filter is

$$N_2 = (\gamma B)^2 \int_{-\infty}^{\infty} \frac{1}{[1 + 4\pi^2 f^2 \tau_0^2]^2} \cdot \left\{\delta(f) + \frac{1}{\sqrt{2}B} e^{-\pi f^2/2B^2}\right\} df. \tag{52}$$

Integrating (52) and assuming that $4\pi B^2\tau_0^2 \gg 1$, we get

$$N_2 = (\gamma B)^2 \left\{1 + \frac{1}{4\sqrt{2}B\tau_0}\right\}. \tag{53}$$

## Appendix III

### Standard Deviation of the Fluctuations of Signal with Noise Out of the Postdetection Filter

*A. Single Low-Pass Filter*

The output of the single low-pass filter, $V_1(t)$, is given by (12). The variance of $V_1(t)$ is equal to

$$\text{Var } V_1(t) = \langle [V_1(t) - \langle V_1(t)\rangle]^2 \rangle. \tag{54}$$

The value of $\langle V_1(t)\rangle$ is found from (16). It can easily be seen, by means of (39) and (40), that

$$\text{Var } V_1(t) = \frac{(\gamma B)^2}{\tau_0^2} \int_{-\infty}^{t}\int_{-\infty}^{t} e^{-(t-\tau_1)/\tau_0} e^{-(t-\tau_2)/\tau_0} \cdot \left\{\rho^2(\tau_2 - \tau_1) + 2F\rho(\tau_2 - \tau_1) g(\tau_1) g(\tau_2)\right\} d\tau_2 d\tau_1. \tag{55}$$

For reasons that will become apparent in the next section, it will be convenient to compute the following integral:

$$H(r, s) = \int_{-\infty}^{t}\int_{-\infty}^{t} e^{-r(t-\tau_1)/\tau_0} e^{-s(t-\tau_2)/\tau_0} \cdot \left\{\rho^2(\tau_2 - \tau_1) + 2F\rho(\tau_2 - \tau_1) g(\tau_1) g(\tau_2)\right\} d\tau_2 d\tau_1. \tag{56}$$

It is evident that

$$\text{Var } V_1(t) = \frac{(\gamma B)^2}{\tau_0^2} H(1, 1). \tag{57}$$

We make the substitution $x = \tau_2 + \tau_1$ and interchange the order of integration in (56) to obtain

$$H(r, s) = \frac{\tau_0}{r + s} \int_0^{\infty} \left[e^{-rx/\tau_0} + e^{-sx/\tau_0}\right] \rho^2(x) dx + \frac{\sqrt{2\pi}\, aF}{2\sqrt{\ln 2}} e^{-(r+s)t/\tau_0} e^{-a^2(r+s)^2/32\tau_0^2 \ln 2} \cdot \int_0^{\infty} \left[e^{(r-s)x/2\tau_0} + e^{-(r-s)x/2\tau_0}\right] \left[\frac{1}{2} + \Phi\left(\frac{4t/\sqrt{\ln 2}}{a} - \frac{2x\sqrt{\ln 2}}{a} - \frac{a(r+s)}{4\tau_0\sqrt{\ln 2}}\right)\right] e^{-2x^2 \ln 2/a^2} \rho(x) dx. \tag{58}$$

We replace

$$\frac{1}{2} + \Phi\left(\frac{4t/\sqrt{\ln 2}}{a} - \frac{2x\sqrt{\ln 2}}{a} - \frac{a(r+s)}{4\tau_0\sqrt{\ln 2}}\right)$$

by its Maclaurin's series in $x$, integrate using the definition of $\rho(x)$ given by (42), and assume that $4\pi B^2\tau_0^2 \gg 1$. Thus, we obtain

$$H(r, s) = \frac{\tau_0}{\sqrt{2}(r+s)B} + \frac{\sqrt{2\pi}\, aF}{2B\sqrt{\ln 2}} e^{-(r+s)t/\tau_0 + (r+s)^2 a^2/32\tau_0^2 \ln 2} \cdot \left[\frac{1}{2} + \Phi\left(\frac{4t/\sqrt{\ln 2}}{a} - \frac{a(r+s)}{4\tau_0\sqrt{\ln 2}}\right)\right]. \tag{59}$$

World Radio History

By combining (57), (59), (50) and (17), we have

$$\frac{\text{Var } V_1(t)}{N_1 - \langle V_0(t)\rangle^2} = 1 + \frac{4\sqrt{\pi}aF}{2\tau_0\sqrt{\ln 2}} e^{-2t/\tau_0 + a^2/8\tau_0^2 \ln 2} \left[\frac{1}{2} + \Phi\left(\frac{4t\sqrt{\ln 2}}{a} - \frac{a}{2\tau_0\sqrt{\ln 2}}\right)\right]. \quad (60)$$

Evaluating (60) for $t=\tau_0/2$ and $\tau_0=0.62a$ results in

$$\frac{\text{Var } (0.31a)}{N_1 - \langle V_0(t)\rangle^2} = 1 + 2.12F. \quad (61)$$

### B. Cascaded Low-Pass Filter

The output of the cascaded low-pass filter is given by (14). The value of $\langle V_2(t)\rangle$ is given by (22). It can easily be seen, by means of (39) and (40), that

$$\text{Var } V_2(t) = \frac{(\gamma B)^2}{\tau_0^4} \int_{-\infty}^{t}\int_{-\infty}^{t} (t-\tau_1)(t-\tau_2) e^{-(t-\tau_1)/\tau_0} e^{-(t-\tau_2)/\tau_0} \cdot \{\rho^2(\tau_2-\tau_1) + 2F\rho(\tau_2-\tau_1)g(\tau_1)g(\tau_2)\} d\tau_2 d\tau_1. \quad (62)$$

But this equals

$$\text{Var } V_2(t) = \frac{(\gamma B)^2}{\tau_0^2} \left.\frac{\partial H(r,s)}{\partial r \partial s}\right|_{r=s=1}. \quad (63)$$

Combing (59), (63), (53), and (17) and setting $t=3/2\tau_0$ and $\tau_0=0.29a$ yields

$$\frac{\text{Var } V_2(0.435a)}{N_2 - \langle V_0(t)\rangle^2} = 1 + 2.22F. \quad (64)$$

## Appendix IV

### Positive Crossing of the Mean of the Noise Process out of the Postdetection Filter

It can be seen from Rice[9] that the expected number per second of positive crossings of the mean of a Gaussian process is given by

$$M = \left[\frac{\int_0^\infty f^2 L(f) df}{\int_0^\infty L(f) df}\right]^{1/2} \quad (65)$$

where $M$ is the expected number of crossings per second and $L(f)$ is the power spectrum (excluding the dc component) of the noise. In the case of the output of the postdetection filter, the amplitude density of the noise process deviates from the Gaussian only in the tails of the distribution. It will be of interest to compute (65) for the noise out of the postdetection filter.

[9] S. O. Rice, "Mathematical analysis of random noise," *Bell Sys. Tech. J.*, vol. 24, pp. 54–55; January, 1945.

### A. Single Low-Pass Filter

Using (44) and (48), it is found that

$$L_1(f) = \frac{(\gamma B)^2}{\sqrt{2}B(1 + 4\pi^2 f^2 \tau_0^2)} e^{-\pi f^2/2B^2}. \quad (66)$$

Defining

$$\Gamma_1(\lambda) = \int_0^\infty \frac{1}{(1 + 4\pi^2 f^2 \tau_0^2)} e^{-\lambda \pi f^2/2B^2} df, \quad (67)$$

it is clear that

$$M_1 = \left[-\frac{2B^2}{\pi} \left.\frac{\partial \ln \Gamma_1(\lambda)}{\partial \lambda}\right|_{\lambda=1}\right]^{1/2}. \quad (68)$$

Integrating (67),

$$\Gamma_1(\lambda) = \frac{1}{2\tau_0} e^{\lambda/8\pi B^2\tau_0} \left\{\frac{1}{2} - \Phi\left(\frac{\sqrt{\lambda}}{2\sqrt{\pi}B\tau_0}\right)\right\} \quad (69)$$

Substituting (69) into (68) and assuming that

$$4\pi B^2 \tau_0^2 \gg 1, \quad (70)$$

we get

$$M_1 = \frac{0.671 B^{1/2}}{(2\pi\tau_0)^{1/2}}. \quad (71)$$

### B. Cascaded Low-Pass Filter

By use of (44) and (51), it is seen that

$$L_2(f) = \frac{(\gamma B)^2}{\sqrt{2}B(1 + 4\pi^2 f^2 \tau_0^2)^2} e^{-\pi f^2/2B^2}. \quad (72)$$

When we define

$$\Gamma_2(\lambda) = \int_0^\infty \frac{1}{(1 + 4\pi^2 f^2 \tau_0^2)^2} e^{-\lambda \pi f^2/2B^2} df, \quad (73)$$

it is clear that

$$M_2 = \left[\frac{-2B^2}{\pi} \left.\frac{\partial \ln \Gamma_2(\lambda)}{\partial \lambda}\right|_{\lambda=1}\right]^{1/2}. \quad (74)$$

Integrating (73), we get

$$\Gamma_2(\lambda) = \left[\frac{1}{4\tau_0} - \frac{\lambda}{16\pi B^2 \tau_0^3}\right]\left[\frac{1}{2} - \Phi\left(\frac{\sqrt{\lambda}}{2\sqrt{\pi}B\tau_0}\right)\right] e^{\lambda/8\pi B^2\tau_0^2} + \frac{\sqrt{\lambda}}{8\sqrt{2}\pi B\tau_0^2}. \quad (75)$$

Substituting (75) into (74) and assuming equation (70), we get

$$M_2 = \frac{1}{2\pi\tau_0}. \quad (76)$$

World Radio History

# Low-Level Garnet Limiters*

F. R. ARAMS†, SENIOR MEMBER, IRE, M. GRACE‡, MEMBER, IRE, AND S. OKWIT†, SENIOR MEMBER, IRE

*Summary*—*S*- and *L*-band low-level passive limiters preselectors using polished single crystals of narrow line-width yttrium-iron-garnet have been developed. The *S*-band limiter employed unsubstituted YIG and has an insertion loss of 0.6 db, a limiting threshold of −26 dbm, and a dynamic range greater than 30 db.

The *L*-band limiter used specially grown gallium-substituted YIG crystals, which, when ground into spheres and polished to a high finish, exhibited extremely narrow line widths. The *L*-band limiter had an insertion loss of 1.1 db, a limiting threshold of −21 dbm, and a dynamic range greater than 25 db. A tuning range from 1120 to 1305 Mc was obtained. Data on frequency sensitivity and SWR are given and indicate that such limiters have a high off-band rejection and a fair power-handling capability. A leading-edge spike of 0.1-$\mu$sec duration was observed.

The decline of the various components of the magnetic susceptibility tensor can be used to construct other novel types of limiters. The operation of three such devices—electronically-tunable preselectors, and cavity-type and comb-type limiters—will be described and experimental data given.

## I. Introduction

FOR a long time there has existed a need for a microwave limiter which would protect microwave receivers against overload and burnout. In addition, requirements exist for microwave power levelers which eliminate power output variations in microwave power sources and in systems. Such limiters should preferably be passive and phase-distortionless. This paper discusses such limiter devices employing single crystals of unsubstituted and gallium-substituted yttrium-iron garnet as nonlinear elements. Limiters have been developed for *L* and *S* bands which have exceedingly low-limiting levels.

## II. Nonlinearity in Ferrites

Experiments had shown that nonlinear effects appeared in ferrites at power levels only about 1 per cent of the level predicted by the simple saturation theory.[1,2] The main resonance line decreases in amplitude and broadens as the power level is increased. An additional rather broad absorption peak appears—usually at a value of applied static magnetic field, ($H_z$) lower than that required for the main resonance. This latter absorption has been called the subsidiary resonance.

The above effects have been explained by Suhl.[3,4] The decline of the main (uniform precessional) resonance is due to the excitation within the ferrite medium of *z*-directed spin waves at the same frequency as the driving-signal frequency. The appearance of the subsidiary absorption peak involves the parametric excitation of non-*z*-directed spin waved near one half the driving-signal frequency. These spin waves can be thought of as spatial disturbances in the normally uniform ferrite magnetization that propagate as plane waves through the medium. As the RF magnetic field is increased beyond an often sharply-defined critical level, the parametric coupling to these half-frequency spin waves increases, so that a subsidiary absorption peak will occur that increases with increasing signal level.

Thus, a limiter can be constructed in which the ferrite is placed in a coaxial line or waveguide, and the magnetic field is biased to an optimum value below resonance. Such subsidiary-resonance limiters have been investigated at *X*-band by Soohoo[5] and Uebele.[6]

For certain combinations of signal frequencies, ferrite geometry, and saturation magnetization, the range of magnetic field in which the subsidiary instability can occur extends through the main resonance. The coincidence of the subsidiary and main resonances is a condition particularly favorable to *low-level* limiting because at resonance maximum energy transfer occurs between the input signal and the spin-magnetization vector. This is shown by a calculation of the critical RF magnetic field ($h_{crit}$) at which nonlinearity sets in:[3]

$$h_{crit} = \frac{\Delta H \Delta H_k}{4\pi M_s} g(\theta). \tag{1}$$

where

$\Delta H$ = line width of uniform precessional resonance,
$\Delta H_k$ = line width of spin wave having wave-number $k$,
$4\pi M_s$ = saturation magnetization,
$\theta$ = angle between $H_z$ and the direction of propagation of the half-frequency spin waves.

* Received by the IRE, November 30, 1960; revised manuscript received, May 23, 1961. This work was supported in part by the Dept. of Defense. It was presented at the 1961 Internatl. Solid-State Conf., Philadelphia, Pa., February 16, 1961.

† Airborne Instruments Lab., Div. of Cutler-Hammer, Inc., Melville, L. I., N. Y.

‡ Airtron, Inc., Morris Plains, N. J. Formerly with Airborne Instruments Lab., Div. of Cutler-Hammer, Inc., Melville, L. I., N. Y.

[1] R. W. Damon, "Relaxation effects in ferrimagnetic resonance," *Rev. Modern Phys.*, vol. 25, pp. 239–245; January, 1953.

[2] N. Bloembergen and S. Wang, "Relaxation effects in para- and ferrimagnetic resonance," *Phys. Rev.*, vol. 93, pp. 72–83; January, 1954.

[3] H. Suhl, "Nonlinear behavior of ferrites at high microwave signal levels," PROC. IRE, vol. 44, pp. 1270–1284; October, 1956.

[4] H. Suhl, "Theory of ferromagnetic resonance at high signal powers," *J. Phys. Chem. Solids*, vol. 1, pp. 209–227; January, 1957.

[5] R. F. Soohoo, "Power limiting using ferrites," 1958 IRE NATIONAL CONVENTION RECORD, pt. 1, pp. 36–47.

[6] G. S. Uebele, "Characteristics of ferrite microwave limiters," IRE TRANS. ON MICROWAVE THEORY AND TECHNIQUES, vol. MTT-7, pp. 18–23; January, 1959.

World Radio History

For regions of limiting described in this paper, the function $g(\theta)$ approaches unity,[3] which is its minimum value.

Single-crystal yttrium-iron-garnet (YIG) is particularly suited to low-level limiting, since it has a very narrow resonance line width, a narrow $\Delta H_k$, and a saturation magnetization of about 1800 gauss.

LeCraw, Spencer, and Porter[7] have demonstrated that for a single-crystal YIG sphere, the line width improves directly with the surface polish. LeCraw and his co-workers obtained resonance line widths as low as 0.52 oersted at 9200 Mc by polishing the sphere to a surface finish of better than 0.1 $\mu$.

Experimental verification of (1) for the limiting threshold under coincidence of the main and subsidiary absorption peaks was also obtained.[8] This coincidence occurs when

$$2N_t 4\pi M_s \geq \frac{f}{\gamma} \geq N_t 4\pi M_s, \qquad (2)$$

where

$f$ = signal frequency in Mc,
$\gamma$ = 2.8 Mc per oersted
(The definition for $\gamma$ used here differs by $2\pi$ from the $\gamma$ used in the References, where it is defined in terms of the angular frequency.)
$N_t$ = transverse demagnetizing factors for spheroid ($=N_x=N_y$).

For a YIG sphere ($N_t=N_z=\frac{1}{3}$), having $4\pi M_s=1800$ gauss, (2) yields lower- and upper-frequency limits of 1680 to 3360 Mc, respectively. Spencer, *et al.*,[8] observed nonlinear effects in the frequency range from 1600 to 3200 Mc with a limiting level at 2200 Mc in reasonable agreement with (1). These measurements were recently extended by Rossel.[9]

A general plot of (2) for various spheroidal geometries is shown in Fig. 1. For example, for low-level limiting (coincidence of subsidiary and main resonance) at $L$ band, a YIG disk with $N_z=0.670$ and $N_t=0.154$ will have optimum operation near 1200 Mc, and a theoretical operating range from 860 to 1720 Mc.

The practical use of single-crystal YIG as a low-level and low-loss passive limiter was first demonstrated by DeGrasse.[10] He used two crossed-strip-transmission-line half-wave resonators oriented at right angles to one another to obtain maximum decoupling between resonators. We have based some of our work on this same circuit arrangement.

[7] R. C. LeCraw, E. G. Spencer, and C. S. Porter, "Ferrimagnetic line width in yttrium iron garnet single crystals," *Phys. Rev.*, vol. 110, pp. 1311–1313; June, 1959.
[8] E. G. Spencer, R. C. LeCraw, and C. S. Porter, "Ferromagnetic resonance in yttrium iron garnet at low frequencies," *J. Appl. Phys.*, vol. 29, pp. 429–430; March, 1958.
[9] F. C. Rossel, "Subsidiary resonance in the coincidence region in yttrium iron garnet," *J. Appl. Phys.*, vol. 31, pp. 2273–2275; December, 1960.
[10] R. W. DeGrasse, "Low-loss gyromagnetic coupling through single-crystal garnets," *J. Appl. Phys.*, vol. 30, pp. 155–156; Suppl. April, 1959.

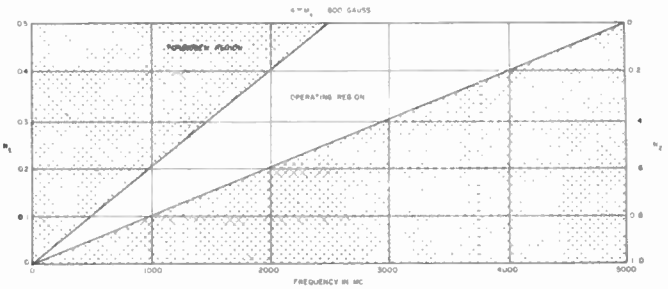


Fig. 1—Frequency region for low-level limiting as a function of ferrite geometry for YIG.

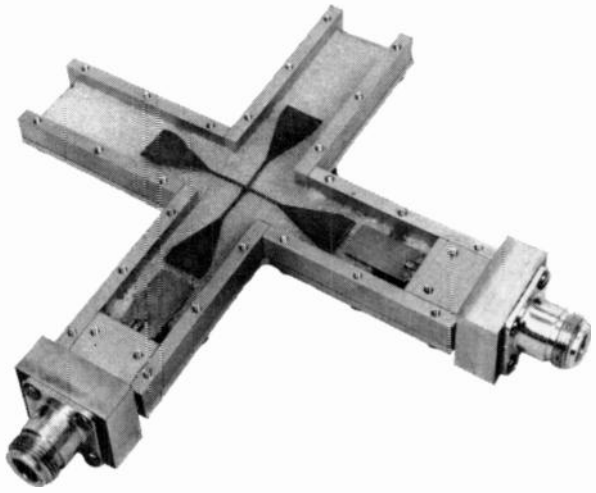

Fig. 2—*S*-band low-level limiter.

## III. *S*-Band Limiter

An *S*-band limiter (with the top ground plane removed) is shown in Fig. 2. The strip-transmission-line resonators are open circuited at each end, so that there is an RF magnetic-field maximum at their centers, where the resonators cross. A 0.020-inch-diameter single-crystal YIG sphere is placed between the strips at their crossover point and biased to ferrimagnetic resonance (uniform precession of the spins). The resonators will then be coupled through the off-diagonal component of the susceptibility tensor. This process can be visualized in the following manner.

The driving RF magnetic field in the input resonator will fan out the spin magnetization vector. The vector will precess about the dc magnetization and in turn will induce an RF magnetic field in the output resonator. Thus, essentially all the RF energy is coupled through the YIG sphere, which can be considered a miniature microwave resonator with a very high unloaded $Q$. For a bandwidth ($\gamma\Delta H$) of 1 Mc, yields an unloaded $Q$ of the order of 3000 at *S*-band. Such a miniature high $Q$ resonator has many other potential applications in microwave circuits: electronically tunable preselector, filter, and panoramic receiver.

The single-crystal YIG resonator is coupled to and, therefore, loaded down by the strip-transmission-line

World Radio History

resonators. This explains why the device has a 3-db bandwidth of approximately 70 Mc instead of a bandwidth of about 1 Mc. In fact, our theoretical investigation of the device has been based on an analysis of a three-resonator filter for minimum insertion loss.[11] This analysis shows that for minimum insertion loss, the input and output couplings should be tight, while the coupling to the center resonator (the YIG sphere) should be relatively loose. The resonators have been substantially reduced in width in the region where the YIG sphere is located in order to increase the RF magnetic field.

The transmission characteristic for the *S*-band limiter is shown in Fig. 3. The insertion loss is 0.6 db and the limiting threshold is $-26$ dbm (3 $\mu$w). The dynamic range is greater than 30 db. The power output actually drops several db from its threshold limiting value. (This characteristic can be changed to a slightly rising output-power slope, if desired, by changing the coupling coefficients.) The limiting threshold level, where the spin precession angle "sticks," is quite pronounced. This is seen more clearly when the YIG sphere is placed in a microwave transmission cavity and insertion loss is measured as a function of input power. The dissipative part of the magnetic susceptibility $\chi''$ can be computed from this measurement. Fig. 4 is a plot of the decline in $\chi''$ as a function of power level. The correlation of the measured values to the theoretical curve is very good.

The YIG sphere used for the above measurements had a line width $\Delta H = 0.37$ oersted measured at 5200 Mc. The dc magnetic field is adjusted to uniform precessional resonance, that is, a signal frequency of 2000 Mc would correspond to 715 gauss. Care must be taken in adjusting the magnetic field to ensure that it is not biased to one of a number of magnetostatic modes[12] in the YIG sphere that have higher insertion loss and, apparently, higher limiting threshold.

Although the limiting characteristic (Fig. 3) was measured at 2000 Mc, we have obtained similar performance at frequencies between 1850 and 3400 Mc by substituting other resonators and readjusting the coupling parameters and the magnetic field.

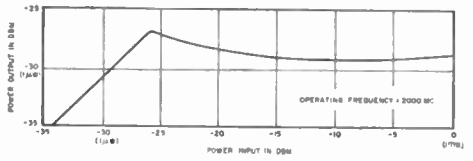


Fig. 3—Transmission characteristic of *S*-band limiter.

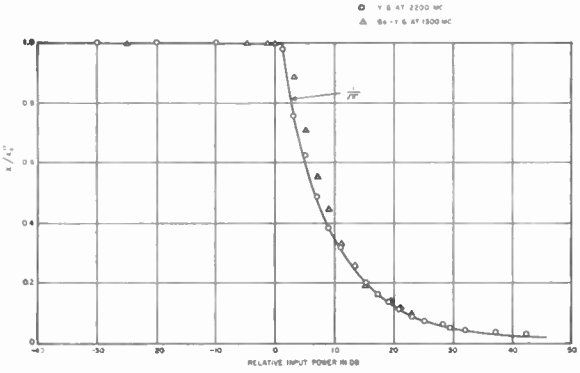


Fig. 4—Magnetic susceptibility of YIG and Ga-YIG spheres as a function of input-power level.

## IV. L-Band Limiter

As Fig. 1 indicates, for low-level limiting at 1200 Mc using pure YIG, an oblate ellipsoid of revolution is required, having $N_z = 0.670$ and $N_t = 0.165$. However, to fabricate such an ellipsoid with a diameter of about 0.030 inch with an optical finish is difficult. A disk was therefore chosen to approximate the ellipsoid.

To achieve the lowest line width possible, YIG disks were X-ray oriented, cut with the hard axis [100] perpendicular to the plane of the disk, and then polished.

Line width and decline of magnetic susceptibility as a function of frequency and power level were measured for three disks of various thickness-to-diameter ratios. These measurements showed that the line width increases rapidly as the frequency is decreased, being 40 oersteds at 1200 Mc. The increase is caused by the YIG disks not being completely saturated at these low frequencies, as well as edge effects.[13] Limiting at low power levels was not obtained.

Another approach is the use of a sphere (easy to polish) having a reduced saturation magnetization, whose value can be determined from (2). Thus, using a narrow line-width material with a saturation magnetization of 1000 gauss, a limiter with a theoretical operating range from 950 to 1900 Mc can be constructed.

Experiments had been reported on decreasing the saturation magnetization of YIG by gallium substitution.[14] The line width remained narrow, increasing linearly with decreasing saturation magnetization in a 1:1 ratio.

Single crystals of Ga-YIG, having a saturation magnetization of 980 gauss and a Curie temperature of 206°C, were obtained from Microwave Chemicals Laboratory. Several spheres of this material were ground and polished to a Linde A finish. Measurements of the polished spheres indicated a very narrow line width (0.72 oersted measured at 5200 Mc), and low-level limiting was successfully obtained.

[11] J. Taub and B. Bogner, "Design of three-resonator dissipative band-pass filters having minimum insertion loss," PROC. IRE, vol. 45, pp. 681–687; May, 1957.

[12] R. L. Walker, "Magnetostatic modes in ferromagnetic resonance," *Phys. Rev.*, vol. 105, pp. 390–399; January, 1957.

[13] R. C. LeCraw, private communication.

[14] E. G. Spencer and R. C. LeCraw, "Line width narrowing in gallium substituted yttrium iron garnet," *Bull. Am. Phys. Soc.*, Ser. II, vol. 5, p. 58; January 27, 1960.

World Radio History

A plot of the magnetic susceptibility as a function of power level that has the same sharp break as pure YIG is shown in Fig. 4. The decline has the $P^{-1/2}$ dependence predicted by Suhl.

An $L$-band limiter with an adjustable permanent magnet is shown in Fig. 5. The measured value for the limiting-threshold power level was $-21$ dbm (8 $\mu$w), which was lower than expected. The operating band over which limiting was measured extended from 1000 to 1500 Mc. The results in an $L$-band crossed-resonator limiter are shown in Fig. 6. An insertion loss of 1.1 db was obtained at the center frequency (1305 Mc). The 0.2-db and 3-db bandwidths for fixed magnetic field are 8 and 43 Mc, respectively; SWR is 1.06 at center frequency.

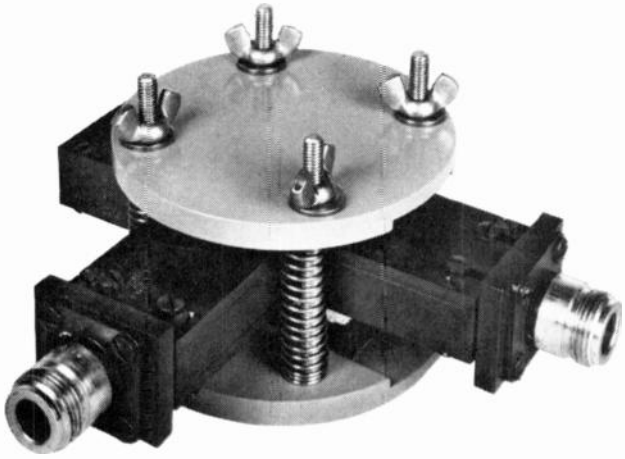

Fig. 5—$L$-band limiter (shown with adjustable permanent magnet).

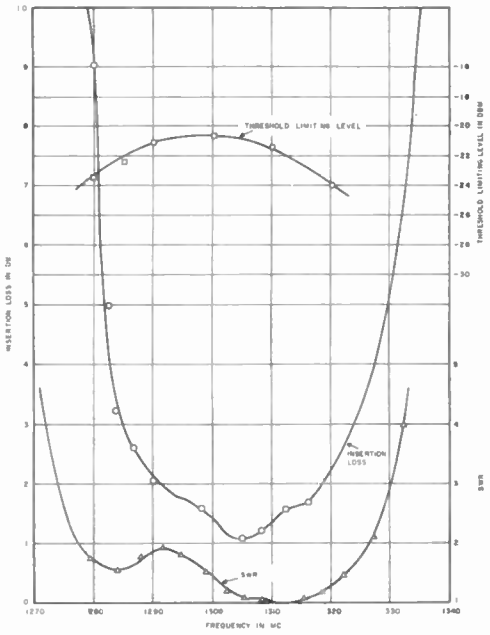


Fig. 6—Operating characteristics of $L$-band limiter

The output-power vs input-power characteristic is shown in Fig. 7, and indicates a dynamic range greater than 25 db. The SWR is also plotted as a function of the input-power level. The reflected portion of the incident power increases sharply as the input power is raised. The remainder of the input power is dissipated in the spin waves within the garnet.

Above limiting threshold, instabilities within the ferrite give rise to oscillations believed to be in the kilocycle region. In response to fast-rising pulses, the limiter exhibits a leading-edge spike about 0.1 $\mu$sec long, caused by the finite build-up time of the spin waves that result in limiting action.

A simple method of tuning the limiter was investigated, that is, capacitively loading the ends of the half-wave resonators with shorting plungers and by optimizing the magnetic field. Measurements showed a linear increase in limiting threshold and insertion loss with decreasing frequency (Fig. 8); a tuning range of 190 Mc was obtained. It is possible to devise other tuning methods in which the insertion loss is essentially independent of frequency.

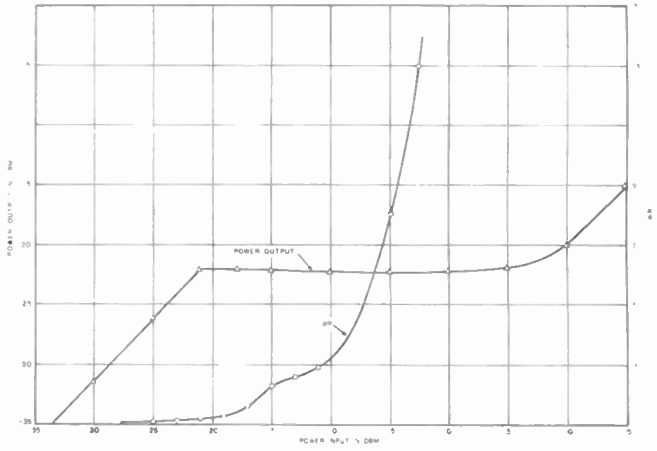


Fig. 7—Transmission characteristics of $L$-band limiter.

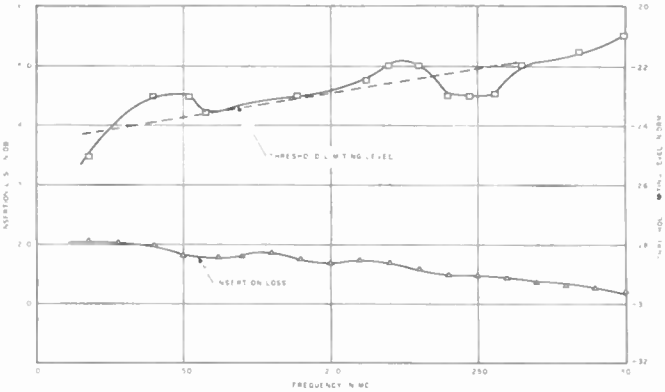

Fig. 8—Tuning characteristics of $L$-band limiter.

World Radio History

## V. Electronically Tunable Limiter-Preselector

Another interesting type of limiter has been operated in which the resonators were replaced by nonresonant transmission lines terminated in open circuits a quarter-wave from the YIG crystal. Thus, the principal frequency-determining parameter is the magnetic resonant frequency of the sphere, and is determined by the applied magnetic field.

By varying the magnetic field, an electronically tunable limiter-preselector was obtained. The test results (using an inferior sphere) were:

| | |
|---|---|
| Frequency tuning range | 2000 to 3400 Mc |
| 3-db bandwidth | 20 Mc |
| Threshold limiting level | −20 to −25 dbm |
| Insertion loss | 4.4 db |

Insertion loss can be reduced by sacrificing threshold limiting level.

## VI. Other Limiting Configurations

In the limiters described, the $\kappa'$ component of the off-diagonal element of the ferrite susceptibility tensor[15] is used to couple two normally-decoupled orthogonal resonators. However, all of the $\chi$ and $\kappa$ elements in the susceptibility tensor are dependent on the RF power level and can be used for the design of other limiters. Two methods for obtaining limiting that use other elements of the susceptibility tensor in appropriate microwave structures are the cavity limiter and the comb limiter.

### A. Cavity Limiter

A cavity limiter has been operated that uses the selectivity of a high-$Q$ single-tuned resonator and the $\chi'$ component of the diagonal element of the susceptibility tensor. The operation of this limiter is as follows.

A quarter-wave resonator is (Fig. 9) tuned to a frequency $f_0$. A ferrite sample is placed on the center conductor near the shorted end of the resonator where the RF magnetic field is maximum. The dc magnetic field is oriented at right angles to the RF magnetic field and adjusted to a field strength slightly less, or greater, than that required for uniform precession at cavity frequency $f_0$. A reactive component will be introduced into the cavity circuit by the ferrite that will retune the cavity to a new resonant frequency $f_1$. The cavity, with RF power levels below $P_{crit}$, will pass a band of frequencies centered about $f_1$ with a minimum of insertion loss. However, when the RF signal is increased above the critical threshold, the decline in the reactive component $\chi'$ will detune the cavity and thereby increase its insertion loss at frequency $f_1$.

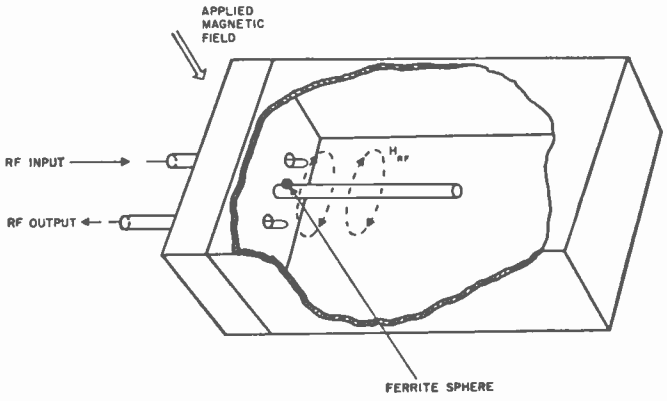


Fig. 9—Slab-line single-tuned cavity power limiter.

An experimental cavity limiter using this technique was constructed in slab-line (Fig. 9). This limiter incorporates a single-crystal YIG sphere with a resonance line width of about 1 oersted. The limiting characteristic is a plateau similar to that in Fig. 6. The measured characteristics are:

| | |
|---|---|
| Center frequency | 2590 Mc |
| Threshold limiting level | −20 dbm |
| Insertion loss (low-level) | 2 db |
| Dynamic range | 20 db |

The insertion loss of the limiter can be minimized by using high-$Q$ microwave circuits, and operating the ferrite at a compromise dc magnetic field. In this way the magnetic losses are small but the reactive component is high enough to sufficiently detune the cavity from its unperturbed resonance.

The power level at which limiting occurs (once a ferrite material has been selected) can be varied by moving the ferrite axially along the center conductor to regions of lower or higher RF magnetic-field strength.

### B. Comb Limiter

A limiter has been operated that uses the inherent decoupling between two adjacent quarter-wave TEM-mode resonators. The garnet spin system is then used as an RF power-level-dependent coupling element between the two resonators (Fig. 10). This configuration has the advantages of compactness and ease in cascading. Furthermore, it is of special interest when used in conjunction with a traveling-wave maser amplifier, where the comb-type slow-wave structure has found wide application.[16,17]

The measured characteristics of a comb limiter are:

| | |
|---|---|
| Center frequency | 2638 Mc |
| Threshold limiting level | −15 dbm |
| Dynamic range | 25 db |
| Insertion loss | 10 db |

[15] The susceptibility tensor is given by

$$\begin{bmatrix} \chi & -j\kappa & 0 \\ j\kappa & \chi & 0 \\ 0 & 0 & 1 \end{bmatrix}$$

where $\chi = \chi' - j\chi''$ and $\kappa = \kappa' - j\kappa''$.

[16] R. W. DeGrasse, E. O. Schulz-DuBois, and H. E. D. Scovil, "Three level solid-state traveling wave maser," *Bell Sys. Tech. J.*, vol. 38, pp. 305–334; March, 1959.

[17] S. Okwit, F. Arams, and J. G. Smith, "Electronically tunable traveling-wave masers at $L$ and $S$ Bands," PROC. IRE, vol. 48, pp. 2025–2026; December, 1960.

World Radio History

The comb limiter that was fabricated is an experimental model for testing feasibility, and it is believed that better performance can be obtained. The comb limiter uses the dissipative part of the diagonal or off-diagonal elements of the susceptibility tensor, or a combination of these elements depending upon the positioning of the garnet sphere in plane A with respect to the comb fingers (Fig. 10). The garnet sphere used for this experiment was the same sphere used for the cavity limiter.

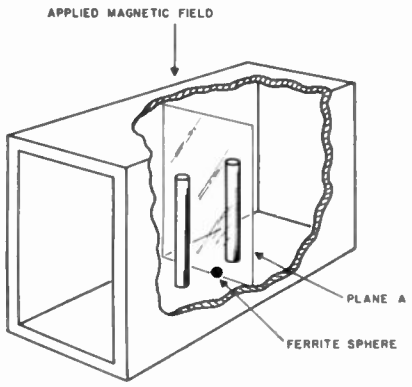


Fig. 10—Comb limiter (coupling not shown).

## VII. Conclusions

The use of a polished single-crystal YIG of narrow line width in *S*-band and *L*-band low-level-limiter preselectors has been investigated.

The *S*-band limiter uses unsubstituted YIG and has an insertion loss of 0.6 db, a limiting threshold of −26 dbm, and a dynamic range greater than 30 db.

The *L*-band limiter uses specially grown gallium-substituted YIG crystals. When ground into spheres and polished to a high finish, these crystals exhibit extremely narrow line widths. The *L*-band limiter has an insertion loss of 1.1 db, a limiting threshold of −21 dbm, a dynamic range greater than 25 db, and a tuning range from 1120 to 1305 Mc. Detailed data on frequency sensitivity and SWR indicates that such limiters have high off-band rejection and fair power-handling capability. A leading-edge spike of about 0.1 μsec duration was observed.

The decline of the various components of the magnetic-susceptibility tensor can be used to construct other types of limiters. The operation of three of these —the electronically-tunable preselector, the cavity limiter, and the comb limiter—has been described and data on experimental models given.

# Correspondence

## The Silicon Cryosar*

For four years members[1] of our laboratory have been studying electrical characteristics of silicon-alloyed *p-n* junction diodes at a very wide range of temperatures, *i.e.*, from 1.9°K to 600°K. During this research on the silicon diode, negative-resistance characteristics have been found in the forward direction of the diodes at 4.2°K. As the result of this research, the silicon cryosar has been developed independently of the study of the germanium cryosar reported by McWhorter and Rediker.[2] The main difference between these two cryosars is that, in the germanium cryosar, negative resistance is observed only when the germanium crystal has compensated impurities; on the other hand, the silicon cryosar shows negative-resistance characteristics with uncompensated impurity silicon crystals.

The silicon cryosar is constructed from one silicon wafer whose thickness ranges from 0.05 mm to 0.3 mm, and from two contacts, which are ohmic at room temperature, attached to both surfaces of this wafer. The resistivity of the silicon wafers investigated ranged from 0.1 to 1000 Ω-cm at room temperature. To form the ohmic contacts, antimony-doped gold is alloyed for *n*-type silicon and aluminum plate, or gallium-doped gold is alloyed for *p*-type.

At room temperature, the silicon cryosar has good conductivity for both directions of current flow; however, at a temperature lower than 10°K, its conductivity becomes quite low at small applied voltages. Fig. 1 shows the dc-voltage-current characteristics of the silicon cryosar at 4.2°K.

As shown in this figure, the dc-voltage-current characteristics of the silicon cryosar at 4.2°K are divided into four regions. In the first region, the silicon cryosar shows high ohmic resistivity up to the breakdown voltage. In the next region, the current increases very rapidly during a small increase in the voltage. In the third region, remarkable negative-resistance characteristics are shown; namely, the voltage decreases to a small value. In the final region, the cryosar again shows low positive-resistance characteristics.

With regard to dynamic characteristics of the silicon cryosar, negative resistance has been observed by the following methods. First, when rectangular voltage was applied to the silicon cryosar through a high resistor, relaxation oscillations were observed. Second, when high-frequency sinusoidal voltage was applied to the silicon cryosar through a moderate-value resistor, it was observed by the voltage-time curve that the terminal voltage of the silicon cryosar decreased suddenly in each half cycle of the voltage.

Fig. 2 shows the waveforms of the relaxation oscillation. In this figure the applied-voltage form is shown in the upper curve. The center curve shows the terminal voltage of the silicon cryosar, and the lower curve is the current waveform of the circuit.

* Received by the IRE, May 8, 1961.

[1] H. Izumi, "The Temperature Dependence of the Electrical Characteristics of the Silicon Alloyed Junction," *Repts. Elec. Commun. Lab., N.T.T.*, vol. 7, pp. 123–132; April, 1959.
H. Izumi, "The Electrical Characteristics of the Silicon Alloyed Junctions at Very Low Temperature," *Repts. Elec. Commun. Lab., N.T.T.*, vol. 7, pp. 339–344; September, 1959.

[2] A. L. McWhorter and R. H. Rediker, "The cryosar—a new low-temperature computer components," Proc. IRE, vol. 47, pp. 1207–1213; July, 1959.

World Radio History

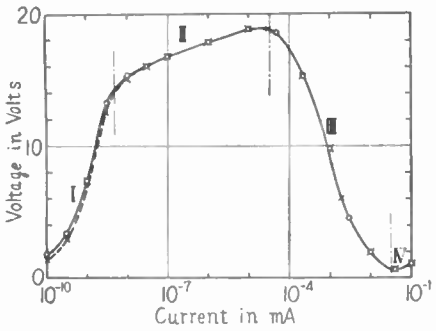


Fig. 1—The dc-voltage-current characteristics of the silicon cryosar. I is the high-impedance region, II is the current-increasing region, III is the negative-resistance region, and IV is low-impedance positive-resistance region. ○ is the normal direction, and × is the reverse direction of current flow.

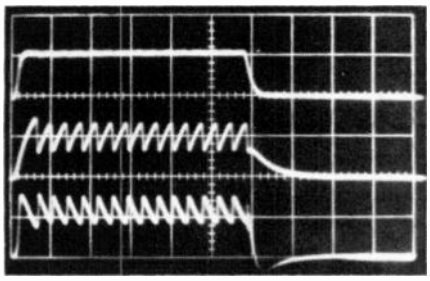

Fig. 2—Three traces illustrate the voltage-time curve of the relaxation oscillation. The time scale of the figure is 1 μsec per large division. The vertical scale for the upper trace (the applied voltage) is 20 volts per large division; for the center trace (the terminal voltage), 10 volts per large division and, for the lower trace (the current through the circuit), 10 volts, *i.e.*, 2 ma per large division.

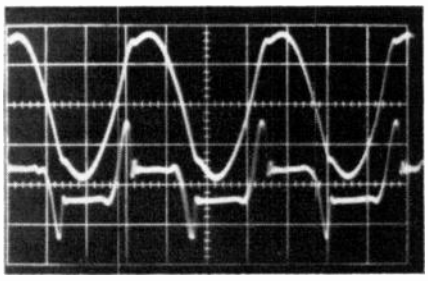

Fig. 3—Two curves indicate the voltage-time curve of the switching action of the silicon cryosar. The vertical scale for the upper curve (the applied) waveform) is 100 volts per large division and for the lower curve (the terminal voltage of the cryosar), 50 volts per large division. The time scale is 1 μ sec per large division.

The repetition frequency of this oscillation is determined mainly from the charging speed of the capacitance of the silicon cryosar (about 100 μμf) through a series resistor. The discharging speed through the negative resistance of the silicon cryosar is less than 0.1 μsec.

When the high-frequency sine wave (about 300 kc) is applied through a resistor to the silicon cryosar from the low-impedance source, the terminal voltage of the cryosar initially increases sinusoidally. However, at the breakdown voltage it falls suddenly to some low value due to negative resistance. This shows that the cryosar switches from the OFF to the ON state.

Fig. 3 shows these voltage changes vs time. The waveform of the terminal voltage of the silicon cryosar is shown in the lower curve of the figure, and the upper curve shows the applied voltage. As can be understood from this figure, the silicon cryosar switches bilaterally because two alloyed electrodes are the same, and the device is symmetrical with respect to both directions of current flow. The switching time is about 50 mμsec, and a maximum-minimum ratio of a voltage as high as 7 is obtained in the optimum case. Higher switching speed can be expected by reducing the inductance of the circuit.

The author wishes to thank N. Inoue and K. Matano for measuring the electrical characteristics and A. Kobayashi for helpful discussion of these phenomena.

H. Izumi
Elec. Commun. Lab.
Nippon Telegraph & Telephone Public Corp.
Tokyo, Japan

## Noise Figure and Stability of Negative Conductance Amplifiers*

Van der Ziel[1] has considered the overall noise figure of a negative conductance preamplifier connected through an ideal transformer to a conventional receiver assuming that the output conductance of the preamplifier, $g_s - g_d$, (Van der Ziel's notation is used) is positive. He considers two cases: a) The turns ratio $n$ is one. He assumes the "high gain" condition $g_s \cong g_d$ and shows that an overall excess noise figure $g_r/g_d$ may be attained. b) The turns ratio is controllable. Here he assumes that the preamplifier output conductance $n^2(g_s - g_d)$ is of such value as to minimize the *receiver* noise figure and shows $g_r/g_d$ may again be attained.

It is the purpose of this note to consider the same problem from a different point of view, namely, to drop the requirement $g_s > g_d$ and to optimize $g_s$ in a way to be described below. This procedure leads naturally to a consideration of stability, and suggests a quantitative definition of stability which can then be introduced into the equations. The results are: 1) For a given stability, neither the high gain assumption nor the assumption in case b) is optimum, and the optimum $g_s$ may be greater than or less than $g_d$. 2) Low noise figure and high stability cannot be simultaneously attained. In particular, the lowest possible overall excess noise figure $g_r/g_d$, (which is also the noise measure and optimum noise measure of the preamplifier[2]) is attained with the preamplifier exactly at the verge of oscillation.

If the exchangeable gain[3] of the preamplifier and the receiver are denoted by $A_{E1}$ and $A_{E2}$ and the exchangeable noise figures[3] by $F_{E1}$ and $F_{E2}$, the overall noise figure may be written $F = F_{E1} + (F_{E2} - 1)/A_{E1}$, where $F_{E1} = 1 + g_r/g_s$, $F_{E2} = 1 + A + R_{n0}(g_s - g_d)/N + g_{n\infty}N/(g_s - g_d)$, $A_{E1} = g_s/(g_s - g_d)$, and $N = 1/n^2$. Combining them, we get a general equation for $F$:

$$F - 1 = (1/g_s)[g_r + A(g_s - g_d) + g_{n\infty}N + R_{n0}(g_s - g_d)^2/N]. \quad (1)$$

The independent variables are $N$ and $g_s$ and there are no restrictions on $g_s$. At this point it is convenient to define a stability factor, $S$, as follows: $S = g_l/g_d + g_s/g_d - 1$, where $g_l$ is the load conductance seen by the preamplifier. If $S$ is equal to or less than zero, the preamplifier is unstable and the more positive $S$ is, the farther is the system from instability. Since $g_l = Ng_i$ where $g_i$ is the input conductance of the receiver we have

$$S = Ng_i/g_d + g_s/g_d - 1, \quad (2)$$

and thus, for given $g_s$, the larger $N$, the greater the stability. The minimum value of the noise figure, regardless of stability, is of fundamental interest. This is determined by minimizing (1) with respect to both $g_s$ and $N$ by the conventional method, and the result is that for $N = 0$ and $g_d = g_s$ (high gain)

$$(F - 1)_{N,g_s} = g_r/g_d, \quad (3)$$

which is in agreement with the conclusion of Van der Ziel and the more general conclusion of Penfield.[2] It should be noted that this lowest possible noise figure is obtained at the expense of stability, for [see (2)] $S$ is equal to zero. Thus, if $g_d$ should become larger by an infinitesimal amount, or if either $g_s$ or $g_l$ should become smaller by an infinitesimal amount, the system would oscillate. In practice then, this lowest possible noise figure is not attainable. Furthermore, the question of the sign of $g_s - g_d$ has not really been touched upon in this degenerate case. What is required is an expression for noise figure as a function of $S$ rather than $N$, in which $g_s$ has been optimized. (The corresponding value of $g_s$ will be designated as $(g_s)_{opt}$).

In principle, this could be done by solving (2) for $N$ and substituting this value into (1) followed by minimization with respect to $g_s$. The resulting expressions are rather unwieldy. Useful equations are obtained as follows. The optimum value of $g_s$ for arbitrary $N$ is obtained from (1).

$$(g_s)^2_{opt} = g_d^2 + g_d N(t - A)/R_{n0} + g_{n\infty}N^2/R_{n0}, \quad (4)$$

where $t = g_r/g_d$. This is inserted in (1) and (2) giving

$$(F - 1)_{g_s} = 2[g_d R_{n0}(t - A)/N + R_{n0}g_{n\infty} + R_{n0}^2 g_d^2/N^2]^{1/2} + A - 2g_d R_{n0}/N, \quad (5)$$

$$S + 1 = Ng_i/g_d + (g_s)_{opt}/g_d. \quad (6)$$

Since low noise figure is associated with small values of $N$, it is useful to write (4)–(6) in the limit of small $N$.

$$(g_s)_{opt} = g_d + Ng'/2, \quad (7)$$

$$(F - 1)_{g_s} = t + (N/g_d)[g_{n\infty} - (g')^2 R_{n0}/4], \quad (8)$$

$$S = N(g_t + g'/2)/g_d, \quad (9)$$

* Received by the IRE, June 6, 1961.

[1] A. Van der Ziel, "Note on the noise figure of negative conductance amplifier," PROC. IRE, (*Correspondence*) vol. 48, p. 796; April, 1960.

[2] P. Penfield, Jr., "Noise in negative-resistance amplifiers," IRE TRANS. ON CIRCUIT THEORY, vol. CT-7, pp. 166–170; June, 1960.

[3] H. A. Haus and R. B. Adler, "An extension of the noise figure definition," PROC. IRE, vol. 45, pp. 690–691; May, 1957.

World Radio History

where $g' = (t-A)/R_{n0}$. Eq. (9) can be substituted into (7) and (8):

$$(g_s)_{opt} = g_d + Sg_d g'/2(g_i + g'/2), \quad (10)$$

$$(F-1)_{g_s} = t + S(g_{n\infty} - (g')^2 R_{n0}/4)/(g_i + g'/2). \quad (11)$$

The quantities $g'$, $g_i + g'/2$ and $g_{n\infty} - (g')^2 R_{n0}/4$ are important. It can be shown that if $t$ is less than the optimum excess noise figure of the receiver (and this is the only case of interest) the last quantity above is positive. $g'$ may be positive or negative since $A$ may be either positive or negative and $R_{n0}$ is always positive. $g_i - g'/2$ must be positive in this first order expansion. This is not a severe restriction and if necessary can be removed by carrying out a higher order expansion.

Eq. (5) may be easily evaluated for large $S$, *i.e.*, large $n$, and the resultant noise figure is $1 + A + 2(R_{n0} g_{n\infty})^{1/2}$ which is just the noise figure of the receiver. Thus, as the stability varies from zero to infinity the overall noise figure varies from $1+t$ to the noise figure of the receiver.

Alan C. Macpherson
U. S. Naval Res. Lab.
Washington, D. C.

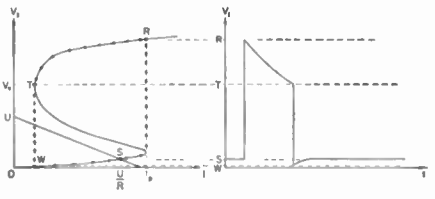

Fig. 1—Low-voltage bias condition.

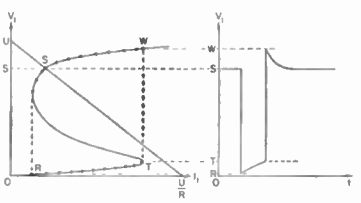

Fig. 3—High-voltage bias condition.

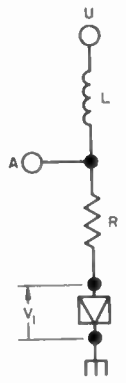


Fig. 2—Tunnel-diode one shot.

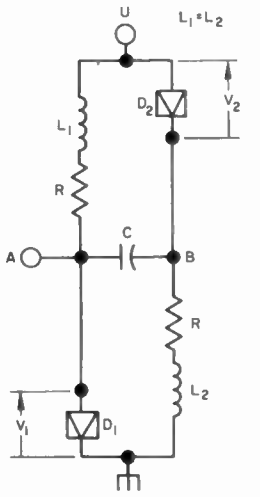


Fig. 4—Triggered oscillator.

## Tunnel-Diode One-Shot and Triggered Oscillator*

A note by Kaenel[1] describes an extremely simple and useful one-tunnel-diode flip-flop. This circuit requires a bidirectional pulse which may not be available. A purpose of this note is to point out that an identical circuit with modified bias will produce the required pulse.

With the use of a supply voltage slightly higher or lower than that used for a bistable operation, the circuit becomes monostable. If a bias condition is selected such that the resistive load line intersects the characteristic tunnel-diode curve at a voltage below that for peak current, as shown in Fig. 1, and a positive spike is applied at point $A$, shown in Fig. 2, the circuit delivers a positive pulse followed by a negative overshoot, as shown in Fig. 1. By selecting a higher bias voltage (and using a negative trigger spike), the circuit delivers a similar but inverted pulse, as shown in Fig. 3. This negative pulse has a larger overshoot and is, therefore, preferable as a driver for the flip-flop described by Kaenel.[1]

The switching action of the circuit will not be discussed, as the switching of tunnel diodes has been described before, and the locus of the operating point of the diode is shown by the arrowed lines in Figs. 1 and 3, point $S$ being the stable operating point.

When two of these circuits are capacitively coupled, an oscillator is obtained; however, this oscillator requires an initiating pulse. The typical oscillator circuit is shown in Fig. 4. This oscillator has two stable states. One is a stable dc state, and the other is a stable ac state where the circuit is in a stable oscillation.

As in the above discussion of the one shot, this circuit can be biased in a low-voltage or high-voltage state. Fig. 1 shows the low-voltage biasing condition. We see that both diodes then have a stable point at $S$. When both diodes are in this stable condition, the oscillator is in its dc state. If a positive trigger pulse is applied at point $A$, the voltage $V_1$ will be as shown in Fig. 1 for the case of the one shot. The sudden jump of $V_1$ from $T$ down to $W$ is transmitted to point $B$ by the capacitor $C$. This causes $V_2$, the voltage across diode $D_2$, to rise suddenly, and the same one-shot action takes place in the right-hand side of the circuit. As $V_2$ jumps downward from $T$ to $W$, it triggers the left side through capacitor $C$. Therefore, the one-shot action takes place alternately on each side, and a stable oscillatory state exists (ac state).

The triggered oscillator can be returned to its dc state from its ac state by grounding point $A$ for a time not less than one period of the oscillator. An additional condition is now imposed on the biasing of the diode which is that $I_p > U/R$ (see Fig. 1). If this limitation does not exist, it is possible for the current through $L_1$ to be greater than $I_p$ when point $A$ is removed from ground, in which case the oscillator will continue in its ac state. After point $A$ is ungrounded, the operating point of $D_1$ moves to point $S$, and the oscillator is back in its dc state, as $D_2$ returned to point $S$ during the period $A$ was grounded.

The high-voltage case is identical in principle to the low-voltage case, except that the oscillator can now be turned off by placing point $A$ at a potential greater than $S$ (see Fig. 3) for at least one period of the oscillator.

One possible application of the triggered oscillator is as a memory unit, as it has two stable states and produces an ac signal for nondestructive readout.

T. W. Flowerday
D. D. McKibbin
Lockheed Missiles and Space Div.
Palo Alto, Calif.

## A Tunnel-Diode Slot Transmission Amplifier*

A negative conductance waveguide transmission type amplifier has been built and operated at 2.7 kMc. The amplifier consists of a tunnel diode mounted within an $S$-band waveguide endplate slot. In operation the slot assembly behaves as a guide-to-guide coupler with reflection and transmission coefficients greater than unity. It is believed that this is the first description of a tunnel-diode microwave amplifier in which a resonated slot or linear electromagnetic radiator provides coupling to the source and

* Received by the IRE, June 7, 1961.

[1] R. A. Kaenel, "One-tunnel-diode flip-flop," Proc. IRE (Correspondence), vol. 49, p. 622, March, 1961.

* Received by the IRE, June 2, 1961. This work was supported in part by AF Cambridge Res. Ctr. under Contract No. AF 19(604)3508 at Hughes Aircraft Co., Culver City, Calif.

World Radio History

load conductances as well as the distributed capacitance and inductance necessary to maintain resonance.

The construction details of the device are shown in Fig. 1. The endplate containing the slot is fabricated in two pieces which are separated by a 0.025 inch mylar insulator. This construction provides microwave continuity between the tunnel diode and the slot while simultaneously permitting an appropriate dc potential to be maintained across the diode. In order to prevent oscillations from occurring in the biasing circuit, a small resistor (not shown in the figure) is connected between the insulated plates near their common perimeter. When the device was used as an endplate guide to guide coupler, it was necessary to place an additional mylar sheet between the split face of the endplate and one waveguide flange in order to prevent the biasing circuit from being shorted.

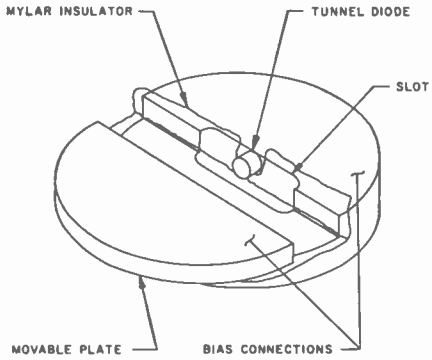


Fig. 1—Tunnel-diode slot amplifier.

In the transmission experiment a tuneable passive endplate slot was inserted into a waveguide system which had been provided with adequate input and output isolation. The slot was then tuned to resonance and the transmitted power level was noted. After the passive endplate slot was removed it was observed that the transmitted power was essentially unchanged. The endplate slot containing the tunnel diode was then inserted into the waveguide system and the transmission gain was measured by introducing sufficient attenuation to produce the same transmitted power as before. Transmission gains of 8, 16 and 21 db have been obtained in the neighborhood of 2.7 kMc; a 3 db bandwidth of 21 Mc was observed for the amplifier which exhibited a center frequency gain of 16 db. The diodes used in the experiment were Hughes Aircraft Company's experimental point contact Gallium Arsenide tunnel diodes with peak currents in the neighborhood of 1 ma, capacitances less than 1 pf, and negative resistances of approximately 300 ohms.

The purpose of the experimental program was to determine the feasibility of obtaining amplification from the elements of a waveguide slotted antenna; consequently no noise figure measurements have yet been attempted. The endplate slot was selected for this experiment because of its geometrical simplicity and the fact that its properties are related in a known way to those of slots cut in the broad wall of a waveguide. The results obtained to date indicate that the development of a multiple element amplifying array is feasible.

During the course of the investigation it was observed that the diode slot configuration could be adjusted to the condition of oscillation. Under this condition the oscillator would lock onto a signal removed in frequency by several megacycles from the natural oscillation frequency. This lock on oscillator effect produced apparent signal gains in excess of 40 db over a 2 Mc bandwidth. The diode slot system acting as a combined microwave source and antenna element produced radiated power levels of 35 dbm. The power level attained was limited by the characteristics of the diode which was selected to match the radiation resistance of the slot.

MELVIN E. PEDINOFF
Electro-Sonic Systems, Inc.
Los Angeles, Calif.

## Neural Analogs*

The present vogue of indiscriminately equating "neural analogs" to biological neurons is as popular as it is erroneous. With a very few exceptions, most of the analogs proposed so far are vastly different from the biological original. The creators of these devices and systems rarely take the trouble to point out these differences, and, in some instances, they appear to be unaware of the essential properties of the neuron. In the recent papers by Hawkins[1] and by Brain[1] a number of misconceptions continued to be propagated.

First, a clarification on anatomy is in order. An abstracted schematic of a neuron is shown in Fig. 1. Axons, the output transmission lines of neurons, branch out into many fine fibers which terminate at synapses. They do not become dendrites, as stated by Hawkins. Dendrites are the converging branched cell inputs and are integral with the cell body.[2] The input signals to a cell are due to axons of other cells which either make synaptic connection with the dendrites of the given cell or which synapse directly onto the cell's body, as shown.

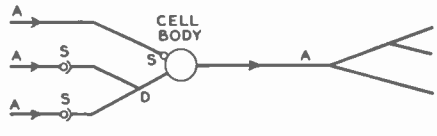


Fig. 1—Simplified representation of a neuron. $A$ = axons. $S$ = synapses, and $D$ = dendrites.

Second, a correction must be made to Hawkins' statement of the function of a synapse. He states that a synapse transmits an attenuated impulse between one neuron and another. This is true only for a minute fraction of the synapses which have been investigated. The majority of synapses do not transmit electrical events at all. Rather, the axon spike (pulse) stops at the synapse where it triggers a chemical release mechanism. After diffusion across the synaptic boundary, the chemical (acetylcholine) initiates a new and different electrical event in the dendrite or at the cell body, depending on its location. The new electrical signal is not a spike; rather it is a long-lasting, low potential signal which then flows slowly and with attenuation.[3]

It is there, at the neuron's inputs, that the functions are continuous-variable, graded, and decremental in contrast to the discrete-variable, lossless axon signals. Thus the logics of a neuron begin to get very complex. These input properties are practically never included in analog descriptions. But it is precisely their intricate functions which play an important part in signal processing. A convincing summary of this complexity is given by Bullock.[4]

All of the so-called "adaptive" systems which have been constructed employ a "synapse" whose transmission varies with use. Although there is some neurophysiological evidence for variable synaptic transmission,[5] it is at best incomplete and controversial. There is no clear evidence that in intact tissue repeated transmission enhances the probability of future transmission. Also, it has been shown that a particular synapse may produce either excitatory or inhibitory effects at various times depending on the instantaneous signal environment in a cell.[6]

In his review, Hawkins points out that it sometimes has been taken into account that immediately after firing, the neuron's threshold briefly becomes infinite (absolute refractoriness). It should be pointed out that the exclusion of this parameter in a model is a most serious omission. Since it appears that the principal business of nerve-net functions involves time-varying interactions, such threshold changes must play an essential role. At least as important is another threshold change which is not mentioned at all. Immediately following the absolute refractory period is the so-called relative refractory phase, an essentially exponential decay toward resting threshold.[7] This decay has a time constant which is quite long compared to axon-spike durations

* Received by the IRE, February 2, 1961.

[1] J. K. Hawkins, "Self-organizing systems—a review and commentary," PROC. IRE, vol. 49, pp. 31–48; January, 1961.
A. E. Brain, "The simulation of neural elements by electrical networks based on multi-aperture magnetic cores," PROC. IRE, vol. 49, pp. 49–52; January, 1961.

[2] F. Brink, Jr., "Excitation and conduction in the neuron," in "Handbook of Experimental Psychology," S. S. Stevens, Ed., John Wiley and Sons, Inc., New York, N. Y., pp. 50–93; 1951.

[3] J. C. Eccles, "The Physiology of Nerve Cells," The Johns Hopkins Press, Baltimore, Md., 270 pp.; 1957.

[4] T. H. Bullock, "Neuron doctrine and electrophysiology," *Science*, vol. 129, pp. 997–1002; April 17, 1959.

[5] J. C. Eccles and A. K. McIntyre, "The effects of disuse and of activity on mammalian spinal reflexes," *J. Physiol.*, vol. 121, pp. 492–516; September, 1953.

[6] S. W. Kuffler and C. Eyzaguirre, "Synaptic inhibition in an isolated nerve cell," *J. Gen. Physiol.*, vol. 39, pp. 155–184; September, 1955.

[7] I. Tasaki, "Nervous Transmission," Charles C Thomas, Springfield, Ill., 164 pp.; 1953.

World Radio History

and repetition rates; hence, it plays an important part in modifying signal processing in the neuron. An example of the significance of this parameter is described in an auditory model by Guttman, van Bergeijk, and David.[8]

Brain implies in his paper that he has devised a "comprehensive" simulation of neural elements. Since he includes even fewer parameters than those mentioned by Hawkins, the simulation is still more remote. Brain has it that the strength of an output signal depends on the previous history of the neuron. Such is certainly not the case in nature where with few exceptions the output is all-or-none, and to a first-order approximation has constant amplitude and duration.[9]

The biological nerve cell operates as an exceedingly complex element. The fact that it is a highly nonlinear device with a large number of time-varying parameters makes it very flexible. Neural modeling is tempting and interesting because abstracting even just a few properties permits a demonstration of a rich variety of behavior.

There has been a sharp increase in neural modeling activity during the last few years, and it is important to point out that two distinct philosophies are involved. One school seeks to make its "neurons" simulate biological function as closely as possible. The emphasis is on small scale and physiologically accurate modeling. Input-output relationships are made to be consistent with what is known of the biological parameters. The intent is to study closely the probable information-processing functions of neurons, and in so doing, to elucidate further the operations of the biological system.

In the second group of modelers (by far the most populous) the idea is to explore the "adaptive" and large-scale behavior of many quasi-neural elements randomly connected. Little care is taken to simulate neural properties accurately or fully. The intent seems to be titillation rather than elucidation. Since these abstractions are generally very imprecise, obviously incomplete, and frequently in error, little relevance to physiological nervous systems should be inferred. Above all, anthropomorphism is unwarranted.

L. D. Harmon
Bell Telephone Labs., Inc.
Murray Hill, N. J.

[8] N. Guttman, *et al.*, "Monaural temporal masking investigated by binaural masking," *J. Acous. Soc. Am.*, vol. 32, pp. 1329–1336; October, 1960.
[9] E. D. Adrian, "The Mechanism of Nervous Action. Electrical Studies of the Neurone," University of Pennsylvania Press, Philadelphia, Pa., 103 pp.; 1932.

## *Author's Comment*[10]

We are indebted to Dr. Harmon for gallantly volunteering to unravel the fascinating complexity of the biological neuron system, and admire his dedication to its simulation down to the last detail. The single-minded tenacity and stoicism of the purist will always command respect, but I would draw a parallel between the present state of affairs in regard to "learning machines" (adaptive pattern-recognition systems which process numerous input signals simultaneously in a statistical manner) and the status of "flying machines" at the end of the nineteenth century. Is it not true that man's progress in the construction of *potentially useful* flying machines, as distinct from interesting scientific curiosities, is measured from the time he ceased to be obsessed with the flapping wings so vital to the birds he took for a model?

Surely the crux of the numerous differences of opinion so prevalent in the field of learning machines lies in basic motivation. The investigation of the detailed mechanism by which a man remembers, recognizes, and extracts generalities out of myriad simultaneous-data samples is assuredly a laudable enterprise, but is it any the less so to seek to construct a *useful* machine to perform in a similar manner? It does not follow that the machine must be an exact model in order to function satisfactorily. The purist has no monopoly of virtue, and the unrepentant urchin who persists in draggling his worm where the water is muddiest frequently catches bigger fish than the "exact copy," dry-fly man.

The word "useful" has been stressed because it has a significant influence on the philosophical attitude being brought to bear on the problem. Reduced to its lowest terms, it is virtually synonymous with "a commercial proposition." It is perhaps unfortunate, but no matter how high their motivation, machine builders sooner or later must face the fact that unlimited funds are not available for the construction of large, expensive, scientific gimmicks. In the present instance, in considering machines which function by simultaneous statistical sampling, one soon finds oneself glibly postulating systems containing upwards of a thousand identical basic building blocks, plus peripheral equipment. With these boundary conditions, simplification to the highest degre possible is mandatory.

With regard to Dr. Harmon's objection to the use of the word "comprehensive," I would merely observe that the four primitive operations

1) addition of signals,
2) absolute inhibition of signals passing through one or more connections by signals in a controlling channel,
3) control on an all-or-none basis by a threshold level, and
4) a weighted connection which can have its value changed in the "learning" phase of operation,

have been made available in compatible components, and that these functions seem to be adequate to satisfy the majority of descriptive models. The circuits given were not intended to constitute an exhaustive list, but rather to be illustrative of the versatility of arrangements using carrier-operated multi-aperture magnetic cores. Thus, should a time-dependent threshold with exponential decay be desired, a gated carrier supplied to Fig. 11, with a little ingenuity, might very well satisfy the requirement. Fig. 6 is, of course, only part of the story; its output is taken along with similar connections to a threshold unit of the all-or-none kind.

As for the need for a weighted connection which can have its value permanently modified in the learning phase of operation, I have no doubt of its usefulness in enhancing the discrimination of pattern recognition machines. With regard to its relevance to human neural operation, I would ask whether anyone has succeeded in finding a plausible mechanism which does not make use of permanently modified connections to explain the retention of human memory through sleep and anesthesia, for 50 years.

A. E. Brain
Applied Physics Lab.
Engrg. Div.
Stanford University
Menlo Park, Calif.

[10] Received by the IRE, March 20, 1961.

## On Self-Organizing Systems*

The recent review by Hawkins[1] represents one possible approach to self-organizing systems that should prove useful. By regarding nervous systems as self-organizing it should be possible for physical scientists and biological scientists interested in this area to engage in a fruitful exchange of ideas. The Hawkins article, unfortunately, illustrates a danger in this approach. In undertaking to relate the nervous system to self-organizing systems an author must assume the responsibility of familiarizing himself with at least the elementary information available in both the physical and biological facets of the problem. Hawkins has failed to do so, at least with regard to biology.

Harmon points out some of the errors in the Hawkins paper; and there are numerous additional errors made by Hawkins. For example, it is stated that the arrival of about ten nearly simultaneous impulses will fire a neuron. In fact, the number of presynaptic spike impulses required to fire a neuron varies tremendously from one type of junction to another with a minimum of one[2] and an undetermined maximum. Related to this error is the statement that each neuron is connected to $10^2$ to $10^3$ other neurons. This property also is tremendously variable with a minimum near one[3] and a maximum that may be of the order of $10^3$.[4] We are also told that "long neurons tend to transmit at a higher speed than short ones." One of the earliest established facts in electrophysiology, however, was that the activity

* Received by the IRE, April 13, 1961.
[1] J. K. Hawkins, "Self-organizing systems—a review and commentary," Proc. IRE, vol. 49, pp. 31–48; January, 1961.
[2] T. H. Bullock, "Properties of a single synapse in the stellate ganglion of squid," *J. Neurophysiol.*, vol. 11, pp. 343–364; 1948. See especially, p. 348.
[3] A. A. Maximow and W. Bloom, "Textbook of Histology," W. B. Saunders Co., Philadelphia, Pa., pp. 188–190; 1952.
[4] D. A. Sholl, "The Organization of the Cerebral Cortex," John Wiley and Sons, Inc., New York, N. Y., pp. 57–58; 1956.

World Radio History

of neural processes of various diameters in a compound nerve could be distinguished by virtue of the fact that speed of conduction over the same distance varies by an order of magnitude.[5] Thus, conduction velocity varies with diameter, not length. Length may be correlated with diameter, but the correlation is low, and the primary relationship is between *diameter* and conduction velocity.

Other statements simplify matters to the point of being misleading. It is mentioned that "the alpha rhythm is sometimes regarded as a scanning mechanism." The evidence indicates that the alpha is probably the summation of fluctuations of certain of the analog voltages referred to by Harmon.[6] Although these local fluctuations will result in changes of threshold in the neurons involved, a network scanning mechanism becomes improbable. These same fluctuations in analog voltage have also been proposed as a possible basis for short-term memory as an alternative to the recirculation of signal sequences mentioned by Hawkins.[7] The distributed memory concept referred to is by no means established. The experiments mentioned in which "memory" is tested following cortical extirpations are difficult to interpret; the deficits in performance following these extirpations may be the result of losses in information handling capacity rather than any losses of storage capacity *per se*.

Harmon also criticizes the designers of adaptive systems for the incorporation of alterations of "synaptic" transmission in their models. His statement, "There is no clear evidence that in intact tissue repeated transmission enhances the probability of future transmission" is entirely unwarranted. Much of the evidence that repeated transmission does alter the probability of future transmission is cited in recent reviews[8,9] of the role of the central nervous system in learning. Although it has not been established with certainty that these alterations of probability of transmission take place at the synapse, evidence of synaptic changes as a result of use and disuse is mounting.[10,11]

Errors such as the ones mentioned above decrease the value of Hawkins' paper to physical scientists by conveying to them incorrect or outdated concepts. In the cases of the biological scientist, they plant a seed of doubt as to the accuracy of the remaining information contained in the paper.

P. D. Coleman
Dept. of Physiology
The Johns Hopkins University
Baltimore, Md.

[5] T. C. Ruch and J. F. Fulton, "Medical physiology and biophysics," W. B. Saunders Co., Philadelphia, Pa., pp. 71–73; 1960.
[6] J. F. Field, Ed., "Neurophysiology," in "Handbook of Physiology," American Physiological Society, Washington, D. C., sect. 1, pp. 293–295; 1959.
[7] B. D. Burns, "The electrophysiological approach to the problem of learning," *Can. J. Biochem. and Physiol.*, vol. 34, pp. 380–388; 1956.
[8] V. E. Hall, Ed., "Annual Review of Physiology," Annual Reviews, Inc., Palo Alto, Calif., vol. 23, pp. 451–484; 1961.
[9] Field, *op. cit.*, pp. 1471–1499; 1960.
[10] E. De Robertis, "Submicroscopic morphology and function of the synapse," *Exp. Cell Research*, suppl. 5, pp. 347–369; 1958.
[11] E. De Robertis, "Submicroscopic morphology of the synapse," *Internat. Rev. Cytol.*, vol. 8, pp. 61–96; 1959.

## Stable Low-Noise Tunnel-Diode Frequency Converter*

A simple nonlinear resistance frequency converter can be represented by the equivalent circuit of Fig. 1(a)[1], provided all image and sum frequencies are short circuited, and the amplitude of the local oscillator voltage is much greater than the sum of the amplitudes of the voltages at the signal and intermediate frequency. In practical positive nonlinear resistances, the conversion conductance $g_c$ must always be less than the average conductance $g_0$.[1] If, however, the incremental value of the nonlinear resistance is negative for some voltages, then $g_c$ may equal or exceed $g_0$.[2]

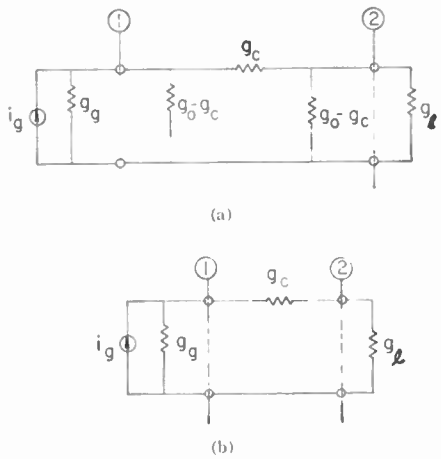


Fig. 1—Equivalent circuit of simple nonlinear resistance mixers. Currents and voltages to the left of port 1 are at the signal frequency $f_s$, those to the right of port 2 are at the intermediate frequency $f_i$. ($f_s = f_i + f_{LO}$; $f_{LO}$ = local oscillator frequency.) (a) $g_0 = g_c$. (b) $g_0 = g_c$. ($i_g$ = generator current, $g_g$ = generator conductance, $g_0$ = average conductance of nonlinear resistance,[1] $g_c$ = conversion conductance of nonlinear resistance,[1] $g_L$ = load conductance.)

For the case $g_c = g_0$, the equivalent circuit of the converter reduces to Fig. 1(b). The conversion gain $G_c$ (*i.e.*, the ratio of the IF output power to the available signal power) is then simply

$$G_c = \frac{4g_g g_l}{\left(g_g + g_l + \frac{g_g g_l}{g_c}\right)^2}. \qquad (1)$$

If the input and output impedances are equal, $G_c$ approaches unity as $g_g/g_c$ approaches zero. In this case, any thermal or shot noise sources in the nonlinear resistance will be completely mismatched from both input and output, so that the converter can be represented by a lossless, noiseless, matched four-terminal frequency translation network.

We are attempting to approach the performance of the ideal converter described above by using tunnel diodes as nonlinear resistances. An initial broadband converter ($f_{LO}$ = 780 Mc, $f_i$ = 30 Mc) had unity conversion gain, a radiometer noise figure of 2.5 db,[3] and was stable with input VSWR's exceeding 10:1 varied through all phases.

It is of interest to note, that both the minimum radiometer noise figure and the minimum conversion loss of a broadband positive resistance frequency converter (image frequency termination equals signal frequency termination) must exceed 3 db.[4] Also, for the tunnel diode used in our converter, $(I_0 R_d)_{min}$ was about 1.2 ($I_0$ = dc current through diode, $R_d$ = magnitude of negative resistance at bias point). The noise figure at high gain of a tunnel diode amplifier using this diode would exceed 3.5 db,[5] while the noise figure at high gain of a system using the converter together with the best commercially available 30-Mc IF amplifier (NF = 0.7 db) would be only 2.9 db.

F. Sterzer
A. Presser
Electron Tube Div.
RCA
Princeton, N. J.

* Received by the IRE, May 17, 1961.
[1] E. W. Herold, "Frequency mixing in diodes," Proc. IRE, vol. 31, pp. 575–581; October, 1943.
[2] K. K. N. Chang, G. H. Heilmeier and H. J. Prager, "Low-noise tunnel-diode down converter having conversion gain," Proc. IRE, vol. 48, pp. 854–858; May, 1960.

[3] Passive circuit losses in front of the converter, amounting to 0.5 db are not included in the quoted gain and noise figure. These losses were due to the local oscillator input circuit and an IF rejection filter, and can, in principle at least, be eliminated by more careful design.
[4] E. W. Herold, R. R. Bush, and W. R. Ferris, "Conversion loss of diode mixers having image frequency impedance," Proc. IRE, vol. 33, pp. 603–609; September, 1945.
[5] M. E. Hines and W. W. Anderson, "Noise performance theory of Esaki (tunnel) diode amplifiers," Proc. IRE, vol. 48, p. 789; April, 1960.

## Thin-Film Cryotrons*

On page 1568 of the paper by the above title, Smallman, *et al.*,[1] state that "the induced current in a tin (film) loop without a ground plane rapidly fell off to a *very low* value in a fraction of a second" (our italics). On page 1571, they state that "residual resistance is present in *many* no-ground-plane cryotrons, and it is significant that the addition of a ground plane completely eliminates it . . ." (our italics).

Hasty reading of these remarks might lead the reader to suppose that unshielded crossed-film cryotrons do not always become superconducting, and cannot be used reliably to store circulating currents. We feel sure that Smallman, *et al.*, did not mean to imply this. In the development by one of the authors, together with Bremer, of the unshielded crossed-film cryotron, which was published last year,[2] we found effects of the type mentioned by Smallman, *et al.*, when our devices were subjected to a field

* Received by the IRE, September 23, 1960; revised manuscript received, November 11, 1961.
[1] C. R. Smallman, A. E. Slade, and M. L. Cohen, "Thin-film cryotrons," Proc. IRE, vol. 48, pp. 1562–1582; September, 1960.
[2] V. L. Newhouse and J. W. Bremer, "High-speed superconductive switching element suitable for two-dimensional fabrication," *J. Appl. Phys.*, vol. 30, pp. 1458–1459; September, 1959.

World Radio History

somewhat larger than that of the earth, directed at right angles to the film surface. Such fields can sometimes arise accidentally if ferromagnetic materials, such as steel clamps for instance, are used near the dewar. The magnetic field of the earth, however, did not affect the performance of our unshielded crossed-film cryotrons to any appreciable extent, nor did it prevent us from storing currents in unshielded cryotron circuits for several hours. In this connection, Crittenden, *et al.*,[3] report that current has been stored in unshielded tin and indium film circuits for many hours. No mention is made in their paper of any precautions to exclude the earth's magnetic field.

It may therefore be concluded that unshielded tin and indium crossed-film cryotrons, persistors, etc. may be operated in the earth's magnetic field. Fields which are large enough to cause trouble may be cancelled out or screened out by any of the well-known methods. A method which is particularly suitable for work on superconductors is that of operating the circuits inside a cup of spun lead, placed in the liquid helium. This causes the lead to become superconducting and expel most of any stray magnetic fields present.

V. L. Newhouse
H. H. Edwards
Appl. Phys. Sect., Research Lab.
General Electric Co.
Schenectady, N. Y.

[3] E. C. Crittenden, Jr., J. N. Cooper, and F. W. Schmidlin, "The 'persistor'—A superconducting memory element," Proc. IRE, vol. 48, pp. 1233–1246; July, 1960.

## Are Electronics Engineers Educated?*

Webster defines engineering as "the art of designing, building, or using engines and machines, or of designing and constructing public works or the like." The concession is further made that engineering may be divided into the particular fields, within each of which the basic definition must be interpreted. One should logically expect, therefore, that a graduate of a good engineering school, with a degree in engineering, should be an engineer—"one who is versed in or practicing any branch of engineering." But is this really the case?

One needs only to attend any of the engineering conventions, symposia, section or professional group meetings to discover that there is an appalling lack of understanding among many of our younger engineers as to the things really important to "the art of designing." At these affairs, intelligent and sincere young men proudly describe their analyses, developments, and achievements. In many cases, original work *has* been done, and its author truly displays a good background of prior work. But too often the dissertation is a rediscovery of work already done, or describes hardware of marginal usefulness, and clearly demonstrates a lack of understanding of many things basic to engineering—"the art of designing."

In this situation is a reason why we have problems with missile reliability, circuit complexity, operational utility, high cost, or even engineering management. In this, the era of the cost-plus-fixed-fee contract, there is but slight financial incentive for industry to genuinely emphasize engineer training. If a young man must spend an extra several months researching the field to select the best components, or redesigning after the catastrophic field test, this is equally profitable to the company. Not only is the salary paid fully reimbursed, but a contribution to overhead helps further to retire the facility, even if no fee is earned. Engineer demand often places a company in the position of assigning engineers project responsibilities far beyond their training or experience. The senior, capable people have long since been removed from such mundane details as selecting the best relay, and now either revolve in the world of the "system" block diagram, the curtained offices and the policy meetings; or else, tiring of the gambit, have become independent consultants or launched their own companies. The public teat succors many a "research" program that, stripped of equations, is nothing more nor less than a learning curve for engineers who have not yet mastered "the art of designing."

In a profit-oriented company (and there are many such companies which refuse all but fixed-price contracts and are choosy about these), we have a similar situation, but for another reason. In these cases, the company cannot afford a plethora of engineers in the futile belief that somehow quantity will make up for quality, nor can it always afford the salary that competence demands. The company selects the best talent it can afford, trains it themselves, and piously hopes through all sorts of inducements to keep it around. But in these cases, the engineer soon finds himself with a work load which is some exponential function of his performance; the better job he does, the more he is assigned, until eventually he, too, cannot devote the time really required for "the art of designing" and must take chances and make guesses.

It is easy to find reasons, but hard to find excuses for this situation. Basically, the heart of the problem is *engineering education*. With a few notable exceptions, our engineering schools are not teaching, and never have taught, "the art of designing." They have taught "the science of analyzing." Throughout the average university curriculum, the emphasis is on *analysis* rather than *synthesis*. Given a circuit, what does it do? Yet the first task usually expected of the engineer is: given the specification, produce the design. The Laplace transform, important though it is, is of no help in deciding which of a dozen makes of capacitors to specify for a particular problem, or in hacking through the jungle of transistor and diode-type numbers. How many of our university catalogs today list courses dealing with what might be called "component sources," or, "who makes what, how good is it, how much does it cost, what are the quantity and OEM discounts, and how is it specified and bought?" How many new engineers even know where to look for product information beyond the magazine advertising? How many professors teach the perils of ground loops or excessive heater-cathode potentials; what are the best printed-circuit base materials; the relative merits of eyelets and plate-through; what constitutes a good solder connection; what plugs can be counted on to give trouble; where solid wire is preferable to stranded; and so on? How many engineering schools have test laboratories equipped with temperature and altitude chambers and random-and-sine vibration-testing equipment? How many show stroboscopic films of the jelly-like behavior of "rigid" components vibrating above their resonant frequencies? How many electronics engineers are taught in school the difference between a coarse and a fine thread, the hole size for a 4-36 screw, or, for that matter, the resistor, capacitor or diode color code? How many students get any appreciation of the *cost* of components as they learn their function? How many new graduates know the effects of stray fields from a transformer? How many know the practical side of what to expect from parasitic oscillations, even in pulse circuits, VR tubes, and Zener diodes, and how to avoid them? How many know what a MIL specification is? How many know how to make by themselves a limited patent search, or even of the existence of the *Patent Gazette*? All of these matters and painfully many more are, in general, left to industry to teach, or for the student to find out for himself, like sex—and to carry the analogy further, often the hard way as he watches his creation cremated on the launch pad. To the extent that industry is unable to do this training, unreliability is naively built into the design.

It is unfair to criticize education for sins of omission without recognizing its side too. Just where, in a four-year or six-year curriculum is there time for such mundane but necessary things, especially in view of the accelerated progress in the past twenty years? Certainly one should not drop the course in Laplace transform in favor of these things. Where does the school obtain qualified professors with practical (and successful) design experience, and how can they be motivated to teach such subjects adequately, with altruistic indifference to the salary received? How can the expense of environmental test equipment be fitted into the budget? And, after all, should an academic institution of "higher learning" teach the things that are really "lower learning"? Of course these are legitimate questions, but they do have answers.

While adequate finance may not be a panacea, it is certainly a necessary remedy to part of the problem. The schools than can afford modern equipment and adequate salaries, and who have working arrangements with nearby industry for laboratory training and summer employment sessions, are turning out the best engineers. Summer periods are an indoctrination into "things

* Received by the IRE, February 7, 1961; revised manuscript received, March 23, 1961.

World Radio History

practical," so essential to "the art of designing." It is to the advantage of both industry and the taxpayer to give generous financial support for such needs. Better engineers will ultimately result, and the investment will be returned many fold.

Additions to engineering curricula of required courses dealing with these practical subjects are needed, even if at the expense of fewer hours of student leisure. Existing courses need greater emphasis on synthesis —working from specifications—not simply in class-A amplifiers or emitter followers, but in digital and RF systems and a host of more complex subjects. The practical side should be taught along with the theory. The student should commit to memory the standard values of 5 per cent and 10 per cent resistors and be required to use these in his designs, and recompute performance in a tolerance (and temperature) analysis. His problem sets should require detailed component selection and specification of critical part locations and lead lengths, hole sizes, types of plugs for interconnections, and so on. Grading could be on how his design would probably withstand temperature, humidity, vibration, shock, corrosion, and whether it would be economical and reliable. Perhaps most of all, the student should be instructed to locate alternate units already commercially available that might satisfy the basic requirements so that he will know whether, in fact, he should be designing such a unit at all except for practice.

We write about engineers who cannot spell, write, or speak in public, and so on, but these things may be secondary to "the art of designing." Such deficiencies are easily tolerable in a man who can turn out a solid, producible, economical, trouble-free, profitable, and useful product. The archives are full of scholarly technical reports on projects long deceased because of poor design.

Only with practical training, in school, government or industry, and preferably all three, can it truly be said that the engineer is *educated* and is "one who is versed in or practicing any branch of engineering—the art of designing."

R. W. Johnson
The R. W. Johnson Co.
Anaheim, Calif.

## A Note on Sugai's Class of Solutions to Riccati's Equation*

In this correspondence, it will be shown that the solution of Riccati's differential equation can be found from the solution of two associated Bernoulli equations provided the coefficients of the Riccati equation satisfy certain relationships to be specified later. This work generalizes the technique presented by Sugai[1] in a recent note. It is accomplished by using a more general transformation of the dependent variable than that used by Sugai. In this note, the notation of Ince[2] is used.

The Riccati differential equation reads

$$\frac{dy}{dx} + \psi y^2 + \phi y + \chi = 0. \tag{1}$$

The transformation proposed here is given by

$$y(x) = \frac{c_1(x)v'(x) + c_2(x)v(x)}{c_3(x)v'(x) + c_4(x)v(x)}, \tag{2}$$

where the prime denotes differentiation with respect to $x$. Substituting the expression for $y(x)$ in (2) into (1), it is seen that $v(x)$ satisfies the following second-order equation:

$$vv''Q_1 - (Q_1 + Q_4)(v')^2 - Q_3vv' - Q_2v^2 = 0, \tag{3}$$

where

$$\begin{aligned} Q_1 &= c_1c_4 - c_2c_3 \neq 0 \\ Q_2 &= c_2c_4' - c_2'c_4 - c_2^2\psi - c_2c_4\phi - c_4^2\chi \\ Q_3 &= c_1c_4' - c_1'c_4 + c_2c_3' - c_2'c_4 \\ &\quad - (c_1c_4 + c_2c_3)\phi - 2c_1c_2\psi - 2c_3c_4\chi \\ Q_4 &= c_1c_3' - c_1'c_3 - c_1^2\psi - c_1c_3\phi - c_3^2\chi. \end{aligned}$$

Eq. (3) will be a linear second-order equation if the condition

$$Q_1 + Q_4 = 0 \tag{4}$$

can be enforced. This condition leads to either one of the following two Riccati equations:

$$c_1' + \frac{\psi}{c_3}c_1^2 + \left(\phi - \frac{c_3'}{c_3} - \frac{c_1}{c_3}\right)c_1 + c_2 + c_3\chi = 0 \tag{5a}$$

$$c_3' - \frac{\chi}{c_1}c_3^2 - \left(\phi + \frac{c_1'}{c_1} + \frac{c_2}{c_1}\right)c_3 + c_4 - c_1\psi = 0. \tag{5b}$$

These equations reduce to Bernoulli's equation, which can be solved in closed form,[3] if in (5a) the condition

$$c_2 = -c_3\chi \tag{6a}$$

is met, or if in (5b) the condition

$$c_4 = c_1\psi \tag{6b}$$

is met. Thus (5a) or (5b) reduces to Bernoulli's equation and $c_1$ or $c_3$ can be determined in closed form.

The condition given in (6a) is satisfied by the first transformation given by Sugai in (4) of his paper. The second given in (6b) is satisfied by the transformation given by Sugai in (5) of his paper.

Now the problem has been reduced to solving the following differential equation:

$$Q_1v'' - Q_3v' - Q_2v = 0. \tag{7}$$

The fact that (1) is equivalent to a second-order linear equation is well known.[4] Hence, in order to benefit from the transformation in (2), one requires that $Q_2$ must also vanish subject to either the condition in (6a) or (6b). The vanishing of $Q_2$ subject to (6a) and (6b) is given in (8a) and (8b), respectively.

$$c_3c_4' - c_3'c_4 - \left(\phi + \frac{\chi'}{\chi}\right)c_3c_4 + c_3^2\chi\psi + c_4^2 = 0 \tag{8a}$$

$$c_1'c_2 - c_1c_2' - \left(\phi - \frac{\psi'}{\psi}\right)c_1c_2 - c_1^2\chi\psi - c_2^2 = 0. \tag{8b}$$

It is noted that (8a) is a Riccati equation in either $c_3$ or $c_4$, and (8b) is a Riccati equation in either $c_1$ or $c_2$, and thus, it is of little value to specify $\psi$, $\phi$, $\chi$. However, at this point it is convenient to point out the results of Sugai's work. It is seen by substitution in (8a) that if one lets

$$c_1 = 0, \quad c_2 = -\chi, \quad c_3 = 1, \quad c_4 = \phi. \tag{9a}$$

which are the conditions in Sugai's transformation given in (4) of his note, then one deduces the condition given in (8) of his note. If one lets

$$c_1 = 1, \quad c_2 = -\phi, \quad c_3 = 0, \quad c_4 = \psi. \tag{9b}$$

then one has the transformation suggested by Sugai in (5) of his note. In this case one deduces the condition in (9) of his note.

New relationships can be derived from the generalized transformation defined in (2) through the study of (8a) and (8b). The study will be facilitated by rewriting (8a) and (8b) in the following forms, namely:

$$\chi' - \frac{c_3\psi}{c_4}\chi^2 + \left(\phi - \frac{c_4}{c_3} + \frac{c_3'}{c_3} - \frac{c_4'}{c_4}\right)\chi = 0 \tag{10a}$$

$$\psi' - \frac{c_1\chi}{c_2}\psi^2 - \left(\phi + \frac{c_2}{c_1} + \frac{c_2'}{c_2} - \frac{c_1'}{c_1}\right)\psi = 0. \tag{10b}$$

Thus it is seen that (10a) and (10b) are Bernoulli's equations in terms of $\chi$ and $\psi$, respectively. The solution of an equation of the form

$$\frac{dz}{dx} + q_1(x)z^2 + q_2(x)z = 0$$

is also a solution of the equation[3]

$$\frac{d}{dx}\left(\frac{1}{z}\right) = q_1(x) + q_2(x)\left(\frac{1}{z}\right).$$

Thus, for example, in (10a), one can specify $c_3$ and $c_4$ in any convenient manner, and since (10a) can be solved in closed form, the functional relationship between $\psi$, $\phi$, $\chi$ necessary to obtain a solution of (1) by these techniques can be found. The coefficients $c_1$ and $c_2$ are now determined by the conditions specified in (5a) and (6a).

Thus, it has been shown that the solution of a Riccati equation can be found by solving two Bernoulli equations provided $\psi$, $\phi$, $\chi$ and the auxiliary coefficients are related as in (10a), (5a) and (6a), or (10b), (5b) and (6b).

David C. Stickler
Antenna Lab.
Dept. of Elect. Engrg.
The Ohio State University
Columbus, Ohio

* Received by the IRE, March 27, 1961.

[1] I. Sugai, "A new exact method of nonuniform transmission lines," Proc. IRE, vol. 49, pp. 627–628; March, 1961.
[2] E. L. Ince, "Ordinary Differential Equations," Dover Publications, Inc., New York, N. Y., pp. 23–25; 1956.
[3] *Ibid.*, pp. 22, 24.
[4] *Ibid.*, p. 23.

World Radio History

## A New RMS Describing Function for Single-Valued Nonlinearities*

Klotter[1] and Prince[2] have at one time or another proposed various unconventional describing functions, but these have not found widespread use because they do not, in general, provide the accuracy of the conventional describing function. The present authors have also looked into a number of other describing functions based on minimizing the average value of error between the fundamental of the output of the nonlinearity for a sine-wave drive and the absolute value of error, etc. Of course, it is apparent that as the linear element of the closed loop tends toward a perfect low-pass

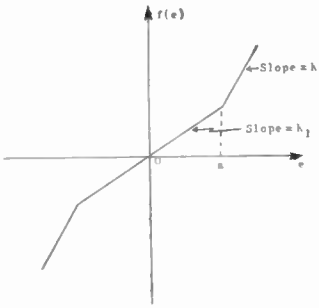


Fig. 1.

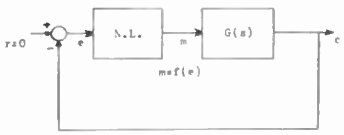


Fig. 2.

filter, the error of the conventional describing function tends towards zero. It is possible, however, that an unconventional describing function could provide better accuracy for many practical systems since perfect filtering is unrealistic.

The authors propose that for single-valued, instantaneous nonlinearities, a possibly superior describing function is obtained by equating the rms value of the equivalent output sine wave of fundamental frequency to the rms value of the actual nonsinusoidal output of the nonlinear element in response to a sine-wave drive. This might be justified on an equivalent energy basis. The definition is thus,

$$K_{eq} \triangleq \left\{ \frac{\frac{1}{2\pi}\int_0^{2\pi} [f(E\sin\theta)]^2 d\theta}{\frac{1}{2\pi}\int_0^{2\pi} (E\sin\theta)^2 d\theta} \right\}^{1/2}, \quad (1)$$

where

$E\sin\theta \triangleq$ input to the nonlinearity

$f(E\sin\theta) \triangleq$ output of the nonlinearity.

For instantaneous nonlinearities, the phase shift through the element will be zero. Consider the nonlinearity shown in Fig. 1. There,

$$f(e) = \begin{cases} k_2(e-a) + k_1 a & (e \geq a) \\ k_1 e & (-a < e < a) \\ k_2(e+a) - k_1 a & (e \leq -a). \end{cases}$$

For this nonlinearity, (1) becomes

$$K_{eq} = \left\{ k_2^2 + \frac{2}{\pi}(k_1^2 - k_2^2) \cdot \left[ \sin^{-1}\frac{a}{E} - \frac{a}{E}\sqrt{1-\frac{a^2}{E^2}} \right] + \frac{8}{\pi} k_2(k_1-k_2)\frac{a}{E}\sqrt{1-\frac{a^2}{E^2}} + 2(k_1-k_2)^2\frac{a^2}{E^2}\left(1 - \frac{2}{\pi}\sin^{-1}\frac{a}{E}\right) \right\}^{1/2} \quad (E > a), \quad (2)$$

which is somewhat more complex than the conventional describing function for the same nonlinearity

$$N = k_2 + \frac{2}{\pi}(k_1 - k_2) \cdot \left[ \frac{a}{E}\sqrt{1-\frac{a^2}{E^2}} + \sin^{-1}\frac{a}{E} \right] \quad (E > a).$$

For the relay with dead band, the rms describing function (1) becomes

$$K_{eq} = \left\{ \frac{2}{\pi}\frac{M^2}{E^2}\left[ \pi - 2\sin^{-1}\frac{B}{2E} \right] \right\}^{1/2} \left( E > \frac{B}{2} \right), \quad (3)$$

and the conventional describing function is

$$N = \frac{4}{\pi}\frac{M}{E}\sqrt{1-\frac{B^2}{4E^2}} \quad \left( E > \frac{B}{2} \right).$$

TABLE 1

| N. L. | $G(s)$ | Method | Predicted Amplitude of Oscillations | Percentage Error | Predicted Period of Oscillations | Percentage Error |
|---|---|---|---|---|---|---|
| 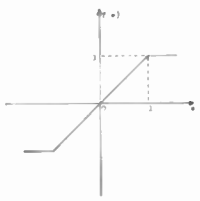 | $\frac{10}{s(s+1)^2}$ | Describing Function | 6.30 | 5.95 | 6.28 | 1.67 |
| | | Proposed rms DF | 6.80 | 1.49 | 6.28 | 1.67 |
| | | Experimental | 6.70 | | 6.38 | |
| | $\frac{5}{s(s+1)^3}$ | Describing Function | 7.45 | 8.25 | 10.90 | 2.68 |
| | | Proposed rms DF | 7.75 | 4.55 | 10.90 | 2.68 |
| | | Experimental | 8.12 | | 11.20 | |
| | $\frac{2}{s(s+1)^4}$ | Describing Function | 4.55 | 3.19 | 15.70 | 3.29 |
| | | Proposed rms DF | 4.75 | 1.06 | 15.70 | 3.29 |
| | | Experimental | 4.70 | | 15.20 | |
| 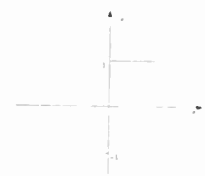 | $\frac{10}{s(s+1)^2}$ | Describing Function | 6.35 | 7.85 | 6.28 | 1.67 |
| | | Proposed rms DF | 7.07 | 2.61 | 6.28 | 1.67 |
| | | Experimental | 6.89 | | 6.38 | |
| | $\frac{5}{s(s+1)^3}$ | Describing Function | 7.15 | 5.92 | 10.90 | 0.925 |
| | | Proposed rms DF | 7.07 | 4.60 | 10.90 | 0.925 |
| | | Experimental | 7.60 | | 10.80 | |
| | $\frac{2}{s(s+1)^4}$ | Describing Function | 4.45 | 4.30 | 15.60 | 0.636 |
| | | Proposed rms DF | 4.95 | 6.45 | 15.60 | 0.636 |
| | | Experimental | 4.65 | | 15.70 | |

An analog computer study of a number of systems has been made to establish an initial feeling for the accuracy of the rms describing function. Two nonlinearities have been considered: 1) saturation or limiting for which the rms describing function is a special case of (2), and 2) the perfect relay, a special case of (3). The linear elements involved are of the third, fourth and fifth order. As might be anticipated, the conventional describing function improves as the filtering becomes heavier, but the rms describing function presents a significant improvement for the lower-order cases. A block diagram of the configuration is shown in Fig. 2 and the results are summarized in Table 1. Work is proceeding on the application of this new describing function to non-single-valued nonlinearities.

Thanks are due D. C. Fosth for analog computer programming.

J. E. Gibson
K. S. Prasanna-Kumar
Control and Information Systems Lab.
School of Elec. Engrg.
Purdue University
Lafayette, Ind.

* Received by the IRE, March 23, 1961.

[1] K. Klotter, "An extension of the conventional concept of the describing function," *Proc. Symp. on Nonlinear Circuit Analysis*, Polytechnic Inst. of Brooklyn, Brooklyn, N. Y., vol. 6; 1956.

[2] L. T. Prince, Jr., "A generalized method for determining closed-loop frequency response of nonlinear systems," *Trans. AIEE*, pt. 2, vol. 73 (*Applications and Industry*) pp. 217–224; September, 1954.

World Radio History

## A Proposed Test of the Constancy of the Velocity of Light*

Einstein's definition of simultaneity and also all accurate measurements that have ever been made of the velocity of light are based upon the assumption that the reflection (by a mirror that is at rest in the observer's frame) of a light signal which is traveling over a return path occurs precisely at the half time for the journey. Because the one-way velocity of light has never been accurately measured,[1] this assumption has never been subjected to a direct test. Stated in another way, it is postulated that the observer's relative space is isotropic to the propagation of light; and this is the underlying and untested assumption upon which the special theory of relativity rests.[2] Recent developments have raised serious questions as to the validity of this postulate.[3,4] I believe, therefore, that it is highly desirable for a direct test of Einstein's concept of simultaneity and of his second postulate to be made at this time, especially since such a test now appears possible with modern techniques.

I offer, by way of example, that two identical maser-controlled clocks, each fashioned to store information on video tape or some similar device accurate to one thousandth of a microsecond, can be first synchronized, while together, by means of identical marker signals on the two tapes, and then can be transported to locations about 18.6 miles apart. The two clocks are hereby stationed 100 microseconds apart by light signal, so that the velocity of light can be timed accurately one-way to ±one mile per second. Selected marker signals at station A are arranged so as to fire a strobe light toward station B, and the tape at station A is marked electronically to indicate each firing. The light signal is detected at station B by a photocell, which marks tape B and simultaneously fires a second strobe light toward station A. The receipt of the return signal is recorded by a photocell, which completes the cycle. Other cycles can be performed as needed.

Upon the assumption that light is some unspecified form of wave propagation, the velocity of the solar system in the universe should produce a first-order effect of $V/C$ on the time required for light to pass in the two directions, when the light signal and the vector $V$ are parallel. This effect equals the time difference in the two directions divided by the total time; i.e.,

$$\frac{t_2 - t_1}{t_2 + t_1} = \frac{v}{c} = \frac{\Delta l}{l}.$$

To this end, the apparatus should be oriented so that at some time during the day it is tangent to our probable orbit about the supergalactic center, located in Virgo. In this case, $V$ should be on the order of 1000 miles per second, and should hence be easily detectable. However, if Einstein's postulate is correct, or if light behaves ballistically, there will be a null effect and relative space will have been proved isotropic to the propagation of light. In this event, a separate, but similar experiment would have to be conducted to decide between Einstein's postulate and the ballistic-like considerations which have been introduced by Prof. Dingle.[2]

PASCAL M. RAPIER
Newtonian Science Foundation
Richmond, Calif.

* Received by the IRE, March 20, 1961.

[1] M. Ruderfer, "Relativity: blessing or blindfold?" PROC. IRE (Correspondence), vol. 48, pp. 1661–1662; September, 1960.
[2] H. Dingle, "A possible experimental test of Einstein's second postulate," *Nature*, vol. 183, p. 1761; June, 1959.
[3] H. Dingle, "Relativity and electromagnetism: an epistemological appraisal," *Phil. Sci.*, vol. 27, pp. 233–253; July, 1960.
[4] P. M. Rapier, "Comments on the article, 'Relativity and the mechanical engineer,'" (by B. D. Mills, Jr.), *Mech. Engrg.*, vol. 82, pp. 91–92; August, 1960.

## Notes on the Structure of Logic Nets*

### Introduction

The purpose of this note is to present an elementary approach to a theory of the role of structure in logic nets and to give examples of some simple applications. We are primarily, although not exclusively, interested in "cellular" or "honeycomb" structures which have a) approximately the form of three-dimensional regular lattices, b) a uniform type of elementary component in a single lattice, and c) simply connected elementary components, *i.e.*, components connected only to adjacent components, or possibly, if located on the periphery, to "system" inputs or outputs. Such structures are termed "peripheral access lattices" or simply PAL's. The composite structure and its behavior, observed at the peripheral connections, is referred to as macrostructure while its constituent elementary components are referred to as microstructures or microcomponents. We are especially concerned with the range of possible macroscopic behavior for nets having a *fixed basic structure but some variability in microscopic behavior.*

### Variability and the Basic Theorem of Composite Structures

Let $N$ represent the number of different possible modes of behavior of a multistable logic structure. Variations in behavior are presumed to correspond to different possible quasi-stable states in which the structure may exist, according to its past history, treatment or conditioning.

If a macrostructure consists of an assembly of $n$ microstructures, then the number of different system-states equals the product of all component state numbers, and thus, obviously,

$$N_{\text{macro}} \leq \prod_{i}^{n} (N_{\text{micro}})_i. \tag{1}$$

* Received by the IRE, February 7, 1961; revised manuscript received, March 17, 1961.

The equality applies if, for every different arrangement of microstates, the macrostructure responds differently, as observed at its periphery. If we define

$$C = \log_2 N, \tag{2}$$

then, from (1),

$$C_{\text{macro}} \leq \sum_{i}^{n} (C_{\text{micro}})_i. \tag{3}$$

$C$ may properly be called the equivalent structural information content and is numerically equal (if an integer) to a minimum number of binary digits required to specify, identify, or describe the behavior or response function of a structure.

### Maximum Capacity of Binary Devices

For a unilateral device having $n_i$ binary inputs and $n_o$ binary outputs, which are functionally dependent on the inputs,

$$C \leq 2^{n_i} n_o \tag{4}$$

The equality applies to a structural unit capable of assuming any describable functional dependence of the output pattern on the input pattern and is essentially the dimensionality of the associated "truth table" or generalized Venn diagram. Such a device is termed a "universal" computer. For example, a unit having two inputs and one output as shown

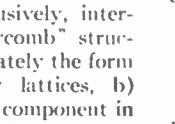


has a maximum structural capacity of 4 bits. If it has such capacity it must be capable of performing as an "and gate," "or gate," "nor gate," "exclusive-or-gate" and all such possibilities (16 in all) including such things, usually considered somewhat trivial in the logical design of computers, as $X=0$, $X=1$, $X=a$, $X=\bar{a}$, $X=b$, or $X=\bar{b}$. With $n_i=1$ and $n_o=2$ the maximum capacity is likewise 4 bits.

### Minimum Size of Universal Binary Machines

If a binary macromachine consisting of a number of identical binary microcomponents is to be universal, then from (3) and (4),

$$n \geq 2^{(N_i - n_i)} \left(\frac{N_o}{n_o}\right). \tag{5}$$

As an example of the implications of this result, consider the structure shown in Fig. 1 where a microcomponent is presumed to be located at each vertex. If the components are universal elements, $(C_{\text{micro}})_i = 4$ bits and, hence,

$$\sum_{i}^{n=60} (C_{\text{micro}})_i = 240 \text{ bits.}$$

But,

$$2^{N_i} N_o = 2^6 \cdot 6 = 384 \text{ bits.}$$

Thus, it is fundamentally impossible for this macrostructure to be universal. In other words, there are apparently some response functions which can be described for $N_i=6$ and $N_o=6$ but which cannot be realized

World Radio History

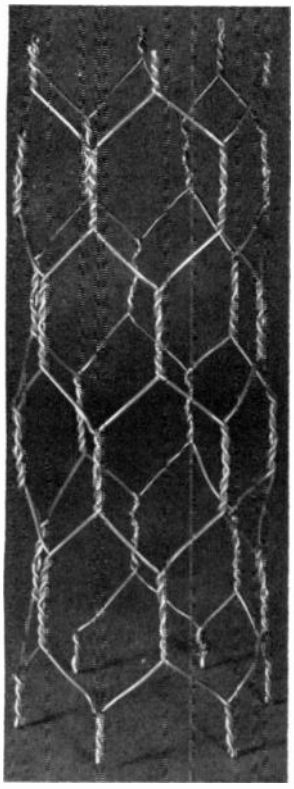

Fig. 1.

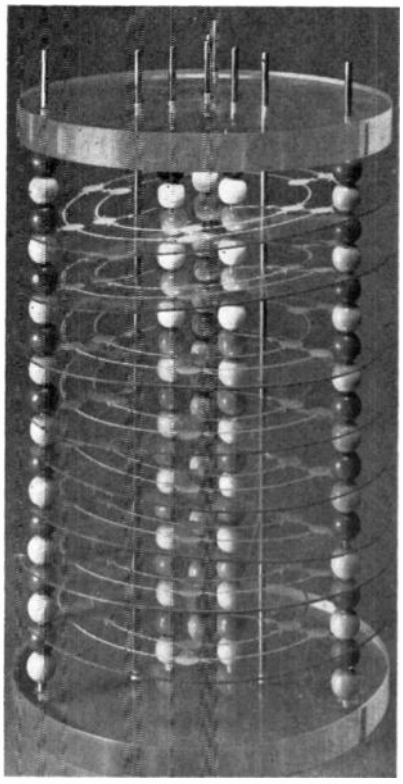

Fig. 2.

with this internal structure and connectivity regardless of how we may choose the behavior of the (binary) internal components. This particular type of structure has a number of interesting special properties and has been the subject of farther intensive study.

### The Closure Rule

A useful theorem in dealing with logic nets is based on the assumption that there are no loose ends, *i.e.*, every input connection to a microcomponent is either a peripheral input to the macrosystem or the output of some microcomponent and that every output of a microcomponent either terminates as an input to some microcomponent or as a peripheral output of the macrosystem. Then, by counting internal connections,

$$\sum^{n} n_i - N_i = \sum^{n} n_o - N_o.$$

When $N_i$ and $N_o$ are much less than $\sum n_i$ and $\sum n_o$ (*i.e.*, many more "internal" connections than peripheral connections), this reduces to

$$\langle n_i \rangle = \langle n_o \rangle, \tag{7}$$

where $\langle n_i \rangle$ and $\langle n_o \rangle$ are respectively the *average* number of inputs and outputs per microcomponent. Under these conditions, this might suggest, for example, that a net partially composed of microcomponents for which $n_i = 2$ and $n_o = 1$ might be completed with approximately an equal number of components for which $n_i = 1$ and $n_o = 2$:

$$a \rightarrow 0 \begin{cases} \nearrow X(a) \\ \searrow Y(a). \end{cases}$$

Another class of structures of interest is that corresponding to a simply connected lattice of closest-packed spheres; for such a lattice,

$$n_i + n_a = 12 \tag{8}$$

for every component except those on the periphery. Therefore, from the modified Closure Rule (7)

$$\langle n_i \rangle = \langle n_o \rangle = 6. \tag{9}$$

If we let $n_i \equiv n_o \equiv 6$, for every component, $C_{\text{micro}} = 384$ bits/component as shown previously.

### Possibilities and Probabilities

Various workers have concerned themselves with calculating and describing theoretical constraints on macrosystem behavior when the constituent microcomponents are constrained in certain special ways. As yet, there has appeared very little analysis involving structural contraints as well. As a simple example, it is probably well-known that an assembly exclusively comprised of any number of "and-gates" and "or-gates," and having just two peripheral inputs $(a, b)$ and one peripheral output $[X(a, b)]$ can behave macroscopically only in the trivial ways, $X \equiv 0$, $X \equiv a$, or $X = b$ or else either as an "and-gate" or as an "or-gate." What may not have been demonstrated is that, if the trivial responses are structurally impossible and if the microcomponent response functions are chosen at random with $p_{\text{and}} = p_{\text{or}} = \frac{1}{2}$ then the macrosystem response probabilities are likewise $P_{\text{and}} = P_{\text{or}} = \frac{1}{2}$. This result is a direct consequence of De Morgan's theorem. This type of analysis of a logic net is directly analogous to the basic aims of physical statistics or statistical mechanics.

The model shown in Fig. 2 represents a machine for which $N_i = 3$, and $N_o = 3$. Hence, $C \leq 2^3 \cdot 3 = 24$ bits. The machine represented actually achieves the theoretical maximum capacity of 24 bits (approximately 16,000,000 different response functions) using just 24 switches (in addition to a fixed section of "nor" elements) and, hence, has a total microcapacity of just 24 bits. Furthermore, if for each bistable component, $P_{\text{open}} = P_{\text{close}} = \frac{1}{2}$, then the probability of occurrence of each possible response function is the same and this machine is, therefore, "structurally homogeneous."

Robert M. Stewart
Space Electronics Corp.
Research and Advanced Techniques Lab.
Glendale, Calif.

## Suppression of Emission from Portions of Barium-Activated Tungsten Dispenser Cathodes and Adjoining Electrodes*

It is often desirable to suppress the emission from portions of cathode surfaces in order to generate electron beams of special shape and also to prevent electron emission from cathode supports and from auxiliary electrodes in close proximity to the cathode. Both objectives are difficult to achieve because most metals become activated by cathode evaporation and migration products.

A technique[1] has been developed to suppress the electron emission from portions of barium-activated tungsten dispenser cathodes[2–5] and from hot tungsten and molybdenum surfaces close to such dispenser or oxide-coated cathodes. The technique consists in carburizing the areas to be rendered nonemitting by completely immersing the part to be treated, save for necessary masks, in finely divided graphite powder and heating for 5 to 15 minutes at a temperature in the range 1500 to 1800°C in an atmosphere of hydrogen. Carbides of molybdenum and tungsten are formed at the treated surfaces for depths of some tens of microns.

The emission from barium-activated dispenser cathodes is reduced by this process by two or more orders of magnitude in the usual operating range of these cathodes (*e.g.*, 900 to 1200°C. The lower limit can be further reduced if the cathode evaporation rate is sufficiently small.) That the inhibition of emission arises solely from the presence of the carbide layer can be demonstrated by grinding the emitter sur-

* Received by the IRE, June 29, 1961.

[1] R. Levi, "Carburization of dispenser cathodes," U. S. Patent No. 2,972,078; February, 1961.
[2] H. J. Lemmens, M. J. Jansen, and R. Loosjes, "A new thermionic cathode for heavy loads," *Philips Tech. Rev.*, vol. 11, p. 341–350; June, 1950.
[3] R. Levi, "New dispenser type thermionic cathode," *J. Appl. Phys.*, vol. 24, p. 233; February, 1953.
[4] R. Levi, "Improved impregnated cathode," *J. Appl. Phys.*, vol. 26, p. 639; May, 1955.
[5] P. P. Coppola and R. C. Hughes, "A new pressed dispenser cathode," Proc. IRE, vol. 44, pp. 351–359; March, 1956.

World Radio History

face down to a depth exceeding that of the carbided region, whereupon the full emission density of the cathode is recovered. This presents another possibility, in addition to masking, for selective carburization of cathode surfaces. The inhibition of emission from dispenser cathodes persists for times of the order of $10^3$ to $10^4$ hours, the higher values applying at lower cathode temperatures. Return of emission coincides with complete disappearance of the carbide layer from the surface of the cathode.

In the case of thin adjoining electrodes of tungsten and molybdenum, provided that embrittlement is not a serious concern, carburization to a depth comparable to the electrode thickness yields negligible emission relative to that from barium-activated tungsten[6] or molybdenum[7] surfaces for times much longer than those observed in inhibited dispenser cathodes. Since the evaporant from these dispenser cathodes is constituted of Ba and BaO,[6,8] carburized tungsten and molybdenum electrodes in close proximity to oxide-coated cathodes will also exhibit emission suppression, provided that they attain a temperature approaching that of the cathode..

The carburization technique has been applied successfully to the generation of hollow beams and to the suppression of emission from cathode supports and auxiliary electrodes such as beam focusing electrodes, disk-shaped grids, accelerating anodes, and guard electrodes. Cathodes containing beam focusing or guard electrodes can be prepared as a single solid structure. A notable success has been the elimination of emission from molybdenum end hats in magnetron cathodes.

R. Levi
Philips Metalonics
Mt. Vernon, N. Y.
E. S. Rittner
Philips Laboratories
Irvington-on-Hudson, N. Y.

[6] E. S. Rittner, R. H. Ahlert, and W. C. Rutledge, "Studies on the mechanism of operation of the L-cathode (1)", *J. Appl. Phys.*, vol. 28, pp. 156–166; February, 1957.
[7] E. S. Rittner and R. H. Ahlert, "Thermionic emission from barium-activated molybdenum," *J. Appl. Phys.*, vol. 29, pp. 61–63; January, 1958.
[8] E. S. Rittner, W. C. Rutledge, and R. H. Ahlert, "On the mechanism of operation of the barium aluminate impregnated cathode," *J. Appl. Phys.*, vol. 28, pp. 1468–1473; December, 1957.

## Transmission Line Model*

In the consideration of transmission line problems, a type of line can be hypothesized which has some interesting characteristics, and which may be used also in theoretically studying radio-wave transmission through various homogeneous isotropic media. Some radio engineers have found the procedures hereafter described to be more convenient in the handling of wave transmission problems through these media than the use of field theory.

This hypothetical transmission line is of the coaxial type, is infinitely long, uses conductors having zero resistance, and the region between conductors is a vacuum; also the ratio of the inner diameter of the outer conductor to the outer diameter of the inner conductor is chosen as equal to $e^{2\pi}$ (that is, 535.5). (In further discussion, the rationalized mks system of units is employed.) From conventional coaxial-line formulas for the fundamental transmission mode, certain properties of the line may be computed. When computed thereby, the capacitance per meter length is found to be the same as the permittivity of free space (or $8.85\times10^{-12}$ farads per meter), the inductance per unit length is found to be the same as the permeability of free space (or $1.257\times10^{-6}$ henries per meter), and the characteristic impedance of the line is found to be the same as the intrinsic impedance of free space (or 376.7 ohms, resistive). Moreover, the propagation velocity of a radio wave along the line is the same as that of light in a vacuum. Phase changes in voltages and currents, with time, along the line, resemble those occurring in the respective counterpart electric and magnetic fields during the passage of a plane radio wave through free space, and the wave is not attenuated during transmission along the line. Thus, the accessible end of this long coaxial line provides a two-terminal electrical network which simulates in several ways the transmission of a plane radio wave through free space.

This hypothetical line may be used in various calculations involving radio-wave transmission through homogeneous isotropic media other than free space. To this end, let it be supposed that the space between the line conductors is completely filled with the particular substance under consideration, rather than being evacuated. Moreover, let it be assumed that the permittivity, permeability and specific conductivity of the material to be examined are known quantities at the frequency of interest. Then, the capacitance, inductance, and conductance per unit length of the filled line may be readily calculated. It is pointed out that the line conductance per unit length is numerically the same as the specific conductivity of the material filling the line, in mhos per meter.

From data on the capacitance, inductance and conductance per unit length of the line, when filled with the chosen medium, conventional coaxial-line formulas for wave transmission may then be used to determine, for the medium of interest, such quantities as wave-propagation velocity, attenuation, and intrinsic impedance. This follows, since the electromagnetic field within the line is confined entirely to the substance filling the line, and does not enter the perfectly conducting coaxial members.

This hypothetical line will now be used, illustratively, to determine certain electromagnetic properties for plane waves in sea water at frequencies less than $10^6$ cycles (1 Mc). Initially, sea water is considered to have the same permeability as free space; a specific conductivity of 4 mhos per meter; and a permittivity of $708\times10^{-12}$ farads per meter, or for the latter quantity, 80 times that of free space. From such data, the inductance, capacity and conductance per unit length immediately follow for the "sea water" line, as already explained. In this case, it is also noted that the susceptance of the shunt-capacitance path in a unit length of line is only 0.11 per cent of that of the conductance thereof at a frequency of $10^6$ cycles; hence, the admittance of a unit length of line may be considered the same as the conductance thereof at frequencies less than just cited, or 4 mhos per meter. This allows further simplification of coaxial-line formulas for the problem at hand.

Accordingly, certain electromagnetic properties of plane waves in sea water may be computed as follows:

$$\alpha = 0.0173\sqrt{f(\sigma - 4.45f\cdot10^{-9})} \cong 0.0173\sqrt{f\sigma} \quad (1)$$

$$\eta = \left[0.00281\sqrt{\frac{f}{\sigma}}\right]\sqrt{j} \quad (2)$$

$$v = \frac{3162\sqrt{f}}{\sqrt{\sigma + 4.45f\cdot10^{-9}}} \cong 3162\sqrt{\frac{f}{\sigma}} \quad (3)$$

where $\alpha$ is the wave attenuation, in decibels per meter; $f$ is the frequency, in cycles per second; $\sigma$ is the specific conductivity, in mhos per meter; $v$ is the wave velocity, in meters per second; $\eta$ is the intrinsic impedance, in ohms; and $j$ is the operator, $\sqrt{-1}$. Certain reference material[1] may be helpful to others who wish to derive the above equations.

It should be remembered that the formulas shown above are somewhat restricted; that is, they are applicable at frequencies less than $10^6$ cycles and with a sea-water specific conductivity not appreciably less than 4 mhos per meter. For example, at a frequency of $2\times10^4$ cycles (20 kc), and with sea water having a specific conductivity of 4 mhos per meter, the above formulas show that the attenuation is 4.9 db per meter, the propagation velocity is 223,600 meters per second, and the intrinsic impedance is $0.199\angle45°$ ohms.

The formulas shown above are identical with those deduced by field theory under similar restrictions, and have been known for decades. However, many practicing radio engineers are more adept in using transmission line theory and equations than in employing field theory. Hence, the transmission line model approach to solution of such problems is suggested as being helpful.

J. D. Wallace
U. S. Naval Res. Lab.
Washington 25, D.C.

[1] The equations cited follow substitution in, and permissible simplification of, the appropriate transmission line equations shown in the handbook, "Reference Data for Radio Engineers," Internatl. Telephone and Telegraph Corp., New York, N. Y., 4th ed., p. 552; 1956. The expression for $\alpha$ of (1), is deduced from the expression for $\alpha$ in the handbook cited, but the unit of (1) is decibels per meter, whereas in the handbook, the unit is nepers per meter. The $\eta$ of (2) is arrived at from the expression for $Z_0$ in the handbook. In (3), $v$ is actually the ratio of $2\pi f$ to $\beta$, the expression for $\beta$ being given in the handbook. In substituting in the handbook equations, the term $R$, the line resistance per unit length, is taken as zero in value, for the line conductors have no ohmic loss.

* Received by the IRE, March 27, 1961.

World Radio History

## Antenna Siting Tests at 3480 and 9640 Mc on a 173-Mile Tropospheric Scatter Path*

During the past three years, scatter propagation measurements have been carried out at 3480 and 9640 Mc over a 173-mile path in southern England using transmitters situated at Start Point, Devon. In addition to the usual propagation measurements made at Wembley, Middlesex, which have been reported elsewhere,[1,2] the signal at each frequency was recorded for a short period at an unfavourable site 1.5 miles from the Wembley terminal. This site, at Kenton, Middlesex, was shadowed by Harrow-on-the-Hill at a distance of 1.8 miles. The angular path distances, $\theta$, of the Start Point-Wembley and Start Point-Kenton paths were respectively 26 and 54 milliradians. The $S$-band signal was recorded simultaneously at the two receiver sites for about 10 days during June, 1959, while a similar period of recording was carried out at $X$ band in January, 1960. In all cases, the signal level was measured in terms of the half-hourly median value of the system transmission loss estimated from low speed pen records of the received transmission. The antennas used on the transmitters and receivers were 8-foot paraboloids. The median value of the decibel difference in level at Wembley and Kenton was, at both $S$ and $X$ band, about 16 db, very close to the value predicted by Norton, *et al.*,[3] on the basis of the angular distance of the paths. Following a suggestion by D. Williams, of SRDE, these measurements have now been examined in more detail and it is the purpose of this note to describe briefly the results.

An analysis was carried out to see how the difference in signal levels measured at the two sites varied as a function of the system transmission loss, $L$, of the Start Point-Wembley path. This is illustrated for $S$ and $X$ band respectively in Figs. 1 and 2. The graphs were obtained by grouping the data for each frequency according to the value of $L$, a grouping interval of 1 db being used. Each of the points through which the curve is drawn represents the arithmetic mean of the measured db differences in level lying within one interval; the second curve in each figure gives the number of measurements available to average in each case. The plot of average difference in level against $L$ is seen to be very similar at the two frequencies. At the higher signal levels there is a region where the difference is fairly constant and of the order of 20 db; as $L$ increases a point is reached at which the average difference starts to fall and beyond this decreases at an approximately constant rate (0.7 db/db at $S$-band and 0.8 db/db at $X$ band). It is interesting to note, that the transition level from a constant to a decreasing difference occurs at both $S$ and $X$ band at about 12 or 13 db above the median value of the signal for the time of the year in which the respective measurements were made. The spread of the measurements within each interval of $L$, as measured by their standard deviation, did not appear to vary significantly with level; the average value of the standard deviation was about 2.6 db at $S$ band and 3.2 db at $X$ band.

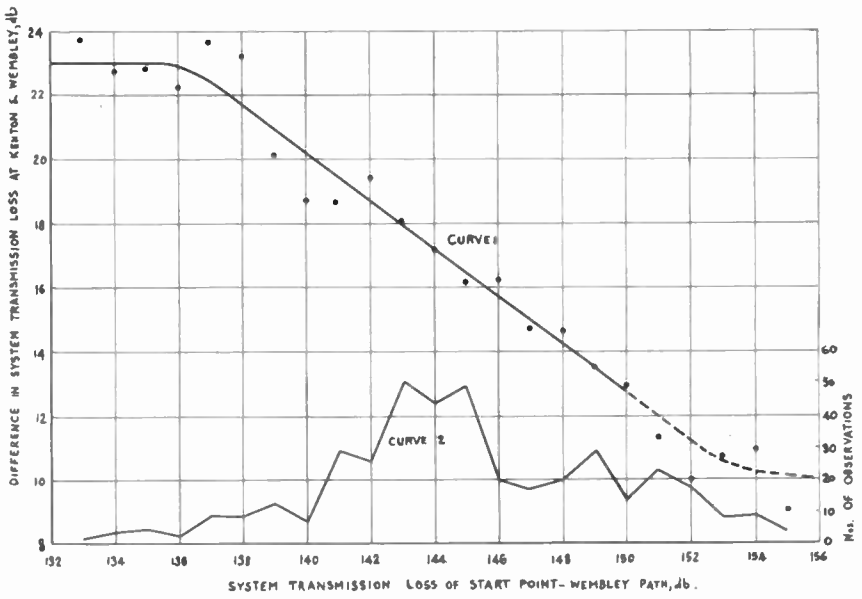


Fig. 1—Average difference in system transmission loss for Kenton and Wembley at $S$ Band. Curve 1—average transmission loss difference. Curve 2—number of measurements available for averaging.

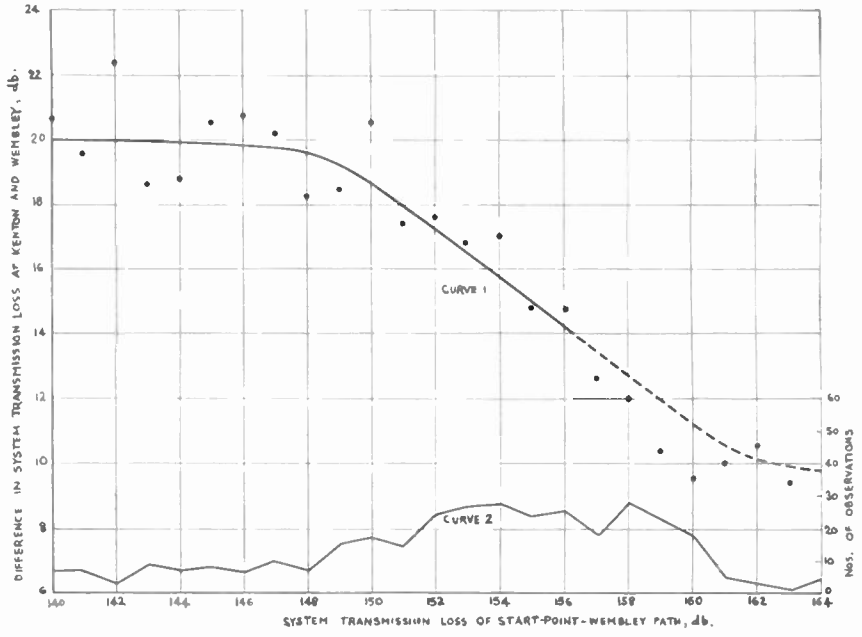


Fig. 2—Average difference in system transmission loss for Kenton and Wembley at $X$ Band. Curve 1—average transmission loss difference. Curve 2—number of measurements available for averaging.

In periods when the transmission loss was high, the Kenton signal occasionally fell below the receiver noise level and the resulting loss of information undoubtedly led to an underestimate of the average difference at the higher values of $L$. The points at which the loss of information started to become significant corresponded to values of $L$ of about 150 and 156 db at $S$ and $X$ band, respectively. It seems probable that, if full information were available, the difference curves in each case would level off to a constant value of perhaps 10 or 11 db. These results are of some practical interest. In a scatter system it is the lower excursions of the median level which are of primary importance since these determine the system reliability. In the event of being forced to accept an antenna site somewhat poorer

* Received by the IRE, April 7, 1961.

[1] B. C. Angell, *et al.*, "Propagation measurements at 3,480 Mc/s over a 173 mile path," *Proc. IEE*, vol. 105, pt. B, suppl. no. 8, pp. 128–142; 1958.

[2] G. V. Geiger, N. D. La Frenais, and W. J. Lucas, "Propagation measurements at 3,480 and 9,640 Mc/s beyond the radio horizon," to be published in *Proc. IEE*.

[3] K. A. Norton, P. Rice, and L. E. Vogler, "The use of angular distance in estimating transmission and fading range for propagation through a turbulent atmosphere over irregular terrain," PROC. IRE, vol. 43, pp. 1488–1526; October, 1955.

World Radio History

than desired, the above results suggest that the actual deterioration in performance may be several db less than might be expected from the theories.

During the propagation program, the amplitude distribution of the *S*-band signal was examined over a large number of periods varying in duration from 5 minutes to 1 hour. In general, it was found that the distribution was similar to that of a Rayleigh vector plus a coherent component, the distributions on the whole approaching the pure Rayleigh case and, therefore, presumably the propagation approaching pure scatter, at the lower values of the median signal level. It is interesting to note that, if it is assumed that in the experiments described above, the difference between the Kenton and Wembley signals tends to a constant value of about 10 db, then the $\theta$ dependence of the received power at low levels is about $\theta^{-3}$ rather than $\theta^{-5}$ given by Norton, Rice, and Vogler.[3]

N. D. La Frenais
W. J. Lucas
The General Electric Co. Ltd.
Central Research Laboratories
Hirst Research Centre
Wembley, England

## On the Linear Circuit Aspects of Cryotrons*

In a recent paper Cohen[1] has presented an expression for the gate resistance of a cryotron in the transition region. It was assumed that the gate resistance is a linear function of the gate and control currents. His expression is of the form

$$R_g = K(ai_G + i_C - I_0), \qquad (1)$$

where $R_g$ is the gate resistance, $i_G$ is the gate current, $i_C$ is the control current, and $K$, $a$, and $I_0$ are constants that depend upon the device configuration. Such an expression is quite adequate for many applications. However, at times it may be desirable to have a more accurate expression for the cryotron characteristic. The expression proposed here has the same form as (1) except that, in order to account somewhat for the nonlinearities present, it is raised to some power. That is

$$\begin{aligned} R_g &= K(ai_G + i_C - I_0)^n \\ &\quad 0 \le K(ai_G + i_C - I_0)^n \le R_n \\ &= 0 \qquad (ai_G + i_C - I_0) < 0 \\ &= R_n \qquad K(ai_G + i_C - I_0)^n > R_n \end{aligned} \qquad (2)$$

where $R_n$ is the normal resistance of the gate.

This expression has been matched with some experimental results,[2] and they are both plotted in Fig. 1. The experimental results are indicated by the plot points. The constants used here were obtained by the usual curve-fitting techniques and are $n=2$, $K=4.7$, $a=0.92$, $R_n=10.7$ millohms and $I_0=0.056$. A better fit to the curves can be obtained by using a more elaborate expression for $R_g$. However, (2) does provide a fairly close fit over much of the region of interest such that more elaborate forms of (2) are required to account for the curvature near the value of normal resistance. However, this region of operation often is not important. In the following discussion it is not, so that (2) suffices here.

Eq. (2) may be used to obtain the gate current vs gate voltage characteristics, which are the output characteristics of the cryotron. The equation that represents these characteristics can be obtained from the relation $e_G = i_G R_g$, where $e_G$ is the gate voltage. The use of this equation results in

$$\begin{aligned} e_G &= i_G K(ai_G + i_C - I_0)^n \\ &\quad 0 \le K(ai_G + i_C - I_0)^n \le R_n \\ &= 0 \qquad (ai_G + i_C - I_0) < 0 \\ &= i_G R_n \qquad K(ai_G + i_C - I_0)^n > R_n. \end{aligned} \qquad (3)$$

A plot of (3) is shown in Fig. 2. An inspection of the results indicates that linear operation of this device similar to that of vacuum tubes and transistors is feasible. Several troublesome features of this operation, such as the thermal hysteresis effect, require further investigation.

In a paper entitled "The Controlled Superconductor as a Linear Amplifier," which is to be published in a forthcoming issue of the IRE Transactions on Component Parts, the authors develop further the above-mentioned ideas. In addition, the authors also derive linear equivalent circuits for controlled superconductors as well as expressions for the gain and efficiencies of cryotrons under various conditions of linear operation.

P. M. Chirlian
V. A. Marsocci
Dept. of Elec. Engrg.
Stevens Inst. Tech.
Hoboken, N. J.

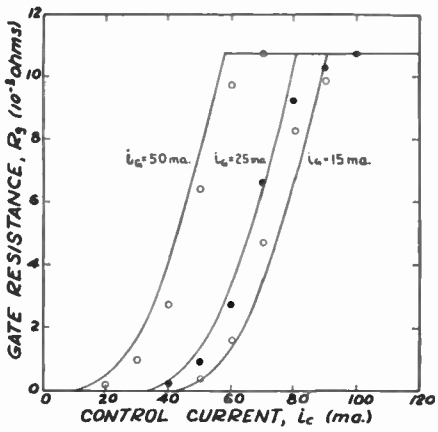


Fig. 1—Gate resistance vs control current, with gate current as a parameter.

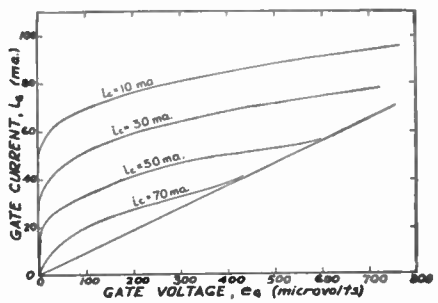


Fig. 2—Cryotron output characteristics.

## A Method for Determining the Base Voltage and Contact Resistance of a Conductivity-Modulated Diode*

The transient behavior of semiconductor diodes is influenced by several parameters including junction voltage, carrier lifetime, base conductivity, and contact resistance. The time rate of decay of an impressed voltage across a diode may be observed by biasing the diode in the forward direction, suddenly opening the circuit, and observing the decay of the injected charge carriers with a cathode ray oscilloscope. Such an oscilloscope trace of the voltage decay in a *p-i-n* junction structure is diagrammed in Fig. 1.

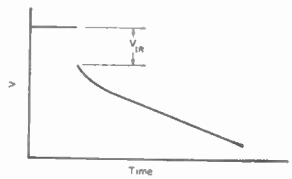


Fig. 1—Voltage decay curve.

Before the switch is opened, the voltage across the device is the sum of the junction voltages, the base voltage, and the voltage developed at the diode contacts. After the switch is opened, the base and contact voltages decay with essentially a zero time constant resulting in the initial vertical portion of the scope trace. The rest of the trace is associated with the transient currents resulting from EMF's developed at the *n-i* and *i-p* junctions due to nonequilibrium concentrations of charge carriers in the junctions. The linear portion of this part of the trace which is associated with the fundamental mode of charge carrier decay is characteristic of the charge carrier lifetime.[1,2] Preceding the linear portion of the curve,

* Received by the IRE, April 12, 1961.
[1] M. L. Cohen, "Thin film cryotrons—Part III," Proc. IRE, vol. 48, pp. 1576–1582; September, 1960.
[2] G. Parkins, "A Cryotron Equivalent Circuit," M.S. Thesis, Dept. of Elec. Engrg., New York University, New York, N. Y.; 1959.

* Received by the IRE, March 3, 1961.
[1] B. R. Gossick, "Post-injection barrier electromotive force of p-n junctions," *Phys. Rev.*, vol. 91, pp. 1012–1013; August, 1953.
[2] S. A. Lederhandler and L. J. Giacoletto, "Measurement of minority carrier lifetime and surface effects in junction devices," Proc. IRE, vol. 43, pp. 477–483; April, 1955.

World Radio History

there is generally a steeper slope which may be attributed to the higher modes of decay[3] and which may not always be distinguishable from the infinite slope associated with the $IR$ component of the voltage, depending on the frequencies of the higher modes and the time constant of the scope.

The contact resistance of a diode is generally deduced from the ohmic portion of the diode impedance by calculating base resistance from the material constants and subtracting from the total ohmic component. However, this is not possible in a conductivity-modulated diode since the base resistance depends on the injection level of the current carriers.

For a $p$-$i$-$n$ diode operated in the conductivity-modulated state, both the conductivity of the base region and the carrier density in the base region are exponentially increasing with applied voltage at the same rate. The result is that the base voltage is relatively independent of current for these high levels of carrier injection.[4] Therefore, the dynamic change in voltage with current in the region of high-level injection is a direct measure of the contact resistance of the device. To determine this dynamic impedance in a particular silicon $p$-$i$-$n$ diode with a 25-mil-wide base, the ohmic component of the voltage-time trace—that is, the quantity $V_{IR}$ shown in Fig. 1—was measured at several current levels and plotted against the current, as shown in Fig. 2.

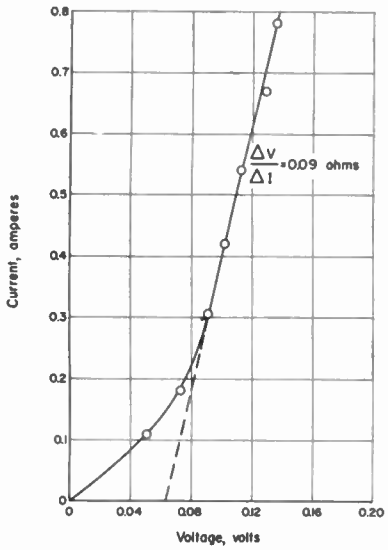


Fig. 2—"Resistive" component ($V_{IR}$) of voltage drop across diode vs forward current.

The higher modes of decay of the injected carriers, which may not be distinguishable on the scope trace from the $IR$ component of the voltage, are assumed to have negligible amplitude. Were the amplitude of the higher modes to be appreciable, the error introduced by this assumption would affect the base voltage only, and not the contact resistance, since the contact resistance is determined from the slope of the curve, and the base voltage from the zero-current intercept.

The conductivity-modulated state of the diode, *i.e.*, constant base voltage, is shown in Fig. 2 to exist above a current load of about 0.3 ampere. The slope of the current-voltage curve in this region is determined by the contact resistance of the device, and represents a resistance of 0.09 ohm.

An extrapolation of the high-level-injection portion of the current-voltage curve to the voltage axis gives the base voltage. Assuming equal resistance at each of the two contacts, a specific contact resistance of 0.0032 ohm cm², and a constant base voltage under conditions of high-level injection of 0.064 volt were obtained.

Since the slope of the conductivity-modulated portion of the $I$-$V_{IR}$ curve represents the contact resistance, decreasing the area of the contacts should result in a proportionate increase in contact resistance. Consequently, the diode was lapped to half its original area and the $I$-$V_{IR}$ data were again taken. The value of contact resistance calculated from the new curve was 0.17 ohm, which is consistent with the reduction of contact area within the limits of experimental error.

J. M. Swartz
H. C. Gorton
Battelle Memorial Inst.
Columbus, Ohio

## Receivers with Zero Intermediate Frequency*

An interesting note was published in these Proceedings on the above subject.[1] A zero-IF (or homodyne) receiver is one in which output is delivered from the first detector or mixer directly at video, or zero IF, rather than at a finite intermediate frequency. The note showed that noise has been considered a major problem in the use of zero IF, and that modern mixers and oscillators have reduced this problem considerably. It is obvious that further improvement is possible by preceding the mixer by low-noise RF amplification.

An experimental zero-IF receiver was set up some years ago by Dr. Charles E. Chase, Jr., of the M.I.T. Lincoln Laboratory. With sufficient low-noise RF gain before the mixer a poor mixer noise figure is unimportant. Such a receiving system was tried, using an RCA experimental A-1038 $S$-band low-noise traveling-wave tube as an RF amplifier. The experimental system is shown in Fig. 1. Two traveling-wave tubes were used in cascade, and the output fed into a balanced mixer with the local oscillator operated at the signal frequency. The mixer output was fed into a video amplifier with balanced input.

If the mixer in a zero-IF system is perfectly balanced, it operates as a perfect multiplier, and interfering signals farther from the stalo frequency than the video bandwidth are rejected. In practice, however, the balance between the two crystals in the balanced mixer is not perfect; consequently, the rectified components at the two crystals do not cancel out and there is detection of signals, to some extent, occurring anywhere in the input pass band.

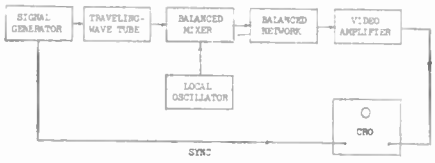


Fig. 1—Zero-IF receiver test apparatus.

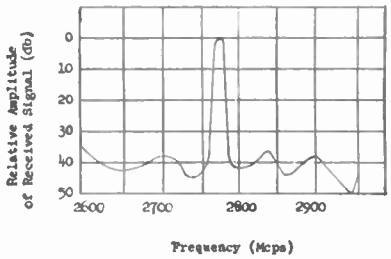


Fig. 2—Rejection of interfering signals by zero-IF receiver.

Although it is possible to balance the output of the crystals at video to cancel interfering signals by perhaps 60 db at some particular frequency, the balance is frequency dependent. Fig. 2 shows the relative amplitude of received signal as a function of frequency, for optimum balance of the above setup over a range of frequencies. The rejection is approximately 40 db, over a range of several hundred Mc, using a standard balanced mixer. For comparison, in a typical superheterodyne system (with an unbalanced mixer) it was found that the interfering signal was rejected by 90 db except at the image, where rejection was only 30 db (and this rejection was due to the TR-tube bandwidth). However, while noise-figure measurements were being made, it was observed that interference from nearby radars was considerably less with the zero-IF receiver than with a similar heterodyne IF receiver of the same over-all gain. This was probably due to the greater ease of shielding the zero-IF receiver.

With the two traveling-wave tubes, having a combined gain of about 45 db, the over-all noise figure, measured with a fluorescent-tube noise source, was 10.8 db. This is the same as the noise figure of the first tube, within experimental error ($\pm 0.2$ db). Thus, the mixer noise contribution was negligible. With a single traveling-wave tube, the noise figure was 17.7 db; because of insufficient gain before the mixer, the video noise contribution of the latter was excessive.

[3] D. T. Stevenson and R. J. Keyes, "Measurement of carrier lifetimes in germanium and silicon," *J. Appl. Phys.*, vol. 26, pp. 190–195; Feburary, 1955.
[4] M. B. Prince, "Diffused p-n junction silicon rectifiers," *Bell Sys. Tech. J.*, vol. 35, pp. 661–684; May, 1956.

* Received by the IRE, March 16, 1961. The research reported in this note was supported by the Dept. of the Air Force under AF Contract No. AF 33(600)39852.
[1] J. C. Greene and J. F. Lyons, "Receivers with zero intermediate frequency," Proc. IRE, vol. 47, pp. 335–336; February, 1959.

World Radio History

It was believed that the relatively poor balance of the balanced mixer was caused by warping of the diaphragm. A new mixer was therefore ordered which used a heavy wedge-shaped member instead of the relatively flimsy diaphragm. Although this mixer was expected to have considerably better balance than the old one, the results were not appreciably different.

If the bandwidth preceding the traveling-wave tube were restricted by a tunable narrow-band filter, then the problem of interfering signals would be considerably reduced. It is also advisable to restrict the input bandwidth since arbitrary received signals over the wide input bandwidth of the traveling-wave tube can be expected to add rms-wise if they occur at the same time, and a total signal can be produced in the traveling-wave tube large enough to reduce seriously the effective dynamic range of the tube. Even with the super-heterodyne, it is helpful to incorporate a tunable filter before the receiver to reduce interference from other radars.

With the zero IF, one has the possibility of a simpler system configuration than with the superhererodyne. In a pulse Doppler radar, the IF strip, synchrodyne, reference oscillator, and IF coherent detector, and any of the specialized power supplies are exchanged for the traveling-wave tubes and their specialized power supplies. This exchange did not appear warranted at the time, in view of the relatively advanced state of design of the former elements. However, with further advances in the traveling-wave tube art, the zero-IF radar may prove to be simpler and easier to maintain.

With the present availability of traveling-wave tubes with noise figures as low as 3 db, the use of zero-IF receivers would be more interesting now and should receive consideration.

M. D. Rubin
The Mitre Corp.
Bedford, Mass.

## A Magnetic Shield for Beam Frequency Standards*

The accuracy of the present cesium-beam atomic frequency standards is limited at least in part by the uncertainty and the inhomogeneties in the magnetic $C$-field region of the machine (see Fig. 1). This uncertainty in the magnetic field arises from two sources: 1) the inability to generate the known uniform magnetic field required to maintain spatial quantization, and 2) the inability to shield out the magnetic field generated by the earth and the environment.

At present, with mu-metal shields it is possible to reduce this uncertainty over the length of the interaction region to about $\pm 2$ milligauss, which corresponds to an uncertainty in the cesium-beam frequency standard of about four parts in $10^{12}$. It should be possible to reduce the error resulting from the externally generated fields by the use of a superconducting magnetic shield. It was shown by Meissner, in 1933, that the magnetic field in a superconductor is zero, and comparatively recently, it has been shown that as long as the magnetic field is well below the critical value, a superconductor behaves as a perfect magnetic shield.[1] However, at the current state of the art, a lower limit of about $10^{-6}$ gauss is set by problems in making an entire closed surface superconducting.

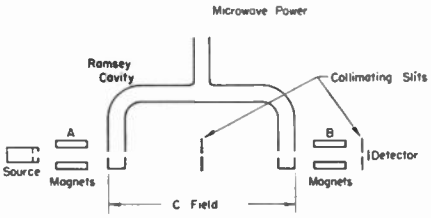


Fig. 1—Schematic of a beam frequency standard.

At present, it is not easy to estimate just how much improvement could be obtained by the use of a superconducting shield in an atomic beam machine which requires a small magnetic field to maintain space quantization of the magnetic dipole moment; however, in the case of a molecular beam machine using an electric dipole transition, it should reduce the small magnetic perturbations to a completely negligible value.

The author wishes to express his appreciation to R. Beehler and C. Snider, of the National Bureau of Standards, for providing a means for making a rough experimental check on the shielding effects of a superconductor, and to the U. S. Army Signal Corps for supporting work on the development of a molecular beam frequency standard.

F. S. Barnes
Elec. Engrg. Dept.
Univ. of Colorado
Boulder, Colo.

[1] J. Babiskin, "Magnetic properties of a hollow superconducting lead sphere," *Phys. Rev.*, vol. 85, pp. 104–106; January, 1952.

* Received by the IRE, May 1, 1961.

## A Monopulse Instrumentation System*

In a conventional RF sum and difference amplitude-sensing monopulse direction finder, the tracking error relative to the beamwidth caused by extraneous phase shifts is (See Appendix)

$$E = \frac{\delta}{2} \sin \psi, \qquad (1)$$

where $\delta$ is the differential phase shift before the comparing hybrid and $\psi$ is the phase shift after the comparing hybrid. (A similar expression applies to phase-sensing systems for amplitude precomparator and phase post-comparator unbalance.)

Since error and reference signals are processed in similar but not identical receivers, the differential phase shift $\psi$ causes boresight shift or imposes unduly small limits on $\delta$, particularly in multiple-pole, narrow-band IF amplifiers. Because of these errors, a method of instrumentation was evolved which eliminates this source of errors.

In the system shown in Fig. 1, the outputs of two elementary antennas are compared in a conventional hybrid to form difference ($\Delta$) and reference ($\Sigma$) array outputs. The difference output, which represents a pointing error signal, is modulated and recombined with the reference output.

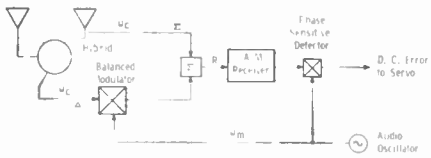


Fig. 1—Block diagram of the monopulse instrumentation system.

The resultant signal is of the form:

$$R = A(\cos \theta + \sin \theta \sin \omega_m t) \cos \omega_c t. \qquad (2)$$

For small error angles:

$$R = A(1 + \theta \sin \omega_m t) \cos \omega_c t. \qquad (3)$$

Thus, the resultant is readily seen to be amplitude modulation whose phase-sensitive amplitude is proportional to directional error. The boresight error, due to parasitic phase shift, is shown by (1).

The receiver output is an audio voltage proportional in amplitude to the error signal. This phase of audio voltage changes 180° upon crossing zero error. This voltage is readily phase compared with the local audio modulation oscillator to provide a dc output for the servo.

Signal processing devices may be very broad-band without affecting system sensitivity and, hence, may be made to produce little or no random phase shift. The critical narrow-band IF amplifier is eliminated as a cause of errors, since reference and error signals undergo the same phase shift in it.

Systems of this type have been built in the laboratory and have exhibited identical results with the usual monopulse system but without sensitivity to phase shifts in the narrow-band amplifiers. Such systems are easy to align and are stable under extremes of environment.

### Appendix

Derivation of (1) is as follows:

$$A(\theta, t) = \sin (k + \theta) \cos \omega_c t$$

where $k$ = offset angle, $\theta$ = error angle.

$$B(\theta, t) = \sin (k - \theta) \cos (\omega_c t + \delta)$$
$$= \sin (k - \theta)(\cos \delta + j \sin \delta) \cos \omega_c t.$$

* Received by the IRE, April 17, 1961.

World Radio History

Here, $A(\theta, t)$ and $B(\theta, t)$ are the amplitude responses of the antenna elements.

$$\Delta = A - B = [\sin(\theta + k) - \cos\delta \sin(k - \theta) - j \sin\delta \sin(k - \theta)] \cos\omega_c t$$

$$= 2\left[\sin^2\left(\frac{\delta}{2}\right) \sin k \cos\theta + 2\cos^2\left(\frac{\delta}{2}\right) \sin\theta \cos k - j \sin\delta \sin(k - \theta)\right] \cos\omega_c t.$$

$$\Sigma = A + B$$

$$= \left[-2\sin^2\left(\frac{\delta}{2}\right) \sin\theta \cos k + 2\cos^2\left(\frac{\delta}{2}\right) \sin\theta \sin k + j \sin\delta \sin(k - \theta)\right] \cos\omega_c t.$$

For many applications, $k = 45°$ (*i.e.*, crossover is at the half-power point) and $\sin k = \cos k = \sqrt{2}/2$. Further near the null, $\theta \ll 1$ and $\delta \ll 1$, hence,

$$\sin\theta \overset{\circ}{=} \theta, \qquad \cos\theta \overset{\circ}{=} 1,$$

$$\sin(k - \theta) \overset{\circ}{=} \sqrt{2}/2$$

and $\sin\delta \overset{\circ}{=} \delta$, $\cos\delta \overset{\circ}{=} 1$.

With these approximations,

$$\Delta = \sqrt{2}\left[\left(\frac{\delta}{2}\right)^2 + \theta - j\frac{\delta}{2}\right] \cos\omega_c t$$

$$\overset{\circ}{=} \sqrt{2}\left(\theta - j\frac{\delta}{2}\right) \cos\omega_c t.$$

$$\Sigma = \sqrt{2}\left[-\left(\frac{\delta}{2}\right)^2 \theta + 1 + j\frac{\delta}{2}\right] \cos\omega_c t$$

$$\overset{\circ}{=} \sqrt{2} \cos\omega_c t.$$

If $\Delta$ is phase detected with respect to $\Sigma$, after a phase shift of $\psi$,

$$\Delta_{dc} = \sqrt{2}\,\theta \cos\psi - \frac{\delta}{2} \sin\psi.$$

Thus, the output voltage $\Delta_{dc}$ is reduced by the factor $\cos\psi$ (which is usually negligible), and an extra error $\delta/2 \sin\psi$ is added.


### Acknowledgment

Much credit is due G. Kruesi whose work and ideas on low-frequency direction finders have contributed substantially to the system shown above. Credit is also due C. Sordal whose analysis of the system has contributed to the understanding of error effects.



Frederic P. Storke, Jr.
Philco Corp.
Western Dev. Labs.
Palo Alto, Calif.


### Bibliography


[1] J. R. Rhodes, "Introduction to Monopulse," McGraw-Hill Book Co., Inc., New York, N. Y.; 1959.

[2] W. Cohen and C. M. Steinmetz, "Amplitude and phase sensing monopulse system parameters," *Microwave J.*, pts. I and II; vol. 2, pp. 33–38; October and November, 1959.


## A Traveling-Wave Maser Using Chromium-Doped Rutile*

An $X$-band traveling-wave maser amplifier which differs in two respects from previously[1,2] reported traveling wave masers has been operated. 1) It is the first time to our knowledge that chromium-doped rutile[3] has been used as the paramagnetic material for traveling-wave masers. 2) Appreciable gain-per-unit length with a very large tunable bandwidth has been obtained without the use of any external slowing structure.

The structure that was employed is shown in Fig. 1. Standard size $X$-band waveguide is used with dielectric tapers leading to and from the active material. The cross-sectional dimensions of the active material are 0.074 inch by 0.150 inch leading to a cutoff frequency of 3 kMc. The small cross section is used because of the large dielectric constant of rutile, 131 for $E$ field perpendicular, and 256 for the $E$ field parallel to the $C$ axis at 4.2°K. The pump frequency is coupled to the system through a $Y$ section and is coupled to the active material by the same dielectric tapers used for the signal frequency. The pass band of the structure is thus limited only by how well one can match into a waveguide filled with a material of high dielectric constant.

Amplification was observed at different frequency intervals from 8 to 10 kMc. At certain frequencies, due to reflections at the dielectric tapers and junctions, cavity $Q$'s between 100 and 1000 were observed. The amplifier at these frequencies exhibited the larger gains and narrower bandwidths which are indicative of cavity operation. The large reflections, and hence the cavities, can be eliminated by known matching procedures.

Some of the characteristics of the amplifier operating at a signal frequency of 8.44 kMc with a 35.85-kMc pump frequency in a magnetic field of 4.4 kilograms are shown in Fig. 2. The gain of 2.4 or 3.8 db with a bandwidth of 20 Mc is for an active material length of 0.75 inch and a rutile-chromium content of 0.07 per cent. This corresponds to a gain of 5 db per inch at 4.2°K. The measured gain at 1.4°K was 6 db or 8 db per inch. These values compare favorably with the calculated values of 3.2 db at 4.2°K and 9.6 db per inch at 1.4°K. The calculated values were based on a slowing factor $S = 15$, $N = 0.54$ (where $N$ is the number of free-space wavelengths) and magnetic $Q$'s of $-90$ and $-30$ at 4.2 and 1.4°K, respectively. It should be noted that this maser was operated using only one ion per unit cell.[3] An amplifier can make use of the two ions per unit cell and thereby increase the gain in db per inch by a factor of two.

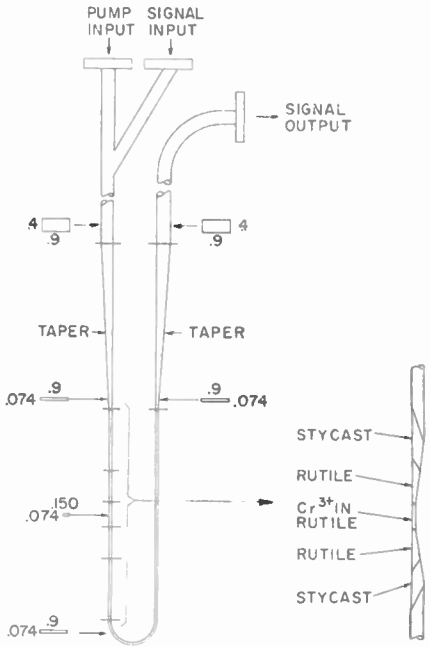


Fig. 1—A traveling-wave maser with no external slowing structure.

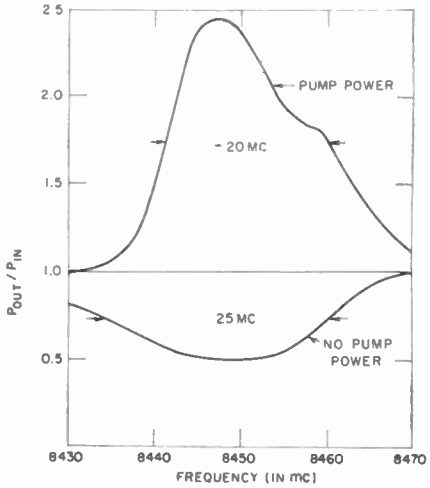


Fig. 2—Normalized power curve for the traveling-wave maser with and without pump power.

The inversion ratio which is defined as the ratio of transmitted power with saturating pump power to transmitted power without pump power both expressed in decibels, was $-1.24$ and $-0.6$ at 4.2 and 1.4°K, respectively. By assuming equal relaxation times, the theoretical value of the inversion ratio is $-1.13$. The experimental value compares favorably at 4.2°K but is surprisingly low at 1.4°K and is probably due to cross relaxation effects.

Fifty milliwatts of pump power was required for saturation. At a signal power output of 30 $\mu$w or $-15$ dbm, the gain of the amplifier is reduced to one half the maximum value. This value of 30 $\mu$w can be compared with the 6 $\mu$w observed for a ruby traveling-wave maser at Bell Laboratory.[1] The power level at which the amplifier sat-


* Received by the IRE, April 19, 1961. This work is partially supported by the U. S. Army Signal Corps, under Contract No. DA 36-039-SC-87386.


[1] R. W. DeGrasse, E. O. Schulz-du Bois, and H. E. Scovil, "The three-level solid state traveling wave maser," *Bell Sys. Tech. J.*, vol. 38, pp. 305–334; March, 1959.

[2] W. S. C. Chang, J. Cromack, and A. E. Siegman, "Cavity and traveling-wave masers using ruby at $S$-band," 1959 IRE WESCON Convention Record, pt. 1, pp. 142–151.

[3] H. J. Gerritsen, S. E. Harrison, and H. R. Lewis, "Chromium-doped titania as a maser material," *J. Appl. Phys.*, vol. 31, pp. 1566–1571; September, 1960.

World Radio History

urates is in agreement with a spin-lattice relaxation time of a few msec. Previous results using pulse techniques gave 2.4 msec.

In an attempt to increase the inversion ratio, the pump frequency was increased to 70 kMc. However, because of insufficient power the pump transition could not be saturated and only small gains for $X$-band signal frequencies were observed at 1.4°K. Gains of 3 db were observed in the 22–24 kMc range with the same structure.

This amplifier using chromium-doped rutile as the paramagnetic material should be a useful device in future systems because of its very large tunable bandwidth and simple structure. To realize this potential, isolation should be incorporated in the structure.

The authors wish to acknowledge the help of M. Heller for assistance in constructing the equipment, and H. Lewis, for his helpful technical discussions.

E. S. Sabisky
H. J. Gerritsen
RCA Labs.
Princeton, N. J.

## Shaping of Distributed RC Networks*

In the study of integrated single crystal and evaporated film circuits, attempts to make adequate inductance have met with only limited success. Therefore it becomes necessary to pay more attention to the possible uses of resistance and capacitance. In "solid" circuitry, resistance and capacitance will generally occur in distributed form, so that new properties may appear which are not realizable in conventional lumped circuitry. Distributed RC networks have been discussed in previous literature.[1-4] The form which has been generally considered is illustrated in Fig. 1 and may be represented by the circuit element of Fig. 2. Johnson[4] analyzed the straight distributed network, for the particular application of vacuum-tube phase-shift oscillators, and set up a design theory taking the grid capacitance into account. In this context only the voltage transfer characteristic was of interest. The analysis showed that with the use of untapered distributed networks, voltage attenuation factors as low as 8 should be realized at the frequency for phase reversal, and it was also concluded that in the limit of steep tapering the attenuation should approach unity. These results indicate a considerable improvement over the more conventional untapered 3-section RC phase-shift network, for which the open-circuit voltage-attenuation factor is 29 at the frequency for a 180° phase shift.

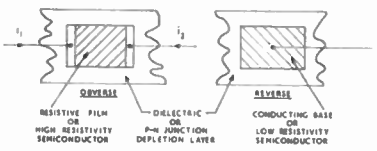


Fig. 1—Linear-distributed RC network.

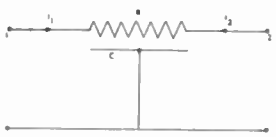

Fig. 2—Circuit representation of distributed network.

In "solid" and evaporated film circuits, the active network elements will be transistors and, in this case, it is appropriate to consider current transfer functions with network loads of the order of 1000 ohms. An investigation of shaped networks is being carried out, with initial emphasis on the realization of current phase reversals with small attenuation. The network was treated as a tapered transmission line, and solutions were obtained in closed form for the case of exponential shaping, in which the RC product per unit length is invariant with position along the line. Thus, with the origin of $X$ at the input 1 of the network, we have

$$R(x) = R_0 e^{mx} \quad \text{ohms/unit length,}$$

$$C(x) = C_0 e^{-mx} \quad \text{farads/unit length.}$$

Solution of the line equations for such a network leads to the following $Z$-parameters:

$$Z_{11} = \frac{R_0}{2\alpha^2 \sinh \frac{\gamma L}{2}} \cdot \left( m \sinh \frac{\gamma L}{2} + \gamma \cosh \frac{\gamma L}{2} \right)$$

$$Z_{12} = \frac{R_0 \gamma e^{mL/2}}{2\alpha^2 \sinh \frac{\gamma L}{2}} = Z_{21}$$

$$Z_{22} = \frac{R_0 e^{mL}}{2\alpha^2 \sinh \frac{\gamma L}{2}} \cdot \left( \gamma \cosh \frac{\gamma L}{2} - m \sinh \frac{\gamma L}{2} \right),$$

where

$$\gamma = \sqrt{m^2 + 4j\omega R_0 C_0},$$

$$\alpha^2 = j\omega R_0 C_0,$$

$R_0$, $C_0$ and $m$ are previously defined,

$$\omega = 2\pi \times \text{frequency},$$

$$L = \text{network length}.$$

Writing

$$R_0 C_0 = T_0 = \frac{1}{\omega_0},$$

we may then use

$$\omega R_0 C_0 = \frac{\omega}{\omega_0} = U$$

as a relative frequency parameter. The curve of Fig. 3 was calculated from the relation

$$T_N = \frac{Z_{12}}{Z_{22} + Z_L},$$

where $T_N$ is the current transfer function for the particular values,

$$m = -5,$$

$$L = 1 \text{ cm},$$

$$R_0 = 10^5 \text{ ohms/cm},$$

$$\text{load} = Z_L = 500 \text{ ohms}.$$

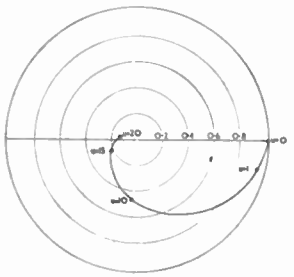


Fig. 3—Polar plot of current transfer function of a distributed RC network. $m = -5$, $L = 1$ cm, $R_0 = 10^5$ ohms/cm, and $Z_L = 500$ ohms.

From this curve, it may be seen that for 180° phase change, $U \doteq 18$ and the current is attenuated by a factor of about 6, *i.e.*, 16 db. Further trial calculations indicated that this was much better than could be obtained with a "straight" network. However the expression for $T_N$ is too complicated to be easily optimized by analytical means.

Several 10-section lumped component analogs have been built, and current and voltage attenuations were measured at the frequency for phase reversal. The theoretical calculations for the above example were first checked, and the agreement was fairly good in that phase reversal occurred at $U \doteq 20$ with a current attenuation factor of 7. Further measurements indicated the existence of an optimum $m$-value depending on the $R_0/Z_L$ ratio. Measurements on open-circuit voltage transfer provided direct comparison with a straight distributed network and the normal 3-section RC phase-shift network. The network with $m = +5$ gave an attenuation factor of 4.5, while the "straight" distributed network and the 3-section network give attenuation factors of 12 and 29, respectively. It is apparent that shaped distributed networks can offer considerable improvement over the more conventional forms. By using the lumped analog to provide feedback from collector to base of a common-emitter transistor amplifier, it was possible to obtain oscillations up to 500 kc. Furthermore, the particular component values used in the feedback circuit were of

* Received by the IRE, April 14, 1961.

[1] C. K. Hager, "Network design of microcircuits," *Electronics*, vol. 32, pp. 44–49; September, 1959.

[2] C. K. Hager, "Distributed parameter networks for circuit miniaturization," *Proc. Electronic Components Conf.*, Philadelphia, Pa.; May 6–8, 1959.

[3] C. Holm, "Distributed Resistor Capacitor Networks for Microminiaturization," Royal Radar Establ., Malvern, England, RRE Tech. Note No. 659; 1959.

[4] R. W. Johnson, "Extending the frequency range of the phase-shift oscillator," Proc. IRE, vol. 33, pp. 597–603; September, 1945.

World Radio History

the same order as the maximum values which may be realized in the practical distributed networks used in micro-circuitry. With suitable design, it should be possible to obtain oscillations well into the megacycle range.

In order to gain a fuller understanding of the characteristics of the shaped networks, the voltage and current transfer functions together with the input and output impedances are being computed for a variety of shapes and loads, and the results so obtained will be reported elsewhere. It should then be possible to set up a design procedure for optimum use of the networks. The experimental data obtained so far indicate new ways of designing "solid" oscillators and selective amplifiers, and it is hoped to do this using a wafer of silicon with distributed capacitance provided by a reverse-bias *p-n* junction. The advantage of using depletion layer capacitance, rather than an evaporated dielectric system, lies in the possibility of tuning by means of the junction bias voltage, and also in the fact that the low dielectric loss is maintained up to very high frequencies.

ACKNOWLEDGMENT

The authors wish to thank the Directors of the Plessey Co. Ltd., for permission to publish this note, and also to the Ministry of Aviation for financial support.

B. L. H. WILSON
R. B. WILSON
The Plessey Co. Ltd.
Caswell, Towcester,
Northants, England

## Proposed Technique For Modulation of Coherent Light*

A technique for the modulation of the coherent-light output of a ruby laser has been proposed[1] at the Millimeter Wave Research Laboratory, Purdue University, Lafayette, Ind. This technique makes use of the Stark effect in the ruby itself. By applying a strong electric field to the ruby, the energy levels involved in the laser action can be shifted, with the shift dependent upon the strength of the applied field. This results in a frequency shift of the coherent-light output. If the applied field is a strong microwave signal, then the resultant output will be frequency modulated.

The required field strength of a reasonable frequency deviation is difficult to calculate, but may be determined experimentally. An estimate of the order of magnitude of the required field may be obtained from a consideration of the Stark shift of an isolated hydrogen atom. Von Hippel[2] gives the equation for the frequency as

$$\nu_e = \frac{3\epsilon_0 h}{2\pi me} nE \approx 1.93 \times 10^4 nE$$

where

$\epsilon_0$ = permittivity of free space
$h$ = Plank's constant
$m$ = electronic mass
$e$ = electronic charge
$n$ = principal quantum number
$E$ = field strength in v/m.

For the chromium ions in ruby, $n=3$, and hence,

$$\nu_e \approx 5.29 \times 10^4 E.$$

For a field strength of $10^5$ v/m, a frequency shift of

$$\nu_e \approx 5.29 \times 10^9$$

or 0.18 $cm^{-1}$ is obtained. This is a large enough frequency deviation to be observed with a good interferometer. Higher field strengths will, of course, result in larger deviations.

A problem which arises is the pump efficiency. In order to obtain the required high field strengths at microwave frequencies, the ruby will have to be placed in a waveguide or a microwave cavity. Thus sufficient light will have to be focussed on the ruby from a source external to the cavity. Since, at present, rather high energy is required from the pump source, difficulties may be encountered in achieving laser action in configuration.

The frequency modulated light may be converted to amplitude modulated light by passing it through a Fabry-Perot etalon which will act as a band-pass filter. The output of the etalon may then be detected by a photosensitive envelope detector.

The relaxation oscillations which have been observed in ruby lasers may make any form of modulation difficult. However, it is assumed that the problem of achieving constant output over the pulse period can be solved.

A. K. KAMAL
S. D. SIMS
Millimeter Wave Res. Lab.
School of Elec. Engrg.
Lafayette, Ind.

* Received by the IRE, June 15, 1961.

[1] Application for patent, "Frequency modulation of coherent light," submitted to Purdue Res. Found.; March, 1961.

[2] A. Von Hippel, "Dielectrics and Waves," John Wiley & Sons, Inc., New York, N. Y.; 1954.

## A Generalization of "Mutual Information"*

As usually defined, "mutual information" relates to two random variables, say $x$ and $y$; their mutual information $I(x:y)$ is the amount of information that one random variable gives about the other, *i.e.*, the information $x$ and $y$ have in common. It can be expressed as

$$I(x:y) = H(x) - H(x \mid y) \qquad (1)$$

in terms of the entropy and conditional entropy (equivocation) of $x$. With the help of Fig. 1, we can find the mutual information of three random variables, *i.e.*, the amount of information common to, say, $x$, $y$, and $z$:

$$\begin{aligned} I(x:y:z) &= I(x:z) - I(x:z \mid y) \\ &= I(y:z) - I(y:z \mid x) \\ &= I(x:y) - I(x:y \mid z), \end{aligned} \qquad (2)$$

in which the last term, for example, is the average conditional value of (1). The last line of (2) says that the information $z$ has in common with both $x$ and $y$ is that part of the information common to $x$ and $y$ which is not independent of $z$; this relation bears a close resemblance to (1). Eq. (2) can also be written in the symmetric form

$$\begin{aligned} I(x:y:z) = H(x) + H(y) + H(z) - H(y, z) \\ - H(x, z) - H(x, y) + H(x, y, z) \end{aligned} \qquad (3)$$

which is reminiscent of the familiar $I(x:y) = H(x) + H(y) - H(x, y)$.

The mutual information of $n$ random variables $x_1, \cdots, x_n$ similarly turns out to be

$$\begin{aligned} I(x_1: \cdots :x_n) = I(x_1: \cdots :x_{n-1}) \\ - I(x_1: \cdots :x_{n-1} \mid x_n), \end{aligned} \qquad (4)$$

which can be expressed in a symmetric form, like (3), as the sum of all entropies of a single variable minus the sum of the entropies of all pairs plus the sum of the entropies of all triples, etc. With the aid of Fig. 1, we can also show that $H(x_1, \cdots, x_n)$ is the sum of all entropies of a single variable minus the sum of the mutual informations of all pairs plus the sum of the mutual informations of all triples, etc.

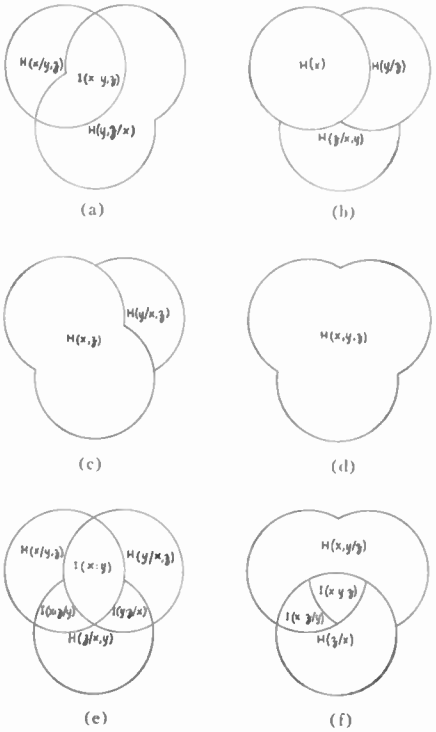


Fig. 1—Relationships among the entropies and mutual informations of $x$, $y$, and $z$. The designation of the central triangle as $I(x:y:z)$ can be justified by noting, for example, that $I(x:y,\ z) = I(x:y) + I(x:z) - I(x:y:z)$.

* Received by the IRE, April 26, 1961.

World Radio History

*Note added in proof:* It has just come to the author's attention that this generalization, though presented somewhat differently, appears in Fano[1] and McGill.[2] The present exposition, however, may help to clarify the idea.

N. M. Blachman
Sylvania Electronic Defense Labs.
Mountain View, Calif.

[1] R. M. Faro, "The Transmission of Information," Massachusetts Institute of Technology Press, Cambridge, and John Wiley and Sons, Inc., New York, N. Y., sec. 2.12, pp. 57–59; 1961.
[2] W. J. McGill, "Multivariate information transmission," IRE Trans. on Information Theory, vol. IT-4, pp. 93–111; September, 1954.

## "A Broad-Band Termination for IF Coaxial Lines"*

Referring to Stull's note,[1] we would like to inform you that a similar problem has been approached and solved in a different manner at CERN, Geneva, Switzerland.

In connection with the construction of an electron accelerator, the question arose concerning feeding a cavity resonator through a nearly lossless transmission line (Fig. 1).

Starting from the transfer impedance function

$$Z_T = \frac{V_2}{I_1} = \frac{Z_0 Z_r}{Z_0 \cos \frac{s}{j\omega_0}\frac{\pi}{2} + jZ_r \sin \frac{s}{j\omega_0}\frac{\pi}{2}}, \quad (1)$$

with

$$Z_r = \frac{\omega_0 \sqrt{L/C}\, s}{s^2 + \frac{\omega_0}{Q} s + \omega_0^2}, \quad (2)$$

and developing the sine and cosine functions into an infinite product, it is possible to find easy expressions for sine and cosine functions in the neighborhood of $s \cong j\omega_0$ ($\omega_0$ being the resonant frequency of the quarter wavelength line and of the resonator). Then

$$\begin{cases} \cos \frac{s}{j\omega_0}\frac{\pi}{2} \cong \frac{\pi}{4\omega_0^2}(s^2 + \omega_0^2) \\ \sin \frac{s}{j\omega_0}\frac{\pi}{2} \cong 1. \end{cases} \quad (3)$$

Introducing (3) into (1) and solving $Z_T$ by means of the root-locus method, we find $Z_T$ to be characterized by 4 poles $p_A$, $p_B$, $p_A^*$, $p_B^*$ in the vicinity of $j\omega_0$. The actual position of these poles is a function of what we call the coupling factor $k$:

$$k = \sqrt{\frac{\sqrt{L/C}}{Z_0}}. \quad (4)$$

By increasing $k$, the coupled poles $p_A$, $p_B$, $p_A^*$, $p_B^*$ move along the lines drawn in Fig. 2.

Magnifying the region around $j\omega_0$, it can be shown that $p_A$, $p_B$ poles lie on a circle centered in $p_L$ with radius

$$\Omega = \omega_0 \sqrt{\frac{\sqrt{L/C}}{\pi Z_0}}, \quad (5)$$

at a distance $\omega_0/4Q$ from the $j$ axis (Fig. 3).

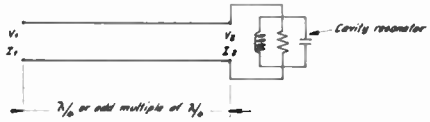


Fig. 1.

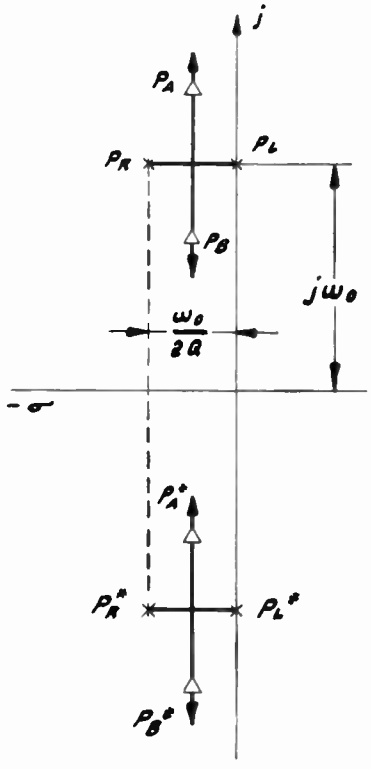


Fig. 2.

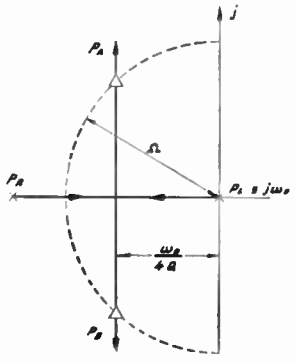


Fig. 3.

If we now feed the line from a constant current source, we find on the resonator either a flat or a double-peaked frequency response, depending on the factor $k$.

Good agreement with (5) has been observed in practice for bandwidths up to 40 per cent.[2]

A. Susini
F. A. Ferger
Accelerator Res. Div.
CERN-European Organization
for Nuclear Research
Geneva, Switzerland

[2] F. A. Ferger and A. Susini, "Wide Band Impedance Matching by the Root-Locus Method, Application to the Design of a High Power Radio-Frequency System for an FFAG Accelerator," CERN Rept. No. 60-41; October, 1960.

## Tracking and Display of Earth Satellites*

There are several errors in the above titled article.[1] A list of the typographical errors follows:

(2) for $y$ should read:

$$y = a\sqrt{1 - e^2} \sin E$$

(8) for $C$ should read:

$$C = e\sqrt{(k_3)^2 + (k_1)^2}.$$

The line immediately following (15) should read:

" . . . for $e \leq 0.1$, produces errors not greater than 1 . . . . "

Slack and Sandberg derived equations for a satellite subtrack. They considered the special case for a circular orbit to reduce the equations to a presentable form. I disagree with their method of reduction. I also question several points in their derivation.

In the first step in the derivation, the equations of motion for a set of axes whose $x$ member coincides with the semimajor axis of the satellite's elliptic path are transformed to a new set of axes in the same orbital plane whose $x$ member passes through the point of maximum latitude. This is a rotation through an angle called $\beta$. The statement is then made that since $\omega = 90° - \beta$, this transformation can be written in terms of $\omega$, the argument of the perigee. I fail to see why the point of maximum latitude was used since the transformation in terms of $\omega$ can be performed directly. It actually may be more convenient to make this transformation through the angle $\omega$ rather than $90° - \omega$. In this case, the $x$ member of the new set of axes would pass through the ascending node.

* Received by the IRE, April 6, 1961.
[1] K. S. Stull, "A broad-band termination for IF coaxial lines," Proc. IRE, vol. 49, pp. 365–366; January, 1961.

* Received by the IRE, February 14, 1961.
[1] F. F. Slack and A. A. Sandberg, "Tracking and display of earth satellites," Proc. IRE, vol. 48, pp. 655–663; April, 1960.

World Radio History

In the third transformation, the equations of motion (referred to a set of axes fixed in space and with the $x$ and $y$ members in the equatorial plane) are fixed to a rotating earth by rotation through the angle $\gamma+\omega_e t$. The authors neglected defining $\gamma$. Obviously it is the angle from $x''$ to $x'''$ at time $t=0$, *but* no $t=0$ is defined. Since the expression for the eccentric anomaly is written in terms of $t-T_p$, the transformation must be through the angle $\gamma+\omega_e(t-T_p)$. Now, when $t=T_p$, $\gamma$ is the angle from $x''$ (fixed in space) to $x'''$ (the reference axis in the equatorial plane—presumably Greenwich). The use of $t-T_p$ leads to changes in (13), (14), (16), (17) and (21).

Besides the typographical error in (8) for C, there are three other errors in these equations. The following are the correct expressions for $\phi$, $\alpha$, and $\rho$:

$$\phi = -\gamma - \tan^{-1}\frac{(k_3+k_2)}{(k_1+k_4)}$$

$$\alpha = -\gamma - \tan^{-1}\frac{(k_4+k_1)}{-(k_2+k_3)}$$

$$\rho = \gamma - \tan^{-1}\frac{k_1}{k_3}.$$

It will be noted that some simplification of the equations given by the authors is possible. Specifically:

$$A = D \qquad \delta = \theta + 90°$$
$$B = F \qquad \alpha = \phi - 90°$$
$$C = G \qquad \rho = \psi + 90°.$$

The authors considered a special case as an example. A circular orbit ($e=0$) was chosen and then it was assumed that $\omega=0$, $T_p=0$, and $\gamma=0$. However, when a circular orbit is assumed, $\omega$ and $T_p$ no longer have any meaning. This indeterminancy can be eliminated if the constants are evaluated before any assumptions are made. One would expect that the magnitude constants ($A$, $B$, $C$ and $H$) are independant of $\omega$ as $e$ approaches zero. It is easily shown, neglecting higher-order terms in $e$, that:

$$A = a\sin^2\left(\frac{i}{2}\right)$$

$$B = a\cos^2\left(\frac{i}{2}\right)$$

$$C = ea\sqrt{1-\sin^2 i\sin^2\omega}$$

$$H = a\sin i$$

$$\theta = \gamma + \omega - 90°$$

$$\phi = -\gamma + \omega - 90°$$

$$\psi = \gamma - 90° - \tan^{-1}(\cos i\tan\omega)$$

$$\tau = \omega - 90°.$$

Hence, to a first-order approximation, $A$, $B$, and $H$ are functions of the semi-major axis and the inclination of the orbit only. If a circular orbit is assumed, $C=0$ regardless of the value of $\omega$. The authors have implied that it is necessary to assume $\omega=0$ to evaluate these constants for the special case. Actually, no assumptions are necessary to evaluate these constants for even the general case.

In order to get a simple illustrative example, one can certainly assume, quite arbitrarily, that the perigee is at the ascending node (therefore $\omega=0$). There is no need to assume $T_p=0$ since all the equations are now in terms of $t-T_p$. We can again, quite arbitrarily, assume a value for $\gamma$. The authors have chosen to use 0° which fixes the reference axis to the longitude where the point of maximum latitude occurs.

When one assumes that $\omega=0$ and $\gamma=0$, the phase angles have the following values: $\theta=-90°$, $\phi=-90°$, $\delta=0$, $\tau=-90°$, $\alpha=-180°$, $\psi=-90°$, $\rho=0$. The last three are incorrectly given in the article.

It is only necessary to calculate two of the subtrack equations given by the authors since a spherical earth has been assumed. (This is a valid assumption since only a 1 per cent accuracy is desired.) Instead of calculating the subtrack in cartesian coordinates, one can just as easily calculate the subtrack in spherical coordinates: $\lambda$ and $\Omega$, where $\Omega$ is measured from $x'''$.

$$\lambda = \sin^{-1}\frac{Z_{ss}}{R}$$

$$\Omega = \cos^{-1}\frac{X_{ss}}{R\cos\lambda}.$$

The error corresponding to a 1 per cent accuracy in the cartesian subtrack equation would be about one-half degree.

A. Van Gelder, Jr.
Kearfott Div.
General Precision, Inc.
Little Falls, N. J.

## High-Level Microwave Detector Using Avalanche Injection*

A semiconductor diode has been built which has interesting properties as a large-signal microwave detector. At 9350 Mc, rectified voltages up to 12 v across 200 Ω have been obtained with input power ranging from 1 to 3 w. In addition, at somewhat lower input power, some of these diodes have delivered more rectified power than was available from the microwave source. Crude measurements at very low levels indicate that these diodes are not useful for small-signal applications. This may be because of the large noise associated with breakdown.

The avalanche-injection microwave (AIM) diode was constructed by placing the point of a tungsten whisker in the bottom of an etchpit in a silicon die of 0.2-ohm-cm resistivity. An ohmic contact was provided by lightly alloying from a thin, vacuum deposited layer of Au-0.6 per cent Sb before plating with nickel for soldering. This assembly was installed in a 1N23 package. The thickness of the silicon between the bottom of the etchpit and the ohmic contact was 10 $\mu$ and the radius of the tungsten point was approximately 2 $\mu$.

Microwave rectification is poor when the point is biased negative with respect to the semiconductor (back direction) and for this reason the back characteristic is not presented here. The I-V characteristic of a typical diode in the forward direction as taken from an oscilloscope trace is shown in Fig. 1. Gunn's[1] treatment of rectification and avalanche at a current constriction leads to a static characteristic closely resembling Fig. 1 below the breakdown current. According to his theory, the nearly flat part of the characteristic just below breakdown is due to the onset of drift velocity saturation. The saturation current density is given by $J_0=qN_dV_{ds}$, where $q$ is the electronic charge, $N_d$ is the donor density, and $V_{ds}$ is the saturation drift velocity. Gunn gives an experimental value of $8.5\times10^6$ cm/sec for $V_{ds}$. Using this value along with our value of $2.5\times10^{16}$/cm³ for $N_d$, a value of $34\times10^3$ amperes is obtained for $J_0$. If we assume that the current just below breakdown in Fig 1. is $J_0A$, where $A$, the contact area, is about $10^{-6}$ cm², a value of $35\times10^3$ amperes is obtained for $J_0$.

The entire negative-resistance region can be understood qualitatively in terms of the avalanche-injection theory of Gunn[1] which postulates that minority carriers from the avalanche are injected into the drift region. Gunn[1] and Gibson and Morgan[2] have developed a quantitative theory for the low-voltage branch of the negative-resistance region which is in agreement with our data.

Rectification measurements were made on commercially available microwave rectifier diodes as well as on AIM diodes using a pulsed microwave source and an oscilloscopic display. The commercial diodes deliver only about 3 v or 40 mw to a 200-ohm load, presumably because of their poor back characteristics, while about half of the AIM diodes delivered 10 v or ½ w to the same

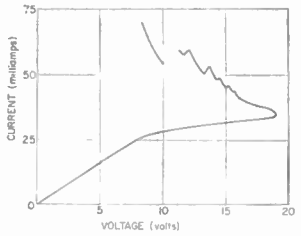


Fig. 1—Static characteristics of the avalanche-injection microwave diode.

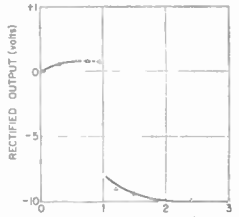


Fig. 2—Rectification characteristics of the avalanche-injection microwave diode at 9350 Mc with the bias at 16 v and the video load at 200 Ω.

* Received by the IRE, May 1, 1961.

[1] J. B. Gunn, "High electric field effects in semiconductors," *Progress in Semiconductors*, vol. 2, pp. 213–247; 1957.
[2] A. F. Gibson and J. R. Morgan, "Avalanche injection diodes," *Solid State Electronics*, vol. 1, pp. 54–69; March, 1960.

World Radio History

load, and an occasional diode has delivered 12 v or 0.7 w.

For the AIM diodes, the dependence of rectified power on available microwave power for fixed tuning and bias depends strongly on the bias. The data plotted in Fig. 2 were obtained at a bias about 3 v below the breakdown voltage. Note that the rectified voltage undergoes a change of polarity at the discontinuity. There is a range of power input, in this case from about 1 to 3 w, in which the output is nearly independent of the input. Just below this, the curve is broken to indicate uncertainty in the measurements due to distortion of the pulse shape as observed on the oscilloscope. A small fraction of the AIM diodes showed power gain as mentioned above. In this case tuning and bias were critical and the power input was in the 30- to 50-mw range. This effect is undoubtedly related to the negative resistance, and of course, the sum of the bias power and the input microwave power exceeds the rectified power.

H. M. Day
A. C. MacPherson
U. S. Naval Res. Lab.
Washington, D. C.

## Coherent Generation of Microwave Power by Annihilation Radiation of a Prebunched Beam*

Coherent electromagnetic power at the 100-mw level has been produced in the millimeter region by the creation and annihilation radiation of a tightly bunched 0.8-Mev electron beam. The creation-radiation process, as in beta emission, results from the sudden creation of a charge moving at a constant velocity. The annihilation-radiation process, on the other hand, is similar to the radiation associated with the two-quanta annihilation process in quantum theory.[1]

In the experiments performed, a prebunched beam enters the structure through a small hole and travels a distance of several wavelengths before impinging on a flat conducting surface, as shown schematically in Fig. 1. The resulting radiation is transmitted through a coaxial horn and then into detection and measuring devices.

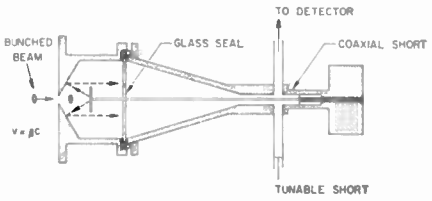


Fig. 1—Schematic of assembly used with a metal target (tellurium copper).

The performance of the device is based on the following considerations: Assume that an infinitely long beam is incident normal to the surface of a conducting material. If the conducting surface is infinite in extent, its effect on the electromagnetic fields can be adequately accounted for by replacing the surface with an image beam traveling in the opposite direction to the electron beam. The resulting power radiated per unit solid angle is

$$P(\Omega) = \sum_n \frac{\eta_0 I_n^2}{8\pi^2} \frac{\beta^2 \sin^2\theta}{(1-\beta^2\cos^2\theta)^2}, \quad (1)$$

where $\eta_0 = 120\pi$ is the free-space impedance, $I_n$ is the beam-harmonic current, $\beta = v/c$ is the ratio of beam velocity to the velocity of light, $\theta$ is the angle between the direction of motion of the beam and the point of observation, and finally the summation in (1) extends over the harmonics of the beam.

To find the total power radiated, (1) is integrated over the solid angle. Due to the special geometry used, the power expression must be integrated over $4\pi$ steradians. The resulting power in terms of the radiation resistance is

$$P = \sum_n \tfrac{1}{2} I_n^2 R_n, \quad (2)$$

where $R_n$, the radiation resistance, is given by

$$R_n = \frac{\eta_0}{2\pi}\left[\frac{1+\beta^2}{2\beta}\ln\left(\frac{1+\beta}{1-\beta}\right) - 1\right]. \quad (3)$$

Thus, for a 0.8-Mev beam, the radiation resistance is 140 ohms. Furthermore, the radiation resistance is independent of frequency, a fact of paramount importance with regard to operation in the submillimeter region.

Experimentally the radiation resistance was measured in the frequency range 30–40 kMc. The results are shown in Fig. 2, wherein the radiation resistance exhibits a seemingly random variation with frequency. This is partly due to the presence of a vacuum glass seal which introduces a dispersive element into the system. In addition, the beam length is comparable to a wavelength.

The fact that the beam is of finite length, and that it enters the structure through a hole whose size is small compared to a wavelength, introduces a new element into the problem. It can be shown that for the above conditions the total power radiated is about twice that calculated for the case of simple beam annihilation.[2] The added power comes from beam-creation radiation at the entrance hole. Thus the total radiation resistance for a 0.8-Mev beam is of the order of 280 ohms and takes into account both creation and annihilation radiation.

Effects of beam scattering at the target surface have been largely neglected. However, there is experimental evidence which indicates that the intense localized heating at the point of impact affects the power level.

For wavelengths below two millimeters, conventional waveguides become lossy. Also mode interference problems preclude the use

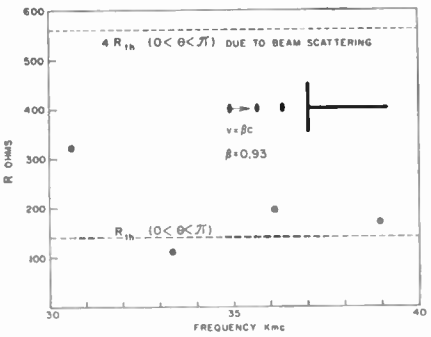


Fig. 2—Radiation resistance as a function of frequency.

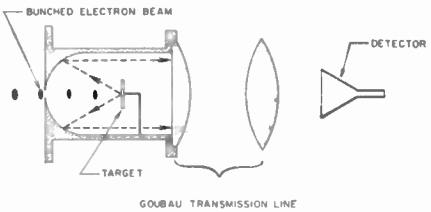


Fig. 3—Proposed optical-electronics method of generating coherent electromagnetic power by creation-annihilation radiation.

of such waveguides below one millimeter. In this region optical techniques become useful and the creation-annihilation scheme is ideally suited for such applications. A schematic of a proposed optical creation-annihilation device is shown in Fig. 3. The dimensions of the device are several orders of magnitude larger than a wavelength. An optical-type Goubau transmission line is used to transmit the power to the detector.

Finally, coherence conditions require that the bunch size be smaller than a wavelength. However, the creation-annihilation radiation phenomenon depends to a large extent on the nature of the beam at two points in space, namely the point where the beam enters the structure and the point where it is annihilated.[3] Therefore, the bunches do not have to retain their tightness over a long distance of interaction as in Cerenkov and other devices. Hence the coherence requirement on the beam is that its bunches be pointwise tight. This obviates the problems involved in preserving the bunches over long distances, and hence lower-energy beams can be used. This improves the over-all efficiency of the system. Also, since the radiation resistance is expected to remain invarient with frequency, the power yield in the submillimeter region should be appreciable.

In conclusion, the authors wish to thank Prof. P. D. Coleman for his support and interest in the problem, and for making available the Rebatron on which the above-mentioned experiments were conducted.

B. W. Hakki
H. J. Krumme
Ultramicrowave Group
University of Illinois
Urbana, Ill.

* Received by the IRE, June 19, 1961.

[1] W. Heitler, "The Quantum Theory of Radiation," Oxford University Press, London, Eng., 1953.

[2] B. W. Hakki and H. J. Krumme, "Coherent Generation of Annihilation Radiation by a Tightly Bunched Megavolt Electron Beam," presented at Conf. on Electron Device Research, Troy, N. Y.; June, 1961.

[3] G. A. Askar'yan, "Pulsed coherent generation of millimeter radiowaves by non-relativistic electron bunches," *Soviet Phys. JETP* (Letter), vol. 3, pp. 613–614; November, 1956.

World Radio History

## WWV and WWVH Standard Frequency and Time Transmissions*

The frequencies of the National Bureau of Standards radio stations WWV and WWVH are kept in agreement with respect to each other and have been maintained as constant as possible with respect to an improved United States Frequency Standard (USFS) since December 1, 1957.

The nominal broadcast frequencies should for the purpose of highly accurate scientific measurements, or of establishing high uniformity among frequencies, or for removing unavoidable variations in the broadcast frequencies, be corrected to the value of the USFS, as indicated in the table below. The corrections reported have been arrived at by means of improved measurement methods based on LF and VLF transmissions.

The characteristics of the USFS, and its relation to time scales such as ET and UT2, have been described in a previous issue,[1] to which the reader is referred for a complete discussion.

The WWV and WWVH time signals are also kept in agreement with each other. Also they are locked to the nominal frequency of the transmissions and consequently may depart continuously from UT2. Corrections are determined and published by the U. S. Naval Observatory. The broadcast signals are maintained in close agreement with UT2 by properly offsetting the broadcast frequency from the USFS at the beginning of each year when necessary. This new system was commenced on January 1, 1960. A retardation time adjustment of 20 msec was made on December 16, 1959; another retardation adjustment of 5 msec was made at 0000 UT on January 1, 1961.

WWV Frequency with Respect to U. S. Frequency Standard

| 1961 May | Parts in $10^{10}$† |
|---|---|
| 1 | −150.5 |
| 2 | −150.3 |
| 3 | −149.7 |
| 4 | −149.4 |
| 5 | −149.6 |
| 6 | −149.8 |
| 7 | −149.9 |
| 8 | −149.9 |
| 9 | −149.9 |
| 10 | −149.8 |
| 11 | −149.9 |
| 12 | −150.0 |
| 13 | −150.3 |
| 14 | −150.6 |
| 15 | −150.3 |
| 16 | −150.2 |
| 17 | −150.1 |
| 18 | −150.0 |
| 19 | −149.6 |
| 20 | −149.8 |
| 21 | −149.8 |
| 22 | −149.6 |
| 23 | −149.5 |
| 24 | −149.7 |
| 25 | −149.6 |
| 26 | −149.3 |
| 27 | −149.6 |
| 28 | −149.7 |
| 29 | −149.6 |
| 30‡ | −149.8 |
| 31 | −150.6 |

† A minus sign indicates that the broadcast frequency was low. The uncertainty associated with these values is $\pm 5\times10^{-11}$.

‡ Frequency adjusted $-1\times10^{-10}$ on May 30 at 1900 UT.

National Bureau of Standards
Boulder, Colo.

* Received by the IRE, June 26, 1961.

[1] Refer to "National Standards of Time and Frequency in the United States," Proc. IRE, vol. 48, pp. 105–106; January, 1960.

## Self-Educating Machines for Recognition and Classification of Patterns*

The direct reading of characters (letters or numbers) by a machine has found many applications. It is rather easy to do when the characters are taken from a given well-restricted set. This leads, for instance, to the automatic recognition of account numbers on bank checks. When the machine is asked, on the other hand, to recognize letters as well as the trained human eye does, the problem becomes a very complex one. It has been suggested, with some success, that a machine which would have the possibility of classifying a great number of input patterns into a small number of output classes should not be worked out to its final details at the designing stage and, in particular, should not rigidly provide automatically a classification of the patterns chosen *a priori*. Indeed, when the number of input patterns becomes very large the implementation of a given classification at the drawing-board level may become quite unwieldy. One may hope for a machine which can traia itself just like the human eye does, provided it is possible to tell the machine when its classification is in error. Such machines are made of an array of input sensing elements, which transform the input pattern laid on them into an input signal in a one to one correspondence with the pattern. This input signal is transformed into an output which is in a one to one correspondence with the classification desired. The output is not only used as an output; it is also fed back into a memory device where the desired correspondence between the input patterns and the output classification has been stored. If the comparison with the memory is satisfactory, the machine is ready for the next input pattern. If it is not satisfactory, the machine transforms certain of its inner parameters (values of certain circuit elements) in such a way that the incorrect result will become less probable when, in the future, the same input pattern shall occur.

The first point one must make is that the memory device mentioned does indeed contain the drawing-board classification which was deemed unwieldy. The only advantage gained is that, possibly, the classification in the memory can be changed at will. This, indeed, provides a very large versatility. One may visualize a machine, for instance, which classifies aerial photographs in certain classes. The classification desired may depend then on the intended use of the photographs at a given time.

The machines in existence today, to my knowledge, have however a very important drawback. Not all possible classifications can be learned and some classifications, while learnable, may necessitate a great number of self-adjustments (a great number of pattern trials) before they are learned. Indeed, most of the literature on the subject is on the mathematics of the restrictions involved and one may wonder why the authors of such articles are so delighted with the shortcomings of their own proposals. Such shortcomings are not inherent to the problem and it is rather easy to propose machines which do not have any. All that is necessary, for instance, is for the input signal, in a one to one correspondence with the input pattern, to move a magnetic memory tape. The motion of the tape will place a location of the tape under an output reading head which is in a one to one correspondence with the input signal. The output reading will be fed back to the memory device described before and compared with the desired output. If this output is not proper, the location on the tape just read will be moved by the machine to a location under an erasing and printing head where the desired output will be printed on the tape. In this manner, any possible classification can be learned and can be learned within the smallest number of trials (equal to the number of different input patterns used). In practice, the memory device could be the tape itself thus eliminating all but the sensing raster, the mechanism moving the tape, and the output reading head. A library of tapes would provide the versatility, and duplication (by just duplicating such tapes) would be quite easy.

P. A. Clavier
Aeronutronic Div.
Ford Motor Co.
Newport Beach, Calif.

* Received by the IRE, April 25, 1961.

## On Parametric Amplification in Transistors*

A mode of parametric amplification using transistors was proposed by Vodicka and Zuleeg,[1,2] who reported on a converter circuit which they say provides very high gain by a combination of mixing and parametric amplification. Their basic circuit, without bias connections, is shown in Fig. 1. The circuit was reconstructed in this laboratory and the gain reported by Vodicka and Zuleeg was reproduced. However, we did not find the reported stability. Also, we differ on some of the theoretical considerations presented.

The principle of operation of the circuit is as follows: The oscillating transistor provides the pump frequency, and its emitter the nonlinear impedance, for parametric amplification of an incoming signal. Therefore, the power level of the difference frequency at the input terminals may be higher than that of the input signal. If this difference frequency is much smaller than the cutoff frequency of the transistor, additional gain is available from the transistor at the output terminals.

The circuit is apparently a two-frequency oscillator. Redrawing Fig. 1 for high frequencies as Fig. 2, we can immediately see

* Received by the IRE, March 21, 1961.

[1] V. W. Vodicka and R. Zuleeg, "Transistor operation beyond cut-off frequency," *Electronics*, vol. 56, pp. 56–60; August, 1960.

[2] R. Zuleeg and V. W. Vodicka, "Parametric amplification properties in transistors," Proc. IRE (Correspondence), vol. 48, pp. 1785–1786; October, 1960.

World Radio History

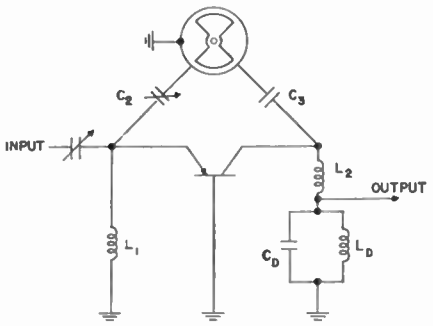


Fig. 1—The ac portion of the circuit proposed by V. W. Vodicka and R. Zuleeg.

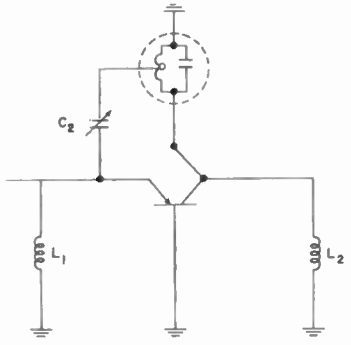


Fig. 2—The high-frequency oscillator.

that the circuit is a Hartley oscillator which will oscillate at a frequency determined by the butterfly, as pointed out by the authors. For low frequencies, Fig. 3 is the equivalent circuit. This is the case for a difference frequency of a few megacycles. As is apparent from Fig. 3, the circuit can also oscillate at a low frequency mostly determined by $L_D C_D$. However, due to the small amount of feedback at the difference frequency $f_D$, conditions are not very favorable for low-frequency oscillation.

Favorable conditions at the butterfly frequency allow oscillation to occur at $f_L$, beginning at fairly low bias currents. Due to the unfavorable conditions at low frequencies, oscillation will occur for $f_D$ only over a fairly narrow current range, *i.e.*, in the neighborhood of maximum power gain.[3] The circuit components are such that unity loop gain at $f_D$ can be obtained only near the power gain maximum.

If the current and collector voltage are set such that the loop gain is not quite sufficient for low-frequency oscillation, a narrow-band high-gain amplifier for $f_D$ is the result. (The transistor is, of course, oscillating meanwhile at $f_L$.)

The circuit mixes an input signal at the frequency $f_S$ with $f_L$ to result in a signal at the difference frequency $f_D$, which is then amplified by the high-gain amplifier. It is apparent that the greater part of the high gain results *not* from parametric amplification but from the narrow-band low-frequency amplifier. This amplifier is operating

[3] As is well known, the power gain varies with the current and has a maximum for drift transistors. The magnitude of the power gain maximum increases with increasing collector voltage.

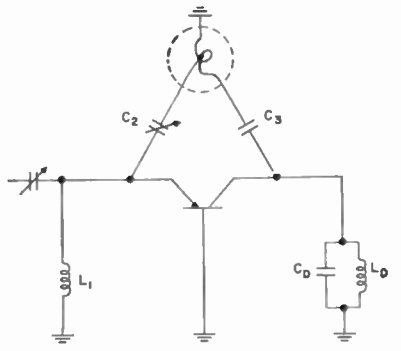


Fig. 3—The basic circuit for low frequencies. $C_2$ adjusts the feedback for both high and low frequencies and is very important for low frequencies.

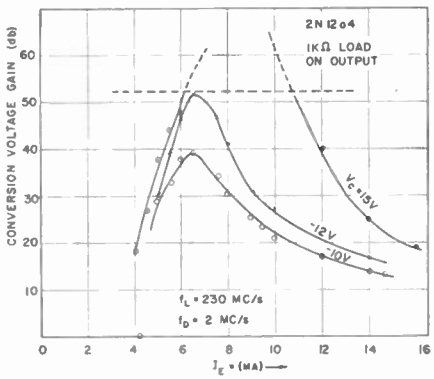


Fig. 4—Conversion gain as a function of emitter current, with collector voltage as a parameter, for a 2N1204 micro-alloy diffused-base transistor. With the 1kΩ load in the circuit, oscillation occurs at $f_D$ above 52-db voltage gain.

far below the transistor's cutoff frequency, and, as the low-frequency oscillatory conditions are approached, the gain becomes extremely large.

According to the above arguments, the maximum gain need not necessarily occur at the point where the input impedance becomes real, as was suggested by Vodicka and Zuleeg.[1] We have found that the input impedance of a 2N1204 micro-alloy diffused transistor is real for $I_E \approx 0.5$ ma. However, the maximum gain occurs at $I_E \approx 7$ ma, which coincides with the maximum in power gain.

Since the high gain is mostly achieved by use of a narrow-band amplifier, the stability is mainly controlled by the properties of the amplifier. As can be seen from Fig. 4, a high gain is extremely dependent upon both voltage and current. If a compromise is made to lower gain, the stability is improved accordingly.

Use of harmonic mixing (in order to extend the frequency limit) results in a worse gain stability for two reasons. First, the difference frequency easily drifts out of the narrow band of the low-frequency amplifier. Second, due to the lower pump power at the harmonics of $f_L$, reasonable gain is obtained only on the brink of low-frequency oscillation, when the third or fourth harmonic is used.

Summarizing the characteristics of the proposed circuit, we can say that it acts as an oscillator, mixer, and low-frequency amplifier. The resulting gain is mainly due to the narrow-band low-frequency amplifier rather than to parametric amplification.

J. Lindmayer
C. Wrigley
Sprague Electric. Co.
North Adams, Mass.

## *Author's Comment*[4]

Our brief letter was not meant to furnish all the answers for the circuit's operation, but rather to point out the possibilities of parametric operation of drift transistors, which have useful, inherent, nonlinear reactances of capacitive and inductive nature. We are grateful for the measurements reported which substantiate the performance of the circuit in general. It is felt that one of the preferred modes of the circuit operation does indeed consist of parametric variation of the input capacitance of the transistor to produce down-conversion (mixing) with little or no conversion loss. The necessary pumping frequency (local oscillator) is here supplied by the transistor itself through the butterfly to the emitter. The additional gain required is supplied by the transistor itself.

Since the specific transistors used in this circuit, and their characteristics, *e.g.*, very low base-resistance, high drift field, small emitter capacitance, are of utmost significance, we would like to point out certain properties of the devices investigated in conjunction with the circuit.

Although the oscillator circuit can be identified as a Hartley type, there is an important deviation in the form of an inductance placed between emitter and base terminals. By proper choice of this $L$ for a certain transistor, a broad-band tuning will occur. Fig. 5(a) is the normal $V_{eb}$-$I_e$ characteristic of a transistor under dc bias. Fig. 5(b) is the $V_{eb}I_e$ characteristic outside of this band, and Fig. 5(c) is the same characteristic at the center of this tuning range with constant RF power from a separate local oscillator. Diode mixing with this type of characteristic has been discussed in the literature.[5] The conditions under which the characteristics exist in the tuned range [Fig. 5(c)] are:

1) Presence of nonlinear resistance and capacitance.
2) Presence of RF-power at the fundamental or the higher harmonic.

The expected electrical performance would be:

1) Down-conversion or mixing with low-conversion losses when the conductance approaches zero and possibly with conversion gain, if very low or slightly negative IF-conductance can be achieved.
2) Greatly reduced noise figures.

We are still investigating several other closely related modes in the transistor, the most important of which is the transit time and the negative impedance occurring in the circuit.

[4] Received by the IRE, May 1, 1961.
[5] R. V. Pound, "Microwave Mixers," McGraw-Hill Book Co., Inc., New York, N. Y., p. 92; 1948.

World Radio History

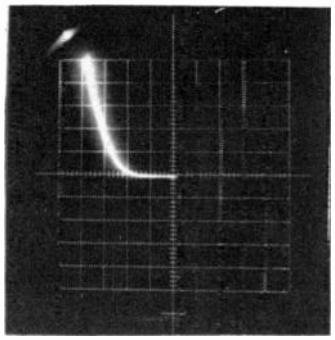

(a)

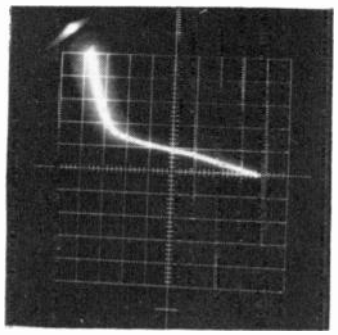

(b)

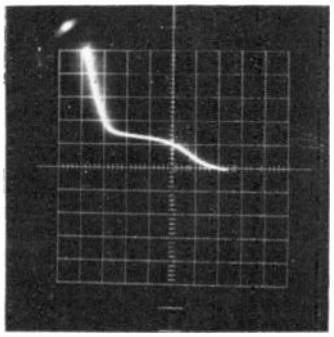

(c)

Fig. 5—*P-N-P* Hughes experimental transistor No. 314-41. (a) DC emitter-to-base characteristic with no RF power applied. (b) DC emitter-to-base characteristic with RF power at 240 Mc. (c) DC emitter-to-base characteristic with RF power at 360 Mc. Scales: Vertical—$I_e$ in 2 ma per division. Horizontal—$V_{eb}$ in 0.1 volt per division.

The circuits, as used, exhibited a low stability in the region of 200 Mc but became stable at frequencies above 400 Mc. For example, operation at 500 Mc produced a shift of 2000 cycles in 24 hours and approximately 2-db variation at 40-db conversion gain. The possibility of the circuit operating as a two-frequency oscillator is not excluded and can occur at certain settings. This would not necessarily explain the high gain, as the feedback, via the emitter capacitor which represents approximately 8000 ohms reactance at 2 Mc, would be facing the inductor $L_1$ which has a reactance of ½ an ohm at 2 Mc.

We have found that maximum gains and the best stability are in the lower current region between 1½ and 2½ ma where the best noise figure is also available. The maximum bandwidth achieved up to now was approximately 1 per cent at 500 Mc.

We hope that within the near future we will be able to present a definite answer as to the transistor action in this mode of operation.

V. W. Vodicka
Advanced Development
Lenkurt Electric Co., Inc.
San Carlos, Calif
R. Zuleeg
Semiconductor Div.
Hughes Aircraft Co.
Newport Beach, Calif.

## Multiple Burst Detection*

Peterson and Brown[1] have demonstrated the potency of cyclic codes when used for error detection. In particular, they have proven that a cyclic code capable of correcting a single burst of length $b$ bits in a block of $n$ bits can be used to detect two bursts of $b$ bits in the same block.

Telephonic data transmission tests have shown that bursts of errors are not distributed according to Poisson's law. The bursts themselves tend to occur in clusters. Multiple bursts of errors within a block occur much more often than would be the case with a Poisson distribution.

There exists a class of cyclic codes which can correct any $t$ bursts of maximum length $b$ in a block of $(2^k-1)$ $b$ bits. The number of check digits required is no greater than $bkt$. From the work of Peterson and Brown, this code can alternatively be used to detect any $2t$ bursts of length $b$ in a block of length $(2^k-1)b$. The following theorem provides the basis for this assertion.

If $P(x)$ is such that the cyclic code, whose feedback shift register (FSR) has $P(x)$ as its characteristic polynomial, is capable of correcting any element of the set $S$ of error polynomials in a block of $n$ bits, then the cyclic code whose FSR has $P(x^b)$ as its characteristic polynomial is capable of correcting any error polynomial in a block of $bn$ bits of the form

$$\sum_{i=0}^{b-1} x^i e_i(x^b) \qquad (1)$$

where $e_i(x)$ represents any element of $S$.

The theorem can be proven by considering two different error polynomials in the class of (1) and demonstrating that division by $P(x^b)$ yields different remainders.

For two such polynomials $E(x)$ and $E'(x)$ we can write

$$E(x) = \sum_{i=0}^{b-1} x^i e_i(x^b)$$

$$= P(x^b) \sum_{i=0}^{b-1} x^i q_i(x^b) + \sum_{i=0}^{b-1} x^i r_i(x^b)$$

$$E'(x) = \sum_{i=0}^{b-1} x^i e_i'(x^b)$$

$$= P(x^b) \sum_{i=0}^{b-1} x^i q_i'(x^b) + \sum_{i=0}^{b-1} x^i r_i'(x^b). \quad (2)$$

Since (2) must hold term by term:

$$e_i(x^b) = P(x^b) q_i(x^b) + r_i(x^b),$$
$$e_i'(x^b) = P(x^b) q_i'(x^b) + r_i'(x^b), \qquad (3)$$

for any $i$.

But $r_i(x^b) = r_i'(x^b)$ implies $e_i(x^b) = e_i'(x^b)$ since all $e_i(x)$ and $e_i'(x)$ have been selected from $S$.

It follows that

$$\sum_{i=0}^{b-1} x^i r_i(x^b) = \sum_{i=0}^{b-1} x^i r_i'(x^b)$$

implies $E(x) = E'(x)$, and this completes the proof of the theorem.

Now, if a Bose-Chaudhuri[2] polynomial $P_{BC}(x)$ is used, we can correct any $t$ errors in a block of $2^k-1$ bits with no more than $kt$ check bits. From the theorem, it follows that, with $P_{BC}(x^b)$, we can correct any $t$ bursts of maximum length $b$ bits in a block of $b(2^k-1)$ bits. The number of check bits is at most $bkt$. There are other patterns which can be corrected by $P_{BC}(x^b)$, and if it is used solely for correcting the $t$ bursts its efficiency is low for practical values of $k$, $b$, and $t$. The value of a $P_{BC}(x^b)$ code is principally in its qualities as an error detector because the decoder needed for error correction is too complex for most practical purposes. As an error detector, the $P_{BC}(x^b)$ code can detect any $2t$ bursts of maximum length $b$ in a block of length $(2^k-1)$ $b$ bits. The number of check digits required is at most $bkt$. There is no minimum "guard space" required between the bursts.

Francis Corr
Centre d'Etudes et Recherches
IBM Corp.
Nice, France

* Received by the IRE, April 3, 1961; revised manuscript received, May 1, 1961.

[1] W. W. Peterson and D. T. Brown, "Cyclic codes for error detection," Proc. IRE, vol. 49, pp. 228–235; January, 1961.

[2] R. C. Bose and D. K. Ray-Chaudhuri, "A class of error-correcting binary group codes," *Information and Control*, vol. 3, pp. 68–79; March, 1960.

## An Analytical Expression for Describing the Write Process in Magnetic Recording*

This note describes analytically the writing process, including self-demagnetization, in magnetic recording on a thin magnetic material. The expression developed enables one to determine the magnetization in the recording medium after writing, in relation to the geometry of the recording head, the variation of the gap field strength with time, and the hysteresis of the magnetic medium. It avoids the use of any linearization process and such terms as trapezoid magnetization function, transition length, etc.

* Received by the IRE, May 9, 1961.

World Radio History

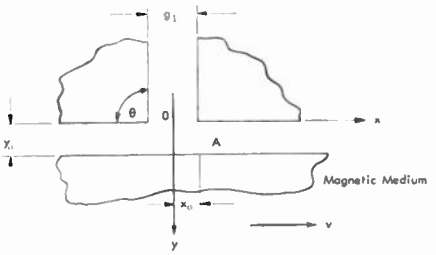


Fig. 1—Typical magnetic-recording system.

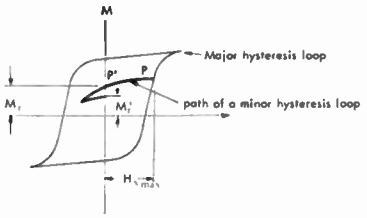


Fig. 2—Typical magnetization behavior.

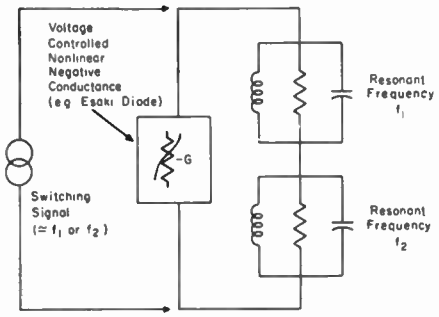


Fig. 1—Equivalent circuit of negative-conductance bistable oscillator, indicating method of switching.

Fig. 1 shows a typical magnetic recording head. In longitudinal recording (such as in a magnetic-tape, disk, or drum) one is concerned only with the $x$ component of the field, $H_x$. For $\theta=\pi/2$ and at a distance $y_0$ from the head, $H_x$ has been shown to be[1]

$$H_x = -\frac{H_0(t)}{\pi}\left\{\tan^{-1}\left[\frac{1+\frac{2x}{g_1}}{\frac{2y_0}{g_1}}\right] + \tan^{-1}\left[\frac{1-\frac{2x}{g_1}}{\frac{2y_0}{g_1}}\right]\right\}, \quad (1)$$

assuming the gap field strength $H_0(t)$ is a known function of time $t$.

Consider any point on the magnetic material, say point $A$ in Fig. 1. At $t=0$, point $A$ is located at $x_0$; at time $t$, the point has moved to

$$x = x_0 + vt, \quad (2)$$

where $v$ is the surface velocity of the material directly below the recording head. Substituting (2) into (1), we have

$$H_x = \frac{H_0(t)}{\pi}\left\{\tan^{-1}\left[\frac{1+\frac{2(x_0+vt)}{g_1}}{\frac{2y_0}{g_1}}\right] + \tan^{-1}\left[\frac{1-\frac{2(x_0+vt)}{g_1}}{\frac{2y_0}{g_1}}\right]\right\}. \quad (3)$$

At some time $t$, point $A$ will experience some maximum field $H_{x_{max}}$ which determines the maximum magnetization for point $A$. This maximum, of course, is the point at which

$$\frac{\partial H_x}{\partial t} = 0 \quad \text{and} \quad \frac{\partial^2 H_x}{\partial t^2} < 0.$$

Substituting this value of $t$ into (3), the value of $H_{x_{max}}$ locates point $P$ on the hysteresis loop, as shown in Fig. 2.

When the material is moved away from the head, the magnetization at point $A$ decreases, as described by the material's minor hysteresis loop, and reaches, at point $P'$ (Fig. 2), a value of $M_r$ corresponding to zero energizing field. The final value of $M_r'$ will be somewhat less than this due to self-demagnetization—a process well described by Bayer.[2]

This procedure can be extended to other points in the material and a complete description of the magnetization in the tape can thus be obtained after the writing process.

T. C. Ku
Development Lab.
General Products Div. IBM Corp.
Endicott, N. Y.

[1] O. Karlqvist, "Calculation of the magnetic field in the ferromagnetic layer of a magnetic drum," *Stockholm Tek. Hogskolans-Handlingar*, no. 86, pp. 1–28; 1954.

[2] R. G. Bayer, "A Theoretical Model for Self-Demagnetization," submitted for publication in *J. Appl. Phys.*

## A Potential Microwave Computer Element*

In recent years there has been a search for some means of performing logic and computing operations at speeds reaching the microwave range using other than pulse operation. This communication is concerned with a bistable oscillator frequency script system of the form proposed by Edson,[1] but employing a tunnel diode as the active element.

One form of bistable oscillator, Fig. 1, consists of the connection in series of two parallel-tuned circuits and a nonlinear negative conductance. In this circuit, free oscillation can occur at either of the frequencies $f_1$ or $f_2$ associated with the two tuned circuits. Due to the nonlinearity, simultaneous oscillation at $f_1$ and $f_2$ cannot occur. The circuit, therefore, is bistable and the frequency of oscillation indicates its state. Switching between states is effected by the injection of a sufficient number of cycles of current large enough in amplitude and sufficiently close in frequency to the frequency to which the circuit is to be switched.

Fig. 2 shows a bistable oscillator which is more suited to high-frequency operation. The bistable oscillator consists of a doubly resonant, quarter-wave trough line with the tunnel diode connected across the ends of the two inner conductors. Advantages of the device are its relatively small size, simplicity, low cost, low power consumption, and relative freedom from shielding problems. An experimental model demonstrates stable oscillation frequencies of 250 Mc and 375 Mc. Experiments established that the device could be switched from one frequency state to the other, but no measurements of switching speed have yet been made. To obtain some idea of the switching speed to be expected, measurements were made with an oscillator of the form in Fig. 1 having resonant frequencies of 600 kc and 735 kc. The results are illustrated in Fig. 3. Assuming that the curve for certainty of switching lies close to that for a switching probability of 0.9, a time of the order of 10 cycles of switching frequency is necessary to effect switching when the oscillator is forced by a signal one-tenth the unloaded output amplitude of an

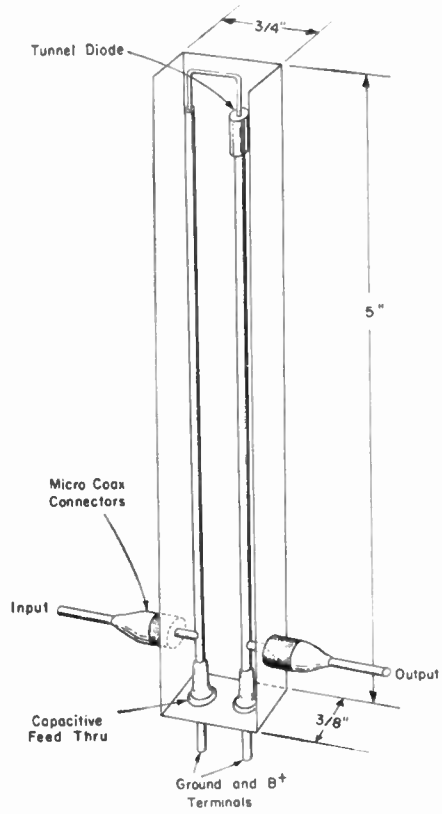


Fig. 2—The trough-line bistable oscillator.

* Received by the IRE, April 17, 1961; revised manuscript received, May 2, 1961.

[1] W. A. Edson, "Frequency memory in multimode oscillators," IRE TRANS. ON CIRCUIT THEORY, vol. CT-2, pp. 58–66; March, 1955.

World Radio History

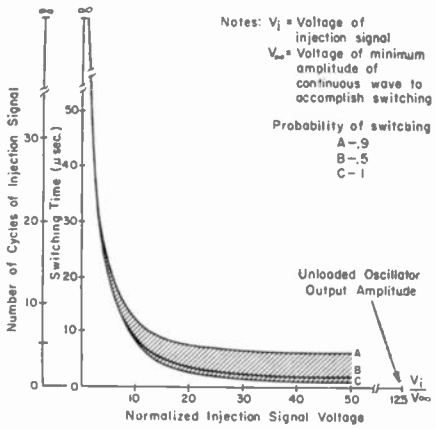


Fig. 3—Illustration of switching uncertainty.

identical oscillator. The results suggest that a useful fan-out ratio can be obtained with a switching time of about 10 cycles of switching frequency.

Bistable oscillator logic operation can be based on the majority principle. That is, if $m$ equal amplitude, in-phase, inputs of frequency $f_1$ and $n$ equal amplitude, in-phase, inputs of frequency $f_2$ are simultaneously applied to the bistable oscillator as switching signals, the final frequency of the oscillator is $f_1$ or $f_2$ depending on whether $m$ or $n$, respectively, is the greater integer. Both AND and OR logic circuits are realized by injecting two input signals and a continuous frequency bias signal, which are all of the same amplitude, into a bistable oscillator. If the bias frequency is $f_1$, an output of frequency $f_2$ is obtained from the oscillator only when both inputs are of frequency $f_2$ (AND circuit); if the bias frequency is $f_2$, an output of frequency $f_2$ is obtained when either of the inputs is of frequency $f_2$ (OR circuit). In the COMPLEMENTATION logic circuit (output of $f_2$ for input of $f_1$, and vice versa), the single input signal is applied via a phase-reversing transformer to the bistable oscillator together with two continuous frequency bias signals, one of each of the frequencies $f_1$ and $f_2$. Due to the phase shift, cancellation between the input and the bias signal of the same frequency occurs, and the output frequency is then determined by the other bias signal. Satisfactory operation of these three logic circuits is obtained only if all inputs, including frequency biases, are of nearly equal amplitude and, when of the same frequency, of essentially the same phase. The bistable oscillator is a bilateral device, but unidirectional transmission of information has been accomplished by using Goto's[2] three-beat clock bias principle. With the bistable oscillator, suitably-phased square-wave bias is applied to each tunnel diode, causing unidirectional flow to occur in a network of logic elements.

Assuming that 10 cycles of switching frequency is the order of time necessary to change the state of the bistable oscillator, it follows that to obtain a switching time of 1 nsec a bistable oscillator with characteristic frequencies of the order of ten kMc would be required.

Advantages of the bistable oscillator are: its regenerative property, coupled with its nonlinearity, results in a self-contained unit with an essentially constant output amplitude; logic can be performed with short switching times and a useful fan-out ratio; and the availability of simple high-frequency constructional techniques and extremely small tunnel-diodes offer small size, low power, and low cost. These advantages make the bistable oscillator a potentially useful microwave logic element.

R. W. Couch
A. F. Rashid
R. Spence
Radio Communication Lab.
Research Div.
General Dynamics/Electronics
Rochester, N. Y.

[2] E. Goto, "The parametron, a digital computing element which utilizes parametric oscillation," Proc. IRE, vol. 47, pp. 1304–1316; August, 1959.

## A Solution to the Shannon Switching Game*

In a recent paper[1] a description is given of a resistor version of the Shannon switching game. A graphical version is as follows. Two players designated "cut" and "short" are presented with a finite unoriented-branch linear graph in which two of the vertices are distinguished. The cut player, in his turn, deletes one of the branches of the graph, his object being to sever all paths between the two distinguished vertices. The short player alternates moves with the cut player. In his turn he makes an unplayed branch invulnerable to deletion, his object being to connect the two distinguished vertices by an invulnerable path. Both players have complete information. The game proceeds until one of the players reaches his goal.

It can be shown by an involved argument in matroids[2] that the short player can win against all possible strategies of the cut player (the cut player playing first) if and only if the graph contains two disjoint cospanning[3] trees connecting the distinguished pair of vertices. The short player can win using a strategy of "repairing" any play (deletion) of the cut player on one tree by a play on the remaining tree. The play in general is not unique, and the strategy need not win in a minimum number of plays. It has one remarkable feature. There exist two disjoint cospanning trees[4] which span all vertex pairs which can be spanned by any tree pair. The two-tree strategy of the short player played with respect to this tree pair will win where possible, and is independent of the chosen pair of vertices. Hence the short player can play and win where possible without knowledge of the chosen vertex pair. Such a strategy is not possible for the cut player.

By duality[5] it is possible to characterize those graphs with two distinguished vertices in which the cut player, playing second, can win against all strategies of the short player. The remaining graphs are those on which the player playing first can win against all strategies of the other player. These graphs differ from those previously discussed by only one branch, and the winning strategies are correspondingly similar.

A. Lehman
Systems Research Center
Case Inst. Tech.
Cleveland, Ohio

[5] All of the results hold for matroids. If the graph is not planar, the matroid dual still exists. Thus the roles of the cut and short player are dual locally (*i.e.*, with respect to a given vertex pair), but not globally.

* Received by the IRE, May 8, 1961.

[1] M. Minsky, "Steps toward artificial intelligence," Proc. IRE, vol. 49, p. 23; January, 1961.

[2] H. Whitney, "The abstract properties of linear dependence," *Am. J. Math.*, vol. 57, pp. 507–533; 1935.

[3] Two trees are cospanning if they connect the same set of vertices.

[4] More properly two forests—these trees need not be connected.

## The Wide Tuning Range of Backward Traveling-Wave Parametric Amplifiers*

In a recent paper, Straus[1] discussed the tuning range of backward traveling-wave parametric amplifiers. He has shown that the TEM mode of operation described by Breitzer and Sard[2] can be modified to provide a wider tuning range. The analytical and graphical examination of Straus gives a clear demonstration of the way of extending the tuning range, and also provides a satisfactory explanation of the experimental results of Breitzer and Sard.[2] Nevertheless, the scheme of Straus actually does not fully cover the maximum tuning range, and it is different from the mechanism used in our earlier reported work for achieving wide tuning ranges.[3] In fact, it is possible to extend still further the tuning range of electronically tunable parametric amplifiers in many different ways.

Fig. 1 shows a typical $\omega$-$\beta$ diagram of the loaded transmission lines of a backward traveling-wave parametric amplifier. The $PQ$ branch belongs to the pump. The $P_sQ_s$ and $P_iQ_i$ branches belong to the signal and idler which propagate in the same transmission line. It is assumed that the periodic

* Received by the IRE, May 12, 1961; revised manuscript received, May 19, 1961.

[1] T. M. Straus, "Tuning range of the backward traveling-wave parametric amplifier," IRE Trans. on Microwave Theory and Techniques (Correspondence), vol. 9, p. 95; January, 1961.

[2] D. I. Breitzer and E. W. Sard, "Low frequency prototype backward-wave reactance amplifier," *Microwave J.*, vol. 2, pp. 34–37; August, 1959.

[3] H. Hsu, "Letter to Editor," dated September 23, 1959, *Microwave J.*, vol. 3, p. 14; January, 1960.
H. Hsu, "Backward Traveling-Wave Parametric Amplifiers," presented at Internatl. Solid-State Circuits Conf., Philadelphia, Pa., February 10–12, 1960, and at the Internatl. Congress on Microwave Tubes, Munich, Germany, June 7–11, 1960.
H. Hsu, "Wide-Band Electronically Tunable Parametric Amplifiers," GE Co., Syracuse, N. Y.; November, 1959. (unpublished)

World Radio History

loading of parametric diodes occurs at intervals of $a$.

The conditions for backward traveling-wave parametric amplification are [3,4]

$$\omega_p = \omega_i + \omega_s, \tag{1}$$

$$\beta_p = \beta_i - \beta_s. \tag{2}$$

In order to satisfy (1) and (2), the sets of points ($P$, $P_s$, $P_i$) and ($Q$, $Q_s$, $Q_i$) in Fig. 1 are linked by the dotted curves which are parallel to the $\omega$-$\beta$ curve of the signal and idler transmission line. Graphically, we can determine $P$, for example, from $P_s$ and $P_i$, and vice versa.

In Fig. 1, the positions of $P_i$ and $Q_i$ are chosen such that the idler frequency is very close to the cutoff frequency, and thus the idler frequency is essentially constant over the whole tuning range. As is shown in Fig. 1, the signal-frequency tuning range ($P_s$, $Q_s$) is larger than 2:1. The tuning range can also be extended further by properly shaping the $\omega$-$\beta$ curve of the pump ($PQ$). Fig. 2 shows a tuning range ($P$,$Q_s$) of about 3:1 when the pump characteristic approaches that of a TEM mode. In Figs. 1 and 2, the signal, idler, and pump frequency bands are still separated from each other. Consequently, the limitations on the tuning range imposed by the condition of separation of these frequency bands, as discussed by Breitzer and Sard[2] and Straus,[1] are no longer severe in the schemes of Figs. 1 and 2. In fact, there is considerable freedom in the choice of circuit parameters, such as the relative phase velocities of the transmission lines; and the tuning range can be extended further.

The schemes of Figs. 1 and 2 have several additional advantages. We have chosen $\omega_i$ at $P_i$ and $Q_i$ to be equal. Thus, the required pump and signal tuning ranges ($\Delta\omega_p$ and $\Delta\omega_s$) are equal, *i.e.*,

$$\Delta\omega_p = \Delta\omega_s. \tag{3}$$

The TEM mode of operation[2] requires a proportional change in the pump and signal frequencies. Thus

$$\Delta\omega_p = (\omega_p/\omega_s)\cdot\Delta\omega_s. \tag{4}$$

In the modified TEM mode,[1] $\Delta\omega_p$ is smaller than the value of (4), but still higher than the value of (3). Thus, the fractional change in the pump frequency ($\Delta\omega_p/\omega_p$) is reduced in the scheme of Figs. 1 and 2. Furthermore, we can now raise $\omega_p$ and $\omega_i$, such that the fractional change in pump frequency becomes smaller. This results in simpler and possibly faster electronic tuning. The noise figure is also better due to the higher $\omega_i/\omega_s$ ratio.

In the construction of Figs. 1 and 2, the points $Q_i$ actually lie in the second Brillouin Zone.[5] Thus, $Q_i$ is identical to $Q_i'$ (Fig. 1) of the first Brillouin Zone. The sets of points $Q_s$, $Q_i'$, and $Q$ correspond to the parametric amplification of the backward traveling

[4] P. K. Tien, "Parametric amplification and frequency mixing in propagating circuits," *J. Appl. Phys.*, vol. 29, pp. 1347–1357; September, 1958.
[5] L. Brillouin, "Wave Propagation in Periodic Structures," Dover Publications, Inc., New York, N. Y.; 1953.

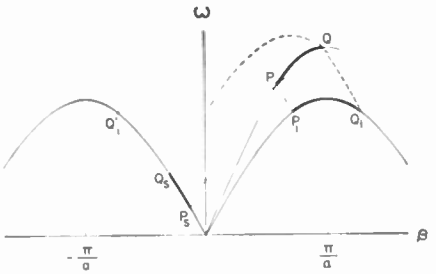


Fig. 1—Graphical illustration of the wide tuning range of backward traveling-wave parametric amplifiers.

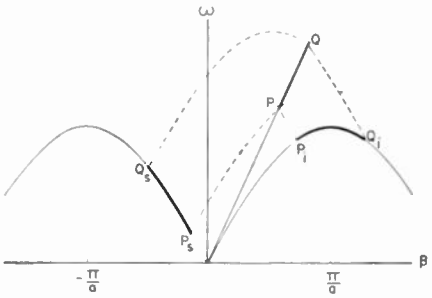


Fig. 2—Graphical illustration showing a further extended tuning range.

waves of the signal ($Q_s$) and idler ($Q_i'$) by a forward pump wave ($Q$). This type of operation is of particular physical significance because it is a typical microwave analogy of the Umklapp process described by Peierls.[6]

The fact that the idler frequency remains essentially constant is characteristic of the schemes of Figs 1 and 2, but these figures are not the only choice. We have achieved various types of parametric interactions with an essentially constant idler frequency in other schemes. For example, it is possible to provide separate idler circuits with a constant idler frequency. It is also possible to operate the idler near the cutoff frequency of the pump circuit when a loaded waveguide is used.

With an essentially constant idler frequency, the signal tuning range is a function of the phase velocities of the pump ($v_{\phi p}$), signal ($v_{\phi s}$) and idler ($v_{\phi i}$). From (1) and (2), we obtain

$$\frac{\omega_s}{\omega_i} = \left[\frac{v_{\phi p}}{v_{\phi i}} - 1\right]\cdot\left[\frac{v_{\phi p}}{v_{\phi s}} + 1\right]^{-1}. \tag{5}$$

By comparing (5) with Fig. 2, for example, we see that the enhanced tuning range is a result of varying $v_{\phi i}$ while keeping $v_{\phi s}$ and $v_{\phi p}$ nearly constant. From (5) or the corresponding graphs reported earlier,[3] the effect of the variations of the phase velocities on the tuning range can be calculated. The result serves as a guide in the design of the microwave structures.

H. Hsu
S. Wanuga
Electronics Lab.
General Electric Co.
Syracuse, N. Y.

[6] R. E. Peierls, "Quantum Theory of Solids," Oxford University Press, Oxford, England; 1955.

## Correction to "Negative Resistance in Transistors Based on Transit-Time and Avalanche Effects"*

The authors would like to make the following correction to the above paper.[1]

The very last factor (exp $i\omega\tau$) in (5) should be changed to $(1+\bar{m}\exp i\omega\tau)$.

The authors wish to thank O. Gandhi of Philco for bringing this error to their attention.

R. A. Pucel
H. Statz
Research Div.
Raytheon Co.
Waltham, Mass.

* Received by the IRE, April 26, 1961.
[1] H. Statz and R. A. Pucel, "Negative resistance in transistors based on transit-time and avalanche effects," Proc. IRE (Correspondence), vol. 48, pp. 948–949; May, 1960.

## Correction to "Communications Satellites Using Arrays"*

In the above paper,[1] the author would like to make the following corrections. In Table I, the figures for Stabilized Dish are reversed. The power for $D=60$ feet should be 22.4 mw and the power for 120 feet should be 5.6 mw.

In addition, the cylindrical array of Fig. 3 does not produce exact reinforcement as the following analysis shows. Referring to Fig. 1 of this letter where half of a cylindrical array with an odd number of elements is depicted, let the elements be spaced uniformly along the projected plane aperture.

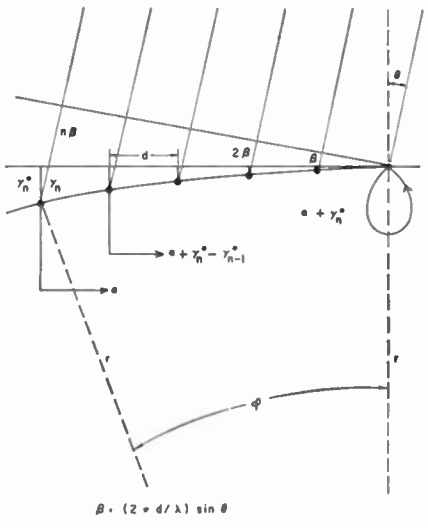


Fig. 1—Half of cylindrical array.

* Received by the IRE, May 22, 1961.
[1] R. C. Hansen, "Communications satellites using arrays," Proc. IRE, vol. 49, pp. 1066–1074; June, 1961.

World Radio History

Suppose also that the connecting line lengths are adjusted to compensate exactly for the cylindrical surface at broadside $\theta=0$. Using the symbols of the figure, the phase correction $\gamma_n{}^0$ for the $n$th element at broadside is given by

$$\gamma_n{}^0 = r - \sqrt{r^2 - n^2d^2}. \quad (1)$$

The actual departure $\gamma_n$ of the $n$th element from the plane aperture is given by

$$\gamma_n = \gamma_n{}^0 \sec\theta. \quad (2)$$

The phase error for the $n$th element as a function of incidence angle $\theta$ is then $\Delta_n$ and is given by

$$\Delta_n = (2\pi/\lambda)(\sec\theta - 1)(r - \sqrt{r^2 - n^2d^2}). \quad (3)$$

For small $n$ and for half-wave effective spacing, this is approximated by

$$\Delta_n \simeq (n^2\pi\lambda/4r)(\sec\theta - 1). \quad (4)$$

Here $r$ is the cylinder radius. The angular factor varies as follows:

| $\theta=$ | 0 | 15 | 30 | 35 | 40 | 45 |
|---|---|---|---|---|---|---|
| $(\sec\theta-1)=$ | 0 | 0.035 | 0.155 | 0.221 | 0.305 | 1.00 |

For a practical example, take a frequency of 8 Gc and a diameter of 2 feet. Table I gives the maximum phase error in radians for two scan angles. Note that $n$ is half the total number of elements minus 1. Now if the correction is chosen to be exactly halfway between $\gamma_n{}^0$ at broadside and $\gamma^{max}$ at $\theta_{max}$, maximum and equal phase errors occur at $\theta=0$ and at $\theta=\theta_{max}$, and these phase errors are just half of those given in the table. Silver[2] shows that a maximum quadratic phase error of 0.79 radian ($\lambda/8$) gives a gain loss of 0.25 db; a phase error of 1.58 ($\lambda/4$) gives a gain loss of 1.0 db. For the synchronous example in the original paper, the cylindrical array is satisfactory. To check the two-term approximation of (4), the ratio of the third term to the second term was examined and found to be less than 0.1 for $n=10$ (corresponding to 21 elements). Thus, the approximation is quite good up to a full quadrant.

TABLE I

| $n$ | Total Elements | $\theta=30°$ | $\theta=45°$ |
|---|---|---|---|
| 2 | 5 | 0.06 | 0.38 |
| 4 | 9 | 0.24 | 1.56 |
| 6 | 13 | 0.54 | 3.48 |
| 8 | 17 | 0.96 | 6.18 |
| 10 | 21 | 1.50 | 9.66 |

In the equatorial synchronous (stationary) satellite case, coverage requirements limit the number of elements and hence limit available directivity. It should be mentioned that active Van Atta systems should offer major advantages for long-distance space communications where narrow beamwidths, and thus high directivities, could be realized.

Norwood has recently pointed out that the decrease of effective aperture away from broadside of the passive array could be compensated by using an element factor which increased away from broadside.[3]

R. C. Hansen
Electronics Lab.
Aerospace Corp.
Los Angeles, Calif.

[2] S. Silver, "Microwave Antenna Theory and Design," M.I.T. Rad. Lab. Ser., McGraw-Hill Book Co., Inc., New York, N. Y., vol. 12, p. 191; 1949.

[3] V. T. Norwood, "A Versatile Reflector Design for Passive Satellite Use," URSI-IRE Spring Meeting, Georgetown University, Washington, D. C.; May 1-4, 1961.

# Contributors

Frank R. Arams (S'44–A'49–SM'55) was born in the Free City of Danzig, on October 18, 1925. He received the B.S.E. degree in electrical engineering and mathematics from the University of Michigan, Ann Arbor, in 1947, the M.S. degree in applied physics from Harvard University, Cambridge, Mass., in 1948, and the M.S. degree in business management from Stevens Institute of Technology, Hoboken, N. J., in 1953. He received the Ph.D. degree in Electrical Engineering (electrophysics from the Polytechnic Institute of Brooklyn in 1961, with a dissertation on cross-relational masers.

F. R. Arams

During World War II, he served in the Army Signal Corps as Communications Chief of Radio Receiver Station WXH, Ketchikan, Alaska. He joined RCA, Lancaster, Pa., in 1948, where he was Project Engineer on various development programs in microwave magnetrons, traveling-wave tubes, and plasma-filled cavities. From 1953 to 1956 he was employed at the Tube Division of RCA, Harrison, N. J., where he was in charge of the microwave-tube application engineering group. In 1956, he joined Airborne Instruments Laboratory, Melville, N. Y., where he is presently associated with the Department of Applied Electronics as Consultant, concerned with theoretical and experimental work on microwave solid-state devices such as new types of solid-state maser amplifiers, microwave linear and nonlinear ferrite devices, and parametric amplifiers. He now directs programs in microwave ferrite, and millimeter-wave and optical maser fields.

Dr. Arams is a member of Tau Beta Pi, Eta Kappa Nu, the American Physical Society, and the Editorial Board of the *Microwave Journal*.

❖

Wolfgang W. Gärtner (M'54-SM'60), for a photograph and biography, please see page 839 of the April, 1961, issue of these Proceedings.

Martin I. Grace (S'57, M'59) was born in New York, N. Y., on June 16, 1936. He received the B.S.E.E. degree from the Polytechnic Institute of Brooklyn, Brooklyn, N. Y., in 1958. He is presently completing the requirements for the M.E.E. from the Polytechnic Institute of Brooklyn. From 1958 to 1961 he was an engineer in the Applied Electronics Department of Airborne Instrument Laboratory where he worked on ferrite devices and backward-wave parametric amplifiers.

M. I. Grace

In March of 1961, he joined the staff of the Advanced Devices Laboratory of Airtron Incorporated, Morris Plains, N. J. as a Group Leader working on the development of parametric amplifiers and ferrite devices. In 1960 he joined the staff of the Department of Electrical Engineering at the Polytechnic Institute of Brooklyn as a part-time Instructor.

World Radio History

Bernard Jaffe was born in Brooklyn, N. Y., on November 28, 1923. He received the B.S. degree in ceramic engineering from the New York State College of Ceramics at Alfred University, Alfred, N. Y., in 1948.

B. JAFFE

From 1948 to 1955, he worked on ceramic dielectrics and on ferroelectric ceramic transducer materials at the National Bureau of Standards in Washington, D. C. Since 1955, he has been working on piezoelectric ceramics at the Electronic Research Division of Clevite Corporation, Cleveland, Ohio, where he is head of the Electro-Ceramic Section.

Mr. Jaffe is a member of the American Ceramic Society and of the Institute of Ceramic Engineers.

❖

Sanford A. Meltzer, for a photo and biography, please see page 532 of the February, 1961, issue of these PROCEEDINGS.

❖

Jin-ichi Nagumo (M'60) was born in Tokyo, Japan, on October 14, 1926. He received the Kogaku-Hakase degree in applied physics from the University of Tokyo, Japan, in 1954.

J. NAGUMO

From 1953 to 1959, he was an Assistant Professor of applied mathematics at the Keio University, Tokyo, Japan. Since 1959 he has been an Assistant Professor of applied physics at the University of Tokyo; since 1948 he has been working mainly on the theory of nonlinear oscillations, nonlinear circuit theory and nonlinear electronics.

Dr. Nagumo is Vice-Chairman of the Professional Group on Nonlinear Circuit Theory of the Institute of Electrical Communication Engineers of Japan.

❖

Seymour Okwit (A'55, SM'61) was born in New York, N. Y., on August 31, 1929. He received the B.S. degree in physics from Brooklyn College, N. Y., and the M.S. degree in applied mathematics and physics from Adelphi College, Garden City, N. Y., in 1952 and 1958, respectively. He is presently working toward the Ph.D. degree in mathematical physics, Adelphi College, Garden City, N. Y.

S. OKWIT

From 1952 to 1954, he was in the armed forces assigned to the detection division of the Chemical and Radiological Laboratories of the Army Chemical Center, Edgewood, Md., where he did extensive development work on instrumentation for the detection and analysis of the poisonous "G" nerve gases. Detection instruments upon which he has worked include an infrared scanning system and a system utilizing microwave spectroscopy. He was associated with the radar department of Arma Corporation, Long Island, N. Y., from 1954 to 1955, where he was concerned with boresight on monopulse antennas. He joined the Airborne Instruments Laboratory, a division of Cutler-Hammer, Inc., Melville, N. Y., in 1955, as an engineer in the Department of Electronics, where he was concerned with the design and development of RF, IF, and microwave components and systems. Since 1958, he has been responsible for, and has performed considerable theoretical and experimental work on solid-state devices such as low-loss circulators, low-level ferrite limiters, and cavity and traveling-wave masers. At present, he is a Section Head in the Applied Electronics Department at AIL, and is directing programs in the development of advanced solid-state devices including masers, parametric amplifiers, and novel ferrite components.

❖

Max J. Schuller (M'60), for a photograph and biography, please see page 840 of the April, 1961, issue of these PROCEEDINGS.

❖

Masamichi Shimura was born in Tokyo, Japan, on April 5, 1936. He received the Kogakushi degree in applied physics from the University of Tokyo in 1960.

M. SHIMURA

He is now a student in the postgraduate course and is engaged in studies of nonlinear electronic circuits under the direction of Assistant Professor J. Nagumo.

❖

Samuel Thaler (A'42–M'60), for a photo and biography, please see page 532 of the February, 1961, issue of PROCEEDINGS.

World Radio History

# Books

## Transistor Circuit Analysis, by Maurice V. Joyce and Kenneth K. Clarke

Published (1961) by Addison-Wesley Publishing Co., Inc., Reading, Mass. 438 pages+11 index pages +xiv pages+5 pages answers to problems. Illus. 6¼×9¼. $10.75.

From the large influx of technical books dedicated to the theme of tutoring the engineer on the fundamentals of transistor circuitry, it is refreshing to review a book that is so well prepared and presented as "Transistor Circuit Analysis," by M. V. Joyce and K. K. Clarke.

The book is orientated in an academic flavor with suggested reference reading and circuit problems at the end of every chapter. The over-all concise preparedness of the text is obviously derived from the academic teaching background of the authors, the late Maurice V. Joyce and Kenneth K. Clarke, associated with the Electrical Engineering Department of the Polytechnic Institute of Brooklyn. The text provides a continuous development of junction transistor circuitry which would benefit the electrical engineer attempting to establish himself in the semiconductor electronics field. It definitely serves as an excellent textbook for the undergraduate electrical engineer engaged in the study of semiconductor electronics during his senior year

The first several chapters describe the junction transistor circuit characteristics and then expand these into the circuit equivalent Tee and the Hybrid and the well-known Hybrid-Pi circuit model. The transistor then is treated in its three basic circuit modes of operation (common base, common emitter, and common collector), and the pertinent characteristics and circuit parameters are analyzed. The following six chapters (4–9) provide an excellent presentation of transistor low freqeuncy small signal amplifiers, power amplifiers, power regulators, broad-band amplifiers, and narrow-band amplifiers. It is felt that in the presentation of the high-frequency equivalent circuit a broader expansion into the characteristics of the Hybrid-Pi equivalent circuit would have been beneficial. Perhaps an entire chapter should have been dedicated to transistor high-frequency characteristics.

Chapter 8 presents an extensive analysis into broad-band transistor amplifiers with excellent coverage on the gain bandwidth tradeoff and feedback techniques to attain this end. The chapter also has an excellent presentation on the analysis of the frequency response of the emitter follower circuit. The last part of Chapter 8 deals with the subject of transistor distributed amplifiers.

Chapter 9 expounds on the characteristics of transistors in band-pass, and it is interesting to note that the authors concentrate their effort on the analysis of the transistor characteristics as applied to the circuit rather than dealing with an extensive dissertation into the characteristics of the associated passive elements. Chapters 10–14 deal with the subject of transistors being employed as switches. The reviewers feel that an incorporation of the junction transistor being treated as a stored charge device would have aided many engineers in their understanding of the fundamental concepts of transistor switching theory. The majority of the circuit examples analyzed in the text are very much the "state-of-the-art" techniques. Chapter 15 gives an up-to-date presentation of circuit characteristics of negative resistance devices such as the tunnel diode and the "PNPN" junction transistor. The final chapter, Chapter 16, goes into the analysis of employing transistors in the conventional sine wave oscillator usage. It is felt that the high-frequency oscillator equivalent circuit could have been expanded upon and perhaps one network analysis example given.

This book is definitely recommended for the transistor circuit engineer to serve him as an excellent circuit reference guide. It should prove to be very popular with the engineer embarking into the semiconductor electronics field for obtaining a complete tutorial background on semiconductor circuitry. The book should especially become popular with the undergraduate electrical engineer as a textbook for transistor electronics during his senior year at college.

J. T. Lynch
J. J. Kakew
Burroughs Corp.
Paoli, Pa.

## IRE Dictionary of Electronic Terms and Symbols (Compiled from IRE Standards)

Published (1961) by the Institute of Radio Engineers, 1 E. 79 St., New York 21, N. Y. 221 pages+ 4 index pages+x pages. Illus. 6¼×9¼. $5.20 members; $10.40 nonmembers.

During the past two decades the IRE has issued over eighty IRE Standards, covering the vast multitudes of fields represented within the IRE Standardization structure. These Standards have been divided approximately equally between Standards on Definitions of Terms and Standards on Methods of Measurements. There have also been Standards issued on graphical and letter symbols. Prior to 1949 these were issued as separate pamphlets. Currently each Standard, as issued, appears in the PROCEEDINGS OF THE IRE.

This Dictionary fills the long-felt need for a compilation of the Definitions Standards under one cover, together with associated letter and graphical symbols. It includes the definitions contained in 37 IRE Standards dealing with electronics terminology and symbology. Thus all Standards in effect as of December, 1959, have been combined in this one volume. Knowing the mass of material put out by the IRE, this reviewer was frankly surprised that it was possible to get it all in such a compact volume (225 pages). Yet they are all there, some 3700 terms, plus five IRE Standards dealing with letter and graphical symbols.

This Dictionary has one definite advantage over other contemporary works, at least with respect to IRE definitions, in that it does not take liberties with printed definitions or notes, but reproduces them verbatim. In other works, modifications are frequently encountered and occasionally the notes are incorporated into the definition, whereas they are intended to be explanatory or complementary. This Dictionary, therefore, preserves the purity of the original IRE context.

The reader should find the inclusion of graphical and letter symbols of particular value, especially in those fields where a profusion of competing, and often confusing, symbols exists. In particular, the semiconductor area is well delineated in both respects. This will prove of great assistance to the novice in this important field, helping him to understand the fine distinctions in usage conveyed by the various combinations of capital and lower-case symbols and subscripts. Possibly a perusal of the remainder of the graphical symbols will convert some readers to a proper usage of the capacitor and relay symbols!

This book will be indispensable to anyone having occasion to deal with legal terminology in the electronics field, as well as to the practicing engineer who wants a handy source of authoritative definitions. It is to be hoped that having established this precedent the IRE will follow at reasonable intervals with either supplements or new editions, adding the later material continually generated in this fast-moving technology.

R. F. Shea
General Electric Co.
Knolls Atomic Power Lab.
Schenectady, N. Y.

## Printed Circuits—Their Design and Application, by J. M. C. Dukes

Published (1961) by Macdonald & Co., Ltd., 16 Maddox St., London, W. 1, England. 196 pages+12 index pages+xii pages+11 bibliography pages+9 appendix pages. Illus. 5¾×8¾. 40s. net.

The widespread interest in new ways of fabricating electronic hardware, as indicated by the large development effort, has resulted in many published papers. This situation has created a problem for the practicing engineer who wishes to stay abreast of the capabilities and limitations of the many competing approaches. The book by Mr. Dukes goes a long way toward solving the problem for the field of printed circuit techniques.

The book starts with an introduction which includes a brief historical review and a classification system for printed circuit techniques. The author makes a valiant attempt to define the term "printed circuit." He concludes that it is a poor term but that it is too commonly used to bear substitution.

The book is broken up into two main parts: the first on Manufacture and the second on Design and Application. In the first part a separate chapter is devoted to a description of each of the following classes of techniques: the direction deposition of a

World Radio History

metallic circuit on a bare insulating surface, the controlled removal of metal from a previously metallized surface, and methods which combine the formation of the substrate and the detailed circuit wiring. The second class covers the most popular technique now employed for printed circuits, that is, the etched-foil technique. An additional chapter in the first part is devoted to these topics: components for printed circuits, automatic assembly machines, dip soldering, and protective coatings.

The part on Design and Application presents information on the preparation of the circuit layout, and a good review is given of materials for use in printed circuits such as ceramics, laminates, and the conducting materials. There is also a discussion of printed component parts including coils, resistors, capacitors, switches, and commutators for use at low and medium frequencies. The last two chapters deal with strip transmission lines and printed microwave components. The author is obviously "at home" in these two chapters since it is in this area that he has made original contributions. The strong emphasis on microwave components is quite proper because of the increasing importance of high speed circuits, of both the analog and digital types, coupled with the need for small size and low cost components and systems.

A generous number of references (173) to British and American literature is provided. It is easy to find sources of more detail on any of these items discussed. The book is thoroughly cross-referenced. Although the author's experience is British, many of the examples include American products.

Two minor weaknesses are apparent. Only a little over one page is devoted to the rapidly developing field of microminiaturization and slight mention is made of the problems of handling transistors in the printed circuit production process. One small irritation is the use in the text of figure numbers that are condensed over those used to identify the figures themselves.

The author describes the book as "a first primer on manufacturing techniques," and he achieves this objective for the field of printed circuits. The book is recommended to the system and equipment designer who is looking for a general understanding of the problems and techniques of circuit fabrication and for anyone entering the field needing references to detailed information.

THOMAS A. PRUGH
Dept. of Defense
Washington, D. C.

### Line Waves and Antennas, by Robert Grover Brown, Robert A. Sharpe, and William Lewis Hughes

Published (1961) by the Ronald Press Co., 15 E. 26 St., New York 10, N. Y. 261 pages+3 index pages +v pages+27 appendix pages. Illus. 6¼×9¼. $10.00.

This book, written by professors at Iowa State University and Oklahoma State University, is intended as an introductory text in the general area of electric energy propagation. The first six chapters present a good practical treatment of transmission lines including pulse transmission and reflection. Smith charts are used in the analysis to determine input impedance, line length or load impedance when two of the quantities are known.

The next five chapters treat guided waves, wave propagation and waveguide circuit elements with heavier mathematics involving Maxwell's equations and the various waveguide modes. The discussion of lossy wave propagation deals with lossy dielectrics, poor conductors and skin effect problems.

The last three chapters briefly cover electromagnetic wave radiation, dipole antenna radiation and antenna systems.

There are eight appendixes, covering reference material and handbook information such as transmission line, parameters, characteristics and charts, vector analysis, phase and group velocities and the scattering matrix.

The text is in the second person classroom vernacular. In the more difficult areas the authors make assumptions which lead to appropriate solutions, thus avoiding tedious proofs. Numerous problems are left for the student to solve. The term "current flow," which used quite often, is redundant since current is a flow of electrons or ions. The directional antenna patterns for broadside and end fire arrays on page 238 are drawn with the same shape, which is untrue.

The authors have written a very usable text for classroom instructions with excellent descriptive material and a minimum of complex mathematics. The brevity of the presentation keeps the size of the book small; hence the instructor will be called on more often to amplify the text and help the student with his problems.

CARL E. SMITH
Cleveland Institute of Electronics
Cleveland, Ohio

### Time-Harmonic Electromagnetic Fields, by Roger F. Harrington

Published (1961) by McGraw-Hill Book Co., Inc., 330 W. 42 St., New York 36, N. Y. 446 pages+8 index pages+xi pages+2 bibliography pages+24 appendix pages. Illus. 6¼×9¼. $13.50.

In essence this book is divided into four parts. The first part reviews some of the basic concepts which are needed for the application of the theory of steady-state electromagnetic waves and fields to the solution of problems in electromagnetic engineering. The second part deals with certain boundary-value problems selected from the theory of waveguides, cavity resonators, antennas, and scattering which can be handled simply by the matching of well-known solutions of Maxwell's equations. The third part introduces the reader to variational and perturbational methods of treating waveguide discontinuities, diffraction, and loaded cavity resonators. And the fourth part provides the reader with an exposition on microwave networks.

The book is easy to read and probably pleasant to teach from. Its subject matter is selected to place in evidence some of the more common mathematical methods used in electromagnetic engineering. At the end of each chapter there are problems which illustrate and augment the material in the text. The topics discussed in the book are timely, but not especially new. Indeed, several other books and monographs that cover the same ground have been on the market for a number of years. However, in general, these other books are intended to satisfy the rather sophisticated tastes of the active researcher, whereas the present book is designed to serve as a senior or first-year graduate text for electrical engineering students.

Unfortunately, the author has neglected to provide the reader with an adequate bibliography of original papers. As a result it becomes difficult for the reader to track down the subject matter to its original sources if he limits himself to the few footnote references that the book contains. Although this detracts from the scholarship of the book, it can be remedied by having the instructor supply the missing information.

This reviewer enjoyed reading the book and considers it a worthwhile contribution to the educational literature of electromagnetic engineering.

CHARLES H. PAPAS
Calif. Inst. Tech.
Pasadena

### Theory of Microwave Valves, by S. D. Gvozdover

Published (1961) by Pergamon Press, Inc., 122 E. 55 St., New York 22, N. Y. 450 pages+5 index pages+xiii pages+6 reference pages+25 appendix pages. Illus. 6¼×9¼. $12.50.

The scope of this book can be most easily conveyed by repeating here the table of contents:

1) Elements of electrodynamics of cavity resonators
2) Static characteristics of the plane diode
3) Alternating voltage applied to a plane diode; basic formulae of microwave electronics
4) Electronics of the plane diode when the influence of space charge is negligible
5) Application of the total-current method to the analysis of the plane diode
6) The influence of transit effects on noise in a plane diode
7) Amplification of high-frequency signals by a triode
8) General theory of single circuit klystron oscillators
9) Theory of the reflex klystron
10) Introduction to the theory of the multi-cavity magnetron
11) The theory of traveling-wave tubes.
12) Noise in the electron beam; the sensitivity of traveling-wave tubes

The technical level of the book is generally high, and some previous acquaintance with the fundamentals of electrodynamics is assumed of the reader. Graduate students in electrical engineering or physics should encounter no serious difficulty in reading this book.

The major part of the book is devoted to a very thorough and detailed presentation of the theory of the plane diode. The reviewer knows of no other single reference

World Radio History

work in which so much of the detailed analysis of the plane diode has been compiled. In the chapter on static characteristics, we are given not only the usual multivelocity analysis of the space-charge limited diode, but also a compilation of detailed single-valued velocity analyses for almost all conceivable cases of electron flow between parallel planes. In the ac analyses, the equivalents of the Llewellyn-Peterson equations and coefficients are derived. In the noise analyses, the usual single-valued velocity assumptions are made. The analyses of reflex klystrons, magnetrons, and traveling-wave tubes are essentially standard and equivalent to those found in many graduate level texts and require no special comment.

Because of its limited scope, this book will probably not be very useful as a text for a formal course in microwave tubes. It should, however, be useful as a rather complete reference on transit-time effects in microwave diodes.

C. W. Barnes
Stanford Research Inst.
Menlo Park, Calif.

### Lectures on Communication System Theory, Elie J. Baghdady, Ed.

Published (1961) by McGraw-Hill Book Co., Inc., 330 W. 42 St., New York 36, N. Y. 603 pages+13 index pages+xii pages+bibliography by chapter. Illus. 6¼×9¼. $12.50.

Models, analytical techniques, representations for signals and channels, as well as coding and detection rules—all appropriate to the design of a single communication link—characterize the material covered in this book. It has grown from a set of notes used in a special two-week summer session on "Reliable Long-Range Radio Communication" offered in August, 1959, at MIT. Most of the material is based on papers written by the chapter authors and published over the past few years in the Proceedings of the IRE and Transactions of IRE Professional Groups. It is the Editor's contention that the book should serve as a reference book for practicing engineers as well as a textbook for students at the senior or graduate level. Nonuniform quality of coverage, absence of exercises, and the necessity for considerable outside reading to extract the full flavor of the subject matter contribute to making the latter view of the Editor border on wishful thinking. This book does not appear to be suitable as an undergraduate text. On the other hand, practicing engineers and sophisticated graduate students can benefit from this book provided they are appraised of both its many excellent features and its important shortcomings. An attempt at providing this balanced assessment follows.

The introductory chapter presents a realistic picture of the role of mathematical models in the design of communication systems and also sets the stage for the four main divisions of the book. The first short division (Chapters 2, 3, and 10) is concerned with statistical notions and techniques for the analysis and representation of linear systems and signals. It is worth noting that Chapter 2 presents a refreshing approach to probability concepts and their relevance to the way in which probability distributions are measured and utilized in communication system design. A more complete appreciation of R. M. Lerner's Chapter 10 on signal representation by sums of elementary signals may be obtained by reference to his paper.[1]

The second principal division emphasizes the characterization of linear time-variant dispersive channels. Chapter 4 serves to motivate the work of this section, while Chapters 5 and 6 delve into the details of channel characterization for relatively rapid channel fluctuations. Canonical descriptions of the linear time variant channel are given in Chapter 6. Long-term variability and its implications in design are examined in detail in Chapter 20.

The third and largest of the four main divisions is devoted to methods for overcoming multiplicative and additive disturbances introduced into the transmission channel. Diversity techniques for combating fading are discussed in Chapter 7. Statistical decision theory is presented in a lucid manner in Chapters 8 and 9. Chapter 11 is concerned with signal design to combat additive noise, both Gaussian and impulsive. Chapter 12 is an excellent treatment of functional receiver design to overcome both multiplicative and additive disturbances. Coding and decoding and pre- and post-decision feedback for error control in digital transmission are treated with precision and clarity in Chapters 13 and 14. Noise characterization and minimization in receiving systems receive adequate attention in Chapters 15–17. Chapter 19, on analog modulation, concludes this section.

Application of the above theory to communication system design is the avowed purpose of the final section of the book. This materializes only in the form of a philosophy for design. A more detailed discussion of Rake (even beyond that in the fundamental paper of Price and Green[2]) might have provided a more concrete illustration of the results obtainable with the application of the theory espoused. The concluding chapter, covering present trends, is appropriately authored by R. M. Fano, who I am sure has been teacher and counselor to many of the authors. Professor Fano advocates overlapping membership in the computing and communication fraternities to bring the present promises of digital communication to fruition.

The significant shortcomings of the book are found in Chapters 7 and 19. Chapter 7 is, by and large, a rewrite by the editor of D. G. Brennan's excellent paper.[3] Unfortunately, the sharpness of the original is dulled in "translation." Chapter 19, on analog modulation, as presented does not integrate well with the close-knit subject matter and crispness of the remainder of the text. Secondly, the exposition is fuzzy and can mislead the unwary. For example, the discussion of "manageable bounds" on the error associated with using the "quasi-stationary" response of a linear network to an FM signal is even more obscure than the Editor's original paper on this subject.[4] In this regard, he invokes a very powerful theorem on asymptotic expansions to arrive at his bounds. After a search and study of the pertinent literature on this subject (Erdelyi, Hardy, Knopf, Bromwich, and DeBruijn) this reviewer is unable to verify the existence of such an unrestricted theorem. The treatment of residual distortion in FM is not given in a useful form. Discussion of Chaffee's FM receiver with feedback is trivial. References at the end of the chapter are inadequate. The most glaring omission is the absence of references to the classic papers of Crosby (experimental) and Rice (theoretical) on noise in FM systems.

Despite the above criticisms, the book can be recommended. In particular it should be useful to the communication system designer interested in gaining insight into how statistical communication theory can contribute to the design of modern communication facilities.

M. R. Aaron
Bell Telephone Labs.
Murray Hill, N. J.

[1] R. M. Lerner, "The representation of signals," IRE Trans. on Circuit Theory, vol. CT-6, pp. 197–216; May, 1959.

[2] R. Price and P. E. Green, Jr., "A communication technique for multipath channels," Proc. IRE, vol. 46, pp. 555–570; March, 1958.

[3] D. G. Brennan, "Linear diversity combining techniques," Proc. IRE, vol. 47, pp. 1075–1102; June, 1959.

[4] E. J. Baghdady, "Theory of low-distortion reproduction of FM signals in linear systems," IRE Trans. on Circuit Theory, vol. CT-5, pp. 202–214; September, 1958.

### Electronic Drafting Handbook, by Nicholas M. Raskhodoff

Published (1961) by The Macmillan Co., 60 Fifth Ave., New York 11, N. Y. 233 pages+7 index pages+xiii pages+159 appendix pages. Illus. 6¼×9¼. $14.75.

There was a time, not too many years ago, when a mechanical draftsman could turn to electronic drafting without requiring much, if any, additional training. Not so today. The impressive growth in the complexity of electronic circuitry, the birth of printed circuitry, and the broadening of the standardized graphical symbology have all contributed to making electronic drafting a highly specialize field requiring special skills.

The author has prepared a handbook that is more than just a reference guide for draftsmen and designers working in the electronics field. It is eminently suited to students preparing for a career in electronic drafting and design. It will also be of considerable value as a reference text for engineering students majoring in electronics.

The book is divided into four parts. Part 1, Basic Electronic Information, contains brief descriptions, as well as pictures, of practically all of the electronic and mechanical components used in electronic equipment. Also included in this section is a chapter on such materials as the more common alloys and plastics. All of this information in Part 1 has been thoughtfully arranged in alphabetical order to facilitate reference.

In Part 2, General Electronic Drafting Techniques, the author describes general drafting room practice, including the use of templates and other drawing tools. A chap-

World Radio History

ter on mechanical design, dealing with the layout of components on a chassis, or rack; space and cooling considerations; and other design criteria also forms part of this section.

Part 3, Special Electronic Drafting Techniques, is the most comprehensive part of this book so far as drafting information, as such, is concerned. Included are chapters on Schematic Diagrams, Wiring or Connection Diagrams, Wiring Harness Drawings, Outline Drawings, Printed Circuits, Industrial Electronic Drawings, Graphical Representation, and Checking Electronic Drawings. In the chapters on schematic and wiring diagrams, the author has drawn heavily—and wisely, we feel, on the American Standards Association standard Y14.15 for his illustrations. This standard reflects industry's coordinated opinion of what information such drawings should contain, and how they should depict this information. The chapter on Printed Circuits contains considerable design information on this comparatively new and radically different approach to electronic wiring. It might have been well to include in this chapter reference to the printed circuit processes described later on page 288.

In Part 4, Reference Information, the author has gathered together such strictly reference information as: Abbreviations, Symbols, Designations, Tube Basing Diagrams, Copper Wire Data, Transistor Types, Screw Sizes, etc. Also included is a digest of the General Specifications for Military Electronic Equipment.

The material in this book is well organized, thus making the book readily adaptable to classroom use. The information is up-to-the-minute, and the data, for the most part, is from authoritative sources. The art work in the illustrations, of which there is an abundance, is excellent. It is too bad, though, that someone did not caution the draftsman preparing the illustrations on pages 136–140 to use the standard resistor symbol which the author illustrates on page 277. And while we are touching on the shortcomings of this book we should also mention that while the author, in Chapter 8 and Appendix A, gives due credit to the military and ASA as sources for the symbols he has shown, he has overlooked giving similar credit to the IRE. The Institute has done considerable work in this field over the years.

These are, however, small faults in a book that is in all respects an excellent treatment of an important subject. Mr. Raskhadoff is to be commended for giving us a book that is authoritative, comprehensive, and—what may seem strange for a text book—readable.

R. T. Haviland
Sperry Gyroscope Co.
Great Neck, N. Y.

### Electronics, by Paul M. Chirlian and Armen H. Zemanian

Published (1961) by McGraw-Hill Book Co., Inc., 330 W. 42 St., New York 36, N. Y. 327 pages+7 index pages+xii pages. Illus. 6¼×9¼. $8.75.

Now that many topics of electronics such as circuit theory, feedback, and modulation have become well-developed fields of study, about all that is left to electronics is a study of the physical electronics of active devices and the development of their equivalent circuits. It is in recognition of this shift of emphasis that "Electronics," by Chirlian and Zemanian, is limited to the physical electronics of tubes and transistors together with a development of their equivalent circuits.

The book is intended as a one-quarter or one-semester upper division college textbook for electrical engineering or science students. The first chapters discuss electron ballistics, electron emission, Child's Law, and the vacuum diode. Then follow chapters on semiconductor physics and the semiconductor diode. A brief chapter on gaseous conduction indicates that this subject is considered of decreasing importance.

Using the physical electronics of the earlier chapters, the characteristics of vacuum tubes and transistors are next developed. The remainder of the text deals with the graphical and linear circuit analysis of vacuum tube and transistor circuits. The chapter on graphical analysis efficiently combines the vacuum tube and transistor analysis and contains standard material on bias, load lines, and distortion. The final chapters discuss linear equivalent circuits at a level assuming familiarity with three-terminal network theory.

The text has the strong point of integrating vacuum tube and transistor analysis so that neither one is predominate. It also takes advantage of modern courses on circuit theory now commonly taught to electrical engineers. It does not pretend to do more than furnish a background for understanding the characteristics of vacuum and semiconductor devices and obtaining their equivalent circuits. To following courses must fall the task of developing linear amplifier theory, pulse and trigger circuitry, etc.

The text is extremely well furnished with problems; without a thorough sampling the student will miss a good share of the value of the text. As an example, the 67 problems at the end of the chapter on linear equivalent circuits introduce the concepts of frequency response, cathode and emitter followers, the grounded grid amplifier, and the impedences and gain of a feedback amplifier; none of these appears as subjects in the text. The instructor using this text should use the problems as a springboard for additonal discussion.

Reading of the material on emission and semiconductor physics leaves one with a feeling of frustration not entirely the fault of the authors. As a practical matter they have assumed that the reader has no knowledge of thermodynamics including statistical mechanics. How much better it will be when electrical engineers can approach physical electronics with such a background.

One can always find a number of matters with which to quarrel. Chapter 1 does not take advantage of the modern field background of the college student. The text also does not clearly relate the practical physical world to the ideal one under discussion. Examples are in assuming a uniform field between two parallel plates and then using the results of this analysis to find the path of an electron just missing the edge of one plate. In the Child's Law derivation the basic assumption made is that the slope of the potential curve is zero at the cathode. It is more fundamental to take the assumptions as zero initial velocity at the cathode and an emitter electron supply greater than the space current; from these one can deduce that the initial slope must be zero.

The final chapter on piecewise-linear equivalent circuits is certainly useful from the standpoint of obtaining a given V-I curve for modeling a system on an analog computer. But for analyzing the behavior of a circuit including a nonlinear element the necessary information is often more easily obtained from the segmental approximation to the curve than from a complex network of diodes, resistors, and voltage and current sources.

W. R. Hill
University of Washington
Seattle

### Progress in Semiconductors, Vol. 5, A. F. Gibson, F. A. Kröger, and R. F. Burgess, Eds.

Published (1961) by John Wiley and Sons, Inc., 440 Park Avenue South, New York 16, N. Y. 315 pages+vii pages. Illus. 6¼×9¼. $11.00.

The primary purpose of this annual series of volumes is to permit the specialist in a particular area to keep abreast of activities in the various aspects of semiconductors without the need of sifting through the massive literature in the field. We have come to expect that this series will do so within the fairly obvious limitations of a series which consists of a single book of reasonable size per year. The present volume is no exception. In general the papers are critical reviews of seven fields. In several cases, very recent work has been included by the expedient of additions made in proof. Comprehensive bibliographies are included with each article.

In "The Electrical Properties of Semiconductor Surfaces," T. B. Watkins begins with a very brief historical outline, followed by a discussion of a surface model with primary emphasis on germanium. Results of basic theoretical calculations are presented, followed by discussions of the measurement techniques used in surface studies and the applications of surface properties.

In "The Absorption Edge Spectrum of Semiconductors," T. P. McLean gives a review of the theoretical analysis of both direct and indirect transitions. After a discussion of the experimental methods used in making measurements, the properties of the absorption edge of both germanium and silicon are presented in detail. Brief references to work on other materials are given in the historical review which opens the paper and in the concluding summary.

"Magneto-Optical Phenomena in Semiconductors" are discussed by B. Lax and S. Zwerdling. Detailed discussions of magneto-absorption, Zeeman effect of excitons, magneto-absorption of impurities, Faraday effect and magneto-plasma effects—both theoretical and experimental—are followed by a brief description of the experimental techniques used in making the measurements. In this fast-moving field any sum-

World Radio History

mary is soon out of date, but an extended note added in proof brings the survey well into 1960.

"Indium Antimonide" by T. S. Moss is a concise survey of this material from preparation to applications. Detailed consideration is given to band structure, optical properties, photo effects and electrical properties. Applications of this material utilizing its photo-response, magnetoresistance and Hall characteristics are discussed in some detail. Potential applications as a low temperature diode and transistor are briefly mentioned.

"The Chemical Bond in Semiconductors" by E. Mooser and W. B. Pearson is a discussion of the intricate relationships between the chemical bond and material properties of semiconductors. A theoretical discussion of "Thermal Conductivity of Semiconductors" is given by J. Appel. R. R. Haering and S. Mrozowski discuss "The Band Structure and Electronic Properties of Graphite Crystals" with particular emphasis on the relationships between these phenomena.

In sum, the present volume continues the tradition of this series in presenting timely topics for those interested in the field fo semiconductors. The writing is good and the book is highly recommended.

W. M. Bullis
Texas Instruments, Inc.
Dallas, Tex.

### Essentials of Dielectromagnetic Engineering, by H. M. Schlicke

Published (1961) by John Wiley and Sons, Inc., 440 Park Avenue South, New York 16, N. Y. 221 pages+6 index pages+xxii pages+5 bibliography pages+8 appendix pages. Illus. 6×9¼. $9.50.

The purpose of this book is to furnish essential facts on magnetics and dielectrics, more particularly on high $\mu$ and $\epsilon$ materials, and serves as a guide to engineers in solving practical problems with actual available materials.

Chapter 1 deals with idealized dielectric and magnetic materials strongly susceptible to electric and/or magnetic fields such as high dielectric ceramics and ferrites and their effect on circuit elements. The fundamental relationships for practical calculations of electrical, magnetic, electromechanical and transmission line parameters are presented in a concise manner. The numerical examples, comparative tables and nomograms are very illustrative.

Chapter 2 is a brief non-mathematical discussion of ferrimagnetism (ferrites) and ferroelectricity (titanates) with typical materials mentioned only.

Chapters 3–5 are concerned with various classes of applications such as lumped reactive circuit elements (Chapter 3), distributed parameter effects (Chapter 4), and finally, a few selected applications are presented connected with nonlinearity, nonreciprocity and losses of these materials (Chapter 5).

It is neither a physics nor a solid-state book. The material and discussion of dielectrics and magnetics are restricted to the basic phenomena and their applications as a reactive circuit element, rather than to fields of applications. Therefore, it does not present details about a number of fields such as amplifiers, computer and memory applications. The bibliography could have been more complete in connection with some topics.

In general, this book is intended to aid engineering thinking in the realm of dielectric and magnetic materials. The presentation of the various conceptional areas along with actual material data and typical numerical examples makes this book very useful for the practicing electronics engineer and the student intending to enter this field.

Charles F. Pulvari
Catholic University of America
Washington, D. C.

### Radio Waves in the Ionosphere, by K. G. Budden

Published (1961) by Cambridge University Press, American Branch, 32 E. 57 St., New York 22, N. Y. 509 pages+13 index pages+xxiv pages+13 bibliography pages+2 appendix pages+5 pages index of symbols. Illus. 6¾×9¼. $18.50.

With the publication of this extensive text on "the mathematical theory of the reflection of radio waves from stratified ionised layers" (the author's subtitle), it can be said, really for the first time, that an adequate collection of books treating the ionosphere now exists.[1] As any author must do in writing a book of this kind, Dr. Budden has drawn heavily on the work of many authors published in the periodical literature. But he has himself contributed much to that literature and is eminently qualified to collect it, interpret it, and fill in the gaps.

After two chapters of introductory material, the book is organized according to the following topical outline:

- Propagation in a homogeneous isotropic medium
- Propagation in a homogeneous anisotropic medium; magneto-ionic theory
- Properties of the Appleton-Hartree formula
- Definition of the reflection and transmission coefficients
- Reflection at a sharp boundary
- Slowly varying medium; the WKB solutions
- Ray theory for vertical incidence when the Earth's magnetic field is neglected
- Ray theory for oblique incidence when the Earth's magnetic field is neglected
- Ray theory for vertical incidence when the Earth's magnetic field is included
- Ray theory for oblique incidence when the Earth's magnetic field is included
- The general problem of ray tracing
- The Airy integral function and the Stokes phenomenon
- Linear gradient of electron density
- Various electron density profiles when the Earth's magnetic field is neglected
- Anisotropic media, coupled wave equations, and the WKB solutions
- Applications of coupled wave-equations
- The phase integral method
- Full wave solutions when the Earth's magnetic field is included
- Numerical methods for finding reflection coefficients
- Reciprocity

In the author's words, it is inevitable that some topics are omitted, though that hardly seems possible after viewing the scope of the coverage. But he points out that he does not treat horizontal gradients, irregularities, reflection from cylindrical structures such as meteor trails and field-aligned ionization, wave interaction, and earth-ionosphere waveguide mode theory. Dr. Budden states that the last named topic is a large one and would fill a book itself. J. R. Wait has recently made a pretty good start in that direction by publishing fifty pages on this subject.[2]

In this reviewer's opinion, the author should have made the effort to restrict himself to conventional and easy to write and say symbols. The Fraktur which he has used is particularly unsatisfactory from this point of view.

Dr. Budden has organized and edited his book very well indeed, and it is indexed and referenced in a very complete yet uncomplicated manner. Given a copy of the book to leaf through, any experienced student of the ionosphere will quickly see that this is a book he can ill afford to be without; but if the publisher's out-of-print record with J. A. Ratcliffe's monograph on the magneto-ionic theory is any example, he is likely to find himself without it.

M. G. Morgan
Dartmouth College
Hanover, N. H.

[1] Notably this book and the following:
S. K. Mitra, "The Upper Atmosphere, Second Edition," The Asiatic Society, Calcutta, 713 pp.; 1952.
J. A. Ratcliffe, Ed., "Physics of the Upper Atmosphere," Academic Press, Inc., New York, N. Y., 586 pp.; 1960.
J. A. Ratcliffe, "The Magneto-Ionic Theory and Its Applications to the Ionosphere," Cambridge University Press, American Branch, New York, N. Y., 206 pp.; 1959.
K. Rawer, "The Ionosphere," Noordhoff (German Edition); 1953. Ungar (English Edition); 1956.
H. Bremmer, "Terrestrial Radio Waves," Elsevier Publishing Co., Amsterdam, Netherlands, 343 pp.; 1949.

[2] J. R. Wait, "Terrestrial propagation of very-low-frequency radio waves," *J. Research NBS*, Pt. D, pp. 153–204; March–April, 1960.

### Scientific Russian, by James W. Perry

Published (1961) by Interscience Publishers, Inc., 250 Fifth Ave., New York 1, N. Y. 476 pages+9 index pages+xxvi pages+62 vocabulary pages. Illus. 6¾×9¼. $9.50.

Teachers and students of scientific Russian will welcome the second edition of Professor Perry's "Scientific Russian." There are many texts available for the teaching of scientific Russian, but none is more thorough and comprehensive than Professor Perry's work. Even for the intense short course where a briefer text may be almost mandatory, the availability of a comprehensive grammar of scientific Russian is a great help to both student and teacher.

Professor Perry has made many improvements in this new edition Emphasis on cognates will be found particularly helpful. Updating of the reading exercises will increase student interest and the clearer type face will make easier the task of learning to recognize unfamiliar characters.

S. D Browne
Mass. Inst. Tech.
Cambridge

World Radio History

**Electrical Noise, by W. R. Bennett**

Published (1960) by McGraw-Hill Book Co., Inc., 330 W. 42 St., New York 36, N. Y. 270 pages+9 index pages+viii pages+bibliography by chapter. Illus. 6¼×9¼. $10.00.

This is an excellent book that should find wide use as a textbook for undergraduate courses dealing with the physics and mathematics of electrical noise and the role of noise in communication systems. It is recommended reading for the expert as a simple and masterful summary of the field. Throughout the book the emphasis is on the physical sources of noise and on the experimental determination of the quantities discussed. Thus, for example, the concept of spectral density is expressed as a reading of a specified meter in a specified circuit. Fundamentals for analyzing basic sources of noise are covered, and methods of design are stressed.

The book starts with a discussion of the general properties of noise. Useful definitions, such as ideal band-pass transmittance, white noise, and noise bandwidth, are introduced.

A discussion of distributions of noise-wave amplitudes is then presented. The way in which this subject is introduced is in keeping with the book's emphasis: a brief description is given of the measurement of distributions by means of a level distribution recorder. Among the distributions discussed and physical examples given are the Gaussian, Rayleigh, and Poisson distributions.

The noise in vacuum tubes is treated at considerable length, yet unnecessary and tedious mathematical detail are avoided. The treatment of transistor noise is to be particularly commended for its clarity and conciseness. A lucid presentation is given of noise in electromagnetic radiation with application to maser noise. One chapter is devoted to noise-generating equipment, another to noise measurements. In the design of low-noise equipment the previously developed theory is applied to the analysis of various important amplifiers, such as the cascode amplifier and the transistor amplifier.

A treatment of the concept of noise measure is given, showing how it applies to low-gain amplifiers and negative-resistance amplifiers. The last two chapters deal with somewhat more sophisticated mathematical methods of noise analysis, and their application to noise in communication systems. Noise in amplitude, phase, frequency, and pulse modulation systems is treated succinctly and clearly. Each chapter contains an extensive bibliography.

This is a book with a judicious choice of content and mathematical tools for dealing with it. The excellent method of presentation is best characterized by the author's own words: "The intent is not to tantalize the reader by referring too often to methods beyond our scope and at the same time not to exhaust him by exploring irrelevant difficulties."

HERMANN A. HAUS
Mass. Inst. Tech.
Cambridge

## RECENT BOOKS

Berman, Arthur I., *The Physical Principles of Astronautics*. John Wiley and Sons, Inc., 440 Park Ave., New York 16, N. Y. $9.25. Designed to furnish an exposition of the basic principles of astronautics at a level suitable for a wide technical audience, and for use as an adjunct text in astronomy and mechanics at an intermediate level.

Dummer, G. W. A. and Robertson, J. M., Eds., *British Miniature Electronic Components and Assemblies Data Annual 1961–62*. Pergamon Press, 122 E. 55 St., New York 22, N. Y. $15.00. The first volume in an annual series containing concise data on miniature components, and information on the effect of potting resins, shock and vibration, and temperature overload.

Legros, Roger and Martin, A. V. J., *Transform Calculus for Electrical Engineers*. Prentice-Hall, Inc., Englewood Cliffs, N. J. $12.00. The first half of the book considers the basic properties of Fourier series, Fourier integrals and Laplace transforms; the second half considers the application of transform methods to linear circuits.

Liller, William, Ed., *Space Astrophysics*. McGraw-Hill Book Co., Inc., 330 W. 42 St., New York 36, N. Y. $10.00. Concerned with astronomical and astrophysical problems investigated from above the atmosphere; a compilation of lectures delivered at the University of Michigan in 1959–1960.

Marshak, R. E. and Sudarshan, E. C. G., *Introduction to Elementary Particle Physics*. Interscience Publishers, Inc., 250 Fifth Ave., New York 1, N. Y. $4.50. Eleventh in a series of "Interscience Tracts on Physics and Astronomy," R. E. Marshak, Ed.

# Scanning the Transactions

**Have you heard?** In an industry which annually produces several billion dollars worth of communication equipment, it is perhaps appropriate to take note here of the remarkable device which, in a sense, is the cause of it all. We refer to the human ear, and to the phenomenon of hearing which enters into so many facets of the communications field. Human hearing is indeed phenomenal. Nerves can scarcely carry 1000 pulses per second, and yet we can hear to 18,000 cycles per second and beyond. With the assistance of a physiological automatic-volume-control mechanism, we can perceive an almost painful sound containing $10^{12}$ times as much energy as the weakest discernible sound. The trained ear can make remarkably good guesses about the pitch of a tone, and a favored few persons have authentic absolute pitch. An especially attentive ear can act as a wave analyzer in identifying the primary constituents of a complex tone or noise. The ear has a poor memory for loudness. On the other hand, it has a remarkable ability for picking out one desired conversation from amongst a babble. If the ear has an impressive range of capabilities, so must the audio and communications engineers who deal with it. For it has been pointed out that the worker in this field is involved with electric circuit theory, vibration theory, electronics, music, psychology, medicine—and to top it off, architecture. (R. A. Long and V. Salmon, "Current research in communications acoustics," IRE TRANS. ON AUDIO, March–April, 1961.)

**The future of radar—the phased array?** If radar system capabilities have increased tremendously during the last 20 years, so have the severity of radar system requirements. In World War II it was generally sufficient to determine the range, height and azimuth of the target. Today, in addition to dealing with range and resolution requirements of a totally different order of magnitude, it is necessary to determine many other factors, such as path, velocity, acceleration, and what kind of target it is. The time has long since passed when we could rely solely on increasing the power of a radar to give the performance improvement needed. During the past decade attention has turned more and more to other techniques for getting more energy on the target, by either

World Radio History

playing with the type of pulse which is transmitted, playing with the method of beam formation, or tinkering with the received signal. In looking to the future of radar and which of the numerous techniques appears most promising, it appears that the electronically steered phased array offers the brightest promise. The basic principle involves feeding power to a large number of individual radiators with complete control of the phase for each element. This leads to a highly flexible system which can generate an extremely high-power beam by viture of the fact that it draws upon a large number of smaller power sources. Indeed, the phased array appears to be the only technique available today for coping with the demands of the space age. (J. S. Burgess, "The future of radar," IRE TRANS. ON MILITARY ELECTRONICS, April, 1961.)

**Viewing antennas as information processors** is leading to an interesting change in antenna design philosophy which may have fundamental implications for the future. Over the past few years the emphasis has been shifting from synthesizing patterns. Instead, the antenna is coming to be regarded as an information processing device, requiring the application of modern information theory concepts to their design and to the optimization of their performance. In this context, the primary design objective is to maximize the information or data rate. This places the various parameters of the antenna system in a new light and suggests the adoption of unconventional techniques for obtaining unusual performance. Among the techniques under investigation are novel nonlinear methods of processing the outputs of the individual elements of an array. In radar applications various kinds of time, frequency or space coding suggest themselves as a means of improving data rate. One can envision, for example, a self-adaptive antenna system which by means of its computer will automatically adjust the intensity of a scanning beam in such a way as to give greater illumination to a target and less to its surroundings. Whatever the direction these investigations take us, we are certain to hear a good deal more about signal processing antennas in the future. (G. O. Young and A. Ksienski, "Signal and data-processing antennas," IRE TRANS. ON MILITARY ELECTRONICS, April, 1961.)

# Abstracts of IRE Transactions

**The following issues of TRANSACTIONS have recently been published, and are now available from The Institute of Radio Engineers, Inc., 1 East 79 Street, New York 21, N. Y., at the following prices. The contents of each issue and, where available, abstracts of technical papers are given below.**

| Sponsoring Group | Publication | IRE Members | Libraries and Colleges | Non-Members |
|---|---|---|---|---|
| Audio | AU-9, No. 2 | $2.25 | $3.25 | $4.50 |
| Automatic Control | AC-6, No. 2 | 2.25 | 3.25 | 4.50 |
| Circuit Theory | CT-8, No. 2 | 2.25 | 3.25 | 4.50 |
| Communications Systems | CS-9, No. 2 | 2.25 | 3.25 | 4.50 |
| Education | E-4, No. 2 | 2.25 | 3.25 | 4.50 |
| Electron Devices | ED-8, No. 3 | 2.25 | 3.25 | 4.50 |
| Industrial Electronics | IE-8, No. 1 | 2.25 | 3.25 | 4.50 |
| Military Electronics | MIL-5, No. 2 | 2.25 | 3.25 | 4.50 |
| Product Engineering and Production | PEP-5 No. 2 | 2.25 | 3.25 | 4.50 |

## Audio

### VOL. AU-9, NO. 2, MARCH–APRIL, 1961

**The Editor's Corner**—Marvin Camras (p. 33)

**PGA News**—William Ihde (p. 35)

**Current Research in Communications Acoustics**—R. A. Long and V. Salmon (p. 37)

Despite the appeal of the visual arts, all persons turn naturally to sound for the rapid, thorough, and precise transmission of both practical and esthetic information. Communications acoustics deals with this flow of acoustic information, and with controlling noise that might interfere with it.

**Acoustical Measurements on a Home Stereo Installation**—John K. Hilliard (p. 41)

This paper describes a two-way 500-cycle crossover loudspeaker system using the infinite baffle principle. A 300-cubic-foot volume is used. Two identical systems are spaced 15 feet apart for stereo reproduction.

A description of the living-room architectural acoustics is included. There are no parallel walls or surfaces, and the splay of the side walls is a minimum of one inch per foot. Reverberation decay charts are provided for different frequencies to indicate the effect of the splayed walls. Sine wave and warble tone curves are shown and sine wave single-frequency levels are plotted for the width and length of the room.

**Intermodulation Distortion Meter Employing the Hall Effect**—A. C. Todd, J. N. Van Scoyoc, and R. P. Schuck (p. 44)

This paper presents a method of measuring intermodulation distortion produced by a nonlinear system operating in the audio-frequency spectrum. The design of the measuring device is based upon the Hall principle. Transistorized circuitry is used throughout. Both the circuitry employed and the theory of operation are discussed. The instrument is simple to operate and permits the measurement of intermodulation distortion at any frequency on a point-by-point basis within the range of 400 to 20,000 cps. Distortion measurements may be made in two ranges; zero to one per cent and zero to five per cent.

**Third-Order Distortion and Cross Modulation in a Grounded Emitter Transistor Amplifier**—Helmut Lotsch (p. 49)

The nonlinear modulation characteristic of a transistor is approached by the first terms of a Taylor-series formula and the output voltage is calculated for a suitably-chosen ac-input voltage. For higher frequencies and different working points, the influence of the diffusion capacity and the emitter admittance are illustrated by experimental results. It is shown that —as in electronic tubes—the third-order distortions (harmonic distortion, distortion of modulation, alteration of the degree of amplitude modulation, degree of cross modulation) are closely connected, but unlike the situation in electronic tubes, the distortions disappear at a special working point. The influence of the base resistance and the internal resistance of the sig-

World Radio History

nal source are discussed in relation to the appearance of this zero point and the frequency dependence.

In an RF amplifier a transistor is modulated, for example, only by a part of the resonant circuit voltage because of the low input resistance in a grounded emitter circuit. Although this voltage transformation is accounted for, the transistor is inferior to the electronic tube with respect to cross modulation. To reduce the cross modulation in a transistor RF stage, two possibilities are described for correcting the distortions with a fixed or controlled working point using a predistortion or a push-pull modulation. In this case the different influences of a resistance in the base lead, or of a resistance blocked for HF but not for LF in the emitter lead, are discussed.

**Contributors** (p. 59)

## Automatic Control

### VOL. AC-6, NO. 2, MAY, 1961

**Foreword** (p. 95)

**The Issue in Brief** (p. 96)

**On a Property of Optimal Controllers with Boundedness Constraints**—H. L. Groginsky (p. 98)

This paper deals with a theory for optimal control systems designed to operate a plant of known characteristics. It is assumed that only limited changes in the system characteristics can be effected by the control variables at the designer's disposal.

It is shown that within the assumed limitations for a wide class of inputs and systems and for a certain class of measures of the system performance, an optimal system behaves as a relay or switched system during the transient period and as a continuous system during periods in which the input is reproduced identically. A procedure is described for determining the switching times during the transient period in terms of the permissible measurements.

**A Minimal Time Discrete System**—C. A. Desoer and J. Wing (p. 111)

A sampled-data control system with a plant having real poles and limited input is considered. The plant forcing function which will bring the system to equilibrium in a minimum number of sampling periods is desired; this function is called an optimal strategy.

To implement this particular optimal strategy, we define a surface in state space called the critical surface. It is shown that this optimal strategy will be generated by the following procedure: at the beginning of each sampling period, the distance $\phi$ from the state of the system to the critical surface is measured along a fixed specified direction; if $\phi \geq 1$ (or $\leq -1$), then the forcing function for that sampling period is $+1$ (or $-1$); if $|\phi| < 1$, then the forcing function is $\phi$. For a third-order plant, it is shown that the critical surface has certain properties which lead to a simple analog computer simulation.

**Theory and Design of High-Order Bang-Bang Control Systems**—M. Athanassiades and O. J. M. Smith (p. 125)

A complete analysis and design is presented of a nonlinear controller to minimize the response time of a limited input plant whose transfer function has $N$ real roots.

The design procedure is based exclusively on the concept of the switching hypersurface of the system in $N$-dimensional state space and on the concept of the "distance function" from the state point to the switching hypersurface.

The linear and nonlinear transformations performed by a nonlinear computer upon the error and its time derivatives, in order to generate the optimal amplitude limited input to the plant, are described in detail, and properties of the switching surfaces, which are subsets of the switching hypersurface, are also described.

**Model Feedback Applied to Flexible Booster Control**—G. E. Tutt and W. K. Waymeyer (p. 135)

The fundamental control problems in the design of flexible space vehicle boosters center around the control of an aerodynamically unstable airframe in a dynamic wind shear (jet stream) environment. This paper presents a feedback model approach to this design problem which shows promise. This system does not adapt to body bending, but instead is contrived to ignore it.

A conventional attitude control system is assumed in which rigid body control considerations have been used to design the control loops. A model of the plant (airframe rigid body dynamics) is derived. The attitude and rate feedbacks are now synthesized by a combination of actual and model rate and attitude. Bending and similar dynamic effects are filtered from the actual attitude and rate signals as required, and the information thus rejected is supplied from the model of the plant. It is readily shown that the performance of this system in response to commands is substantially identical in all important respects to the original rigid body system.

**Terminal Control System Applications**—R. K. Smyth and E. A. O'Hern (p. 142)

This paper deals with certain theoretical extensions of earlier work on terminal control techniques and their application to an aircraft landing system. The case considered is of a system having a second-order response from altitude rate command to altitude rate. The terminal time equations for this case are developed together with the various closed-loop weighting functions by transform methods. From the terminal equations developed, the terminal controller equations are synthesized for a two-condition terminal controller which controls altitude and altitude rate at the terminal (touchdown) time. The mechanization of these terminal controller equations are presented.

The flight test results of the terminal control system using the system developed in this paper are described briefly. A comparison between flight test and simulation results is included.

**A Parameter Perturbation Adaptive Control System**—M. J. McGrath, V. Rajaraman, and V. Rideout (p. 154)

Theoretical and simulator studies of some new forms of a parameter perturbation self-adaptive system are presented in this paper. Here, the response of the control system is subtracted from that of a reference model to obtain the error signal. As in the previous studies, the controllable parameters of the system are sinusoidally perturbed. Somewhat different methods of processing the perturbation and error signals have been employed to obtain the parameter control signal which is used in the automatic optimization of the control system.

Computer studies are made with both random and deterministic input signals and parameter disturbances. The results are compared with the analytical results.

**Adaptive Servo Tracking**—A. I. Talkin (p. 167)

This paper describes a self-adapted sampled-data radar tracking loop. The tracking loop may be considered to be a low-pass filter with a variable bandwidth. The loop is designed to adapt rapidly to changes in the input signal by monitoring both the apparent error and the loop output.

Results show a mean tracking error 25–34 per cent less than that of a comparable linear system, at a receiver SNR of 10 db.

**Transfer-Function Tracking and Adaptive Control Systems**—C. N. Weygandt and N. N. Puri (p. 162)

In an adaptive system in which the plant parameters are varying, it is necessary to track or measure the plant parameters. Two separate schemes are proposed for tracking the transfer function of a multi-order system.

The first scheme is based on perturbing the normal process with small amplitude sinusoidal perturbation signal consisting of different frequencies. The tracking system is a closed-loop system.

The second scheme does not depend upon perturbation signal, but does require knowledge of the form of the transfer function of the system. It is more suitable for tracking systems which have a number of first-order lag units connected in tandem.

**Precision of Impulse Response Identification Based on Short Normal Operating Records**—R. B. Kerr and W. H. Surber, Jr. (p. 173)

An identification scheme is presented for estimating in a short time the impulse response of a system from normal operating records.

Maximum-likelihood estimates of the impulse response are discussed, and a "sufficiency" criterion on the input signal is defined based upon the expected integrated squared difference between the actual and estimated impulse responses. Examples of sufficient and insufficient test signals are given in terms of a "sufficient record length" criterion. Experimental results illustrating this latter criterion are presented.

The time variation of the system parameters sets an upper bound on the useful record length. Some preliminary results relating this time variation to the useful record length are also presented.

**Some Techniques of Linear System Identification Using Correlating Filters**—W. W. Lichtenberger (p. 183)

Random signals and cross-correlation can be used to determine the impulse response of a system. If, instead of a random testing signal, one is employed which has certain properties similar to the random signal, a linear filter may be constructed which performs the necessary cross correlation. No multiplication is involved, and the output is a continuous function of time. Thus, a single filter obtains the impulse response for all values of time. A disadvantage of this method is that in a practical situation, there is usually a great amount of noise present. This "noise" consists mostly of process actuating signals since the measurements must be made "on line."

**A Modified Lyapunov Method for Nonlinear Stability Analysis**—D. R. Ingwerson (p. 199)

The Lyapunov stability criterion deals with arbitrarily small disturbances. A generalization of the original theorem which applies to arbitrarily large and arbitrarily small disturbances, and to intermediate conditions as well, is given in this paper.

In contrast to the success that has been achieved in advancing the theoretical concepts of stability by this method, little has been accomplished in the way of formulating practical means for applying them to specific problems. A method which is easily applied to many of the systems encountered in automatic control and which has given good results for numerous examples is presented here.

**A Mean-Weighted Square-Error Criterion for Optimum Filtering of Nonstationary Random Processes**—K. Sahara and G. J. Murphy (p. 211)

A procedure for use in the design of a physically realizable time-invariant linear system for optimum filtering of a nonstationary random process in the presence of nonstationary random noise is presented. The criterion used to measure system performance is a mean-weighted square error.

It is shown that the use of this generalization of the mean square-error criterion leads to a

World Radio History

generalization of the Wiener-Hopf integral equation. A technique for solving this modified Wiener-Hopf integral equation is presented, and the application of the theory is illustrated in an example of the optimum synthesis of a missile interception system.

**A General Performance Index for Analytical Design of Control Systems**—Z. V. Rekasius (p. 217)

A performance index which enables one to specify the desired response of the optimum system in terms of the differential equation describing the response of an ideal model is proposed.

A simple straightforward procedure of calculating this performance index is outlined in the paper. This procedure consists of solution of a set of linear algebraic equations. Simultaneous solution of these algebraic equations yields the value of performance index in terms of gain and time constants of the actual system. It is then a simple matter to calculate the numerical values of the free gain and time constant parameters for the optimum system (*i.e.*, to minimize the performance index). The procedure of optimization is illustrated by means of an example of a third-order system.

**Stability of Servomechanisms with Friction and Stiction in the Output Element**—P. K. Bohacek and F. B. Tuteur (p. 222)

Servomechanisms with friction in the output element are often observed to oscillate, even though the Bode diagram indicates stability. This paper investigates the conditions for this instability and the type of oscillation that can occur. It finds that an overdamped system with a lag equalizer is stable if $L<2C/C-1$, where $L$ is the lag ratio and $C=$ static friction + Coulomb friction; with a lag-lead equalizer it is stable if

$$\frac{L}{1+a/b} < \frac{2C}{C-1},$$

where $a/b$ is the ratio of the two zeros of the network. Experimental results that correlate with the theory are also included.

**Sensitivity Considerations for Time-Varying Sampled-Data Feedback Systems**—J. B. Cruz, Jr. (p. 228)

A synthesis procedure for linear time-varying sampled-data feedback systems is described. The plant and compensators are characterized by transmission matrices first introduced by Friedland. Part of the specification involves a deviation or error matrix for the time-varying plant and an allowable deviation matrix for the closed-loop system. Noise considerations are also included. Using a technique analogous to that of Horowitz which was originally used for fixed multivariable continuous control systems, the digital compensator transmission matrices are derived. The corresponding time-varying digital compensators are realized by means of zero-order hold circuits, switches, resistors, and adders. An example using a digital computer simulation is included.

**Direct Cycle Nuclear Power Plant Stability Analysis**—D. Buden and R. F. Miller (p. 237)

A power plant with a heat exchanger such as a nuclear reactor substituted for the conventional chemical interburners in a jet engine will cause a considerable change in dynamic performance. The instantaneous power generated by the heat source is not the same as the instantaneous power delivered to the turbine. The basic control problems are analyzed using fixed control parameters and partial derivatives around a given operating point. A mathematical criterion is developed and correlated with power plant test data.

An understanding of the inherent limitations of combining a reactor, or any heat exchanger having a thermal lag, with a basic jet engine makes it possible to devise a means of control. The introduction of an effective operational speed control makes it possible to operate a complete power plant under any desired condition.

## Circuit Theory

### Vol. CT-8, No. 2, June, 1961

**Optimum Design of Single-Stage Gyrator-RC Filters with Prescribed Sensitivity**—I. M. Horowitz (p. 88)

The design of low-frequency filters by means of RC feedback around active elements has long been known. The advent of the transistor has renewed interest in this field and has necessitated a more exact synthesis procedure. This is because in the classical design the active element is assumed to be an ideal voltage amplifier with infinite input impedance, zero output impedance and zero reverse transmission. The transistor satisfies the dual ideal assumptions to a considerably lesser degree than the vacuum tube. The sensitivity of the transistor parameters to temperature also requires more attention to be paid to the effect of parameter variations on the filter response.

The paper extends the classical theory in several directions:

1) A synthesis procedure is developed in which the finite input and output impedances and reverse transmission of the active element are taken into account in an exact manner.

2) The freedom that exists is used to optimize the synthesis so as to permit design with a "least active" element.

3) Expressions are developed for the sensitivity of the filter to the four low-frequency active parameters and to the passive parameters. It is presumed that the design specifications include a statement of the extent of active and passive parameter variation and the tolerances on the filter response. The procedure for satisfying such specifications is an integral part of the design procedure.

4) Under the constraint of fixed source and load impedances and desired parameter insensitivity, the design achieves maximum gain.

An example which includes all the above features is worked out in detail.

The principal limitations of the design procedure are:

1) It is restricted to a transfer function of second degree so that if sharper cutoffs are needed, several basic sections must be used, separated by isolating stages.

2) It is best suited to achieve low-pass or moderate band-pass characteristics.

**Power Conversion with Nonlinear Reactances**—E. Della Torre and M. D. Sirkis (p. 95)

Mixing of several frequencies in any nonlinear reactance having a characteristic that can be represented by a power series is considered. The purpose of this paper is to cite the importance of the nature of the nonlinearity in mixing processes occurring in nonlinear reactances. Power relationships are derived, and limitations imposed by a finite degree of nonlinearity are considered. Restrictions on the source frequencies are found, and it is shown that in practice incommensurability is not required. The special cases of harmonic generation and subharmonic generation are considered.

For the case in which the circuit considered in this paper is identical to that analyzed by Manley and Rowe, the results obtained here agree with theirs.

**Solving Steady-State Nonlinear Networks of "Monotone" Elements**—G. J. Minty (p. 99)

This paper treats the problem of finding the steady-state currents and voltage drops in an electrical network of two-terminal elements, each of which has the property that its current-voltage-drop graph, or "characteristic," is a curve going upward and to the right. (Thus, "tunnel diodes" are excluded, but nonlinear resistances, current and voltage sources, rectifiers, etc. are permitted.)

The construction methods are specifically designed for digital computation techniques (either automatic or manual). The principal tools are: 1) the application of theorems from graph theory ("network-topology"), and 2) quantization of the variables (permitting them to take on only a discrete set of values).

**Some Necessary Conditions for a Non-Negative Unit Impulse Response and for a Positive Real Immittance Function**—Paul M. Chirlian (p. 105)

The fact that the unit impulse response of a network is non-negative imposes certain conditions on the real part of the transfer or immittance function. Such conditions are derived in this paper. In addition, when the real part of the immittance function is non-negative, necessary conditions are imposed upon the impulse response. Such conditions are also presented here. These conditions are in a graphical form, which can be utilized without the necessity of lengthy calculations.

**The Zeros of Transient Responses**—A. H. Zemanian (p. 109)

This paper considers the zeros of the transient responses corresponding to rational Laplace transforms whose poles are all real and whose zeros are allowed to be either real or complex. The possible values for the number of zeros of the transient responses are determined under various assumptions on the Laplace transforms. For instance, when the poles of the transform are allowed to have any multiplicity, the possible values for the number of zeros of the transient response are found in terms of the number of zeros of the transform. On the other hand, when the poles are all simple and the pole and zero locations of the transform are known, a stronger result is obtained.

These results are developed for the function obtained by extending to all time the expression for the transient response that holds for positive time. The possible values for the number of its zeros are determined for positive time and for negative time separately.

**Zero Cancellation Synthesis Using Impedance Operators**—Don Hazony (p. 114)

Through an extension of Richards' theorem, an RLC driving-point impedance function, $Z$, is synthesized by a prescribed, realizable, four-terminal network terminated with another driving-point impedance function, $\zeta$, four less in rank than $Z$. $Z$ is completely arbitrary except that it may not have a pole or a zero at the origin or infinity.

The initial four-terminal network consists of a capacitor, a perfectly-coupled transformer, and an ideal gyrator. Other equivalent networks are derived which do not require transformers and gyrators but in which the cascade nature of the synthesis is lost.

**The Effects of Time Weighting the Input to a Spectrum Analyzer**—Will Gersch (p. 121)

The effects of time weighting the input to a spectrum analyzer are considered. The spectrum analyzer is assumed equivalent to a bank of similar filters whose overlapping pass bands cover a region of spectral interest and whose outputs are measured at a single instant in time. The term transient selectivity is defined as the magnitude of the envelope of the response of a filter with center frequency $\omega+\Delta\omega$, at the time instant $T$, to an input $e^{j\omega t}$ over the interval $0\leq t\leq T$. The transient selectivity characteristics of an arbitrary bank of filters can be achieved using a bank of single-tuned filters and time varying the magnitude of the envelope of the input to the filter bank system. This property is called the time-weighting principle.

Spectrum analyzer systems are employed to detect the presence and specify the fre-

World Radio History

quency of fixed-duration constant-frequency signals immersed in noise. For a system whose objectives include distinguishing the presence of several simultaneous signals, two measures of system performance are the sharpness of the system's transient selectivity and the system's signal-to-noise ratio (SNR). Time weighting functions are presented which can realize arbitrarily sharp transient selectivity characteristics. An equation for the SNR for arbitrary filters and arbitrary time weighting functions is also presented. The transient selectivity and SNR performance for a bank of filters time weighted with a $\sin^N \pi t/T$ weighting function is illustrated.

**Stability Margins and Steady-State Oscillations of ON-OFF Feedback Systems**—Erik V. Bohn (p. 127)

Exact methods of determining the steady-state oscillations in feedback systems incorporating one nonlinear element of the ON-OFF type have been developed by Hamel and Tsypkin. It is shown that these methods are not generally applicable. A general method is developed which overcomes these limitations, and suitable stability margins are derived.

**Impedance Transformation Using Lossless Networks**—James D. Schoeffler (p. 131)

Two impedances are said to be compatible if one of them can be realized as the input impedance to a two-terminal-pair lossless network terminated in the other impedance. A uniqueness property of the Darlington realization procedure and the methods of cascade synthesis are used to determine a simple, concise set of necessary and sufficient conditions under which two given realizable impedances can be compatible. Applications are discussed.

**Broad-Band Matching Between Load and Source Systems**—Daniel C. Fielder (p. 138)

This paper discusses impedance matching between an arbitrary load and a particular type of source network, by means of a lossless two-terminal-pair matching network. The source network consists of an LC ladder in series with a generator resistance. This study is devoted principally to theoretical considerations of low-pass systems utilizing lossless matching networks between source networks and arbitrary load impedances. The present effort is one possible extension of previous work of Fano. Fano's system, however, did not include a two-terminal-pair source network. The value of the present work is derived from an investigation of constraints imposed by the source system and the load, rather than just the load itself.

**A Unified Approach to Two-Terminal Network Synthesis**—P. M. Kelly (p. 153)

The problem of two-terminal immittance function realization is considered in terms of the reflection coefficient. A conceptually basic method of synthesis is developed which has important implications in exact and approximate synthesis techniques. Consideration of the practical shortcomings of this method lead directly to the standard methods of exact synthesis which are demonstrated to be all applications of the Schwarz lemma. Among the methods considered are those of: Foster, Cauer, Miyata, Brune, Bott-Duffin, Fialkow-Gerst, and Darlington.

**Correspondence** (p. 165)
**Contributors** (p. 178)

## Communications Systems

### Vol. CS-9, No. 2, June, 1961

**The Examination of Error Distributions for the Evaluation of Error-Detection and Error-Correction Procedures**—T. A. Maguire and E. P. G. Wright (p. 101)

The factors influencing the speed at which data can be transmitted, and those determining the error rate, are summarized as an introduction to a statement in respect to error rates measured. Different applications for data transmission are considered in relation to the amount of error correction which may be justified.

Various forms of error detection and correction are illustrated, and the probability of undetected errors is considered from a theoretical point of view for a random distribution of errors. These results are then compared with records obtained by practical tests using various redundancy arrangements.

It is concluded that there is a substantial advantage in the use of large (500-bit) rather than small (50-bit) blocks for detecting errors. It is also suggested that the practical evidence of error patterns which remain undetected should enable more effective detection designs to be produced.

**RF Spectra and Interfering Carrier Distortion in FM Trunk Radio Systems With Low Modulation Ratios**—R. G. Medhurst (p. 107)

This paper provides formulas for evaluating RF spectral shape and interfering carrier distortion in connection with FM trunk radio systems having low modulation ratios. Numerical results are given for 1800-speech-channel systems. The curves showing interfering carrier distortion are of particular interest in connection with systems using RF multiplex (*i.e.*, systems consisting of a number of carriers each modulated with a signal built up from a large number of speech channels). Preferred carrier spacings, originally determined for 600-channel systems, have been recommended by the CCIR 9th Plenary Assembly, 1959, for use with up to 1800 channel systems. It appears from the analysis that with these larger numbers of channels, a considerable amount of attenuation by filtering or by isolators will be required to give adequate protection against intermodulation distortion.

**Consideration of Nonlinear Noise and its Testing in Frequency Division Multiplex Voice UHF Radio Communication Systems**—Leang P. Yeh (p. 115)

In UHF radio communications systems, the thermal noise limits the performance under weak received signal conditions. When the signal is strong, the nonlinear noise (sometimes called the intermodulation noise) may become the limiting factor, It is, therefore, imperative to control the intermodulation distortion contribution from the system components by careful equipment design and from the medium by appropriate choice of system parameters.

In single-sideband systems, nonlinear noise may be attributed to two main causes: 1) transmitter nonlinearity and 2) receiver nonlinearity. Multipath effects in the medium do not seem to produce any nonlinear distortion, except selective amplitude fading or frequency distortion. Amplitude nonlinearity is the sole contributing factor in nonlinear noise.

There is no set rule on the subdivision of nonlinear noise among both the transmitter and the receiver. Equal distribution seems to be a reasonable assumption. In some cases, an entirely different distribution may be desired, according to actual requirements.

How to distribute the transmitter or receiver nonlinear noise among its components depends on the characteristics of the components. The general principle is to have the most economical design on every piece of the components, if possible and practicable.

The nonlinear noise in single-sideband systems may be assumed to consist of only 3rd- and 5th-order products. It is further assumed that 3rd- and 5th-order products contribute to the total nonlinear noise in equal amounts in power.

In frequency modulation systems, nonlinear noise may be attributed to three main causes: 1) transmitter nonlinearity, 2) multipath effect in the medium, and 3) receiver nonlinearity. Both amplitude and phase nonlinearities are equally important in the contribution to the noise and each should be considered carefully.

The subdivision of nonlinear noise may be done in two ways. It may be distributed among the transmitter, the path and the receiver, or among the amplitude and phase nonlinearities. In either way, further subdivision is necessary in order to specify the amplitude or phase linearity requirements for the various components of the system.

There is, again, no set rule on the distribution of nonlinear noise among the various causes. The same principle as applied to single-sideband systems as mentioned before may be used for frequency-modulation systems.

The nonlinear noise in frequency-modulation systems may be assumed to consist of only 2nd- and 3rd-order products. It is further assumed that 2nd- and 3rd-order products contribute to the total nonlinear noise in equal amounts.

Methods for performance evaluation, based on signal-to-nonlinear-noise ratio, are given and sample calculations are made to illustrate the methods.

In the test of a complete system, either two-tone or noise loading tests may be used. Assuming that only 3rd-order nonlinear noise is predominant and that a peak factor of 10 db for random noise is chosen, the noise loading test signal-to-nonlinear ratio is 8 db higher than the two-tone test ratio if the rms power in the two tests are equal. However, if the peak power in the two tests is equal, both ratios are the same.

**Model of Impulsive Noise for Data Transmission**—Pierre Mertz (p. 130)

It has often been found more necessary in the engineering of data transmission systems to consider impulsive noise than conventional Gaussian white noise. A model is proposed for the impulsive noise, which describes empirically an amplitude distribution and a time distribution. Because the latter has been described in experimental work principally in terms of error occurrences, the description is translated into these. The notable characteristics of impulsive noise are that at low occurrence frequencies the amplitudes are much larger than for Gaussian noise, and that impulses or errors tend to be more "bunched" than expected from a Poisson distribution.

**Diversity Combining for Signals of Different Medians**—J. Granlund and W. Sichak (p. 138)

Over-the-horizon communication systems normally use two identical antennas at each end. It is shown that an asymmetrical arrangement, for example,

60′( )60′
30′( )30′

is better than a symmetrical arrangement when both antennas at one end are used for diversity reception and the larger antenna at the other end is used for transmitting. This arrangement is important because for a given performance it costs less than the symmetrical arrangement. Depending on the exact relationship between cost and antenna gain, the cost is a minimum when the difference in antenna gains lies between 3.2 and 4.8 db. Statistical performance for various combining methods and degrees of diversity are presented. As for the case of equal medians derived previously, selector diversity combining is decidedly inferior to equal gain combining, which in turn is about one db worse than maximal ratio combining.

The "instantaneous" SNR's (applicable to data transmission) are derived and compared to the usual short-term SNR's applicable to telephony.

**Diversity Reception for Meteoric Communications**—A. W. Ladd (p. 145)

One of the first goals of the research effort on meteoric communications was to establish the advantage, if any, of diversity reception.

World Radio History

Three types of diversity were investigated: frequency, space, and polarization.

Nearly perfect correlation of the signals was found for frequency diversity reception with a frequency separation of 4 kc and for space diversity reception for antenna spacings of up to 1200 feet.

Only polarization diversity appears to provide any advantage. Two identical eight-element Yagi receiving antennas were erected, one horizontally polarized and the other vertically polarized. The transmitting antenna was horizontally polarized. Analysis of the data shows that about 34 per cent of the signals on the vertical antenna equal or exceed in amplitude the signals on the horizontal antenna, but the shapes of the bursts on the two antennas are identical in most cases.

It is concluded that there is not enough increase in system performance to justify the use of any of the three types of diversity.

**Digital Computer Simulation for Prediction and Analysis of Electromagnetic Interference**—D. R. J. White and W. G. James (p. 148)

A digital computer simulation program is described for use by communications systems and equipment designers who must consider electromagnetic interference. The program determines the interference experienced by a test receiver in a signal environment resulting from its associated transmitter, a large deployment of potentially interfering transmitters, and by atmospheric and cosmic noise sources. Simulation models are designed to represent such transmitter characteristics as antenna gain and scan patterns, polarization and emitted power spectrum; other models represent propagation phenomena such as scattering, reflection, fading and tropospheric refraction; and such receiver characteristics as antenna gain patterns, frequency selectivity and demodulator transfer characteristics. Signal acceptability criteria are included to permit system scoring. Program flexibility is stressed so that optimum system design may be achieved through rapid evaluation of successive approximations.

**Preliminary Study of a Miniature Under-Water Cable System**—B. G. King, G. Raisbec L. O. Schott, and L. R. Wrathall (p. 159)

Certain aspects of feasibility of a miniature submarine cable-transmission system have been studied. The system is small and light, and designed for use in military applications as an expendable item where submarine cables of conventional design would be uneconomical.

It weighs about 125 pounds per mile, transmits 1.35 million pulses per second of a pulse-code modulated (PCM) signal, and is powered by 4.5 ma with a voltage drop of about 2 volts per mile.

Several armorless cables were tested. All have a steel core with a layer of copper for the center conductor, and extruded polyethylene dielectric. They differ in the way in which the center conductor is fabricated, in the materials of the outer conductor, and in the way in which it is held in place over the dielectric.

The transistor repeater uses one transistor and eight passive components. It has a 17-db gain and an output of 0.8 volt into a 75-ohm line.

The repeater housings are hollow cylinders of beryllium copper, $2\frac{1}{8}$ inches by $\frac{7}{16}$ inch. The insulation of the transmission line is joined to the ends of the housing by an adhesive and by a mechanical seal. The cable tension is transferred to the housings by hollow ceramic insulating cones. The housings were tested in 13,200 psi hydrostatic pressure and to 120 pounds axial tension.

A system of five repeaters in 18,000 feet of line was laid in Sandy Hook Bay and was operable for thirteen months.

**Development of Sydney, Nova Scotia-St. John's, Newfoundland Canadian National Telegraphs Microwave System**—C. J. Bridgland, A. Piechota, and B. P. MacKenzie (p. 165)

A 650-mile radio-relay system composed of 22 "line-of-sight" paths was constructed to supplement the Canadian National Communications between Sydney, Nova Scotia, and St. John's, Newfoundland. Relay repeater points were chosen by means of all available contoured maps and on-site surveys of the various points, bearing in mind radio transmission characteristics and also accessibility for maintenance. All the radio paths were field-tested to confirm their transmission capabilities. The over-water hop between Cape North and Red Rocks, which is 69 miles long, required careful consideration, and special arrangements were made to ensure that this hop would provide a satisfactory performance. Standard Telephones and Cables Ltd., were requested to provide this system using their latest equipment. This is 5-watt equipment working on 4000 Mc and able to carry the equivalent of 600 toll quality message circuits or one video program.

To handle the present Canadian National requirements, three channels were installed in an eastward direction and two in a westward direction. The system is divided into three sections with back-to-back terminals at Corner Brook and Gander for general communications and television branching circuits. Each section has a separate comprehensive supervisory control facility for providing dual information and controls at both section terminals.

**Analytical Prediction of Electromagnetic Environments**—W. H. Tetley (p. 175)

The problem of transmitting digital data through electromagnetic environments of high ambient-pulse density is one of growing concern. The appearance of pulsed radar in the 10-mw range, and sensitive receivers in the −100-dbm range, will aggravate this situation. This paper discusses three efforts made by the government to predict the status of future environments. In all cases, the basic technique of analytical prediction calls for the solution of mathematical models by digital computer. Results from these analyses are useful to the designer of future systems as well as to the operators who must use them. The responsibility of keeping the signal congestion within bounds rests with the designer and user alike.

**Correspondence** (p. 186)
**Contributors** (p. 190)

## Education

### Vol. E-4, No. 2, June, 1961

**Editorial**—W. R. LePage (p. 47)

**Today's Dilemma in Engineering Education**—Gordon S. Brown (p. 48)

The present wide-scale activity to increase the science content of engineering curricula can, if not skillfully accomplished, result in the teaching of science, and not the engineering of science, to engineers. The changes experienced in the substance of the curricula are sometimes so great that faculties encounter great difficulty in providing worthwhile engineering examples to support their presentations of engineering science.

**Programmed Learning in Engineering Education—A Preliminary Study**—E. M. Williams (p. 51)

A recent study of programmed learning, including experimental use in an electrical engineering department, indicated that the most fruitful application of teaching machine methods is in the presently nonprogrammed or loosely programmed hours spent by students outside classroom or laboratory periods. Programs already developed for use in this study have been concerned with analytical skills; further programs under development are concerned with concepts. Larger scale experiments are planned in which additional questions can be answered, particularly as to whether exposure to programmed instruction adversely affects the capacity of the student to learn independently.

**TV Production Techniques and Teaching Efficiency**—John B. Ellery (p. 59)

Educators who venture into the realm of television immediately encounter this question: What equipment is required, and what can be done with it? This paper attempts to provide some basis for an intelligent answer.

In designing the research from which this report derived, attention was focused upon basic television production techniques. A series of instructional segments were produced utilizing these techniques; a second series was subsequently produced with the same instructors and subject matter, but with more elaborate techniques. The two series were then presented for viewing by various student audiences. A control group viewed the first series; an experimental group was shown the second series. Preliminary knowledge of subject matter was determined by a pre-test; degree of learning and retention were measured by an immediate post-test, and a delayed post-test. Those data were then analyzed by means of standard statistical instruments.

In collating and appraising the obtained results it was apparent that a one camera production, with true flat lighting, utilizing close-up camera coverage and a modicum of technical skill and imagination, was as effective as the more elaborate production in ordinary lecture-teaching situations.

**An Experiment in Laboratory Education**—G. Kent and W. H. Card (p. 62)

A departure from traditional forms of undergraduate laboratory education has been incorporated into the electrical engineering curriculum at Syracuse University. In this paper is presented a summary of the reasons for this innovation, a description of the course, and an evaluation of our experiences with it.

As curricula in electrical engineering become more science centered, it is essential that the undergraduate engineering laboratory take as its prime objective the development of skills requisite to the planning and execution of meaningful experiments and the promotion of an understanding of the relationships between theory and experiment. Briefly, the objective is an education in the experimental aspects of scientific method.

This objective has not been well served in the past by the traditional laboratories. Too frequently, student motivation has been poor enough to limit substantially the learning process, and the typical experiment was not likely to afford an opportunity for education in science.

To attempt to fulfill the objectives stated, a separate course in laboratory was initiated. The separation of the laboratory from its traditionally dependent role was expected to permit greater freedom in the technical content of the course and to emphasize the importance of the laboratory to science. The plan of the course was inspired by the belief that motivation, the prime force in the learning process, is determined in part by the significance of the experiments the student is asked to perform, and that an education in science can be obtained only by the exercise of its method. Accordingly, the experiments were conceived as nontrivial real engineering problems whose solutions demand independent study and planning on the part of the student. The technical content of the experiments was arranged to constitute an organized development of scientific knowledge.

Consistent with this general conception, the course is built around a sequence of problems which the student is expected to solve. These assignments state the problem and discuss its origin and significance. A list of apparatus, ref-

World Radio History

erences to the literature, and occasionally some experimental hint in the form of a provocative statement are given. The students plan their experiments and proceed with them at their own pace. The only time limitations are that a reasonable number of projects must be completed during the course. In addition to keeping laboratory notebooks, the students are required to prepare several specific kinds of reports. In contrast to the common practice of marking solely on the report, grades are determined by total laboratory performance.

The evaluation of this program is a continuous process. Although at this date no conclusive judgments can be made, early indications of student response have stimulated great enthusiasm among the teaching staff. We are confident that progress toward our objectives is substantial.

**The Computer Revolution in Engineering Education**—Robert E. Machol (p. 67)

The ready availability of high-speed digital computers has wrought a fundamental and unprecedented change in engineering education. Described herein are one university's experiences with a small digital computer, on which thousands of undergraduates have been taught to program within the past year. A new approach to the teaching and administration of computers is required, as is a new approach to almost every aspect of the engineering curriculum. The shape of things to come is briefly examined.

**Engineering Education in Canada and the Co-operative Electrical Engineering Program at the University of Waterloo**—B. R. Myers and J. S. Keeler (p. 71)

Although co-operative engineering is practiced at several universities in the United States, that at the University of Waterloo is unique in Canada. The baccalaureate program requires five years of continual attendance, during which the student spends alternate three-month periods in school and in industry.

A distinctive feature of the plan is the maintenance of a Co-ordination Department within the University organization. Staffed by senior professional engineers, this department acts as liaison between industry and the students.

Two programs of study are offered in the undergraduate electrical engineering curriculum. One of these is designed for the heavy electromechanical and power systems engineer. The other embraces electronics, communication and computery disciplines, with a greater concentration of theoretical studies.

Although the University is still in its infancy, both industrial and student acceptance of the co-operative plan has exceeded initial expectations. There is every indication that co-operative engineering education will rapidly assume a dominant role in the Canadian academic scene.

**Letter to the Editor**—Samuel Seely (p. 79)

**Contributors** (p. 80)

## Electron Devices

### Vol. ED-8, No. 3, May, 1961

**Concentration-Modulation Electron-Beam Devices**—Herbert Lashinsky (p. 185)

Electron-beam devices are considered in which a form of concentration modulation, as defined by Gabor, is utilized. In the devices described here a scalloped electron beam is produced by a combination of crossed electric fields and a magnetic field, and strikes a collector after passing through a fixed aperture. The points of minimum width of the scalloped beam are "images" of the cathode which are reproduced along the longitudinal axis of the system by virtue of the cyclotron motion of the electrons. The application of an additional alternating electric field, parallel to the fixed electric field, causes a periodic variation in the longitudinal position of the cathode images, giving rise to an alternating component in the current which reaches the collector. Concentration modulation is compared with other modulation methods. Transit-time limitations are evaluated and possible applications are considered, including frequency multiplication at microwave frequencies. The use of the concentration-modulation technique in modulating a high-density electron beam at audio frequencies in an experimental system is described.

**A Stagger-Tuned Five-Cavity Klystron with Distributed Interaction**—Hellmut Golde (p. 192)

This paper describes the operation of a five-cavity klystron with distributed interaction using stagger-tuned cavities. A bandwidth of 64 Mc with a gain of about 30 db at 40 per cent efficiency is typical of the performance of the amplifier.

**Electron Beam Coupling in Interaction Gaps of Cylindrical Symmetry**—Garland M. Branch, Jr. (p. 193)

In a ballistic analysis in which space-charge effects have been neglected, the method of describing the performance of re-entrant cavity resonators in terms of beam-coupling coefficients, beam-loading conductance ratios, the shunt impedance $R$, and the cavity quality factor $Q$ has been generalized and extended for the treatment of any kind of resonator with electric fields of arbitrary spatial distribution. As one consequence, the properties of resonant helix sections and cavity resonators can be directly compared in terms of the same physical concepts.

**Noise Temperature in Distributed Amplifiers**—A. Yariv and R. Kompfner (p. 207)

The subject of noise generation in certain types of RF amplifiers is treated. The different physical mechanisms by which noise is generated within the amplifier are discussed. Expressions for the "effective source noise temperature" are derived for distributed amplifiers of the maser, parametric, and tunnel type.

**Traveling-Wave Tube Analysis of the Adler Tube**—R. W. Fredricks (p. 212)

The cyclotron waves on an electron beam in the pump field of the Adler tube are studied with respect to their circular polarization. It is found that positive and negative circularly polarized beam waves are coupled through the pump electric field. As a consequence of the coupling, the small signal traveling-wave analysis leads to the conclusion that the positive circularly polarized beam wave is comprised of the fast signal wave and all idlers of frequencies $n(\omega \pm \omega_p)$ where $n$ is an even integer, while the negative circularly polarized wave is comprised of all idlers with odd integral values of $n$. This information appears to be new, and can perhaps be used to design input and output couplers which discriminate against unwanted idler waves.

**Bridge Measurement of Tunnel-Diode Parameters**—W. Howard Card (p. 215)

A specific bridge measurement technique is presented for measuring the important small-signal parameters of the tunnel diode at frequencies up to 100 Mc and at all significant operating levels. Particular attention is paid to the problem of biasing the tunnel diode to eliminate instability in the negative resistance region which would otherwise prevent significant measurements being made in this region. Requirements for stable bias circuits are analyzed in detail and specific criteria for stable operation given.

A circle diagram method is presented which allows the significant parameters to be determined from a set of measurements made for a sequence of bias voltages, at a chosen frequency. From the results, curves of shunt capacitance and conductance as a function of bias voltage may be plotted.

Measurements made using a Wayne Kerr Type B.801 VHF Admittance Bridge on a particular tunnel diode are presented. The experimentally determined capacitance vs voltage curve is found to agree closely with the theoretical curve of the normal junction diode, with no pecularities through the negative resistance region. Further results show that approximate parameter values may be obtained even when oscillatory or bistable behavior prevents satisfactory measurement in the negative resistance region.

**Four-Terminal Analysis of the Hall Generator**—D. L. Endsley, W. W. Grannemann, and L. L. Rosier (p. 220)

The four-terminal parameters of the Hall generator are derived and then used to develop expressions for input impedance, output impedance, current gain, and voltage gain. The theoretically determined expressions are then verified for a Hall generator using indium antimonide. The four-terminal equations are given as a function of conductivity, Hall constant, temperature, magnetic field, and dimensions of the material. Thus, the designer may use these expressions in the application of Hall-effect devices.

**Focus Reflex Modulation of Electron Guns**—Kurt Schlesinger (p. 224)

High resolution and low drive features have been successfully combined in a new type of electron gun for cathode-ray tubes. The gun has a spot-defining aperture of 0.007 inch upon which emission from a large cathode area is concentrated by a retarding electron lens. This unit modulates the beam by electron reflection, while focusing it upon the aperture ("Focus Reflex Modulation").

Immediately ahead of the aperture, a modulated virtual cathode is formed with an emission capability of over four amperes per square centimeter.

A 1000-$\mu$a beam with a 6° divergence is controlled by a signal of 12 volts centered at ground potential. Highlight brightness of 250 foot lamberts was read at 17,500 volts, while more than 500 lines were resolved on a television test pattern.

In more recent forms of the FRM gun, 1600 $\mu$a are measured in the screen return, out of 1800-$\mu$a cathode current. This is 88 per cent over-all transmission, using the same defining aperture (0.007 inch). 18 volts of drive signal will completely modulate the above current.

**Anode Effect: the Influence of Electron Bombardment of the Anode on Flicker Noise**—H. J. Hannam and A. Van Der Ziel (p. 230)

Experiments are presented which indicate the existence of two types of flicker noise in vacuum tubes with oxide-coated cathodes. The first is "normal" flicker noise that is present for anode voltages below 10 volts; the second is the "bombardment-enhanced" flicker noise that is added when the anode voltage is above 10 volts. It seems that the latter can be attributed to the arrival of neutral oxygen on the cathode. Since most pentodes and triodes operate with anode voltages above 10 volts, the "bombardment-enhanced" flicker noise should be a rather common source of flicker noise in these tubes.

**Experimental Investigation of Large-Signal Traveling-Wave Magnetron Theory**—J. R. Anderson (p. 233)

Experiments conducted on a beam-type backward-wave amplifier which closely approximates the theoretical thin-beam model used in the large-signal analysis of Sedin have resulted in gain and phase shift characteristics which are in good quantitative agreement with the adiabatic portion of both the Sedin and Gandhi-Rowe theories. Efficiencies approaching the theoretically-predicted maximum have been observed. By driving the amplifier to very large signal levels a conversion efficiency for power available from the initial potential energy of the beam of 63 per cent was obtained with a corresponding value of 45 per cent for the total electronic efficiency. An important feature of this experimental amplifier is the electron gun design which is based on a theory by Kino. That this gun is capable of producing a well-confined, rectilinear-flow thin beam is

World Radio History

demonstrated by visual observations of the beam thickness which indicate that $\omega_c/\omega_p$ is as low as 1.17, a value close to that for a laminar-flow Brillouin beam ($\omega_c=\omega_p$).

**Contributors** (p. 240)

## Industrial Electronics

### Vol. IE-8, No. 1, May, 1961

**An Event Recorder Using Transistor Switches**—J. W. Streater (p. 1)

An improved event recorder has been developed which is capable of resolving the time-relationships among two-state events to within two milliseconds. Conducting styli, writing on electrosensitive chart paper, are switched on or off by transistor circuits functioning as non-mechanical relays having fast response, high sensitivity, and minimum size.

**A Device to Determine the Number of Turns and the Presence of Short-Circuited Turns on Cylindrical Coils**—Walter F. Praeg (p. 5)

A device to measure the number of turns and the presence of short circuits between turns is described. It will measure, depending on the construction of the magnetic comparator, cylindrical coils with or without a ferromagnetic core. The accuracy for the number of turns measured is ±0.1 per cent. Short-circuited turns, either intentional or accidental, affect only slightly the accuracy of the measurement of the number of unfaulted turns. On coils without an iron core, the presence of one short-circuited turn of No. 25 AWG copper wire can be detected.

**Transistorized Switching Control of a Variable-Speed DC Motor**—Jack Allison and Paul Vergez (p. 19)

Where a dc motor is supplied energy from a storage battery or other fixed voltage source, variable-speed operation is usually accomplished by adding resistance in series with the motor supply. In this type of control, only part of the total energy delivered by the source is available at the motor to do useful work. The balance of the energy is converted into heat by the series resistance and is lost.

A more desirable approach to speed control, as presented in this report, is to insert a switch rather than a resistor in series with the motor's supply. Here the switch would be opened and closed at regular intervals which would represent infinite or zero series resistance, respectively. In either state, the switch would present no energy losses to the circuit. The motor speed varies with the percentage of time the switch remains closed.

The latter system has the advantage that for a given speed setting, variations in load will not cause fluctuations in speed due to IR drop in any series resistor.

The transistorized switching circuit described in detail in this report represents an efficient method of switching the motor supply current for good speed control. The laboratory model, which gave very satisfactory performance, was designed to control 20 amperes at 24 volts, or approximately a one-half horsepower motor. This rating may be increased with only minor modifications to the circuit.

**A Transistorized Tension and Loop Control**—T. E. DeViney (p. 24)

With the introduction of power semiconductors, it is possible to accomplish many functions statically that were previously accomplished with electro-mechanical devices. The use of static components results in improved performance with reduced maintenance. The tension and loop control described in this paper features the use of static circuits.

**High-Speed Welder for Crossbar Switch Contacts**—J. S. Gellatly and R. Spillar (p. 30)

A novel-design welding machine has been constructed to attach the precious-metal contacts required on the switch springs of the crossbar-type telephone central office equipments. Parts are carried through the various checking stations and the multiple welding nest by a geneva-driven high-speed transfer mechanism. The electronic weld control is a 20-unit modular minimum-size packaged capacitor discharge welder utilizing circuits designed to provide a high degree of reliability with semi-skilled electrical maintenance. Carded units of ten switch springs are transferred through the welding nest where 20 contacts are fed, welded, clipped, and checked on ¾-second cycle. The speed of 100,000 welds per hour permits this machine to replace 20 previous machine units, thus realizing large manufacturing-cost reduction.

**A Digital Storage "Language" for Engineering and Production Information**—William S. Bennett (p. 36)

In addition to the present uses of electronic data processing machines in computation, business accounting, simulation, literature retrieval, and the like, these devices could also be used as a central repository for the storage and rapid retrieval of the information we now put on engineering drawings, specifications, process sheets, bills of material, and so forth. However, the data formats commonly used in computation and accounting do not appear to be adequate to the retrieval problem involved, while literature retrieval methods do not have the precision required in production work. A data format or "language" is proposed which is loose enough to contain all possible engineering or production information, but precise enough to permit accurate retrieval. The price paid for these features is the formulation of a large dictionary of identifiers, and some inflation of storage requirements.

## Military Electronics

### Vol. MIL-5, No. 2, April, 1961

**Frontispiece**—James M. Bridges (p. 29)

**A New Generation of Radar**—James M. Bridges (p. 30)

**The Future of Radar**—John S. Burgess (p. 32)

In this paper an attempt is made to forecast the direction in which the radar state-of-the-art will aim. The paper will begin with a description of a few of the radars of World War II, to set the stage for a comparison and evaluation of the various techniques that have been added.

Since World War II, various components and techniques developments have been designed for our more modern-day radar, and a tremendous increase has been realized in capability for handling smaller, faster and more distant targets. Particular emphasis is placed on the problems of high resolution, discrimination and pattern recognition.

The effect of our entry into the space age on the design of radar equipments will be discussed. These new radars must cope with problems which are at least an order of magnitude greater than the air-breathing threat in all of its aspects.

The conclusion made is that the phased-array type of radar offers the only long-range solution to the complex problems faced today by the radar engineer. Its combination of flexibility, limitless power, high-frequency capability, electronic scanning, etc., makes it the only logical choice for the future.

**High-Power Traveling-Wave Tubes for Radar Systems**—J. A. Ruetz and W. H. Yocom (p. 39)

Data obtained on high-power traveling-wave tubes at *S* and *C* band indicate performance suitable for the final amplifier in a wide bandwidth phase coherent radar transmitter. Static phase measurements demonstrate the capability of parallel operation of tubes and the feasibility of use in pulse compression systems. Gain and power output data show that for the most efficient operation a programmed drive is needed. Data taken at constant drive power displays a compressed gain variation and a somewhat lower output. An extrapolation of present data indicates the feasibility of obtaining 25- to 30-per cent bandwidth in high-power traveling-wave tubes with other improved characteristics.

**Automatic Frequency Control of Magnetrons**—Austin R. Sisson (p. 45)

A practical AFC system for both *X*-band and *Ku*-band magnetron radar transmitters has been developed. This system meets the needs of three radar systems currently in production. Frequency stabilization is accomplished by electronically controlling the magnetron load impedance. Therefore, the magnetron "pulling figure" is put to use.

The closed loop AFC system maintains frequency stability to better than ±2 Mc at *Ku*-band and ±1.5 Mc at *X*-band frequencies over wide environmental conditions. The system dynamically compensates for deviations in frequency due to temperature, vibration, shock, changes in duty cycle, drift with life, and poor voltage regulation. The response time of the AFC system is such that, starting at the limits of the capture range, "on frequency" response is obtained within the first five pulses of the magnetron. One of the radar systems requires a considerable delay between groups of pulses. For this radar, the AFC system provides a memory to hold the conditions for "on frequency" response during the delay periods.

A qualitative analysis of the closed-loop system is made with reference to the Rieke Diagram. It is shown how a single magnetron has been used to meet two different sets of system performance requirements.

System operation and hardware are discussed with reference to practical difficulties.

**The Radar Measurement of Range, Velocity and Acceleration**—E. J. Kelly (p. 51)

This paper is a study of the ultimate attainable accuracy in the radar measurement of range, range rate, and range acceleration. It is assumed that these quantities are to be measured by a coherent radar with a large output signal-to-noise ratio. The approach is entirely theoretical, and the accuracy evaluated is the accuracy that would be attained with an ideal receiver which performs maximum-likelihood estimates of the unknown parameters. The transmitted waveform is fixed and arbitrary, and the error variances and covariances are evaluated in detail in terms of the amplitude and frequency modulation of the transmitted wave. Specific results are also given for constant amplitude pulses carrying arbitrary combinations of linear and quadratic frequency modulation.

**Masers for Radar Systems Applications**—H. R. Senf, F. E. Goodwin, J. E. Kiefer, and K. W. Cowans (p. 58)

This paper is intended to provide the systems engineer with a practical introduction to the use of solid-state maser amplifiers in radars. Various environmental problems involved in the successful application of masers are discussed. An elementary survey of reflection-cavity and traveling-wave masers, together with some experimental results are presented. Another section treats the problem of saturation in masers and discusses some of the methods available for protecting masers from the TR leak-through pulses in radar. Progress made in the development of open- and closed-cycle liquid helium cryogenic systems suitable for masers is described. The authors' personal evaluations of the state of the art of ruby masers and closed-cycle helium refrigerators are given in appendixes.

**The Electron Beam Parametric Amplifier as a Radar System Component**—R. Adler and W. S. Van Slyck (p. 66)

Practical experience is now available with the Electron Beam Parametric Amplifier (EBPA) used as a low-noise preamplifier in radar systems. Principles of operation of the

World Radio History

EBPA are briefly recapitulated. Among its desirable characteristics are unilateral behavior, high stable gain and a double-channel noise figure (NF) of 1 db or less; its bandwidth, input and output impedance remain constant as gain is adjusted. An $L$-band amplifier is described in detail. A discussion of various ways of handling the idler channel follows. The technique of in-pass-band pumping achieves an effective NF of 2.5 db or better in radars with conventional detection. Complications arise with Moving Target Indicator (MTI) systems; remedies are described.

The paper reports on field tests in which these techniques were used, including a few flight tests. The results show substantial improvements in sensitivity and range. They also spotlight the ability of the EBPA to tolerate high overload and to act somewhat like a TR switch.

**Design Considerations for Parametric Amplifier Low-Noise Performance**—C. R. Boyd, Jr. (p. 72)

The basic characteristics of parametric amplifiers are reviewed briefly, with particular emphasis on the limitations on low-noise performance resulting from diode losses. Normalized curves showing the minimum excess temperature of a parametric amplifier for various spectrum arrangements are presented, where the normalizing factor is the degenerate-mode gain cutoff frequency. Experimental evidence consisting of noise figure measurements on an $X$-band amplifier is used to relate this cutoff frequency to an easily and commonly measured diode quality factor. Design considerations for a hypothetical $L$-band parametric amplifier are discussed to illustrate the implications of the noise analysis.

**Steerable Array Radars**—Frank C. Ogg, Jr. (p. 80)

The general characteristics of radars using large planar steerable array antennas are discussed. The need for an amplifier for each element is shown, and the tolerances and stability requirements for the amplifiers are discussed. Array geometry, pattern formation and gain, mutual coupling, and beam-steering techniques are summarized. Element minimization and signal-processing techniques are analyzed.

**Signal and Data-Processing Antennas**—G. O. Young and A. Ksienski (p. 94)

This paper treats the antenna as an information processing device, and applies the concepts of modern information theory to the design of antennas and to the optimization of their performance. The principal optimization criterion employed is maximization of information or data rate.

The general procedure is to treat the antenna as a spatial frequency filter which is being optimized subject to a given set of control inputs. Given these specifications, the information rate is maximized with respect to the antenna system parameters subject to the physical constraints of the system.

It is shown that in a general antenna system where noise is introduced in both the object and image space, the optimum antenna aperture distribution is uniform. When the image, or receiver, noise is zero, the useful output information content and rate are independent of the aperture distribution. An equation relating the signal and noise spectra and the aperture distribution is derived which shows the way in which the signal should be coded so as to maximize the information content. Processing is discussed generally, and a specific nonlinear processing scheme is analyzed. The general conclusion is that nonlinear processing degrades the useful information rate when the SNR is low whereas it may improve the rate at high SNRs. Finally, a number of specific military and space applications of information processing antennas are considered.

**Signal Processing Techniques for Surveillance Radar Sets**—C. A. Fowler, A. P. Uzzo, Jr., and A. E. Ruvin (p. 103)

One of the major recent advances in radar technology has been in the processing of the received signals. Several techniques have been developed to enhance the desired signals (aircraft) relative to ground clutter, sea clutter, rain, interference from other radars, and active countermeasures.

The following techniques are discussed: MTI, Sweep Integration, and Blanking and Switching. A signal processing system utilizing these techniques is described.

**Principles of Pulse Compression**—H. O. Ramp and E. R. Wingrove (p. 109)

For good radar system performance, a transmitted waveform is desired that has 1) wide bandwidth for high range resolution and 2) long duration for high velocity resolution and high transmitted energy. In a pulse-compression system, a long pulse of duration $T$ and bandwidth $F$ (product of $T$ and $F$ greater than one) is transmitted. Received echoes are processed to obtain short pulses of duration $1/F$. Compression ratio (the ratio of long-pulse duration to short-pulse duration) is thus the product $T \cdot F$, and is a measure of the combined range and velocity resolution.

Pulse compression occurs if a waveform with a nonlinear phase spectrum is passed through a filter "phase matched" to the waveform. Phase matched means that the nonlinear part of the network phase response is the negative of the nonlinear part of the waveform phase spectrum.

The waveform with rectangular amplitude spectrum and parabolic phase spectrum is ideally suited for pulse compression. Bandwidth and duration can be independently specified, duration-bandwidth products of 100 or more are presently feasible, and the waveform remains phase matched to one filter over a wide range of Doppler frequency shifts.

**Airborne Pulse-Doppler Radar**—L. P. Goetz and J. D. Albright (p. 116)

Doppler radars are employed for the detection of moving targets whose radar echo area is much smaller than the ground clutter return. Moving targets are separated from clutter on a frequency basis by utilizing the Doppler phenomenon. Continuous-wave Doppler radars have a practical maximum-range capability because the leak-through between the transmitter and receiver causes receiver saturation. This limitation is overcome in pulse-Doppler radar by time-sharing the transmitting and receiving cycles. This paper discusses a typical pulse-Doppler radar and the basic design considerations for the selection of the pulse-recurrence frequency, elimination of clutter, range determination, and oscillator stability requirements.

**A High-Resolution Radar Combat-Surveillance System**—L. J. Cutrona, W. E. Vivian, E. N. Leith, and G. O. Hall (p. 127)

An account is given of the development of the AN/UPD-1 (XPM-1) system. This airborne mapping radar, by synthesizing an extremely long antenna which expands in length in direct proportion to radar range, provides a linear resolution in the azimuth direction that is constant for all radar ranges.

**The Evolution and Application of Coherent Radar Systems**—N. R. Gillespie, J. B. Higley, and N. MacKinnon (p. 131)

A brief introduction to coherent radar applications is given by discussing some basic pulse and CW systems. Comments on the historical development of these systems are followed by a general discussion of coherent radar parameter variations as they relate to the accuracy, resolution and ambiguity of target position or speed measurements.

**Interferometer Techniques Applied to Radar**—E. Gehrels and A. Parsons (p. 139)

A method is described for measuring the angular rate of a radar target by measuring the rate of change of the phase difference between radar echoes received at two widely separated antennas. It is shown that it is possible by the interferometer technique employed to obtain a direct measure of target angular velocity in much the same manner that Doppler measurements yield radial velocities.

Three main questions existed concerning the basic feasibility of such an approach:

1) Will the effect of the fluctuations in time of arrival arising from inhomogeneities in the atmosphere render the data incapable of interpretation?
2) Is sufficient phase stability obtainable in the equipment and in the transmission paths between widely separated sites to permit phase measurements of the required accuracies?
3) Will serious degradations in the data occur as a result of shifts in the phase center of irregularly shaped tumbling objects?

**New Techniques in Three-Dimensional Radar**—Murray Simpson (p. 146)

The definition and basic equations defining the performance of three-dimensional radar systems are given. In particular the parameters defining data rate for different classes of three-dimensional radar are analyzed. Three-dimensional radars are divided into three classes as follows: single beam-rapid scan systems; multiple beam-scanning systems; and multiple beam-nonscanning systems. Each of these types is defined and compared in terms of important characteristics. It is shown that new developments in electronic scanning and multiple beam antennas have made feasible many of these new three-dimensional radar systems. A number of the more important antennas and their method of utilization in the three-dimensional radar equipment are described. Examples are given of two types of three-dimensional radar that are typical of two classes of this equipment. Finally, some of the more important applications for modern three-dimensional radar equipment are noted.

**Recent Advancements in Basic Radar Range Calculation Technique**—L. V. Blake (p. 154)

A procedure for radar range calculation is described, reflecting current knowledge of the effects of external natural noise sources, atmospheric-absorption losses, and the refractive effect of the normal atmosphere. The range equation is presented in terms of explicitly defined and readily evaluated quantities. Curves and equations are given for evaluating the quantities that are not ordinarily known by direct measurement. Some conventions are proposed for use in general radar range calculation, including an antenna-noise-temperature curve, minimum-detectable signal-to-noise ratio ("visibility factor") curves, and a formula for the reflection coefficient of a rough sea. A noise-temperature table and a work-sheet for range calculation are included in the Appendix.

**Prediction of Coverage for Trans-Horizon HF Radar Systems**—G. F. Ross and L. Schwartzman (p. 164)

Coverage patterns for trans-horizon radar systems can be predicted both analytically and empirically. Empirical methods are preferred because of their rapid application and lack of need for elaborate computing facilities. In addition, the coverage techniques introduced may be used eventually to determine the slant range, absorption, and effective noise temperature of trans-horizon radar systems. Some of the fundamental considerations which influence the prediction of coverage, such as geographical location, and the diurnal, seasonal, and anomalous behavior of the ionosphere, are discussed qualitatively. In spite of these factors, however, it is shown how HF radar systems overcome the line-of-sight limitations imposed upon conventional microwave radar systems and theoretically permit up to four or five times the range for a single hop.

**A New Display for FM/CW Radars**—Herbert H. Naidich (p. 172)

World Radio History

One of the limitations of FM/CW radars, often quoted in the literature, is in their inability to handle multiple targets. Several variations of a comparatively simple Range/Range Rate Display, capable of handling and resolving a large number of targets when used in conjunction with an FM/CW radar, are presented. The FM/CW plane and means for resolving target ambiguities are discussed, as well as system features, which, when used in conjunction with the displays, enable multiple target range and velocity information to be obtained and utilized simultaneously.

**Contributors** (p. 179)

## Product Engineering and Production

### VOL. PEP-5, NO. 2, JUNE, 1961

**Message from the Editor** (p. 1)

**Call for Papers** (p. 2)

**Digital Microelectronic Equipment Problems and Potentials**—Aaron H. Coleman (p. 3)

Major problems encountered in the design of a micromodule digital computer (MICROPAC) for tactical operation within the Field Army are described and solutions presented. Such problems include module heat transfer, interconnection of modules and module assemblies and selection of module assembly size and configuration.

The utilization of the circuitry booklet configuration for module mounting, interconnection and cooling is described. It is shown that reasonable air cooling will provide adequate heat transfer for several thousand modules dissipating an average of 120 milliwatts per module. The quantitative dependence of over-all circuitry packaging density upon connector pin per module requirements, type of booklet and harness wiring, booklet size and configuration, etc. is presented in analytical form. It is concluded that an over-all circuitry section (including connectors, backplane wiring, etc.) packaging density of 150,000 components per cubic foot is obtainable by the utilization of micromodules with an average packaging density of slightly less than 500,000 components per cubic foot.

The extent to which the equipment designer and user will achieve their objectives by the application of micromodules to military digital equipment is discussed. It is indicated that more than 60,000 modules (each containing such logical elements as a flip-flop, two logic gates or equivalent) can be mounted, interconnected and adequately cooled within a volume occupied by a 6-foot rack. This dramatic reduction of volume (and weight) is accompanied by a corresponding decrease in the equipment support or overhead cost per module.

**Philco High Speed Card Reader**—N. M. Emslie (p. 13)

This paper describes the mechanical and electrical design and operating characteristics of a high speed tabulating card reader. This unit, a prime input device to the Philco 2000 Computer System, handles, and reads and checks cards at a peak rate of 38 full size tabulating cards per second.

Design problem solutions in the picking and stacking area which make novel use of wrap clutches to provide an indexing card pick and an incremental stacking sensor are described in detail. The characteristics of the photosensitive reading station are also discussed.

**Investigation of Production Requirements for Solderless Wire Wrapped Electrical Connections**—S. Plasker, A. H. Wenner, and C. A. Selzo (p. 17)

A solderless wire wrapped electrical connection consists of tightly wrapping solid bare wire around a stationary terminal to produce a durable pressure connection.

Properly made, the wrapped connection is a permanent, reliable electrical connection that can be produced faster than soldered connections. The elimination of solder and heat detriments are distinct advantages over the soldered connection. Wire wrapping lends itself to automation, and connections can be easily made on closely spaced terminals. While it is a mechanically strong connection, an individual connection is easily removed, simplifying modification and repair. However, this may be less of an advantage in multi-level wrapping.

The increase in complexity of electronic equipment during the last decade has presented industry with some unique production problems. Not the least of these has been the great increase in the number of electrical connections. The need for speed in making this many connections, without decreasing quality, prompted IBM to expend considerable effort in identifying the variables that affect solderless wire wrapping connections in order to define the controls needed in production. At the present time, these connections are widely used by IBM in both commercial and military applications, and over 100 million solderless wrapped connections were made by IBM in 1960.

The use of the solderless wrapped connection has grown steadily since the Bell System first made the new connection public in 1952. Extensive laboratory tests, performed principally by Bell Laboratories, and field experience have verified the reliability of the connection.

This paper describes the effect of the variables involved in the wire wrapping process which were determined from the results of laboratory tests and manufacturing experience and the process controls required to assure the quality and reliability of production connections.

To meet process requirements consistently, the many variables inherent in the solderless wire wrapping process must be considered. These variables will be discussed under the major variable factors involved in the process.

**A Miniature 90×10 Solid State Multiplexer**—S. G. Kritzstein and A. V. Ottaviano (p. 29)

The evaluation of a completely solid state electronic multiplexer, with a capacity of 90 channels, is presented. Electrical operation is described as well as mechanical fabrication. A comparison of two types of packaging techniques is made.

**Analysis of a Tri-Dimensional Feed Horn Support Structure**—Z. M. Slusarek (p. 38)

The design and test analysis of a space structure is presented.

A correlation coefficient, developed from experimental stress analysis and performed on a full scale model under partial loading in the laboratory was used to predict the performance of the structure under actual loading. The results from over 100 tests are shown and discussed.

**The Atlas Missile Autopilot—A Case History of PGPEP Principles in Action**—John H. Hauser (p. 50)

The approach used in introducing electronic packaging utilizing printed wiring boards in the production design of the ATLAS MISSILE AUTOPILOT is described. An integrated system design approach from circuit schematic to finished product is demonstrated by explanation of design standards adopted and the use of eleven (11) specifications, which covered materials, parts, processes and assembly techniques, as requirement documents on applicable part and assembly drawings.

The role of the specialist as coordinator and integrator of cognizant departmental functions involved in the task is discussed. Printed wiring board parts are used as a specific example to show how Engineering, Purchasing, Processing, Assembly, Inspection, Testing and Quality Assurance tasks are related.

**Design Production Coordination for Reducing Lead Time in the AHSR Radar System**—Judd Blass, Eugene Arelt, and W. L. Maxson (p. 63)

**Thermal Design Solutions for Micro-Modular Equipment**—Gerard Rezek and Paul K. Taylor (p. 71)

**The Product Engineer and the Magnetic Thin Film**—P. Kuttner (p. 85)

Magnetic thin films have great potential as memory elements in digital computers. The properties of thin films are such that memories can be operated at speeds of the order of 100 nanoseconds or less, non-destructively in certain instances. While the elements themselves show great promise, there are many problems attendant to their use, the solution of which must come from experts in packaging techniques.

**Value Engineering and Product Engineering**—Carlos Fallon (p. 93)

Value Engineering is coming of age. In the hands of experienced product engineers it can grow into a truly professional tool for improving the competitive position of a company. It applies the precise techniques of science and engineering to those areas of evaluation, programming, and decision-making which have heretofore been governed by intuition. In estimating, bidding, and scheduling, Value Engineering saves not only money but also elapsed time. In design, development and production, it seeks the best ratio between desirable qualities and their cost in available resources.

This paper will illustrate how Value Engineering can be utilized within the conventional engineering disciplines to provide the quantitative data necessary for better balanced specifications, for reducing areas of uncertainty in product planning, and for better decisions in both product design and program management.

**Epoxy Resin Molds for Encapsulating Electronic Circuitry into Modules**—John J. Tallent (p. 98)

This paper discusses the various procedures, methods and recommendations involving the encapsulation of electronic modules utilizing conventional components. In addition this streamlined approach provides Engineering and Manufacturing a means to produce molds easily and economically, as well as a tool, which offers fabrication flexibility.

**Development of a Thermally Conductive Ceramic Component Board**—Gerald H. Kriss and Louis J. Polaski (p. 104)

This paper describes the development and evaluation of a ceramic component board having all circuit connections electrically insulated but thermally grounded.

Individual circuits are encapsulated in epoxy parallelopipeds having large diameter leads of nickel clad copper wire. The leads in turn are resistance welded to metallic (Kovar) studs which have been brazed into an inorganic (Beryllium Oxide Ceramic) wafer having exceedingly good thermal conductance.

Interconnections between weld studs are accomplished by metalized plated runs.

The component board assembly was then evaluated under simulated operating conditions, *i.e.*, edge clamped to an infinite heat sink and in a vacuum environment. Internal heat rise within the circuit modules was monitored and compared to that found in another module which had not been welded to the board, and plots of the thermal gradients across the ceramic wafer were made.

**Sub-Modular Packaging of Airborne Electronic Systems**—John F. Dalton (p. 112)

A packaging concept has been developed to meet the flexible requirements demanded when producing systems for both large and small production runs of airborne electronic systems.

**Multilayer Etched Laminates: A New Packaging Design Tool**—Norman Schuster and William Reimann (p. 114)

**High Density Electronic Packaging Via Welded Honeycomb Structures (Abstract)**—Charles W. Johnson (p. 128)

**Contributors** (p. 129)

World Radio History

# Abstracts and References

**Compiled by the Radio Research Organization of the Department of Scientific and Industrial Research, London, England, and Published by Arrangement with that Department and the *Electronic Technology* (incorporating *Wireless Engineer* and *Electronic and Radio Engineer*) London, England**

**NOTE: The Institute of Radio Engineers does not have available copies of the publications mentioned in these pages, nor does it have reprints of the articles abstracted. Correspondence regarding these articles and requests for their procurement should be addressed to the individual publications, not to the IRE.**


| | |
|---|---|
| Acoustics and Audio Frequencies | 1358 |
| Antennas and Transmission Lines | 1358 |
| Automatic Computers | 1359 |
| Circuits and Circuit Elements | 1359 |
| General Physics | 1361 |
| Geophysical and Extraterrestrial Phenomena | 1362 |
| Location and Aids to Navigation | 1364 |
| Materials and Subsidiary Techniques | 1364 |
| Mathematics | 1368 |
| Measurements and Test Gear | 1368 |
| Other Applications of Radio and Electronics | 1368 |
| Propagation of Waves | 1368 |
| Reception | 1369 |
| Stations and Communication Systems | 1369 |
| Subsidiary Apparatus | 1370 |
| Television and Phototelegraphy | 1370 |
| Tubes and Thermionics | 1371 |
| Miscellaneous | 1372 |


The number in heavy type at the upper left of each Abstract is its Universal Decimal Classification number. The number in heavy type at the top right is the serial number of the Abstract. DC numbers marked with a dagger (†) must be regarded as provisional.

## UDC NUMBERS

Certain changes and extensions in UDC numbers, as published in PE Notes up to and including PE 666, will be introduced in this and subsequent issues. The main changes are:

| | | |
|---|---|---|
| Artificial satellites: | 551.507.362.2 | (PE 657) |
| Semiconductor devices: | 621.382 | (PE 657) |
| Velocity-control tubes, klystrons, etc.: | 621.385.6 | (PE 634) |
| Quality of received signal, propagation conditions, etc.: | 621.391.8 | (PE 651) |
| Color television: | 621.397.132 | (PE 650) |

The "Extensions and Corrections to the UDC," Ser. 3, No. 6, August, 1959, contains details of PE Notes 598–658. This and other UDC publications, including individual PE Notes, are obtainable from The International Federation for Documentation, Willem Witsenplein 6, The Hague, Netherlands, or from The British Standards Institution, 2 Park Street, London, W. 1, England.

**A list of organizations which have available English translations of Russian journals in the electronics and allied fields appears each June and December at the end of the Abstracts and References section.**

**The Index to the Abstracts and References published in the PROC. IRE from February, 1959 through January, 1960 is published by the PROC. IRE, June, 1960, Part II. It is also published by *Electronic Technology* (incorporating *Wireless Engineer* and *Electronic and Radio Engineer*) and included in the March, 1961 issue of that Journal. Included with the Index is a selected list of journals scanned for abstracting with publishers' addresses.**

## ACOUSTICS AND AUDIO FREQUENCIES

**534.213.4** 2063

**On the Transmission of Acoustic Waves through a Circular Channel of a Thick Wall**—Y. Nomura and S. Inawashiro. (*Sci. Repts. Res. Inst. Tohoku Univ., Ser. B*, vol. 12, no. 1, pp. 57–71; 1960.)

**534.232–14:534.6.089.6** 2064

**Sonar Transducer Pulse Calibration System**—J. D. Wallace and E. W. McMorrow. (*J. Acoust. Soc. Am.*, vol. 33, pp. 75–84; January, 1961.) The development of equipment and techniques for making measurements on underwater transducers is described.

**534.283–8:537.312.62** 2065

**Ultrasonic Attenuation in Superconductors**—T. Tsuneto. (*Phys. Rev.*, vol. 121, pp. 402–415; January, 1961.) A general treatment of ultrasonic attenuation of both longitudinal and transverse waves in superconductors is given on the basis of the Bardeen-Cooper-Schrieffer theory.

**534.441.2** 2066

**An Acoustic Spectrum Analyser with Electronic Scanning**—D. J. H. Admiraal. (*Philips Tech. Rev.*, vol. 21, pp. 349–356; October, 1960.) Improvements have been made to earlier equipment [*ibid.*, vol. 7, pp. 50–58; 1942 (Beljers)] by using semiconductor diodes and transistors.

**534.614–8:621.3.018.75** 2067

**Pulse Superposition Method for Measuring Ultrasonic Wave Velocities in Solids**—H. J. McSkimin. (*J. Acoust. Soc. Am.*, vol. 33, pp. 12–16; January, 1961.) Details are given of a pulse superposition technique which takes into account the coupling effect when a quartz transducer is cemented to the specimen.

**534.8** 2068

**Some Periodic Variations in Low-Frequency Acoustic Ambient Noise Levels in the Ocean**—G. M. Wenz. (*J. Acoust. Soc. Am.*, vol. 33, pp. 64–74; January, 1961.)

**534.84** 2069

**New Distortion Criterion**—E. R. Wigan. (*Electronic Tech.*, vol. 38, pp. 128–137 and 163–174; April and May, 1961.) A formula, described as the "distortion criterion," is derived from the results of an analysis of audience reaction to nonlinear distortion.

**534.84** 2070

**The Damping of 'Eigentones' in Small Rooms by Helmholtz Resonators**—F. J. van Leeuwen. (*E.B.U. Rev.*, pp. 155–161; August, 1960.) The natural oscillation or "boom" of small rooms is considered theoretically. Damping of this effect can be achieved by means of small Helmholtz resonators. A design formula is given for these resonators, and suggestions are made regarding installation.

**534.844.1+621.317.2:538.566.08** 2071

**Reverberation Chamber Technique and Construction of a Large Reverberation Chamber for Electromagnetic Waves**—Meyer, Helberg, and Vogel. (See 2325.)

**621.395.623.7.001.4** 2072

**Performance Tests on Loudspeakers**—M. T. Haitjema, W. Kopinga, and S. J. Porte. (*Philips Tech. Rev.*, vol. 21, pp. 362–372; October, 1960.) Sound pressure, electrical impedance and efficiency are measured as a function of frequency. Methods of determining transient response, resonance frequency and directivity are given.

## ANTENNAS AND TRANSMISSION LINES

**621.372.2** 2073

**The Helix as a Transmission Line for Waveguide Modes**—G. Piefke. (*Nachrtech. Z.*, vol. 13, pp. 335–341; July, 1960.) Results of earlier work (*e.g.*, 2459 of 1949) are summarized and discussed treating the helical line as a waveguide in any external medium and taking account of the finite wire thickness.

**621.372.2:537.312.62** 2074

**Field Solution for a Thin-Film Superconducting Strip Transmission Line**—J. C. Swihart. (*J. Appl. Phys.*, vol. 32, pp. 461–469; March, 1961.) A sinusoidal wave solution is found for a superconducting transmission line. This solution gives a slow mode of propagation. At low temperatures and frequencies where losses are low, the velocity is dispersionless. The solutions are continuous through the critical temperature. A lumped-circuit interpretation is given.

**621.372.2:621.319.74** 2075

**The External Electromagnetic Fields of Shielded Transmission Lines**—J. D. Meindl and E. R. Schatz. (PROC. IRE, vol. 49, p. 816; April, 1961.)

**621.372.2:621.372.44:621.375.9** 2076

**Interpretation of the Transmission-Line Parameters with a Negative-Conductance Load and Application to Negative-Conductance Amplifiers**—C. T. Stelzried. (PROC. IRE, vol. 49, pp. 812–813; April, 1961.) Expressions are given for the reflection coefficient, power available and standing-wave ratio.

**621.372.2:621.372.51** 2077

**Note on a Balun: Solution by a Tapered Potential**—C. C. Eaglesfield. (PROC. IRE, vol. 49, pp. 810–811; April, 1961.) The intuitive design of Duncan and Minerva (1489 of 1960) has been replaced by a design depending on an analytic approach.

World Radio History

621.372.8.049.7 2078
**Waveguide Components—a Survey of Methods of Manufacture and Inspection**—D. J. Doughty. (*J. Brit. IRE*, vol. 21, pp. 169–189; February, 1961). 59 references.

621.372.81 2079
**Theory of Waveguides and Cavities: Part 3—Perturbation Theory and Its Applications**—R. A. Waldron. (*Electronic Tech.*, vol. 38, pp. 178–183; May, 1961). Two applications are considered: a) the use of a cavity to measure the dielectric constant of a solid, and b) the attenuation in a waveguide due to the dielectric loss. Part 2: 1723 of June.

621.372.823 2080
**Effect of a Radial Discontinuity in a Circular Waveguide on the Propagation of a $TE_{01}$ Wave**—M. Jouguet. [*Câbles & Trans.* (*Paris*), vol. 14, pp. 270–274; October, 1960.] The relative amplitudes of various $TE_{0n}$-type parasitic waves ($n \geq 2$) introduced by the discontinuity are determined.

621.372.823 2081
**Mode Conversion in Metallic and Helix Waveguide**—H. G. Unger. (*Bell Sys. Tech. J.*, vol. 40, pp. 613–626; March, 1961.) Mathematical solutions are given for mode conversion and transmission losses due to mechanical imperfections.

621.372.823 2082
**Winding Tolerances in Helix Waveguide**—H. G. Unger. (*Bell Sys. Tech. J.*, vol. 40, pp. 627–643; March, 1961. Various causes of losses in circular electric waves are considered. The most significant loss is shown to be due to an irregular tilt of the winding, for which an expression is derived.

621.372.823:621.372.83 2083
**Reflections and Mode Conversions in Imperfect Junctions of $TE_{01}$-Wave Transmission Line**—K. Noda. (*Rev. Elec. Commun. Lab., Japan*, vol. 8, pp. 549–559; November/December, 1960.) The effects of tilt and offset between the waveguide axes, and of an elliptical cross section in one waveguide are calculated.

621.372.823:621.372.852.23 2084
**The $H_{on}$ Mode in Circular Waveguide with Equidistant and Coaxially Arranged Band-Shaped Rings of Perfect Conductivity**—H. Buchholz. (*Arch. Elektrotech.*, vol. 45, pp. 249–264; July, 1960.) The effect of a periodic structure consisting of thin narrow rings inside a perfectly conducting waveguide is investigated. An approximate solution is derived for the phase shift along this system.

621.372.826+621.391.814:537.56 2085
**Propagation of Electromagnetic Waves along a Thin Plasma Sheet**—Wait. (See 2352.)

621.372.826+621.391.814.029.64 2086
**TE Surface Waves Guided by a Dielectric-Covered Metal Plane**—Morris and Mungall. (See 2353.)

621.372.829:621.396.677.7 2087
**Electromechanically Scanned Trough Waveguide Array**—W. Rotman and A. Maestri. (*Electronics*, vol. 34, pp. 54–57; March, 1961.) An asymmetrical obstacle introduced into a trough waveguide changes transmission from a nonradiating to a radiating mode.

621.372.852.323 2088
**Theoretical Study of Nonreciprocal Resonant Isolators**—J. B. Davies. (*Philips Res. Repts.*, vol. 15, pp. 401–432; October, 1960.) The attenuation in each direction is calculated as a function of frequency for various ferrite shapes within rectangular waveguide propagating the dominant TE mode. Perturbation theory is used and the results are valid only for small volumes of ferrite.

621.396.67.012.12:621.317.3 2089
**Measurements on Transmitter Aerials of the Austrian Broadcasting Service with the aid of a Helicopter**—E. Kohlgruber. (*Radioschau*, vol. 10, pp. 248–250; July, 1960.) A brief description is given of the procedure and technical equipment used for the measurement of horizontal and vertical radiation diagrams of broadcast and television transmitter antennas.

621.396.673.011.21 2090
**Impedance of a Monopole Antenna with a Circular Conducting-Disk Ground System on the Surface of a Lossy Half-Space**—S. W. Maley and R. J. King. (*J. Res. NBS*, vol. 65D, pp. 183–188; March and April, 1961.) The base impedance of a $\lambda/4$ monopole is calculated by three different methods, and measured experimentally at 3 cm $\lambda$ using a water-filled tank.

621.396.677:523.164 2091
**The Radio Telescope for 7.9 Metres Wavelength at the Mullard Observatory**—Costain and Smith. (See 2177.)

621.396.677.029.45/.51 2092
**Some Preliminary Experimental Tests of a Novel Method of Radiating at Very Low Frequencies**—R. N. Gould. (*Nature*, vol. 190, pp. 332–333; April, 1961.) Experiments have been conducted in Scotland to assess the suitability of a long narrow strip of land as a radiator and to determine its characteristics. 3000 yards of cable were laid across the base of a peninsula 10 miles long, each end of the cable being earthed in the sea, and the transmitter output of 50 w at 10 kc was applied to the midpoint. Preliminary results demonstrate the feasibility of the proposals, though measurements were marred by capacitance effects between the cable and earth.

621.396.677.3 2093
**Equivalence between Continuous and Discrete Radiating Arrays**—A. Ksienski. (*Canad. J. Phys.*, vol. 39, pp. 335–349; February, 1961.) The agreement between the radiation patterns of arrays of sources and those of continuously illuminated apertures is shown to be close. The effect of varying element spacing is found.

621.396.677.3 2094
**Two-Element Aerial Array**—V. G. Welsby. (*Electronic Tech.*, vol. 38, pp. 160–163; May, 1961.) A two-element multiplicative system is described in which signal waveforms composed of a number of sinusoidal components are used to obtain a directional pattern comparable with that of a multi-element additive array. The principle may be applied to give a simplified electronic beam-scanning system.

621.396.677.3.012.12:681.142 2095
**An Analogue Computer for Aerial Radiation Patterns**—H. Page, G. J. Phillips, and J. A. S. Fox. (*E.B.U. Rev.*, no. 62A, pp. 146–149; August, 1960. *Electronic Engrg.*, vol. 33, pp. 206–212; April, 1961.) A detailed description is given of a computer for determining the horizontal radiation patterns of arrays consisting of identical elements. The currents in the elements may have any desired amplitude and phase. See also 2235 of 1960 (Mitchell).

621.396.677.4 2096
**Plane Aerial with Periodically Bent Conductor**—G. V. Trentini. (*Frequenz*, vol. 14, pp. 239–243; July, 1960.) A directional antenna is investigated which consists of a conductor bent periodically in one plane arranged in parallel with a sheet reflector at a spacing of about $\lambda/10$. Narrow-beam radiation can be achieved, the direction of the main beam depending on frequency. Several arrangements, including a four-antenna array for omnidirectional radiation, are discussed.

621.396.677.8 2097
**Fresnel Region Fields of Circular Aperture Antennas**—M. K. Hu. (*J. Res. NBS*, vol. 65D, pp. 137–147; March and April, 1961.) An analysis is given, with numerical results, for antennas with nonuniform illumination.

621.396.677.8 2098
**Transient Behaviour of Aperture Antennas**—B. R. Mayo and C. Polk. (PROC. IRE, vol. 49, pp. 817–819; April, 1961.) Corrections to 3373 of 1960 are given, together with additional conclusions.

621.396.677.85:621.396.965 2099
**A High-Speed Scanning Radar Antenna**—F. Valster. (*Philips Tech. Rev.*, vol. 22, pp. 29–35; November, 1960.) A description is given of an experimental installation using a Luneberg-lens scanning system at speeds up to 10 rps. At these speeds the observation of fast-moving objects is greatly improved.

## AUTOMATIC COMPUTERS

681.142 2100
**A Versatile Forcing-Function Generator**—J. Morrison. (*Electronic Engrg.*, vol. 33, pp. 155–159; March, 1961.) An electronic generator for use with analog computers, which produces sine, square, triangular, ramp, step or impulse functions over the range 0.001–100 cps to an accuracy within $\frac{1}{4}$ per cent is given.

681.142:517.512.2 2101
**A Successful Version of the Beevers-Macewan Fourier Synthesizer using Dekatron Counters**—J. W. Jeffery. (*J. Sci. Instr.*, vol. 38, pp. 119–125; April, 1961.) A Fourier synthesizer is described which allows a possible 100 harmonics to be specified with amplitudes ranging from 1–100 units. Both positive and negative harmonic components are acceptable. See 248 of 1943 (Macewan and Beevers).

681.142:537.226 2102
**A Dielectric Drum Storage System**—S. Morleigh. (*J. Brit. IRE*, vol. 21, pp. 211–219; March, 1961.) The basic theory of a dynamic electrostatic storage system is given. Experimental results with a ceramic drum are given; packing densities of 40 bits per inch were obtained with SNR's of 12:1.

681.142:538.221:539.23 2103
**Designing Thin Magnetic Film Memories for High Speed Computers**—E. E. Bittmann. (*Electronics*, vol. 34, pp. 39–41; March, 1961.) A storage system has been built which will store 320 words each of 8 bits and which has a cycle time of 0.2 $\mu$sec.

681.142:621.374.33 2104
**Current-Operated Diode Logic Gates**—H. Reinecke, Jr. (*Commun. and Electronics*, pp. 762–772; January, 1961.) The basic logic circuits are described and practical examples are given.

681.142:621.396.677.3.012.12 2105
**An Analogue Computer for Aerial Radiation Patterns**—Page, Phillips, and Fox. (See 2095.)

## CIRCUITS AND CIRCUIT ELEMENTS

621.318.57:621.372.44:539.23 2106
**Stable-Oscillation Conditions for the Magnetic-Film Parametron**—R. M. Sanders. (*J. Appl. Phys.*, vol. 32, pp. 478–482; March, 1961.) A mathematical analysis of a parametron is given. This parametron uses a single-domain magnetic film as the core of a nonlinear inductor absorbing energy from an alternating pump field and delivering energy to a signal

World Radio History

winding. Graphical means of determining stability conditions, amplitudes and phases of the oscillating variables, and the range of operating frequencies are discussed.

621.318.57:621.382.23:621.372.44 2107
**Microwave Bistable Circuits using Varactor Diodes**—C. L. Heizman. (PROC. IRE, vol. 49, pp. 829–830; April, 1961.) Using a 10-Gc carrier frequency, switching speed between states was less than 10 nsec. A threshold logic circuit with power gain is illustrated.

621.318.57:621.382.3:621.376 2108
**Symmetrical Transistors as A.C. or D.C. Switches and their Applications in Modulator and Demodulator Circuits**—J. F. O. Evans, D. A. Gill, and B. R. Moffitt. (*J. Brit. IRE*, vol. 21, pp. 143–149; February, 1961.)

621.319.45 2109
**An Investigation of Columbium as an Electrolytic Capacitor Metal**—A. Shtasel and H. T. Knight. (*J. Electrochem. Soc.*, vol. 108, pp. 343–347; April, 1961.) The characteristics of capacitors prepared from Cb are very similar to those of Ta, except that the working voltages are about one third and the dc leakage currents about double that of similar Ta capacitors.

621.372.4 2110
**Extension of a Theorem for Normal Passive Electrical Two-Poles in the Steady State**—L. Lunelli. (*Alta Frequenza*, vol. 29, pp. 377–388; June-August, 1960.) The theorem of R. M. Cohn (*Proc. Am. Math. Soc.*, vol. 1, pp. 316–324; June, 1950) which gives the terminal resistance of a two-pole network as a function of the resistances of its elements, is extended to allow for $n$ degrees of freedom of the network satisfying the reciprocity condition.

621.372.4/.5:681.142 2111
**The Representation of Coupling-Free Branched Circuits on an Analogue Computer**—W. Schüssler. (*Arch. elekt. Übertragung*, vol. 14, pp. 327–334; August, 1960.) A method is given for simulating branched circuits on an analog computer so that each circuit component can be varied independently to determine its effect on circuit characteristics. See also 3737 of 1960.

621.372.4:681.142 2112
**Realization of Second-Order Two-Pole Functions with Transformerless Canonical Circuits by means of Program-Controlled Computers**—R. Unbehauen. (*Nachrtech. Z.*, vol. 13, pp. 321–326; July, 1960.)

621.372.413:621.318.134 2113
**The Size Effect of Ferrite Spheres**—W. Hauser and L. Brown. (*Quart. J. Mech. Appl. Math.*, vol. 13, pt. 3, pp. 257–271; August, 1960.) The integral-equation technique is used to derive an approximate formula for the apparent susceptibility of a small ferrite sphere within a microwave cavity. Using a variational principle a first-order estimate is obtained for the effect of a plane wall and the effect of the size of the sphere. See 27 of 1960.

621.372.5 2114
**Calculation of the Transfer Function from the Magnitude of the Transmission Factor**—G. Wunsch. (*Frequenz*, vol. 14, pp. 244–247; July, 1960.) A generalization and modification of Küpfmüller's system theory to eliminate certain contradictions with practical systems is given.

621.372.5 2115
**The Matrix of a Recurrent Network of Equal Quadripoles (Representation of Any Power of a Matrix)**—G. Doetsch. (*Arch. elekt. Übertragung*, vol. 14, pp. 335–340; August, 1960.) An explicit expression is derived for the $n$th power of a matrix representing $n$ equal four-terminal networks in cascade.

621.372.54 2116
**Synthesis of Electrical Filters from Operating Parameters by Means of Zolotarëv Fractions**—A. F. Ufel'man. [*Radiotekhnika* (*Moscow*), vol. 15, pp. 64–72; May, 1960.] Design formulas are given in which special functions are avoided by using mathematical tables of Glowatzki (see 2051 of 1957) and which involve less calculation than is required using the Grossman formulas (2053 of 1957).

621.372.54 2117
**Electrical Wave Filter with Prescribed Operating Characteristics**—J. B. Fischer. (*Arch. elekt. Übertragung*, vol. 14, pp. 283–298; July, 1960.) Calculations are simplified by the application of image-parameter theory to filter design, which may outweigh the advantages of economy in circuit components resulting from the use of insertion-loss methods. Exact relations are derived between the quadripole and insertion-loss characteristics of reactance quadripoles, and examples are given.

621.372.54 2118
**Gaussian-Response Filter Design**—M. Dishal. (*Elec. Commun.*, vol. 36, pp. 3–26; 1959.) Exact data are given for the design of both low- and band-pass filters having characteristics which are $n$th-order approximations to the perfect Gaussian amplitude response, $n$ being the number of elements in the complete filter.

621.372.54 2119
**General Low-Pass and High-Pass Antimetric Filters Inserted between Equal Resistances**—J. E. Colin. [*Câbles & Trans.* (*Paris*), vol. 14, pp. 262–269; October, 1960.]

621.372.54:681.142 2120
**The Application of Electronic Digital Computers in Network Theory**—H. Härtl. (*Nachrtech. Z.*, vol. 13, pp. 313–316; July, 1960.) The applications discussed are a) the synthesis of a quadripole reactance filter, and b) network analysis.

621.372.54+621.372.57].029.42 2121
**Filter Circuits for Extremely Low Frequencies without the Use of Inductances**—H. G. Jungmeister and H. L. König. (*Arch. elekt. Übertragung*, vol. 14, pp. 317–324; July, 1960.) Filter-design procedure using double-T RC networks is described. Passive and active filter circuits are given.

621.372.543.2:534.143 2122
**Electromechanical Quadripoles as Coupling Filters**—E. Trzeba. (*Hochfrequenz. und Elektroak.*, vol. 69, pp. 108–117; June, 1960.) The equivalent circuits of mechanical resonators and electromechanical transducers are derived and the design of band-pass filters consisting of input and output electromechanical transducers coupled by a mechanical transmission line is described.

621.372.543.2:621.372.412 2123
**Ceramic I.F. Transformers**—R. C. V. Macario. (*Wireless World*, vol. 67, pp. 253–256; May, 1961.) The principles of design of the radial-mode resonator as used in IF circuits is discussed. See 2124.

621.372.543.2:621.372.412 2124
**Design Data for Band-Pass Ladder Filters employing Ceramic Resonators**—R. C. V. Macario. (*Electronic Engrg.*, vol. 33, pp. 171–177; March, 1961.) Graphical and tabulated design data based on image-parameter theory are given for filters comprising piezoelectric disks resonating in a radial mode with or without capacitors. The ranges of center frequency, bandwidth and image impedance achievable are discussed.

621.373.029.6:621.372.44 2125
**An Analysis of the Magnetic Second-Subharmonic Oscillator**—A. Lavi and L. A. Finzi. (PROC. IRE, vol. 49, pp. 779–787; April, 1961.) The analysis refers to a parametric oscillator with two ferromagnetic cores. The steady-state operation with both current and voltage pump drives is studied to determine the values of the circuit parameters which will give subharmonic oscillations. The experimental waveforms are close to those predicted.

621.373.42:621.372.44 2126
**Oscillator Circuits with Variable Parameters (Rheolinear Oscillators)**—E. G. Woschni. (*Hochfrequenz. und Elektroak.*, vol. 69, pp. 103–108; June, 1960.) Approximation formulas are given for determining pull-in range and gain of parametric oscillators; sinusoidal variation of capacitance and of attenuation are the cases particularly considered. See also 3560 of 1956.

621.373.42.029.55:621.396.933 2127
**An Airborne Frequency Generating Unit for the H.F. Communication Band**—T. F. Hargreaves, J. H. Gifford, and G. E. Smythe. (*J. Brit. IRE*, vol. 21, pp. 129–136; February, 1961.) The unit gives an output frequency, with channel spacing of 1 kc, in the band 3.5–26.5 Mc. A variable oscillator is phase-locked to a frequency derived from a 5-Mc standard.

621.373.421.13 2128
**Piezoelectric Excitation of Quartz Oscillators Operating in the Thickness Mode by means of a Parallel Field**—R. Bechmann. (*Arch. elekt. Übertragung*, vol. 14, pp. 361–365; August, 1960.) The parallel-field excitation of AT- and BT-cut crystals is considered and its advantages are discussed. Equivalent circuits are given of two experimental oscillators, for 750 kc and 1 Mc using AT-cut quartz crystal resonators. See also 3544 of 1960.

621.373.431.1 2129
**Frequency Control and Frequency Fluctuations of the Astable Multivibrator**—G. Linckelmann. (*Arch. elekt. Übertragung*, vol. 14, pp. 299–313; July, 1960.) A modified multivibrator circuit is given which permits frequency variation over the range 1:400 by means of grid bias control. The causes of fluctuations of pulse repetition frequency are investigated and design formulas are derived for minimizing these effects.

621.373.52 2130
**High-Frequency Transistor Polyphase Oscillator**—T. Takagi and K. Mano. (*Sci. Repts. Res. Inst. Tohoku Univ., Ser. B*, vol. 12, no. 1, pp. 27–39; 1960.) Conditions for oscillation of a polyphase transistor oscillator are developed from its tube equivalent (791 of March). Experimental results show the relative performances of single, polyphase, and push-pull transistor oscillators and demonstrate the superiority of the polyphase oscillator when a high power output is required at high frequencies.

621.374.4:621.372.8 2131
**Waveguide Harmonic Generators**—J. Brown. (PROC. IRE, vol. 49, p. 825; April, 1961.) The generator suggested by Hedderly (4144 of 1960) is regarded as a multiphase rectifier circuit.

621.374.4:621.396.62 2132
**The Synthesis of High-Purity Oscillations Suitable for Single Sideband Receivers**—P. S. Carnt and E. Ribchester. (*J. Brit. IRE*, vol. 21, pp. 237–240; March, 1961.) A phase-locked oscillator has its output mixed with part of a 100-kc spectrum to form an IF in the region

World Radio History

900–1000 kc. An interpolating signal with unwanted components 40 db down is used to lock the loop. Frequencies at 1-kc intervals between 3 and 30 Mc are derived.

621.374.4.029.65 2133
**Harmonic Generators for the 40000-Mc/s Band**—L. Grifone. (*Ricerca Sci.*, vol. 30, pp. 1214–1220; August, 1960.) A description of two signal generators covering the ranges 31–41 and 39–51 Gc is given. They incorporate a 9-Gc klystron oscillator and Si-diode frequency multipliers (665 of 1955.)

621.375.221 2134
**Increase of the Gain of a Wide-Band Distributed Amplifier by Compensation of its Zeroes and by Arrangement of the Residual Poles in a Tchebycheff Ellipse**—J. Koch. (*Arch. elekt. Übertragung*, vol. 14, pp. 348–360; August, 1960.) A set of equations is obtained for a two-tube distributed amplifier, and its component values and characteristics are calculated for a limiting frequency of 300 Mc. General formulas for distributed amplifiers with any number of tubes are derived. Theoretical results are verified with the aid of an experimental two-tube circuit. The Tchebycheff-type amplifier is shown to have a gain greater, by a factor of 1.84, than the conventional distributed amplifier.

621.375.4 2135
**Bandpass Transistor Amplifiers**—C. J. McCluskey. (*Electronic Tech.*, vol. 38, pp. 183–187; May, 1961.) A determinant method is given for the analysis of amplitude and phase responses of tuned amplifiers having complex internal feedback circuits.

621.375.9:621.372.44 2136
**A Wide-Band Single-Diode Parametric Amplifier using Filter Techniques**—A. G. Little. (Proc. IRE, vol. 49, pp. 821–822; April, 1961.) An arrangement is described using parallel-tuned circuits at appropriate points along the signal line to give bandwidths up to 130 Mc at a center frequency of 3.3 Gc.

621.375.9:621.372.44 2137
**A Nondegenerate *S*-Band Parametric Amplifier with Wide Bandwidth**—G. Schaffner and F. Voorhaar. (Proc. IRE, vol. 49, pp. 824–825; April, 1961.) Band-pass filters in the input and idler circuits are used to give a bandwidth of 80 Mc at a center frequency of 2.5 Gc. Operation in four different modes is possible.

621.375.9:621.372.44 2138
**A Nearly Optimum Wide-Band Degenerate Parametric Amplifier**—M. Gilden and G. L. Matthaei. (Proc. IRE, vol. 49, pp. 833–834; April, 1961.) A double-resonator single-diode design with 3-db bandwidth of 210 Mc centered on 1 Gc is given.

621.375.9:621.372.44:621.372.2 2139
**Interpretation of the Transmission-Line Parameters with a Negative-Conductance Load and Application to Negative-Conductance Amplifiers**—Stelzried. (See 2076.)

621.375.9:621.372.44:621.385.6 2140
**Behavior of Thermal Noise and Beam Noise in a Quadrupole Amplifier**—R. Adler and G. Wade. (Proc. IRE, vol. 49, p. 802; April, 1961.)

621.375.9:621.382.23 2141
**A Broad-Band Tunnel-Diode Amplifier**—N. F. Moody and A. G. Wacker. (Proc. IRE, vol. 49, p. 835; April, 1961.) A first-order theory for an amplifier using tunnel diodes is presented. The series resistance and inductance of the diodes is neglected except where stability is concerned. The amplifier could be built using strip or coaxial lines.

621.376.223 2142
**Elimination of Even-Order Modulation in Rectifier Modulators**—D. G. Tucker. (*J. Brit. IRE*, vol. 21, pp. 161–167; February, 1961.) The time-varying-resistance function of the modulator is considered not to be a square wave but to contain even-order carrier harmonics.

621.376.223 2143
**The Relative Magnitude of Modulation Products in Rectifier Modulators and some Effects of Feedback**—D. P. Howson. (*J. Brit. IRE*, vol. 21, pp. 275–281; March, 1961.) The various modulation products occurring in series, shunt and ring modulators are evaluated for square-wave switching of the rectifiers assuming that the terminations are resistive. The information is used in the design of feedback modulators.

621.376.33 2144
**The Round-Travis Discriminator**—K. R. Sturley. (*Electronic Tech.*, vol. 38, pp. 186–189; May, 1961.) A re-examination of Johnstone's analysis of the Round-Travis amplitude discriminator (1220 of 1957) shows that the conditions indicated are not those giving minimum distortion; a correction is proposed.

## GENERAL PHYSICS

530.162:621.391.822 2145
**Thermal Noise in Dissipative Media**—H. A. Haus. (*J. Appl. Phys.*, vol. 32, pp. 493–500; March, 1961.) To account for the spontaneous thermal fluctuations in a general dissipative medium, a current-source term is introduced into Maxwell's equations. The results are applicable to nonuniform media and to media at nonuniform temperatures.

537.311.33 2146
**Theory of Electron-Phonon Interactions**—G. D. Whitfield. (*Phys. Rev.*, vol. 121, pp. 720–734; February, 1961.) "The theory of the interaction of electrons and acoustic phonons in nonpolar crystals has been formulated in terms of a new set of basis states, whose wave functions are essentially Bloch functions that deform with the lattice. The major part of the interaction may then be calculated in terms of the strain tensor rather than the displacement of the lattice. A result of the theory is a generalization of the deformation potential theorem."

537.525.72:538.569 2147
**A Gas Discharge Free in Space, Glowing at the Focus of a Radar Paraboloid**—J. Geerk and H. Kleinwächter. (*Z. Phys.*, vol. 159, pp. 378–383; August, 1960.) An electrodeless gas discharge in a low-pressure vessel was achieved using an arrangement of two paraboloidal mirrors and coherent EM radiation at 3 cm λ.

537.529:537.311 2148
**On the Relation between Zener Breakdown and Residual Resistance in Crystals**—P. Gosar. (*Nuovo Cim.*, vol. 18, pp. 241–250; October, 1960. In English.) The theory of Zener breakdown in crystals is extended to the case of very strong electric fields.

537.533.8 2149
**Energy Dissipation and Secondary Electron Emission in Solids**—H. Kanter. (*Phys. Rev.*, vol. 121, pp. 677–681; February, 1961.) Experiments show a proportionality between secondary-electron yield and energy dissipation by incident electrons.

537.533.8 2150
**Contribution of Back-Scattered Electrons to Secondary-Electron Formation**—H. Kanter. (*Phys. Rev.*, vol. 121, pp. 681–684; February, 1961.) The contribution observed was large even in materials of low Z; it was 40 per cent in Al for 10-kev electrons.

537.56 2151
**Pulse Conduction in Decaying Plasma**—V. Arunasalam and J. D. Trimmer. (*Rev. Sci. Instr.*, vol. 32, pp. 282–285; March, 1961.) Apparatus has been constructed in which plasma, ionized by 144-Mc RF excitation, is subjected to repeated submicrosecond voltage pulses immediately after excitation is removed; the current is measured.

537.56 2152
**Generation and Measurement of Highly Ionized Quiescent Plasmas in Steady State**—R. C. Knechtli and J. Y. Wada. (*Phys. Rev. Lett.*, vol. 6, pp. 215–217; March, 1961.) A simple generation technique is described. Experimental results validate double-probe measurements, indicate purely ambipolar diffusion in homogeneous dc magnetic fields and give a recombination coefficient of Cs plasmas below $10^{-10}$ cm$^3$ sec$^{-1}$.

537.56 2153
**Drift Velocities of Slow Electrons in Helium, Neon, Argon, Hydrogen and Nitrogen**—J. L. Pack and A. V. Phelps. (*Phys. Rev.*, vol. 121, pp. 798–806; February, 1961.)

537.56:537.533 2154
**Electromagnetic Interaction of a Beam of Charged Particles with Plasma**—J. Neufeld and P. H. Doyle. (*Phys. Rev.*, vol. 121, pp. 645–658; February, 1961.) The theory of growing plasma waves is generalized to include waves propagated in directions other than the beam direction.

537.56:538.566 2155
**A Method for Measuring High Electron Densities in Plasmas**—S. Takeda and M. Roux. (*J. Phys. Soc. Japan*, vol. 16, pp. 95–98; January, 1961.) It is proposed that the standing-wave pattern produced by plane microwaves at the plasma boundary be measured to give the complex reflection coefficient which is related to the electron density and collision frequency.

537.56:538.63 2156
**Diffusion of Plasma across a Magnetic Field**—J. B. Taylor. (*Phys. Rev. Lett.*, vol. 6, pp. 262–263; March, 1961.)

537.56:621.372.8 2157
**The Influence of the Langmuir Stratum between Plasma and Container Wall on Wave Propagation in a Plasma Cable**—W. O. Schumann. (*Z. angew. Phys.*, vol. 12, pp. 298–300; July, 1960.) See also 1121 of April.

538.12:538.221 2158
**Field External to Open-Structure Magnetic Devices Represented by Ellipsoid or Spheroid**—H. Chang (*Brit. J. Appl. Phys.*, vol. 12, pp. 160–163; April, 1961.) Mathematical expressions for the fields are given and curves are plotted with dimensional ratio as parameter.

538.56:537.56 2159
**The Electromagnetic Fields of a Dipole in the Presence of a Thin Plasma Sheet**—J. R. Wait. (*Appl. Sci. Res.*, vol. B8, nos. 5/6, pp. 397–417; 1960.) An extension of Poeverlein's work (3604 of 1958) is given. Under the assumption that the thickness of the slab is small, expressions for the resultant fields are obtained See also 2352.

538.566 2160
**Impedance Boundary Conditions for Imperfectly Conducting Surfaces**—T. B. A. Senior. (*Appl. Sci. Res.*, vol. B8, nos. 5/6, pp. 418–436; 1960.) It is shown how the exact EM boundary conditions at the surface of a material of large refractive index can be approximated to yield the usual impedance or Leontovich boundary conditions. [See, *e.g.*, 1901 of 1947 (Leontovich and Fock)].

World Radio History

538.566 2161
**Propagation of Electromagnetic Surface Waves along Wedge Surfaces**—W. E. Williams (*Quart. J. Mech. Appl. Math.*, vol. 13, pt. 3, pp. 278–284; August, 1960.) The conditions under which surface waves can be excited by a plane EM wave incident on a wedge are determined.

538.566 2162
**Impedance Boundary Conditions for Statistically Rough Surfaces**—T. B. A. Senior. (*Appl. Sci. Res.*, vol. B8, nos. 5/6, pp. 437–462; 1960.)

538.566:535.42 2163
**Scalar Diffraction by a Prolate Spheroid at Low Frequencies**—T. B. A. Senior. (*Canad. J. Phys.*, vol. 38, pp. 1632–1641; December, 1960.)

538.566:535.43 2164
**Scattering by a Narrow Unidirectionally Conducting Infinite Strip**—S. R. Seshadri. (*Canad. J. Phys.*, vol. 38, pp. 1623–1631; December, 1960.) Expressions for the far-zone fields and the first two terms in the series for the total scattering cross section are obtained.

538.566:535.43 2165
**Backscattering from a Conducting Cylinder with a Surrounding Shell**—M. A. Plonus. (*Canad. J. Phys.*, vol. 38, pp. 1665–1676; December, 1960.)

538.566:535.43 2166
**Scattering by a Grating: Parts 1 and 2**—R. F. Millar. (*Canad. J. Phys.*, vol. 39, pp. 81–118; January, 1961.) Anomalies occur in the angular spectrum of plane waves scattered by a grating when any of the waves propagate tangentially along the surface. This behavior is analyzed theoretically for a wave function vanishing on the grating elements, and for the derivative of the wave function vanishing.

538.566:537.56 2167
**Nonlinear Interaction of an Electromagnetic Wave with a Plasma Layer in the Presence of a Static Magnetic Field: Part 1—Theory of Harmonic Generation**—R. F. Whitmer and E. B. Barrett. (*Phys. Rev.*, vol. 121, pp. 661–668; February, 1961.) Theory of propagation through an anisotropic ionized layer, as a function of $H$, $n_e$, $\nu$, incident field strength, and layer thickness, is presented.

538.566.2 2168
**Penetration of Microwaves into the Rarer Medium in Total Reflection**—J. J. Brady, R. O. Brick, and M. D. Pearson. (*J. Opt. Soc. Am.*, vol. 50, pp. 1080–1084; November, 1960.) Using right-angle prisms separated by a narrow air gap, transmission and reflection coefficients of paraffin, sulphur and NaCl have been measured at 3 cm $\lambda$ as a function of the gap width.

538.566.2 2169
**Refraction and Diffraction of Pulses**—W. E. Williams. (*Canad. J. Phys.*, vol. 39, pp. 272–275; February, 1961.) A solution for reflection and refraction of a plane pulse at a plane surface is obtained by Fourier synthesis using a method which is also valid when total reflection occurs.

538.569.4:535.853 2170
**A Spectrometer for Paramagnetic Electron Resonance with Different Methods of Detection**—D. Bösnecker. (*Z. angew. Phys.*, vol. 12, pp. 306–314; July, 1960.) The equipment described can be used for the klystron frequency-modulation and magnetic sweep methods of measurement.

538.569.4:538.221 2171
**Theory of Ferro- and Antiferro-magnetic Resonance Absorption**—T. Oguchi and A. Honma. (*J. Phys. Soc. Japan*, vol. 16, pp. 79–94; January, 1961.)

538.569.4:538.221:621.318.134 2172
**Longitudinal Ferrimagnetic Resonances**—R. K. Wangsness. (*Phys. Rev.*, vol. 121, p. 472; January, 1961.) Susceptibility components are calculated for a triangular ferrimagnetic system when the oscillating field is parallel to both the constant field and the net magnetization. See also 499 of February.

538.569.4:538.221:621.318.134 2173
**The Relation of Transition Parameters for Linear Processes to Measurable Parameters in Ferrimagnetic Resonance**—P. E. Seiden. (*J. Phys. Chem. Solids*, vol. 17, pp. 259–266; January, 1961.) Calculated expressions include the effect of the reaction of spin waves back on to the uniform precession. The consequences of its neglect in previous calculations by others are discussed.

538.569.4:621.375.9:535.61-1/2 2174
**Confocal Multimode Resonator for Millimetre through Optical Wavelength Masers**—G. D. Boyd and J. P. Gordon. (*Bell Sys. Tech. J.*, vol. 40, pp. 489–508; March, 1961.) The mode patterns and diffraction losses are obtained for a resonator formed by two concave spherical reflectors. These are shown to be a minimum when the reflector spacing equals the common radius of curvature of the reflectors. The optical alignment is not extremely critical.

538.569.4:621.375.9:535.61-2 2175
**Resonant Modes in a Maser Interferometer**—A. G. Fox and T. Li. (*Bell Sys. Tech. J.*, vol. 40, pp. 453–488; March, 1961.) A theoretical investigation is made of the diffraction of EM waves in Fabry-Perot interferometers when used as resonators in optical masers. Curves for field distribution and diffraction loss are given for different mirror geometries and different modes.

539.2 2176
**Collective Excitation of Electrons in Degenerate Bands: Part 2—Collective Excitations in a Metallic $p$-Band**—T. Izuyama. (*Prog. Theoret. Phys.*, vol. 24, pp. 899 907; October, 1960.) Part 1: 827 of March.

## GEOPHYSICAL AND EXTRA-TERRESTRIAL PHENOMENA

523.164:621.396.677 2177
**The Radio Telescope for 7.9 Metres Wavelength at the Mullard Observatory**—C. H. Costain and F. G. Smith. *Monthly Notices Roy. Astron. Soc.*, vol. 121, no. 4, pp. 405–412; 1960.) The pencil-beam system described is based on the principle of aperture synthesis and has a resolution of $0.8° \times 0.8°$. A survey of the sky between R.A. $05^h$ and $17^h$, declination $+10°$ to $+50°$ is given.

523.164.4 2178
**The Radio Spectrum of the Andromeda Nebula.**—J. E. Baldwin and C. H. Costain. (*Monthly Notices Roy. Astron. Soc.*, vol. 121, no. 4, pp. 413–417; 1960.) New observations have been made at 38 and 178 Mc. Results are compared with those made at Jodrell Bank at 408 Mc by Large, *et al.* (2937 of 1959) and show that all parts of the nebula have a similar spectrum.

523.165 2179
**Asymmetry in the Recovery from a Very Deep Forbush-Type Decrease in Cosmic-Ray Intensity**—D. C. Rose and S. M. Lapointe. (*Canad. J. Phys.*, vol. 39, pp. 239–251; February, 1961.) The intensity-time curve for cosmic rays recorded at 30 locations all over the world is analyzed. Recovery occurred at each station at the same effective local time, corresponding to arrival from directions making 15° and 165° with the sun-earth line.

523.165:523.75 2180
**Cosmic-Ray Flare of November 20, 1960**—R. T. Hansen. (*Phys. Rev. Lett.*, vol. 6, pp. 260–262; March, 1961.) A solar flare was observed visually at a height at least $10^5$ km above the chromosphere, at a time which corresponds with a period of increased cosmic-ray neutron flux and a burst in solar noise flux [1496 of May (Covington and Harvey)].

523.165:550.383.4 2181
**The Drift Velocity of Charged Particles in the Magnetic Dipole Field**—M. Siebert. (*Naturwiss.*, vol. 47, p. 351; August, 1960.) A more accurate expression for the drift velocity of particles in the vicinity of the equator is derived by allowing for a second centrifugal-force term in the original equation.

523.165:550.385 2182
**Equation of a Charged Particle Shell in a Perturbed Dipole Field**—R. H. Pennington. (*J. Geophys. Res.*, vol. 66, pp. 709–712; March, 1961.) The equation obtained agrees with the shell measured by satellite 1958 E following the nuclear explosion of September 6, 1958.

523.165:550.385.4 2183
**Effect of Hydromagnetic Waves in a Dipole Field on the Longitudinal Invariant**—E. N. Parker. (*J. Geophys. Res.*, vol. 66, pp. 693–708; March, 1961.) Hydromagnetic waves of period 1 second and amplitude $10^{-3}$ G at 6 earth radii may cause a systematic lowering of mirror points with subsequent loss of particles in atmospheric collisions. Two models for electron density variation along a field line are investigated. Particle acceleration by the Fermi process is dominated by particle loss at mirror points, and it is suggested that only high-frequency waves will give effective acceleration. See also 533 of February.

523.165:550.385.4 2184
**Preliminary Report on Cosmic-Ray Intensity during Magnetic Storms in July 1959**—J. G. Roederer, O. R. Santochi, J. C. Anderson, J. M. Cardoso and J. R. Manzano. (*Nuovo Cim.*, vol. 18, pp. 120–130; October, 1960. In English.) Observations at three stations show that there was no appreciable change in the primary variation spectrum for three successive Forbush decreases. This may be interpreted as an indication of a linear superposition of cosmic-ray modulation effects during the July disturbances. For an analysis of cosmic-ray intensity recorded at Mina Aguilar during this period as a function of time, see *Ibid.*, pp. 131–135.

523.165:550.385.4 2185
**Cosmic-Ray Intensity Variations during the Magnetic Storm in May 1959**—J. R. Manzano, J. G. Roederer and O. R. Santochi. (*Nuovo Cim.*, vol. 18, pp. 136–146; October, 1960. In English.) The primary variation spectrum has been estimated in a similar manner to that used for the July storms (see 2184). Results for both storm periods have been compared, showing a number of common features.

523.3:621.396.96 2186
**Some Properties of Radio Waves Reflected from the Moon and their Relation to the Lunar Surface**—T. Hagfors. (*J. Geophys. Res.*, vol. 66, pp. 777–785; March, 1961.) The properties of the echoes are described in terms of the correlation of the complex amplitudes of two sine waves at frequencies separated by $\Delta\omega$, reflected from the surface. The correlation technique can be extended to two-dimensional mapping of a rotating rough body. A statistical model of the lunar surface roughness is derived in which rms slopes of 1/20 to 1/10 are assumed.

World Radio History

523.3:621.396.96 2187
**A Method of Evaluating the Intensity of Radio Signals Reflected from the Surface of the Moon**—M. P. Dolukhanov. (*Radiotekhnika (Moscow)*, vol. 15, pp. 5–8; May, 1960.) Propagation losses can be determined by supposing that the reflected wave is formed within the limits of the first Fresnel half-zone and taking account of the curvature of the reflecting surface. The method provides a more accurate picture of the reflection phenomena.

550.385 2188
**Some Evidence of Hydromagnetic Waves in the Earth's Magnetic Field**—M. Sugiura. (*Phys. Rev. Lett.*, vol. 6, pp. 255–257; March, 1961.) Combining changes in the $H$ and $D$ components of field indicate that the horizontal magnetic vector is elliptically polarized. This may be due to a hydromagnetic wave traveling obliquely to the earth's magnetic field.

550.385 2189
**Low-Latitude and High-Latitude Geomagnetic Agitation**—E. R. Hope. (*J. Geophys. Res.* vol. 66, pp. 747–776; March, 1961.) Detailed study is made of geomagnetic agitation ($\Delta H$). Above 60° the three daily maxima of $\Delta H$ have spiral loci. Agitation is an order of magnitude lower at middle latitudes increasing again towards the equator. Ionospheric current systems (with auroral electro-jets) are examined in the above context. The occurrence frequency of sudden commencements at one station exhibits a diurnal variation. A recent theoretical explanation of this is examined. Over 100 references.

550.385.2 2190
**On the Seasonal Variation in Lunar and Solar Geomagnetic Tides in the Geomagnetic Equatorial Region**—K. S. Raja Rao. (*J. Atmos. Terr. Phys.*, vol. 20, pp. 289–294; April, 1961.)

550.385.4:523.746 2191
**Influence of Sunspots on Geomagnetic Disturbance**—F. Ward and R. Shapiro. (*J. Geophys. Res.*, vol. 66, pp. 739–746; March, 1961.) "The hypothesis that the ejection of solar corpuscles is influenced by interactions of 'active region' magnetic fields is tested empirically. The results do not support the hypothesis."

550.385.4:551.594.5 2192
**Dipole-Field Type Magnetic Disturbances and Auroral Activities**—B. K. Bhattacharyya. (*Canad. J. Phys.*, vol. 39, pp. 350–366; February, 1961.) The magnetic perturbation produced at the ground by the current system associated with an electric dipole at 100 km is calculated. Magnetograms obtained during an auroral display are analyzed to deduce the position and motion of the equivalent dipoles. These correspond closely with prominent visual auroral forms.

551.507.362.2 2193
**Minimum Range to Artificial Earth Satellites**—K. Toman. (*Nature*, vol. 190, pp. 333–334; April, 1961.) A complete expression for calculating, from Doppler measurements, the minimum passing range between satellite and observer is derived, and its application under various orbital conditions is discussed.

551.507.362.2 2194
**Loss of Mass in Echo Satellite**—I. I. Shapiro and H. M. Jones. (*Science*, vol. 133, p. 579; February, 1961.) A correction to 1157 of April and comparison of predictions with observed orbital data are given.

551.507.362.2 2195
**Spin-Rate of the Satellite Echo I as Determined by a Tracking Radar**—G. E. K. Lockwood. (*Canad. J. Phys.*, vol. 38, no. 12, p. 1713; 1960.) Radar observation of Echo I (1960 $\iota$) indicate that between passes 131 and 217 the spin rate increased from 1.63 to 1.88 rpm. Between these two observations the satellite first started passing into the earth's shadow, which possibly resulted in changes in internal pressure and subsequent deformation of the balloon.

551.507.362.2:621.396.934 2196
**New Satellite Tracking Station in Great Britain**—(See 2375.)

551.510.53 2197
**Magnesium and Calcium Ions in the Upper Atmosphere of the Earth**—V. G. Istomin. (*Dokl. Akad. Nauk SSSR*, vol. 136, pp. 1066–1068; February, 1961.) The presence of $Mg^+$ and $Ca^+$ ions was recorded by a rocket-borne mass spectrometer launched from a moderate latitude. Peaks in the $Mg^+$ ion concentration reaching $1.36\times10/^4cm^3$ were observed at heights of 103.5 and 105 km.

551.510.53:551.507.362 2198
**Daytime and Nighttime Atmospheric Properties Derived from Rocket and Satellite Observations**—H. K. Kallmann-Bijl. (*J. Geophys. Res.*, vol. 66, pp. 787–795; March, 1961.) A summary of the values of atmospheric density obtained during the interval from 1957 to 1960 from rockets and satellites is presented, and is fitted into a model atmosphere obtained by integrating the hydrostatic equation. A general decrease since 1957 in atmospheric density at all altitudes is confirmed.

551.510.535 2199
**Rocket Electron Density Measurements at Fort Churchill, Canada**—A. W. Adey and W. J. Heikkila. (*Canad. J. Phys.*, vol. 39, pp. 219–221; January, 1961.) A discussion is given of the results of a rocket flight during quiet ionospheric conditions using the two-frequency phase-comparison technique of Seddon (402 of 1954.)

551.510.535 2200
**Longitudinal and Latitudinal Effect of the Ionosphere Estimated by Observation on Board the Soya**—H. Shibata, K. Sawada and S. Taguchi. (*J. Radio Res. Labs., Japan*, vol. 7, pp. 575–582; November, 1960.) Values of $f_0F_2$ at hourly intervals are plotted against geomagnetic latitude for the range 10°S–70°S covered by the voyages from Japan to Antarctica in December and January, 1956–1957, 1958–1959, and 1959–1960.

551.510.535 2201
**Ionization of $E$ Layer by X-Rays**—S. N. Ghosh and S. Nand. (*Indian J. Phys.*, vol. 34, pp. 516–526; November, 1960.) The total amount of solar X-ray energy absorbed within the $E$ layer is calculated from available rocket and absorption measurements. Only X rays in the wavelength region 5–100°A are absorbed, the amount of energy involved being estimated at 0.19 erg $cm^{-2}$ $sec^{-1}$.

551.510.535 2202
**Some Observations of the Occurrence and Movement of Sporadic-$E$ Ionization**—J. Harwood. (*J. Atmos. Terr. Phys.*, vol. 20, pp. 243–262; April, 1961.) An analysis is given of simultaneous observations of $E_s$ clouds in Europe by ionosondes at various locations, by a 17-Mc rotating-antenna back-scatter sounder at Slough, England, and by an oblique-propagation experiment at 17 Mc over 700 km. The mean cloud diameter was about 200 km. About twice as many clouds occurred to the south of Slough as to the north with an average duration of 2½ hours. Of 143 clouds, one third drifted, predominantly to the southwest, at a mean speed of 60 m. The movement of the clouds did not correlate with wind velocities.

551.510.535 2203
**The $F$ Layer at Sunrise**—M. Rishbeth and C. S. G. K. Setty. (*J. Atmos. Terr. Phys.*, vol. 20, pp. 263–276; April, 1961.) Observations at Cambridge and Slough, England, show that at fixed heights in the $F$ region, just after layer sunrise, the electron density increases faster in winter than in summer, and faster at sunspot maximum than at sunspot minimum. It is postulated that seasonal changes of atmospheric composition alter the rates of electron production and loss, thereby causing both the "noon" and "sunrise" seasonal $F_2$-layer anomalies.

551.510.535 2204
**Diffusion of Ionization in the Sunrise $F$ Layer**—H. Rishbeth. (*J. Atmos. Terr. Phys.*, vol. 20, pp. 277–288; April, 1961.) Some idealized calculations support the assumption made in the previous paper that the rare of increase of $F$-region electron density, just after sunrise, depends primarily on the rate of production of ionization. At this time the loss, diffusion and transport of ionization are of secondary importance.

551.510.535 2205
**Travelling Disturbances in the $F$ region over Waltair**—E. B. Rao and B. R. Rao. (*J. Atmos. Terr. Phys.*, vol. 20, pp. 296–297; April, 1961.) A description is given of the general diurnal and seasonal characteristics of traveling disturbances as observed on $P'(t)$ and $P'(f)$ records extending over two years.

551.510.535:523.164:550.385.37 2206
**Simultaneous Observations of Pulsations in the Geomagnetic Field and in Ionospheric Absorption**—S. Ziauddin. (*Canad. J. Phys.*, vol. 38, pp. 1714–1715; December, 1960.) On September 20 and 21, 1959, at 0700 L.M.T. regular pulsations were recorded simultaneously on a) a riometer operating on a frequency of 34 Mc and b) a magnetometer measuring the $H$ component of the geomagnetic field. For many cycles the pulsations remain in phase but on occasions they are in antiphase. The period of the geomagnetic pulsations suggests that they are due to toroidal hydromagnetic oscillations of the outer atmosphere; possible connections with ionospheric absorption are briefly considered.

551.510.535:523.745 2207
**Analysis of the Variation of $f_0E$ and Index of Solar Activity**—H. Shibata and S. Watanabe. (*J. Radio Res. Labs, Japan*, vol. 7, pp. 621–635; November, 1960.) It is assumed that, for both the diurnal and annual changes in $f_0E$, the critical frequency is proportional to $\cos^{\frac{1}{4}}\chi$. The values of $f_0E$ are extrapolated to $\chi=0$ for several stations and an empirical relation between the values for $\chi=0$ and the sunspot number is derived.

551.510.535:550.385 2208
**Vertical Drift in the $E$ layer of the Ionosphere during Geomagnetic Disturbances**—H. Kohl. (*Arch. elekt. Übertragung*, vol. 14, pp. 314–316; July, 1960.) The velocity is estimated of the vertical drift due to geomagnetic disturbances. The possible rise of the $E$ layer is shown to be only a few hundred meters which cannot be measured by ionospheric recorders. For an investigation of $F$-layer movements, see 1848 of June.

551.510.535:621.3.087.4 2209
**Active High-Frequency Spectrometers for Ionospheric Sounding: Part 1—Direct Recording of Ionospheric Characteristics**—K. Bibl. (*Arch. elekt. Übertragung*, vol. 14, pp. 341–347; August, 1960.) On the basis of the method not noted earlier (2729 of 1956), equipment has been designed which provides direct records of M.U.F., $h'$ and $f_n$ as a function of time. Sample records are reproduced and applications of the method are discussed. A method of distinguish-

World Radio History

ing height ranges in $F$-layer $f_n(t)$ records using color film is noted.

551.510.535:621.391.812.3 2210
**Analysis of Random Fading Records**—Khastgir and Singh. (See 2357.)

551.510.535:621.391.812.63 2211
**Measurement of the Ionospheric Absorption during the I.G.Y. at Kokubunji**—J. Yasuda and H. Sugiuchi. (*J. Radio Res. Labs., Japan*, vol. 7, pp. 551–574; November, 1960.) The diurnal variation in absorption shows an asymmetry about noon which is attributed to the changes in vertical drift motion in the $D$ layer associated with the $Sq$ current system. The marked winter anomaly effect cannot be explained by a change in the electron density distribution in the normal $D$ layer.

551.510.535:621.391.812.63 2212
**Ionospheric Motions Observed with High Frequency Back-Scatter Sounders**—L. H. Tveten. (*J. Res. NBS*, vol. 65D, pp. 115–127; March and April, 1961.) "Techniques for determining the characteristics of movements of irregularities in the $F_2$-region by the use of backscatter records are described. The results of an analysis of backscatter data obtained during December 1952, at Sterling, Virginia, at a frequency of about 13.7 Mc/s are presented and found to be in good agreement with those of other investigators of ionospheric motions."

551.510.535:621.391.812.63.029.62/.63 2213
**Effect of the Magnetic Field in Ionospheric Back-Scatter**—E. E. Salpeter. (*J. Geophys. Res.*, vol. 66, pp. 982–984; March, 1961.) Backscatter spectral lines may be used to calculate magnetic field, ion mass and plasma temperature. See also 1290 of April (Fejer).

551.510.535(98):621.391.812.631 2214
**High-Frequency Radio-Wave Blackouts at Medium and High Latitudes during a Solar Cycle**—Collins, Jelly, and Matthews. (See 2351.)

551.594.5 2215
**Theory of Auroral Morphology**—J. W. Kern and E. H. Vestine. (*J. Geophys. Res.*, vol. 66, pp. 713–723; March, 1961.) The theory is based on the production of instabilities in electron sheets. It predicts observed features relating to the duration of homogeneous arcs and the transition from glow to homogeneous arcs to ray arcs and draperies. Other observations explained are certain phenomena in flaming auroras and the lowering of mirror points in certain conditions.

551.594.5 2216
**Reply to Some Comments by Malville concerning the Midnight Auroral Maximum**—E. H. Vestine and J. W. Kern. (*J. Geophys. Res.*, vol. 66, pp. 989–991; March, 1961.) The preponderance of aurora near magnetic midnight is discussed. See 149 of January (Malville).]

551.594.5:550.385.4 2217
**The Relationship between Unique Geomagnetic and Auroral Events**—Y. Sobouti. (*J. Geophys. Res.*, vol. 66, pp. 725–737; March, 1961.) At eleven Canadian stations, a high correlation is found between the geomagnetic latitudes of the southern extents of auroras and the most southerly current lines. A southward drift occurs simultaneously in an aurora and the accompanying ionospheric currents.

551.594.5:551.510.535 2218
**Relationship between Red Auroral Arcs and Ionospheric Recombination**—G. A. M. King and F. E. Roach. (*J. Res. NBS*, vol. 65D, pp. 129–135; March and April, 1961.) An auroral arc (6300 Å), observed photometrically to be north of Boulder, Colo., has been identified with oblique echoes on ionograms taken near Boulder.

551.594.6 2219
**Generation of Very-Low-Frequency Noise in the Exosphere by the Cerenkov Effect**—R. Gendrin. (*Compt. rend. Acad. Sci., Paris*, vol. 251, pp. 1122–1123; September, 1960.) The Čerenkov effect, produced by relatively slow-moving particles of solar origin, is considered as a possible mechanism for the generation and propagation of VLF noise. The theory is briefly discussed in relation to a "traveling-wave tube" model proposed by Gallet (1575 of 1959) to explain similar VLF emissions.

551.594.6 2220
**Energy Fluxes from the Cyclotron Radiation Model of VLF Radio Emission**—W. B. Murcray and J. H. Pope. (PROC. IRE, vol. 49, pp. 811–812; April, 1961.) Comment on a paper by Santirocco (4253 of 1960) is given.

551.594.6 2221
**Classification of the Waveforms of Atmospherics**—S. R. Khastgir and R. S. Srivastava. (*J. Inst. Telecommun. Engrs., India*, vol. 6, pp. 260–265; October, 1960.) A review with 28 references is given.

551.594.6 2222
**The Determination of the Distance of Atmospherics from their Waveform**—R. Schminder. (*Met. Zeit.*, vol. 14, pp. 212–217; July-September, 1960.) Diagrams facilitating the determination of the distance of atmospherics are given; their use is discussed with reference to the results of measurements. A reflection height of 70 km was assumed for daytime conditions, and 90 km for nighttime propagation.

551.594.6 2223
**Guidance of Radio Whistlers by the Earth's Magnetic Field**—R. Gendrin. (*Compt. rend. Acad. Sci., Paris*, vol. 251, pp. 1085–1087; August, 1960.) In an anisotropic medium there is for each frequency an emission angle ($\theta \neq 0$ of such a value that the ray propagates strictly along the line of magnetic force with a velocity which is independent of frequency.

551.594.6 2224
**Remarks on the Annual and Diurnal Variations of the Occurrence of Whistlers**—L. Klinker and G. Entzian. (*Met. Zeit.*, vol. 14, pp. 207–212; July-September, 1960.) The annual variation of whistler density observed at Kühlungsborn appears to be correlated with the thunderstorm activity of South Africa and not with that of the conjugate point which is at a higher geomagnetic latitude. Noctural variations of whistler density show phase differences between summer and winter, which are attributed to absorption in the lower ionosphere.

551.594.6 2225
**The Hydrogen Ion Effect in Whistler Dispersion**—R. E. Barrington and T. Nishizaki. (*Canad. J. Phys.*, vol. 38, pp. 1642–1653; December, 1960.) Careful analysis of four low-altitude whistlers shows deviations at low frequencies from the law $tf^{\frac{1}{2}} = \text{const}$. This observation is explained in terms of a simple atmospheric model in which the gas above about 1000 km is mainly hydrogen.

551.594.6:621.3.087.4 2226
**Initial Results of a New Technique for Investigating Sferic Activity**—G. Hefley, R. H. Doherty and R. F. Linfield. (*J. Res. NBS*, vol. 65D, pp. 157–166; March and April, 1961.) The system was developed for the automatic measurement of the complex spectral characteristics and for the automatic high-speed processing of statistical data. Typical results are presented and discussed.

## LOCATION AND AIDS TO NAVIGATION

534.88 2227
**Prospects and Limitations of the Use of Low Frequencies in Echo Location**—G. Pazienza. (*Alta Frequenza*, vol. 29, pp. 323–336; June-August, 1960.) The frequency dependence of the parameters which determine the range of underwater echo-location equipment is investigated. The ranges obtainable at frequencies between 2 and 30 kc are calculated, and the problem of noise interference is discussed.

621.396.96:621.375.9:621.372.44 2228
**Radar Sensitivity with Degenerate Parametric Amplifier Front End**—J. C. Green, W. D. White, and R. Adler. (PROC. IRE, vol. 49, pp. 804–807; April, 1961.)

621.396.962.3:621.372.54 2229
**General Matched-Filter Analysis of Linear FM Pulse Compression**—G. E. Cook. (PROC. IRE, vol. 49, p. 831; April, 1961.) An extension of earlier work (2023 of 1960) is given.

621.396.963:621.396.65 2230
**Remote Presentation of Radar Information**—G. N. S. Taylor. (*Point to Point Telecommun.*, vol. 5, pp. 18–27; February, 1961.) The use of microwave links is discussed.

621.396.969.36 2231
**Proposed Monocycle-Pulse Very-High-Frequency Radar for Air-Borne Ice and Snow Measurement**—J. C. Cook. (*Commun. and Electronics*, no. 51, pp. 588–594; November, 1960. Discussion.) A method is proposed for investigating from the air the thickness of ice and snow masses. The system operating at about 100 Mc would radiate a single wave train from a spark gap, with the charge conductors shaped to encourage radiation of all frequency components in the spectrum of a short pulse.

## MATERIALS AND SUBSIDIARY TECHNIQUES

531.788.7 2232
**Hot-Cathode Magnetron Ionization Gauge for the Measurement of Ultra High Vacua**—J. M. Lafferty. (*J. Appl. Phys.*, vol. 32, pp. 424–434; March, 1961.) To extend the low pressure limit, an increase in the ratio of ion current to X-ray photocurrent is necessary. A magnetron gauge is discussed which is linear down to a pressure of $4 \times 10^{-14}$ mm Hg.

533.583:621.385.832 2233
**The Determination of the Quantity of Barium Evaporated from Getters**—P. Della Porta and S. Origlio. (*Le Vide*, vol. 15, pp. 446–455; November/December, 1960. In French and English.) The complexometric method described is applied in the determination of the distribution of Ba on the screen of a television tube when using different shapes of getter.

535.215 2234
**Effect of Photoexcitation on the Mobility in Photoconducting Insulators**—R. H. Bube and H. E. MacDonald. (*Phys. Rev.*, vol. 121, pp. 473–483; January, 1961.) The Hall mobility of carriers in photoconducting insulators can be varied over an appreciable range by the effects of photoexcitation. Suitable use of the phenomena leads to knowledge about carrier density, sign and mobility, and also gives information about the charge on and the cross section of the imperfection centers. Experiments on CdS and CdSe single crystals with conductivities in the range $10^{-9}$–$10^{-1}$ mho/cm illustrate the potentialities of the technique.

World Radio History

535.215:546.28 2235
**Some Preliminary Experiments Concerning the Influence of Band Bending on Photoelectric Emission**—J. J. Scheer. (*Philips Res. Repts.*, vol. 15, pp. 584–586; December, 1960.) "The theory that *p*-type semiconductors should exhibit a higher photoelectric quantum efficiency than *n*-type semiconductors is verified by measurements of the photoemission from cesium-covered silicon surfaces."

535.215:546.48'221 2236
**Cadmium Sulphide Photoconductive Sintered Layers**—M. J. B. Thomas and E. J. Zdanuk. (*J. Electrochem. Soc.*, vol. 106, pp. 964–971; November, 1959.) Dependence of photoconduction characteristics on the composition and formation of layers is investigated.

535.215:546.48'221 2237
**The Effect of Mechanical Surface Treatment on the Fine Structure of the Spectral Curves of Photoconductivity in Cadmium Sulphide Crystals**—E. F. Gross and B. V. Novikov. (*Fiz. Tverdogo Tela*, vol. 1, pp. 1882–1885; December, 1959.)

535.215:546.48'221 2238
**The Change of the Real Structure of CdS Single Crystals due to the Evaporation of Lattice Constituents in a Vacuum**—K. W. Böer, H. Hornung, and K. Zimmermann. (*Mber. dtsch. Akad. Wiss. Berlin*, vol. 2, nos. 3/4, pp. 159–161; 1960.) A report of heat-treatment tests on high-purity CdS crystals is given. Evaporation of Cd was observed at 380°C.

535.215:546.48'221 2239
**Influence of a Hydrogen Atmosphere on the Photoconduction of CdS Single Crystals**—M. Asche and F. Eckart. (*Mber. dtsch. Akad. Wiss. Berlin*, vol. 2, no. 5, pp. 261–266; 1960.)

535.215:546.48'221 2240
**Remarks on the Photoconduction of CdS Single Crystals with Excitation at the Fundamental Lattice Absorption Edge**—H. Gutjahr. (*Mber. dtsch. Akad. Wiss. Berlin*, vol. 2, no. 5, pp. 269–271; 1960.)

535.215:546.48'221 2241
**The Influence of Annealing in Vacuum and in Sulphur Vapour on the Real Structure of CdS Single Crystals**—K. W. Böer, H. Gutjahr, and H. Hornung. (*Z. Phys.*, vol. 159, pp. 495–504; August, 1960.) Investigations of the spectral distribution of photoconductivity are given. [See also 1190 of April (Berger, *et al.*)].

535.215:546.48'221 2242
**Photoconductivity of CdS-Type Photoconductors in the Vicinity of the Absorption Edge**—N. N. Winogradoff. (*J. Appl. Phys.*, vol. 32, pp. 506–609; March, 1961.) A new model for the photoconductivity mechanism is discussed.

535.215:546.48'221:538.63 2243
**The Influence of Temperature and Ambient Conditions on the Photoelectromagnetic (PEM) Effects in CdS**—(*J. Phys. Chem. Solids*, vol. 18, pp. 261–262; February, 1961. In German.)

535.215:546.817'231 2244
**The Preparation of Vapour-Deposited Lead Selenide Films of High Mechanical and Electrical Stability**—H. Gobrecht, F. Niemeck and K. E. Boeters. (*Z. Phys.*, vol. 159, pp. 533–540; August, 1960.)

535.376:546.47'221 2245
**Electroluminescence—a Disorder Phenomenon**—D. W. G. Ballentyne. (*J. Electrochem. Soc.*, vol. 107, pp. 807–810; October, 1960.) Experimental investigations show that electroluminescence only occurs in ZnS powders containing both sphalerite and wurtzite. This observation suggests that electroluminescence is a disorder phenomenon associated with stacking faults in the crystal.

535.376:546.47'221 2246
**The Action of Nickel and Cobalt in Electroluminescent Zinc Sulphide Phosphors**—P. Goldberg. (*J. Electrochem. Soc.*, vol. 106, pp. 948–954; November, 1959.) Luminescence characteristics are studied as a function of voltage, frequency, and concentration of Ni and Co. See also 2082 of 1956 (Lehmann: Haake).

537.226.8 2247
**The Temperature Dependence of Dielectric Constants**—E. E. Havinga. (*J. Phys. Chem. Solids*, vol. 18, pp. 253–255; February, 1961.) For isotropic and for cubic materials three factors contribute to the temperature dependence: the influences of volume expansion and of temperature on polarizability, and a direct volume-expansion effect. A simple method is given for determining the values of the separate contributions.

537.227 2248
**Contribution to the Theory of Ferro- and Antiferro-electrics**—V. I. Klyachkin. (*Fiz. Tverdogo Tela*, vol. 1, pp. 1874–1877; December, 1959.)

537.227:546.431'824–31 2249
**Quantitative Study of Low-Frequency Hysteresis Loops of Polarized Polycrystalline Barium Titanate**—G. W. Marks and D. A. Hanna. (*Commun. and Electronics*, pp. 799–808; January, 1961.)

537.227:547.476.3 2250
**Measurement of the Dielectric Nonlinearity of Rochelle Salt**—H. E. Müser. (*Z. angew. Phys.*, vol. 12, pp. 300–306; July, 1960.) Discrepancies between measured values of coercivity and those predicted by the theory of the dielectric properties of Rochelle salt are investigated with reference to ferroelectric hysteresis measurements (3008 of 1959).

537.227:547.476.3 2251
**The Origin of the Optical Representation of the Ferroelectric Domains of Rochelle Salt Crystals**—H. Flunkert. (*Z. Phys.*, vol. 159, pp. 253–271; July, 1960.) A quantitative interpretation of observed interference effects is given, and an appropriate domain model is proposed.

537.228.1:546.431'824–31 2252
**Effect of Pressure on the Piezoelectric Properties of Barium Titanate**—B. A. Rotenberg. (*Fiz. Tverdogo Tela*, vol. 1, pp. 1777–1781; December, 1959.)

537.228.1:546.431'824–31 2253
**The Depolarization Charge of Barium Titanate and its Connection with the Piezoelectric Effect**—F. I. Kolomoĭtsev and I. A. Izhak. (*Fiz. Tverdogo Tela*, vol. 1, pp. 1791–1793; December, 1959.) The sign of the surface charge during depolarization always corresponds to the sign of the piezoelectric charge during compression. The charge released during heating near the Curie point is directly proportional to the size of the piezoelectric modulus.

537.228.1:549.514.51 2254
**Piezoelectric Behaviour of Impacted Quartz**—R. A. Graham. (*J. Appl. Phys.*, vol. 32, p. 555; March, 1961.)

537.311.31+537.312.62]:538.632 2255
**Frequency-Dependent Hall Effect in Normal and Superconducting Metals**—P. B. Miller. (*Phys. Rev.*, vol. 121, pp. 435–450; January, 1961.) Calculations are made of the Hall current flow when an EM wave is incident on the metal in a static magnetic field. The entire frequency range is considered, with emphasis on the microwave region.

537.311.33 2256
**Recombination of Charge Carriers in Semiconductors with Any Conception of Recombination Centres**—K. Thiessen. (*Mber. dtsch. Akad. Wiss. Berlin*, vol. 2, nos. 3/4, pp. 149–158; 1960.) Calculations of lifetimes are based on the existence of two trapping levels.

537.311.33 2257
**Disturbances of Carrier Concentration in High Electric Field**—E. M. Conwell. (*J. Phys. Chem. Solids*, vol. 17, pp. 342–344; January, 1961.) Consideration of recombination of hot carriers on the basis of the Shockley-Read model for thermal carriers (420 of 1953) leads to a prediction of changes in carrier concentration occurring as a bulk effect in high fields.

537.311.33 2258
**Decay of Excess Carriers in Semiconductors: Part 2**—K. C. Nomura and J. S. Blakemore. (*Phys. Rev.*, vol. 121, pp. 734–740; February, 1961.) Theory of recombination of excess carriers, for large or small excess carrier densities, is presented for the case in which the trapping level and Fermi level of the intrinsic gap lie in opposite halves. Part 1: 1915 of 1959.

537.311.33 2259
**Physical Properties of Several II–V Semiconductors**—W. J. Turner, A. S. Fischler, and W. E. Reese. (*Phys. Rev.*, vol. 121, pp. 759–767; February, 1961.) Energy gaps and mobilities have been measured in $Zn_3As_2$, $ZnAs_2$, ZnSb, $Cd_3As_2$, $CdAs_2$ and CdSb. For $CdAs_2$ the resistivity and mobility anisotropy have also been investigated.

537.311.33 2260
**Composition Stability Limits of Binary Semi-conductor Compounds**—R. F. Brebrick. (*J. Phys. Chem. Solids*, vol. 18, pp. 116–128; February, 1961.)

537.311.33 2261
**Extended Curves of the Space Charge, Electric Field, and Free Carrier Concentration at the Surface of a Semiconductor, and Curves of the Electrostatic Potential Inside a Semiconductor**—C. E. Young. (*J. Appl. Phys.*, vol. 32, pp. 329–332; March, 1961.) The work of Kingston and Neustadter (3300 of 1955) has been extended, and curves are given which apply to materials of higher energy gap. Curves of electrostatic potential inside a semiconductor supplement are those given by Dousmanis and Duncan (848 of 1959).

537.311.33:538.569.4 2262
**Cyclotron and Paramagnetic Resonance in Strained Crystals**—G. E. Pikus and G. L. Bir. (*Phys. Rev. Lett.*, vol. 6, pp. 103–105; February, 1961.) Possible applications of resonance measurements on strained crystals are discussed, in particular the determination of the ratio of deformation potentials, investigation of semiconductors with toroidal energy surfaces, and the observation of spin resonance of free carriers in *p*-type Ge and Si.

537.311.33:546.23 2263
**The Influence of Tl and TlCl Impurities on the Conductivity and Photoconductivity of Selenium**—I. P. Shapiro. (*Fiz. Tverdogo Tela*, vol. 1, pp. 1782–1785; December, 1959.)

537.311.33:546.24 2264
**Magnetic Susceptibility and Galvanomagnetic Effects in Pure and *p*-Type Tellurium**—G. Fischer and F. T. Hedgcock. (*J. Phys. Chem. Solids*, vol. 17, pp. 246–253; January, 1961.)

World Radio History

Experimental studies between 4.2° and 500° K are described and the results discussed.

537.311.33:[546.28+546.289 2265
**The Influence of Deformation of the Electrical Properties of *p*-Germanium and Silicon**—G. E. Pikus and G. L. Bir. (*Fiz. Tverdogo Tela*, vol. 1, pp. 1828–1840; December, 1959.) Based on expressions derived earlier (4285 of 1960) a quantitative theory is developed and the changes in conductivity, Hall coefficient and magnetoresistance during uniform deformation are calculated. See 1657 of 1960 (Pikus).

537.311.33:[546.28+546.289 2266
**Segregation and Distribution of Impurities in the Preparation of Germanium and Silicon**—J. Goorissen. (*Philips Tech. Rev.*, vol. 21, pp. 185–195; June, 1960.) Two variants of the zone-melting technique are described which yield a product in which the concentration of the impurity is uniformly distributed.

537.311.33:546.28 2267
**Thermal Expansion of Silicon at Low Temperatures**—S. I. Novikova and P. G. Strelkov. (*Fiz. Tverdogo Tela*, vol. 1, pp. 1841–1843; December, 1959.)

537.311.33:546.28 2268
**Recombination Radiation from Silicon under Strong-Field Conditions**—L. W. Davies and A. R. Storm, Jr. (*Phys. Rev.*, vol. 121, pp. 381–387; January, 1961.) In an attempt to determine the distribution in energy of hot electrons and holes in Si placed in a strong electric field, measurements have been made of the spectral distribution of recombination radiation. The results indicate that intrinsic recombination radiation arises mainly from the decay of excitons rather than from direct recombination of electrons and holes.

537.311.33:546.28 2269
**Impurity Conduction in Silicon**—R. K. Ray and H. Y. Fan. (*Phys. Rev.*, vol. 121, pp. 768–779; February, 1961.) Various *n*- and *p*-type Si samples, of low impurity content, were studied, and conduction due to charge exchange between impurity centers which may be ionized by some compensating impurity was observed. The results are compared with current theories.

537.311.33:546.28 2270
**Impact Ionization of Impurities in Silicon**—J. C. Sohm. (*J. Phys. Chem. Solids*, vol. 18, pp. 181–195; February, 1961. In French.) Above a certain value of electric field impact, ionization multiplies by avalanche. This phenomenon has been observed in Ge, InP and Si. Experimental data for *n*- and *p*-type Si are given.

537.311.33:546.28 2271
**Residual Thermoelastic Stresses in Bonded Silicon Wafers**—T. D. Riney. (*J. Appl. Phys.*, vol. 32, pp. 454–460; March, 1961.) Stresses are investigated photoelastically. Methods normally employed with isotropic birefringent materials can be used.

537.311.33:546.28 2272
**Excess Tunnel Current in Silicon Esaki Junctions**—A. G. Chynoweth, W. L. Feldmann, and R. A. Logan. (*Phys. Rev.*, vol. 121, pp. 684–694; February, 1961.) The unexpectedly high excess current flow in Esaki junctions, when a medium forward bias is applied, has been studied experimentally. The results can be accounted for by a mechanism suggested by Yajima and Esaki (1257 of 1959), and an expression is derived for the excess current.

537.311.33:546.281'26:537.583 2273
**Electron-Emission-Microscope and Velocity-Distribution Studies on Silicon Carbide *p-n* Junction Emitters**—P. H. Gleichauf and V. Ozarow. (*J. Appl. Phys.*, vol. 32, pp. 549–550; March, 1961.)

537.311.33:546.289 2274
**Temperature Dependence of the Low-Frequency Fluctuations of Conductivity in Germanium**—M. I. Kornfel'd and D. N. Mirlin. (*Fiz. Tverdogo Tela*, vol. 1, pp. 1866–1868; December, 1959.) The results of measurements at temperatures between −20° and +100°C show that conductivity fluctuations in impure crystals are due to intrinsic conduction and are related to the generation and recombination of electron-hole pairs.

537.311.33:546.289 2275
**The Electrical Properties of Semiconductor Grain Boundaries**—H. A. Schell and H. F. Mataré. (*Met. Zeit.*, vol. 52, pp. 86–91; January, 1961.) Measurements of electrical characteristics were made at medium-tilt grain boundaries in oriented-growth Ge crystals. Devices based on grain-boundary effects are mentioned.

537.311.33:546.289 2276
**Resistivity Striations in Germanium Single Crystals**—H. Ueda. (*J. Phys. Soc. Japan*, vol. 16, pp. 61–66; January, 1961.) The relationship shown to exist between the period of the striations, growth rate and temperature gradient near the solid/liquid interface is explained by assuming a super-cooled state in the crystallizing solid/liquid interface.

537.311.33:546.289 2277
**Theory of the Magnetic Susceptibility of Holes in Germanium**—J. M. Luttinger and P. J. Stiles. (*J. Phys. Chem. Solids*, vol. 17, pp. 284–291; January, 1961.) "The theory of the magnetic susceptibility of free holes is given. A general method of calculation which will work for degenerate as well as simple bands is described, and applied to the valance band of Ge. Results are given for both Maxwell-Boltzmann and Fermi-Dirac statistics, and the possibility of comparison with experiments is discussed."

537.311.33:546.289 2278
**Electron-Hole Scattering and Minority-Carrier Mobility in Germanium**—T. P. McLean and E. G. S. Paige. (*J. Phys. Chem. Solids*, vol. 18, pp. 139–149; February, 1961.) An extension of earlier work by Paige (1567 of May) by the specific application of the theory to Ge in the temperature and impurity concentration ranges where measurements of the minority-carrier mobility have been made.

537.311.33:546.289 2279
**Diffusion of Silver, Cobalt and Iron in Germanium**—L. Y. Wei. (*J. Phys. Chem. Solids*, vol. 18, pp. 162–174; February, 1961.)

537.311.33:546.289 2280
**Recombination of Excess Carriers at Twin Structures in Germanium**—J. P. McKelvey. (*J. Appl. Phys.*, vol. 32, pp. 442–445; March, 1961.) The continuity equation is solved for recombination of excess carriers at twin structures. The twin boundary recombination velocity is determined from lifetime measurements.

537.311.33:546.289 2281
**Relation between Surface Concentration and Average Conductivity in Diffused Layers in Germanium**—F. B. Cuttrias. (*Bell Sys. Tech. J.*, vol. 40, pp. 509–521; March, 1961.) An expression is derived for the average conductivity of a diffused layer in semiconductor material as a function of the surface concentration of the diffused impurity and the background impurity concentration.

537.311.33:546.289:539.12.04 2282
**Change of Surface State of Ge by Electron Bombardment**—K. Komatsubara. (*J. Phys. Soc. Japan*, vol. 16, pp. 125–126; January, 1961.) Changes are deduced from observed variations of reverse current.

537.311.33:546.289:539.23 2283
**Hall Effect and Conductivity of Thin Vapour-Deposited Germanium Films**—F. Eckart and G. Jungk. (*Mber. dtsch. Akad. Wiss. Berlin*, vol. 2, no. 5, pp. 266–269; 1960.) A preliminary report and discussion of Hall-effect and conductivity measurements on films of thickness 800 to 4100 Å at magnetic field strengths up to 10 kg are given.

537.311.33:546.289:539.23 2284
**The Low-Temperature Interaction of Oxygen with Evaporated Germanium Films**—M. J. Bennett and F. C. Tompkins. [*Proc. Roy. Soc. (London)*, vol. 259, pp. 28–44; November, 1960].

537.311.33:546.289–31 2285
**Donor Equilibria in the Germanium-Oxygen System**—C. S. Fuller, W. Kaiser, and C. D. Thurmond. (*J. Phys. Chem. Solids*, vol. 17, pp. 301–307; January, 1961.) A more detailed account is given of work reported earlier (1229 of April). Donor formation has been investigated over a wide temperature range in Ge single crystals with well-defined oxygen concentrations. Results confirm that four oxygen atoms are involved in the formation of one donor.

537.311.33:546.33'86 2286
**A New Intermetallic Semiconductor Compound**—Ya. A. Ugai and T. N. Vigutova. (*Fiz. Tverdogo Tela*, vol. 1, pp. 1786–1788; December, 1959.) A note on the preparation and properties of NaSb with a band gap of 0.82 ev is given.

537.311.33:546.48'811'19 2287
**Preparation and Properties of $CdSnAs_2$**—A. J. Strauss and A. J. Rosenberg. (*J. Phys. Chem. Solids*, vol. 17, pp. 278–283; January, 1961.) Infrared transmission measurements indicate that the energy gap is about 0.23 ev at room temperature. The absorption edge shifts to shorter wavelengths with increasing electron concentration.

537.311.33:546.681'86 2288
**Optical Determination of the Conduction Band Structure of GaSb**—M. Cardona. (*J. Phys. Chem. Solids*, vol. 17, pp. 336–338; January, 1961.)

537.311.33:[546.682'19+546.681'19 2289
**Electron Effective Masses of InAs and GaAs as a Function of Temperature and Doping**—M. Cardona. (*Phys. Rev.*, vol. 121, pp. 752–758; February, 1961.) Faraday rotation and infrared reflectivity measurements were used.

537.311.33:546.682'19 2290
**Observation of Oscillatory Magnetoresistance in InAs at Microwave Frequencies**—G. Bemski and B. Szymanski. (*J. Phys. Chem. Solids*, vol. 17, pp. 335–336; January, 1961.) Experimental technique and results are described and advantages of microwave measurements over dc measurements are discussed. Similar oscillations have been observed in InSb.

537.311.33:546.682'19:538.639 2291
**Magnetothermal Nernst-Ettingshausen Effects in Indium Arsenide**—O. V. Emel'yanenko, N. V. Zotova and D. N. Nasledov. (*Fiz. Tverdogo Tela*, vol. 1, pp. 1868–1871; December, 1959.) Graphs show the variation of the Nernst-Ettinghausen coefficients of *n*-type InAs with temperature up to 600°K. With increase of electron density the point at which the transverse and longitudinal coefficients change sign is displaced towards lower temperatures.

537.311.33:546.682'86 2292
**Growth Twins in Indium Antimonide**—

World Radio History

R. K. Mueller and R. L. Jacobson. (*J. Appl. Phys.*, vol. 32, pp. 550–551; March, 1961.)

**537.311.33:546.682'86** 2293
**Preparation and Properties of Grown *p-n* Junctions of InSb**—H. C. Gorton, A. R. Zacaroli, F. J. Reid, and C. S. Peet. (*J. Electrochem. Soc.*, vol. 108, pp. 354–356; April, 1961.) Grown *p-n* junctions were produced by doping high-purity *n*-type melts with Zn. The curves of current density as a function of temperature showed that leakage currents predominate at lower temperatures and saturation currents at higher temperatures.

**537.311.33:546.682'86'241** 2294
**A New Semiconducting Compound in the In-Sb-Te System**—N. A. Goryunova, S. I. Radautsan, and G. A. Kiosse. (*Fiz. Tverdogo Tela*, vol. 1, pp. 1858–1860; December, 1955.) A note on the physico-chemical properties of five InSb-InTe alloys, in particular $In_4SbTe_3$, a semiconductor, is given.

**537.311.33:546.812'231** 2295
**Electrical Properties of Sb-Doped *n*-Type SnSe**—J. Umeda. (*J. Phys. Soc. Japan*, vol. 16, p. 124; January, 1961.)

**537.311.33:547.533** 2296
**Current/Voltage Characteristics of the Autoelectron Current from Semiconductors**—Yu. V. Zubenko, A. K. Klimin and I. L. Sokol'skaya. (*Fiz. Tverdogo Tela*, vol. 1, pp. 1845–1847; December, 1959.) A note is given on field-emission data for $W_2C$ and Ge at variance with other published data [see, *e.g.*, 1922 of 1959 (Gofman, *et al.*)].

**537.311.33:621.317.3** 2297
**A Thermal Shutter Phenomenon in Field-Effect Measurements**—N. B. Grover and Y. Goldstein. (*J. Phys. Chem. Solids*, vol. 17, pp. 338–340; January, 1961.) The phenomenon may lead to misinterpretation of field-effect data taken on samples whose temperature differs from that of their surroundings. The nature of the thermal shutter depends only on the mounting of the sample.

**537.311.33:621.375.9** 2298
**New Possibilities of Amplification by Carrier Motion in Semiconductors**—E. Groschwitz. (*Z. angew. Phys.*, vol. 12, pp. 370–382 and 400–410; August and September, 1960.) A detailed consideration is given without mathematical treatment, of the theory underlying the transport processes in semiconductors, on the basis of a hypothetical model. 64 references.

**537.311.33:621.391.822** 2299
**On the Influence of Diffusion and Surface Recombination upon the GR Noise Spectrum of Semiconductors**—K. S. Champlin. (*Physica*, vol. 26, pp. 751–760; September, 1960.) Several theories of generation-recombination noise in nearly intrinsic semiconductors [see, *e.g.*, 2422 of 1959 (Van Vliet and Van der Ziel)] are critically examined, and it is shown that these theories do not allow for the correlation between Fourier coefficients of different spatial modes of the fluctuations in carrier density. A treatment based on a transmission line analogy is presented and the result examined for the cases when the recombination process is limited by a) volume, b) surface, and c) diffusion.

**537.323** 2300
**Investigation of the Thermoelectric Properties of $CoSb_3$ Compound with Sn, Te and Ni Impurities**—B. N. Zobnina and L. D. Dudkin. (*Fiz. Tverdogo Tela*, vol. 1, pp. 1821–1827; December, 1959.)

**537.323** 2301
**Anomalous Thermoelectric Properties of Gadolinium Selenide**—R. C. Vickery and H. M Muir. (*Nature*, vol. 190, pp. 336–337; April, 1961.) Anomalies in parameter interrelations of a high *Z*-value GdSe-$Gd_2Se_3$ composition can be explained in terms of a transport mechanism which is visualized as EM waves of thermal frequency ("thermons") acting as charge carriers.

**537.583** 2302
**Change in the Work Function of Molybdenum on Deposition of Thin Sodium and Caesium Films**—V. N. Lepeshinskaya and V. N. Belogurov. (*Fiz. Tverdogo Tela*, vol. 1, pp. 1806–1812; December, 1959.)

**538.221** 2303
**Threshold Concentration for the Existence of Ferromagnetism in Dilute Alloys**—M. Coopersmith and R. Brout. (*J. Phys. Chem. Solids*, vol. 17, pp. 254–258; January, 1961.) See also 817 of 1960 (Brout).

**538.221** 2304
**Magnetization of Iron-Nickel Alloys under Hydrostatic Pressure**—J. S. Kouvel and R. H. Wilson. (*J. Appl. Phys.*, vol. 32, pp. 435–441; March, 1961.)

**538.221** 2305
**The Relation between Switching Coefficient and Limiting Frequency of Ferromagnetic Materials**—R. Boll. (*Z. angew. Phys.*, vol. 12, pp. 364–370; August, 1960.) The dynamic characteristics of ferromagnetic materials, including thin films, allowing for spin-relaxation and eddy-current losses are investigated. For related work on metal tapes, see 1581 of May. 49 references.

**538.221:534.231–8** 2306
**Movement of Bloch Walls in Ultrasonic Fields**—G. Haacke and J. Jaumann. (*Z. angew. Phys.*, vol. 12, pp. 289–297; July, 1960.) Investigations were made on single-crystal Ni in a 1-Mc ultrasonic field. Changes in Bitter patterns are illustrated and the results interpreted.

**538.221:537.533.7** 2307
**Antiparallel Weiss Domains as Biprisms for Electron Interference Effects**—H. Boersch, H. Hamish, D. Wohlleben and K. Grohmann. (*Z. Phys.*, vol. 159, pp. 397–404; August, 1960.) The interference effects used in electron-optics investigations of domain patterns (see 2313 below) are studied experimentally; results obtained are in agreement with theory proposed by Aharonov and Bohm (821 of 1960).

**538.221:538.213** 2308
**Locus Curves of Complex Permeability of Thin Tapes**—R. Boll. (*Frequenz*, vol. 14, pp. 227–238; July, 1960.) Measurements of permeability on tapes of Ni-Fe and Cu-Fe alloy give results which differ considerably from locus curves based on classical eddy-current theory. These differences are attributable to electron-spin relaxation and resonance effects. See 1581 of May.

**538.221:538.613** 2309
**Limitations of the Magneto-optic Kerr Technique in the Study of Microscopic Magnetic Domain Structures**—D. Treves. (*J. Appl. Phys.*, vol. 32, pp. 358–364; March, 1961.)

**538.221:539.23** 2310
**The Interaction of Thin Nickel Films in Ni-Cu Multilayer Systems with Stress-Induced Uniaxial Anisotropy**—W. Ruske. (*Mber. dtsch. Akad. Wiss. Berlin*, vol. 2, nos. 3/4, pp. 161–163; 1960.) The coercive force is plotted as a function of Ni-film spacing for Ni-film thicknesses of 275, 575 and 1350 Å. See also 3204 of 1960.

**538.221:539.23** 2311
**The Investigation of Slow Magnetization Processes in Thin Films**—W. Hellenthal. (*Naturwiss.*, vol. 47, p. 371; August, 1960.) A note is given on the investigation of magnetic reversal in thin films as a function of time and reverse field strength; typical curves are reproduced.

**538.221:539.23:538.614** 2312
**Microscopic Observation of Straight and Curved Magnetization Structure by means of the Faraday Effect**—H. Boersch and M. Lambeck. (*Z. Phys.*, vol. 159, pp. 248–252; July, 1960.) Magnetic domains in thin vapor-deposited Fe films are rendered visible by the method given in 1162 of 1957 (Fowler and Fryer) in conjunction with a high-resolution microscope technique. See also 4324 of 1960 (Boersch, *et al.*).

**538.221:539.23:621.385.833** 2313
**Electron-Optics Investigations of Weiss Domains in Thin Iron Films**—H. Boersch, H. Raith and R. Wohlleben. (*Z. Phys.*, vol. 159, pp. 388–396; August, 1960.) A schlieren method [3964 of 1960 (Boersch and Raith)] and a shadow-projection method [*e.g.*, 2085 of 1960 (Fuller and Hale)] are described and results obtained with these methods are illustrated and discussed.

**538.221:621.318.134** 2314
**The Ionic Distribution in the Garnets $Gd_3Al_3Fe_2O_{12}$ and $Y_3Al_3Fe_2O_{12}$**—C. E. Miller (*J. Phys. Chem. Solids*, vol. 17, pp. 229–231; January, 1961.)

**538.221:621.318.134** 2315
**On the Structure and Oxygen Content of Copper and Copper-Manganese Ferrite**—A. Bergstein and L. Červinka. (*J. Phys. Chem. Solids*, vol. 18, pp. 264–265; February, 1961.)

**538.221:621.318.134** 2316
**Magnetocrystalline Anisotropy of Cobalt-Substituted Manganese Ferrite**—J. V. Slonczewski. (*J. Phys. Chem. Solids*, vol. 18, pp. 269–271; February, 1961.)

**538.221:621.318.134** 2317
**Ultra-High-Frequency Properties of Yttrium and Lutecium Ferrite with Garnet-Type Structure**—A. G. Gurevich, I. E. Gubler and A. P. Safant'evskii. (*Fiz. Tverdogo Tela*, vol. 1, pp. 1862–1865; December, 1959.) Results of measurements of ferromagnetic resonance, permeability and permittivity are reported.

**538.221:621.318.134** 2318
**Growing Single Crystals of Yttrium Ferrite**—A. G. Titova. (*Fiz. Tverdogo Tela*, vol. 1, pp. 1871–1873; December, 1959.) Crystals 12 mm high were obtained using $B_2O_3$ in the solvent. See 1289 of 1959 (Nielsen and Dearborn).

**538.221:621.318.134:538.569.4** 2319
**Ferromagnetic Resonance in Yttrium Ferrite Single Crystals**—A. G. Gurevich and I. E. Gubler. (*Fiz. Tverdogo Tela*, vol. 1, pp. 1847–1850; December, 1959.) A report is given of measurements at 3.25 cm λ on $Y_3Fe_5O_{12}$ single crystals obtained from solution.

**538.221:621.318.134:538.569.4** 2320
**Paramagnetic Resonance of $Fe^{3+}$ in Octahedral and Tetrahedral Sites in Yttrium Gallium Garnet (YGaG) and Anistropy of Yttrium Iron Garnet (YIG)**—S. Geschwind. (*Phys. Rev.*, vol. 121, pp. 363–374; January, 1961.)

**538.221:621.318.134:538.569.4** 2321
**Relaxation Mechanisms in Ferromagnetic Resonance**—T. Kasuya and R. C. LeCraw. (*Phys. Rev. Lett.*, vol. 6, pp. 223–225; March, 1961.) Recent observations of the relaxation time of spin waves with zero wave vector in Y-Fe garnet are given and theory accounting for the results is outlined.

World Radio History

548.0:538.6 2322
**Direction Dependence of Physical Properties in Crystals with Particular Regard to Galvanomagnetic and Thermomagnetic Effects**—H. Bross. (*Z. Naturforsch.*, vol. 15a, pp. 859–874; October, 1960.) A method is given for determining the influence of crystal symmetry on the direction dependence of the tensors defining crystal properties. A phenomenological theory of galvanomagnetic and thermomagnetic effects is developed.

## MATHEMATICS

517.56:621.372.44 2323
**Analytical Representation of the Characteristics of Nonlinear Two-Poles**—W. Böning. (*Arch. Elektrotech.*, vol. 45, pp. 265–278; July, 1960.) Nonlinear characteristics are approximated by simple algebraic and transcendental functions. Curves are given for the determination of the requisite coefficients. For related graphical methods, see 3459 of 1956 (Fischer and Moser).

519.281.1:621.391 2324
**The Significance of Moments in Time and Frequency Functions**—H. Dobesch and H. Sulanke. (*Nachrtech. Z.*, vol. 10, pp. 240–246; June, 1960.) The statistical method of moments is outlined and its application to the determination of transmission characteristics of communication channels is discussed.

## MEASUREMENTS AND TEST GEAR

621.317.2:538.566.08]+534.844.1 2325
**Reverberation Chamber Technique and Construction of a Large Reverberation Chamber for Electromagnetic Waves**—E. Meyer, H. W. Helberg, and S. Vogel. (*Z. angew. Phys.*, vol. 12, pp. 337–346; August, 1960.) The use of reverberation-chamber techniques for the measurement of EM absorption is discussed with reference to absorption measurements in a small echo chamber. The large chamber described (see 1393 of May) is also intended for acoustic measurements.

621.317.3.029.65:621.391.822:621.387 2326
**Determination of Noise Temperature of a Gas-Discharge Noise Source for Four-Millimeter Waves**—W. Jasinski and G. Hiller. (PROC. IRE, vol. 49, pp. 807–808; April, 1961.) The hot body standard was a heated Si wedge in a waveguide.

621.317.335:621.372.413 2327
**Correction Term for Dielectric Measurements with Cavity Resonators**—E. S. Hotston. (*J. Sci. Instr.*, vol. 38, pp. 130–131; April, 1961.) "The effect of varying the diameter of a polystyrene disk on the value of its dielectric constant when measured in a resonator of fixed diameter is investigated. Agreement is obtained with results predicted by perturbation theory."

621.317.335.3:538.221:621.318.134 2328
**Measurement Equipment for the Determination of the Permeability Tensor and Dielectric Constant of Ferrites at 3000 Mc/s**—W. Nowak. (*Hochfrequenz. und Elektroak.*, vol. 69, pp. 83–94; June, 1960.) The principle used is that of measurement inside a circularly polarized cavity resonator; the method of resonator excitation has been simplified.

621.317.341.2.029.4 2329
**Nyquist Diagram Tracer for A.F.**—A. R. Bailey. (*Electronic Tech.*, vol. 38, pp. 156–159; May, 1961.) Details are given of a laboratory instrument for determining the Nyquist diagram of a circuit in the frequency range 20 cps–20 kc.

621.317.6:621.396.663 2330
**Frequency-Independent Measurement of Complex Ratios by means of the Goniometer**—H. Fricke. (*Elektrotech. Z., Edn A* vol. 81, pp. 422–427; June, 1960.) The principle of operation of the inductive goniometer is outlined and procedures for determining the ratio of electrical quantities in terms of phase and amplitude are described. A diagram is given for evaluating the ratio when the position and magnitude of the goniometer minimum are known. See also 3613 of 1960.

621.317.7:621.391.822 2331
**Sampling Technique for Generating Gaussian Noise**—A. J. Rainal. (*Rev. Sci. Instr.*, vol. 32, pp. 327–331; March, 1961.) The noise has a uniform power spectrum from 0.1 cps to 5 kc.

621.317.75:621.374:681.142 2332
**Accurate Amplitude Distribution analysed combining Analogue and Digital Logic**—T. A. Brubaker and G. A. Korn. (*Rev. Sci. Instr.*, vol. 32, pp. 317–322; March, 1961.) A new precision analyzer yields digital read-out of probability or probability density for random waveforms at low audio frequencies. The use of analog computer techniques permits convenient assembly of such instruments. See 1737 of 1960 (Bickart).

## OTHER APPLICATIONS OF RADIO AND ELECTRONICS

551.508.71:537.322.15 2333
**An Automatic Dew-Point Hygrometer using Peltier Cooling**—P. Gerthsen, J. A. Gilsing, and M. van Tol. (*Philips Tech. Rev.*, vol. 21, pp. 196–200; June, 1960.)

551.510.62:621.372.413 2334
**Free-Balloon-Borne Meteorological Refractometer**—J. F. Theisen and E. E. Gossard. (*J. Res. NBS*, vol. 65D, pp. 149–154; March and April, 1961.) A 400-Mc refractometer for the investigation of layer-type discontinuities in the troposphere is described.

621.362:621.387 2335
**Interpretation of Experimental Characteristics of Cesium Thermionic Converters**—E. N. Carabateas, S. D. Pezaris, and G. N. Hatsopoulos. (*J. Appl. Phys.*, vol. 32, pp. 352–358; March, 1961.) Two types of $V/T$ curves can be distinguished in the operation of a Cs converter: collision-free type and sheath type. A method is outlined for obtaining the electron temperature from the sheath-type curve. The emitter work function and temperature can then be estimated.

621.398:681.142 2336
**An Equipment for Automatically Processing Time-Multiplexed Telemetry Data**—N. Purnell and T. T. Walters. (*J. Brit. IRE*, vol. 21, p. 257–274; March, 1961.) Details are given of the way in which the input signals are derived and the method by which the recordings are made. The equipment produces two forms of output: a) analog graphs on paper film and b) digital records on punched cards. Methods of checking performance are described.

681.175:621.374.3 2337
**A Novel Digital Clock**—A. Russell. (*Electronic Engrg.*, vol. 33, pp. 150–154; March, 1961.) An indicator of the minute, hour and date, together with a four-figure test number which employs telephone-type uniselectors, is operated by a separate seconds generator. The output is suitable for operating a tape perforator of an electronic typewriter.

## PROPAGATION OF WAVES

621.391.812.6.029.45 2338
**A Note on Phase Velocity of V.L.F. Radio Waves**—J. R. Wait and K. P. Spies. (*J. Geophys. Res.*, vol. 66, pp. 992–993; March, 1961.) The phase velocity is plotted as a function of frequency in the range 8–30 kc for ionospheric heights of 60–100 km using formulas given earlier (4367 of 1960).

621.391.812.6.029.6:537.56 2339
**Microwave Propagation through a Magneto plasma**—R. L. Phillips, R. G. DeLoch, and D. E. White. (*J. Appl. Phys.*, vol. 32, pp. 551–552; March, 1961.) Plasma sheaths surrounding space vehicles can severely attenuate radio signals. By using a sufficiently strong magnetic field aligned along the direction of propagation, this attenuation can be reduced. The preliminary results of laboratory experiments are given.

621.391.812.61 2340
**Weather and Reception Level on a Troposphere Link—Annual and Short-term Correlations**—L. G. Abraham, Jr., and J. A. Bradshaw. (*J. Res. NBS*, vol. 65D, pp. 155–156; March and April, 1961.) "The weather parameters suggested by the Booker-Gordon theory (1757 of 1950) are correlated with data from a troposphere link not previously reported. While the correlations over the whole year's weather cycle are high, the short-term correlations practically vanish. The former without the latter lend little support to this theory."

621.391.812.62 2341
**Properties of Tropospheric Scattered Fields**—N. R. Ortwein, R. U. F. Hopkins, and J. E. Pohl. (PROC. IRE, vol. 49, pp. 788–802; April, 1961.) Scatter tests were made in Southern California in conjunction with meteorological measurements. The observed angular scattering of the received field varies as $\theta^{-14/3}$ which is consistent with turbulent spectra varying as $k^{-5/3}$. Reflections from layers become important in the lower frequency range when the atmosphere begins to stabilize.

621.391.812.621 2342
**Graphical Determination of Radio Ray Bending in an Exponential Atmosphere**—C. F. Pappas, L. E. Vogler and P. L. Rice. (*J. Res. NBS*, vol. 65D, pp. 175–179; March and April, 1961.) A simplified method is given for calculating the approximate refraction angle as a function of height, for values of surface refractivity ranging from 200 to 450.

621.391.812.621 2343
**A Formula for Radio Ray Refraction in an Exponential Atmosphere**—G. D. Thayer. (*J. Res. NBS*, vol. 65D, pp. 181–182; March and April, 1961.) The formula is derived by integration of a differential equation, assuming that $(n-1)\times 10^6$ decreases exponentially with height above a smooth spherical earth.

621.391.812.622 2344
**The Effect of Multiple Atmospheric Inversions on Tropospheric Radio Propagation**—F. H. Northover. (*J. Atmos. Terr. Phys.*, vol. 20, pp. 295–296; April, 1961.) A method of analysis developed for a single inversion is extended to account for the collective effect of several simultaneously occurring inversions.

621.391.812.63 2345
**A Theory of Incoherent Scattering of Radio Waves by a Plasma**—J. P. Dougherty and D. T. Farley. [*Proc. Roy. Soc.* (*London*), vol. 259, pp. 79–99; November, 1960.] The amplitude and frequency spectrum of the scattered radiation are calculated, making use of a generalized version of Nyquist's noise theorem, and the results are applied to incoherent scatter from the ionosphere. The amplitude is consistent with independent scattering by electrons; the mean Doppler broadening corresponds roughly to the speed of the ions rather than the electrons. The spectral shape is not Gaussian; there is a slight dip at the center frequency. Plasma resonance effects are negligible for frequencies in use at present.

World Radio History

621.391.812.63 2346
**The Reflection of Radio Waves from an Iceshelf**—W. R. Piggott and L. W. Barclay. (*J. Atmos. Terr. Phys.*, vol. 20, pp. 298–299; April, 1961.) Information concerning the RF properties of the iceshelf is deduced from certain properties of the vertical-incidence ionospheric records made at Halley Bay, Antarctica.

621.391.812.63 2347
**Correlation Analysis of the Fading of Radio Waves Reflected Vertically from the Ionosphere**—G. F. Fooks and I. L. Jones. (*J. Atmos. Terr. Phys.*, vol. 20, pp. 229–242; April, 1961.) The fading of HF waves, after reflection from the *E* and *F* layers, has been analyzed. Magnetic conditions were quiet. The results, obtained from spaced receivers, give the size and shape of an average irregularity in the ground pattern, the drift velocity and the relative importance of random changes to drift in producing fading.

621.391.812.63 2348
**Effect of Antenna Radiation Angles upon H.F. Radio Signals Propagated over Long Distances**—W. F. Utlaut. (*J. Res. NBS*, vol. 65D, pp. 167–174; March and April, 1961.) Observations on a 20-Mc CW signal over E-W paths of 6800 km and 8400 km indicate that antennas with very low radiation angle may be advantageous for long-distance reception.

621.391.812.63.029.62 2349
**Relationship between $f_0E_s$ and Field Intensity depending on Sporadic-*E* Propagation in the 50-Mc/s Band**—M. Yamaoka. (*J. Radio Res. Labs., Japan*, vol. 7, pp. 599–613; November, 1960.) Transmissions from Okinawa on 49.68 Mc were received at five points in Japan at distances from 1100–2390 km. The field intensity is shown graphically as a function of distance and $E_s$-layer critical frequency.

621.391.812.631 2350
**Polar-Cap Blackout and Auroral-Zone Blackout**—Y. Hakura. (*J. Radio Res. Labs., Japan*, vol. 7, pp. 583–597; November, 1960.) A statistical analysis of ten polar-cap events during the I.G.Y. is used to examine the characteristics of the two types of blackout. A detailed examination of the event of July 29, 1958, demonstrates that the two types represent distinct phases; the solar corpuscles responsible are considered.

621.391.812.631:551.510.535(98) 2351
**High-Frequency Radio-Wave Blackouts at Medium and High Latitudes during a Solar Cycle**—C. Collins, D. H. Jelly, and A. G. Matthews. (*Canad. J. Phys.*, vol. 39, pp. 35–52; January, 1961.) An examination of ionograms for the occurrence over Canada of blackouts correlating with riometer measurements of Type II (auroral) and Type III (polar-cap) absorption events has revealed distinct geographical patterns of blackout occurrence. Study of ionosonde data back to 1949 shows different sunspot cycle variations for the two events.

621.391.814:537.56]+621.372.826 2352
**Propagation of Electromagnetic Waves along a Thin Plasma Sheet**—J. R. Wait. (*Canad. J. Phys.*, vol. 38, no. 12, pp. 1586–1594; 1960.) "It is shown that a thin ionised sheet will support a trapped surface wave. The effect of a constant and uniform magnetic field is to modify the phase velocity and polarization of the surface wave. The essential features are illustrated by numerical results for selected values of the electron density, collision frequency, and gyro frequency. The effect of locating the plasma sheet near and parallel to a conducting plane is also considered. In this situation other modes of a waveguide type are possible in addition to the surface wave."

621.391.814.029.64+621.372.826 2353
**TE Surface Waves Guided by a Dielectric-Covered Metal Plane**—D. Morris and A. G. Mungall. (*Canad. J. Phys.*, vol. 38, pp. 1553–1559; December, 1960.) Surface waves were excited over a sand-covered metal plane and the phase velocities of the first three TE modes were determined, as a function of the sand depth, at a frequency of 9300 Mc. The simultaneous existence of two modes with different velocities, predicted theoretically for certain sand depths, was confirmed experimentally. For a report of similar measurements on TM mode surface waves, see 2892 of 1960 (Mungall and Morris).

## RECEPTION

621.376.23:621.391.82 2354
**Questions of Potential Noise Immunity when the Signal Fades**—D. D. Klovskiĭ. [*Radiotekhnika* (*Moscow*), vol. 15, pp. 17–25; May, 1960.] Criteria are obtained for coherent and noncoherent detection processes in an ideal receiver in the presence of fluctuating interference and rapid smooth fading. Error probabilities are calculated for different systems.

621.376.23:621.391.822 2355
**Further Results on the Detectability of Known Signals in Gaussian Noise**—H. C. Martel and H. V. Mathews. (*Bell Sys. Tech. J.*, vol. 40, pp. 423–451; March, 1961.) Solutions are given for a maximum-likelihood detector operating on a finite number of samples of the stimulus, and for an optimum integral operator treating the stimulus as a continuous function.

621.376.23:621.396.962.3 2356
**Summary and Comparison of Known Methods for the Detection of Periodic Pulses in the Presence of Noise**—D. Haussig. (*Hochfrequenz. und Elektroak.*, vol. 69, pp. 94–103; June, 1960.) The improvement of SNR, *e.g.*, for radar, by integration or cross-correlation methods is discussed. Practical pulse correlator and integrator circuits are proposed; experimental results are illustrated.

621.391.812.3:551.510.535 2357
**Analysis of Random Fading Records**—S. R. Khastgir and R. N. Singh. (*Indian J. Phys.*, vol. 34, pp. 527–530; November, 1960.) An analysis is given of experimental results obtained using three spaced receivers on a frequency of 3.8 Mc. See also 3859 of 1960.

621.391.823:621.396.669 2358
**Interference Suppression of PTT Motor Vehicles**—E. Meister. (*Tech. Mitt. PTT*, vol. 38, pp. 271–277; August, 1960. In German and French.) An analysis is given of the results of tests on motor vehicles of the Swiss Post Office fitted with interference-suppression devices, to assess the effectiveness of the methods of suppression adopted and any influence they may have on the running efficiency of the vehicle. See also 1627 of May (Walter).

621.391.823:621.396.669 2359
**Interference Suppression of Vehicles with Petrol Engines**—(*Tech. Mitt. PTT*, vol. 38, pp. 314–315; September, 1960. In German, French, and Italian.) A suppression method and installation instructions are given. See also 2358.

621.396.62 2360
**The Effectiveness of Methods of Increasing the Dynamic Range of a Panoramic Radio Receiver**—N. I. Svetlov. [*Radiotekhnika* (*Moscow*), vol. 15, pp. 29–32; May, 1960.] Experiments show that an automatically re-aligned filter comprising two reactance tubes in a bandpass circuit not only decreases crosstalk but reduces nonlinear distortion.

621.396.62:523.164.32 2361
**Voltage-Tuned Swept-Frequency Receiver**—J. J. Riihimaa. (*Rev. Sci. Instr.*, vol. 32, pp. 289–291; March, 1961.) A voltage-tuned solar spectrum analyzer, employing Si tuning capacitors, has been developed. It covers the range 15–30 Mc at sweep rates up to 10 per second.

621.396.62.029.62 2362
**Fundamental Requirements for a Good F.M. V.H.F. Broadcast Receiver**—E. Wey. (*Tech. Mitt. PTT*, vol. 38, pp. 257–271; August, 1960. In German and French.) A summary touching on sensitivity, selectivity and quality requirements and dealing with the measurement and reduction of interference is given.

621.396.62.029.62 2363
**A New Swiss Radio Receiver with V.H.F. Stage, conforming to PTT (Swiss Post Office) Specifications**—W. Strohschneider. (*Tech. Mitt. PTT*, vol. 38, pp. 304–311; September, 1960. In German and French.) Circuit diagram and design details are given. See also 2362.

621.396.62.029.64:523.164 2364
**A Low-Noise *X*-Band Radiometer using Maser**—J. J. Cook, L. G. Cross, M. E. Bair and R. W. Terhune. (PROC. IRE, vol. 49, pp. 768–778; April, 1961.) A reflection cavity maser with voltage-gain×bandwidth products up to 300 Mc at 4.2°K is used. The gain instability is less than 1 per cent up to 10 minutes and 2 per cent up to 30 minutes. A noise factor of 0.6 db (43°K) has been obtained with rms noise fluctuations of 0.01°K and 0.007°K for integration times of 12 and 43 seconds, respectively.

## STATIONS AND COMMUNICATION SYSTEMS

621.376.5 2365
**Pulse Transmission by A.M., F.M. and P.M. in the Presence of Phase Distortion**—E. D. Sunde. (*Bell Sys. Tech. J.*, vol. 40, pp. 353–422; March, 1961.) Performance in pulse transmission systems using various carrier modulation and detection methods is formulated in terms of a common basic function known as the carrier pulse transmission characteristic. A comprehensive theoretical evaluation of transmission impairment caused by various types of phase and envelope delay distortion is made.

621.391.64:621.376.223 2366
**Solid-State Modulators for Infrared Communications**—P. W. Kruse and L. D. McGlauchlin. (*Electronics*, vol. 34, pp. 177–181; March, 1961.) Free carrier absorption in a semiconductor may be used to modulate a beam of infrared radiation. Ge modulator characteristics and circuit details of a transmitter/receiver with a range of greater than one mile are given.

621.396.215 2367
**A Comparison between Alternative H.F. Telegraph Systems**—W. Lyons, J. V. Beard, and A. J. Wheeldon. (*Point to Point Telecommun.*, vol. 5, pp. 11–17; February, 1961.) Comment on 1026 of March and authors' reply are given.

621.396.4:621.376.23 2368
**Suppressed-Carrier Double-Sideband Systems**—G. W. Short. (*Wireless World*, vol. 67, pp. 242–243; May, 1961.) Summaries receiving techniques and system advantages and difficulties are given.

621.396.43:[523.3+551.507.362.2 2369
**Use of Moon or Satellite Relays for Global Communications**—L. P. Yeh. (*Commun. and Electronics*, no. 51, pp. 607–615; November, 1960.) Results of the major moon-echo experiments are summarized and compared in tabular form. General conclusions regarding the use of

World Radio History

the moon as a passive and an active relay are discussed in relation to the performances expected of similar satellite relays.

621.396.43:621.391.812.826 2370
**Analysis and Detection of Echo Signals on Microwave Radio Paths**—G. E. Rosman. [*Proc. IRE (Australia)*, vol. 21, pp. 810–820; November, 1960.] The permissible echo parameters for a 600-channel circuit and the effects of antenna directivity for a 40-mile path at 4 Gc are assessed.

621.396.65 2371
**The Radio Telephone Terminal**—B. W. Bardwell. (*Point to Point Telecommun.*, vol. 5, pp. 28–54; February, 1961.) Deals with the functions of the terminal, especially with reference to independent-sideband working, are given.

621.396.65:621.391.812.624 2372
**A Tropospheric Scatter Link over a 200 Mile Path**—G. L. Grisdale and D. A. Paynter. (*Point to Point Telecommun.*, vol. 5, pp. 34–59; October, 1960.) Operating experience with the 1958–1959 Start Point–Galleywood link showed that, using diversity reception, communication with a 24-telephone channel system on 858 Mc was reliable for 99 per cent of the time.

621.396.65:621.398 2373
**Telemetering and Remote Control over Radio Links**—S. Skoumal. (*Point to Point Telecommun.*, vol. 5, pp. 15–33; October, 1960.) A discussion of different methods and systems is given.

621.396.932 2374
**Use and Service Time of Short Waves: Predictions for the Spanish Sea Routes**—R. Gea Sacasa. [*Rev. Telecommun. (Madrid)*, vol. 16, pp. 2–16; September, 1960.] See also 1779 of 1960.

621.396.934:551.507.362.2 2375
**New Satellite Tracking Station in Great Britain**—(*J. Brit. IRE*, vol. 21, pp. 150–152; February, 1961.) A general description of the 136-Mc Minitrack radio interferometer is given. For a similar account, see *Electronic Engrg.*, vol. 33, pp. 160–161; March, 1961.

621.396.945 2376
**Radio-Wave Propagation in the Earth's Crust**—H. A. Wheeler. (*J. Res. NBS*, vol. 65D, pp. 189–191; March and April, 1961.) A note is given on the presence of a "waveguide," in the earth's crust, composed of low-conductivity basement rock, and its application to VLF communication problems.

621.396.946:621.391.63 2377
**Interstellar and Interplanetary Communication by Optical Maser**—R. N. Schwartz and C. H. Townes. (*Nature*, vol. 190, pp. 205–208; April, 1961.) An examination is given of the possibility of transmitting an optical beam from a planet associated with a star at a sufficiently high power level to establish communications with the earth.

## SUBSIDIARY APPARATUS

621.3.017.7:621.373.421.13 2378
**The Change-of-State Crystal Oven**—D. J. Fewings. (*J. Brit. IRE*, vol. 21, pp. 137–142; February, 1961.) The action of the oven depends upon the constancy of the melting point of crystalline material and the thermal ballasting due to the latent heat of fusion. An oven of this type can restrict the frequency shift to 2.8 parts in $10^8$ for a temperature change of 10°C.

621.311.68:621.316.726 2379
**Precise Frequency Control for a Rotary Convertor**—M. J. Tucker. (*Electronic Engrg.*, vol. 33, pp. 240–241; April, 1961.) "The Royal Research Ship 'Discovery II' has been provided with a 50 c/s power supply whose frequency is precise to approximately 1 part in $10^9$, by locking the phase of a small rotary convertor to that of a 50 c/s reference signal derived from a quartz-crystal oscillator."

621.311.69:621.383.5 2380
**Detailed Balance Limit of Efficiency of *p-n* Junction Solar Cells**—W. Shockley and H. J. Queisser. (*J. Appl. Phys.*, vol. 32, pp. 510–519; March, 1961.) A theoretical upper limit for efficiency is deduced assuming that recombination is entirely radiative. Maximum efficiencies of 30 per cent are found.

621.311.69:621.383.5 2381
**Characteristics of a High Solar Conversion Efficiency Gallium Arsenide *p-n* Junction**—E. G. Bylander, A. J. Hodges, and J. A. Roberts. (*J. Opt. Soc. Am.*, vol. 50, pp. 983–985; October, 1960.) Spectral emissivity and response data are given for GaAs photocells which have an open-circuit voltage of about 0.85 v and short-circuit current density 13–15 ma/cm².

621.314.1:621.382.3 2382
**The Choice and Design of D.C. Convertors**—J. S. Bell and P. G. Wright. (*Electronic Engrg.*, vol. 33, pp. 226–231; April, 1961.) The design of single- and two-transformer converters using transistors is discussed and their performances are compared. Design steps are indicated and two practical examples are given.

621.314.631 2383
**Power Semiconductor Ratings under Transient and Intermittent Load**—F. W. Gutzwiller and T. P. Sylvan. (*Commun. and Electronics*, no. 52, pp. 699–706; January, 1961. Discussion.) Methods of calculating maximum allowable dissipation are discussed, with examples.

621.314.63 2384
**Transient Thermal Impedance of Semiconductor Devices**—E. J. Diebold and W. Luft. (*Commun. and Electronics*, no. 52, pp. 719–726; January, 1961.)

621.316.72:621–52 2385
**A New D.C. Level Control for Adaptive Systems**—R. A. Johnson and J. D. Hill. (*Electronic Engrg.*, vol. 33, pp. 242–244; April, 1961.) A novel electronic circuit is described and analyzed which maintains the potential drop across a load constant to within a fraction of one per cent while permitting the dc level of the load to be varied through a wide range. The circuit requires only standard-tolerance electronic components, and high precision is obtained by an error compensation technique.

## TELEVISION AND PHOTOTELEGRAPHY

621.397.13 2386
**Television Standards**—H. Dobesch. (*Radio und Fernsehen*, vol. 9, pp. 447–449; July, 1960.) Comparative data tables and waveform diagrams are given for the seven monochrome television systems in present use.

621.397.132 2387
**Distortion due to System and Transmission Faults in Colour Television based on the N.T.S.C. System**—H. Schönfelder. (*Rundfunktech. Mitt.*, vol. 4, pp. 158–172; August, 1960.) Faults likely to occur in the NTSC system are reviewed; their effect on picture quality is shown to be small in most cases.

621.397.132 2388
**Critical Consideration of the "Henri de France" Colour Television System and a Modification with Better Vertical Resolution**—P. Neidhardt. (*Nachrtech Z.*, vol. 10, pp. 286–290; July, 1960.) A comparison is given of the "Henri de France" system (*e.g.*, 3660 of 1960) and the NTSC system, with suggestions for improving the former.

621.397.334 2389
**Modern Aspects of the Design of Colour Television Film Scanners with Flying-Spot Tubes**—P. Neidhardt. (*Elektron. Rundschau*, vol. 14, pp. 307–313; August, 1960.) A review is given of the optical and mechanical problems involved in the design of flying-spot scanners with details of some of the solutions adopted in various systems.

621.397.334 2390
**Optical Problems with Flying-Spot Colour Scanners**—G. Emmrich. (*Nachrtech. Z.*, vol. 10, pp. 290–295; July, 1960.) Difficulties of optical system design are discussed with reference to existing types of scanner.

621.397.334 2391
**Experiences with a Colour-Television Transparency Scanner**—M. Samlenski. (*Nachrtech. Z.*, vol. 10, pp. 295–298; July, 1960. Plate.) Design problems of a flying-spot scanner for color transparencies are discussed.

621.397.334 2392
**Prospects for Colour Picture Tubes with only One Electron-Beam System in Comparison with the Triple-Beam Mask-Type Tubes**—I. Bornemann. (*Nachrtech. Z.*, vol. 10, pp. 305–309; July, 1960.)

621.397.612 2393
**New Problems in the Design of Video Switching Installations**—L. W. Germany. (*Rundfunktech. Mitt.*, vol. 4, pp. 145–152; August, 1960.) The factors governing the choice of a television studio master control system are reviewed and various methods of switching and program control are described, including a system in which timing is controlled automatically by punched paper tape.

621.397.62:621.382.3 2394
**The Transistorized TV Receiver using a New Horizontal Deflection System**—T. Miura and K. Mano. (*Sci. Repts. Res. Inst. Tohoku Univ., Ser. B.*, vol. 12, no. 1, pp. 41–55; 1960.) The horizontal deflection system described uses six power transistors in a series/parallel combination in the output stage. Sufficient output is provided to operate a 17-inch 90° tube.

621.397.62:621.396.67 2395
**The Influence of Mismatch on Television Picture Quality in Single- and Common-Aerial Installations**—A. Köhler. [*Funk-technik (Berlin)*, vol. 15, pp. 604–607; September, 1960.] Attenuation and reflection effects are considered and practical aspects of installation design minimizing mismatch are discussed.

621.397.621:621.385.832 2396
**A Low-Power Cathode for Television Picture Tubes**—H. E. Smithgall. (*Sylvania Technologist*, vol. 13, pp. 118–121; October, 1960.) A heater-cathode assembly with a diameter of 0.05 inch, thickness of 0.011 inch and rated power of 0.21 w, is described. It is rugged mechanically, operable over a range of 1.2–1.6 v, and has a heating time of 10 seconds for stable operation.

621.397.7–182.3 2397
**Television Outside-Broadcasting by the Radio-diffusion-Television Française**—(*E.B.U. Rev.*, no. 62A, pp. 150–164; August, 1960.) Light-weight equipment is described and methods of outside-broadcast operation are mentioned.

621.397.74 2398
**Requirements for and Measurements on Long-Distance Television Links**—J. Müller.

World Radio History

(*Nachrtech. Z.*, vol. 13, pp. 327–334; July, 1960.) CCIR recommendations are outlined and results are given of measurements based on these, which were made on a 4-Gc radio link over 2000 km. Tests to assess the suitability of the system for NTSC color television are proposed.

621.397.74(485) 2399
**The Development of the Television Network in Sweden**—T. Rosenlund. (*E.B.U. Rev.*, no. 62A, pp. 162–165; August, 1960.)

## TUBES AND THERMIONICS

621.382.2/.3:061.3 2400
**International Symposium on Semiconductor Devices**—A. V. J. Martin. (*Électronique et Automatisme*, no. 9, pp. 145–150; 168; March-April, 1961.) A report of a UNESCO symposium held in Paris, February 20–25, 1961, is given. The titles of all papers presented are given and selected papers are reviewed.

621.382.23 2401
**Effect of Fluctuations in Density on the Esaki Effect**—D. G. Dow. (Proc. IRE, vol. 49, p. 837; April, 1961.) Some theoretical expressions are developed and numerically evaluated to assess the extent of spatial fluctuations of tunnel current to be expected in an Esaki diode.

621.382.23 2402
**Tunnel-Diode Large-Signal Simulation Study**—S. B. Geller and P. A. Mantek. (Proc. IRE, vol. 49, pp. 803–804; April, 1961.) An equivalent circuit is investigated for dynamic response using both analog simulation and graphical analysis.

621.382.23 2403
**Oscillations in the Longitudinal Tunnel Current of Tunnel Diodes**—R. R. Haering and P. B. Miller. (*Phys. Rev. Lett.*, vol. 6, pp. 269–271; March, 1961.) Small fluctuations in the electron term level are proposed to explain observed oscillations in tunnel current in a longitudinal magnetic field [1239 of April (Chynoweth, *et al.*)].

621.382.23 2404
**Influence of the State of the Surface on the Breakdown Voltage of Alloy-Type Silicon Diodes**—Zh. I. Alferov and E. V. Silina. (*Fiz. Tverdogo Tela*, vol. 1, pp. 1878–1879; December, 1959.) A note on the change in breakdown voltage when the surface states are cyclically reproduced is given. Typical *I-V* characteristics are shown for air, vacuum and after heating in vacuum.

621.382.23 2405
**'Breakdown' of Alloy-Type Silicon Diodes in the Forward Direction**—Z. I. Alferov and É. A. Yarv. (*Fiz. Tverdogo Tela*, vol. 1, pp. 1879–1882; December, 1959.) The absence of any effect of illumination or magnetic field on the breakdown voltage, and other experimental data indicate that breakdown is due to leakage effects of a nonohmic character.

621.382.23:621.317.33 2406
**Measurement of Tunnel-Diode Negative Resistance**—C. D. Todd. (*Rev. Sci. Instr.*, vol. 32, pp. 338–342; March, 1961.) Several methods are presented, including an accurate null technique. Test equipment which will allow stabilization of most tunnel diodes is described.

621.382.23:621.372.44 2407
**Three-Layer Negative-Resistance and Inductive Semiconductor Diodes**—W. W. Gärtner and M. Schuller. (Proc. IRE, vol. 49, pp. 754–767; April, 1961.) Combinations of effects in three-layer semiconductor diodes may lead to many negative-resistance and inductive devices with applications to microwave circuit design. The theory underlying these devices and the problems involved are discussed.

621.382.23:621.372.44 2408
**Capacitance Coefficients for Varactor Diodes**—R. D. Weglein and S. Sensiper. (Proc. IRE, vol. 49, p. 810; April, 1961.)

621.382.23:621.372.44 2409
**Comparative Figures of Merit for Available Varactor Diodes**—K. Siegel. (Proc. IRE, vol. 49, pp. 809–810; April, 1961.)

621.382.23:621.372.44 2410
**Parametric Diodes: Design and Fabrication**—D. B. Day. (*J. Brit. IRE*, vol. 21, pp. 283–286; March, 1961.) Short notes are given on theory, design and fabrication of diodes with cutoff frequencies in the region of 50 Gc.

621.382.23:621.373.029.631.64 2411
**Tunnel-Diode Microwave Oscillators**—F. Sterzer and D. E. Nelson. (Proc. IRE, vol. 49, pp. 744–753; April, 1961.) Diodes working between 610 and 8350 Mc are described, with power outputs ranging from 0.01 mw at 7130 Mc to 10 mw at 610 Mc. Problems relating to frequency, power output and waveform are treated analytically.

621.382.23:621.375.9 2412
**A Broad-Band Tunnel-Diode Amplifier**—Moody and Wacker. (See 2141.)

621.382.23:621.375.9 2413
**A Noise Investigation of Tunnel-Diode Microwave Amplifiers**—A. Yariv and J. S. Cook. (Proc. IRE, vol. 49, pp. 739–743; April, 1961.) The agreement between the measured noise figure and the theoretical results is an indirect check on the existence of full shot noise in Ge tunnel diodes at microwave frequencies. The approach to the limiting noise temperature in an amplifier by the use of appropriate circuits is discussed.

621.382.23:621.376.23 2414
**The Tunnel Diode as a Highly Sensitive Microwave Detector**—M. D. Montgomery. (Proc. IRE, vol. 49, pp. 826–827; April, 1961.) Good sensitivity has been obtained by biasing the diode near oscillation and operating it as a square-law detector . Experimental results are quoted at frequencies near 1 Gc.

621.382.3 2415
**Transistor Internal Parameters for Small-Signal Representation**—R. L. Pritchard, J. B. Angell, R. B. Adler, J. M. Early and W. M. Webster. (Proc. IRE, vol. 49, pp. 725–738; April, 1961.) A summary report is given of a working group which studied a) the parameters which emphasize the physical mechanism of transistors, b) symbols for these parameters and c) the relation between these parameters and those employed in circuit analysis and design. 35 references.

621.382.3.012.8 2416
**A Complete Transistor Equivalent Circuit**—R. H. Beeson. (Proc. IRE, vol. 49, pp. 825–826; April, 1961.) The circuit given is implicit in the analysis of Ebers and Moll (884 of 1955).

621.382.333 2417
**Measurement of the Number of Impurities in the Base Layer of a Transistor**—H. K. Gummel. (Proc. IRE, vol. 49, p. 834; April, 1961.) The collector current is measured as a function of emitter-to-base voltage. $N_B$ is then calculated from the simple expression given.

621.382.333 2418
**Silicon Surface Alloy Transistors for High-Frequency Switching and Chopper-Amplifier Applications**—P. A. Charman. (*J. Brit. IRE*, vol. 21, pp. 201–204; February, 1961.)

621.382.333.33 2419
**The Dependence of Current Gain of Drift Transistors on Emitter Current**—G. Schwabe. (*Z. angew. Phys.*, vol. 12, pp. 314–320; July, 1960.) The differences in the gain characteristics of drift and diffusion-type transistors are discussed; at high emitter currents their characteristics become similar.

621.383.5 2420
**GaAs, a Sensitive Photodiode for the Visible**—G. Lucovsky and P. H. Cholet. (*J. Opt. Soc. Am.*, vol. 50, pp. 979–983; October, 1960.) Highly sensitive photodiodes have been formed by diffusion of Cd and Zn in *n*-type GaAs. Operated as photovoltaic detectors, the diodes have half-sensitivity points at 9100 and 5600 Å and a dynamic impedance of the order of 1 mΩ with time constant 1 ms. Certain diodes are equally sensitive when operated in the photoconductive mode.

621.385.032.213.23 2421
**On the Electron Emission from Oxide-Coated Cathode subject to Strong Electric Field**—C. Shibata. (*J. Phys. Soc. Japan*, vol. 16, pp. 51–61; January, 1961.) Deviation of emission from the Schottky value is explained by an avalanche effect in the oxide layer. Calculated and measured values are compared.

621.385.032.213.23 2422
**Oxide-Cathode Emission under Positive-Ion Bombardment**—I. A. Abroyan. (*Fiz. Tverdogo Tela*, vol. 1, pp. 1854–1856; December, 1959.) Commercial oxide cathodes 5 mm in diameter were bombarded with potassium ions of energy 1–10 kev and hydrogen ions of 5–70 kev. The increase in emission current from the cathode under postassium-ion bombardment reached values of 1000 to 5000 electrons per incident ion.

621.385.032.213.23 2423
**Application of Shot-Noise Techniques to the Study of Emission in Oxide Cathodes**—B. Wolk. (*Sylvania Technologist*, vol. 13, pp. 129–136; October, 1960.)

621.385.6 2424
**Small-Signal Space-Charge Density in Drifting Ion-Neutralized Rectilinear-Flow Beams Immersed in an Axial Magnetic Field of Finite Magnitude**—V. Bevc. (Proc. IRE, vol. 49, pp. 815–816; April, 1961.)

621.385.6:621.375.9:621.372.44 2425
**Behavior of Thermal Noise and Beam Noise in a Quadrupole Amplifier**—R. Adler and G. Wade. (Proc. IRE, vol. 49, p. 802; April, 1961.)

621.385.63 2426
**RF Focusing of an Electron Stream**—C. K. Birdsall, G. W. Rayfield, E. Sugata, M. Terada, and K. Ura. (Proc. IRE, vol. 49, pp. 819–821; April, 1961.) Attention is drawn to an error in 3330 of 1960 and further comments by Sugata, *et al.*, are included.

621.385.632 2427
**Matching between Travelling-Wave-Tube Helix and Waveguide**—T. Unotoro. (*Rev. Elec. Commun. Lab., Japan*, vol. 8, pp. 560–572; November-December, 1960.) The optimum dimensions of the coupling circuit for mass-produced tubes are determined by a statistically designed series of measurements.

621.385.632.1 2428
**Experiments on a Series of *S*-Band Crestatrons**—J. E. Rowe, G. T. Konrad, and H. W. Krage. (*Commun. and Electronics*, no. 52, pp. 828–833; January, 1961.) The operation of this device is discussed and experimental data are given for fixed length and variable-length tubes.

World Radio History

The tube is small and operates at high efficiency. See 2427 of 1959 (Rowe).

621.385.832:621.397.62 2429
**Some Electron Trajectories in a Nonuniform Magnetic Field**—T. N. Chin. (PROC. IRE, vol. 49, pp. 832–833; April, 1961.) The nonuniformity is introduced to improve thin cathode-ray tube deflection sensitivity and reduce the width of the scan-producing electromagnet. The equations of the resulting trajectories are derived.

621.385.832:621.397.621 2430
**A Low-Power Cathode for Television Picture Tubes**—Smithgall. (See 2396.)

621.387:621.362 2431
**Interpretation of Experimental Characteristics of Cesium Thermionic Converters**—Carabateas, Pezaris, and Hatsopoulos. (See 2335.)

## MISCELLANEOUS

061.6:621.37/.39 2432
**Report of the United States of America National Committee to the XIII General Assembly of the International Scientific Radio Union, London, England, September 5 to 15, 1960**—(*J. Res. NBS*, vol. 64D, pp. i–v and 591–767; November–December, 1960.) A brief report is given by each Commission of the progress made in its field during the period 1957–1960.

538.569.2.047 2433
**Some Technical Aspects of Microwave Radiation Hazards**—W. W. Mumford. (PROC. IRE, vol. 49, pp. 427–447; February, 1961.) A review of information available and of the safety measures adopted by Bell Laboratories is given. A recommended method of calculating power densities is derived and some commercial power-density meters are described. 78 references.

621.3(083.7) 2434
**Supplement to I.R.E. Standards on Graphical Symbols for Electrical Diagrams, 1954**—(PROC. IRE, vol. 49, pp. 467–468; February, 1961.) Standard 54 IRE 21.S1.

621.37/.38].029.6 2435
**Recent Developments in Microwave Physics**—H. Severin. (*Naturwiss.*, vol. 47, pp. 217–221; May, 1960.) A review dealing particularly with improved ferromagnetic and ferrimagnetic materials and semiconductors, and their applications in new microwave devices is presented.

621.38.004.6 2436
**Reliability of Electronic Equipment**—H. J. Fründt. (*Elektrochem. Z.*, Edn A, vol. 81, pp. 338–341; April, 1960.) A method of determining the operational reliability of complex equipment on the basis of the known failure rates of its components is described.

621.39(047.1) 2437
**Communication Engineering and Radiolocation**—(*VDI Z.*, vol. 103, pp. 189–203; February, 1961.)A progress report covering recent developments, with references mainly to German literature is given. The following sections are surveyed:

a) **Telecommunications**—W. Althans, pp. 189–191.

b) **Sound Broadcasting and Television**—K. Müller, pp. 191–194. 99 references.

c) **Radar and Radio Navigation**—W. Stanner, pp. 195–196.

d) **Electroacoustics**—H. Harz, pp. 197–200. 64 references.

e) **High-Frequency Measurements**—A. Egger, pp. 201–203. 65 references.

World Radio History